European Commission

Community Research

Studies

An expert chemical model for determining the environmental conditions needed to prevent salt damage in porous materials

Research report No 11

ENERGY, ENVIRONMENT
AND SUSTAINABLE DEVELOPMENT

EUROPEAN COMMISSION

Technologies to Protect and Rehabilitate European Cultural Heritage

A RESEARCH AREA FUNDED BY THE EC R&D PROGRAMME
'ENVIRONMENT AND CLIMATE'

An Expert Chemical Model for Determining the Environmental Conditions Needed to Prevent Salt Damage in Porous Materials

PROTECTION AND CONSERVATION OF THE EUROPEAN CULTURAL HERITAGE

Edited by Clifford Price

Cooperation between:
Institute of Archaeology, University College London (UK)
School of Environmental Sciences, University of East Anglia (UK)
Institut für Anorganische und Angewandte Chemie, Universität Hamburg (Germany)

Project ENV4-CT95-0135 (1996–2000)

FINAL REPORT

RESEARCH REPORT NO 11

Directorate-General Science, Research and Development 2000

Acknowledgements

The project partners wish to record their gratitude to the European Commission for funding and to Julia Acevedo for her unfailing support and encouragement.

An Expert Chemical Model for Determining the Environmental Conditions Needed to Prevent Salt Damage in Porous Materials (Contract No. ENV4-CT95-0135). Protection and Conservation of the European Cultural Heritage. Research Report no 11.

Edited by Clifford Price.

Published and distributed by Archetype Publications Ltd, London (`www.archetype.co.uk`).

ISBN 1873132 52 2

The cover illustration appears on the opening page of the ECOS program. It shows a foot from an Egyptian limestone statue, covered with salt crystals. The crystals grew out from the surface of the stone as a result of fluctuating humidity in the temporary storage area where the foot was kept during the First World War (W. A. Oddy, ed., 1992. *The Art of the Conservator*, London: British Museum Press). © The British Museum.

This volume was typeset in 11pt Computer Modern Roman by Kris Lockyear using LaTeX 2_ε; he would like to thank Lisa Usman for her invaluable help.

Contents

List of Figures

List of Tables

1
Introduction

This report is the outcome of European Commission contract ENV4-CT95-0135: *an expert chemical model for determining the environmental conditions needed to prevent salt damage in porous materials.*

The contract was undertaken by three partners:

- Institute of Archaeology, University College London (Clifford Price, Shaiba Mahmoud, Julie Eklund and Alison Sawdy)
- School of Environmental Sciences, University of East Anglia (Simon Clegg, Peter Brimblecombe and Nick Reeves)
- Institut für Anorganische und Angewandte Chemie, University of Hamburg (Michael Steiger, Roland Beyer, Joachim Dorn and Anke Zeunert)

The aim of the contract was to develop a thermodynamic model that could describe the behaviour of aqueous salt solutions in porous materials such as stone, wall-paintings and ceramics. Given the ionic analysis of the salts, the model can predict the combination of solid minerals that is present under equilibrium conditions at any given ambient conditions (temperature and relative humidity). By linking this to the mineral densities, it is possible to predict the total volume of minerals present, and thereby to predict ranges of relative humidity and temperature that do not entail any sudden changes in volume. By maintaining these conditions around the object/monument in question, damage due to the growth of salt crystals may be minimised.

It would have been impracticable to include in the model every system that might ever be encountered in practice. Taking account of those ions most commonly found, attention was focused on the following systems:

Na^+–K^+–Ca^{2+}–Mg^{2+}–NH_4^+–Cl^-–NO_3^-–SO_4^{2-}–H_2O

Na^+–K^+–Cl^-–NO_3^-–SO_4^{2-}–HCO_3^-–H_2O

Na^+–K^+–Cl^--NO_3^-–SO_4^{2-}–CO_3^{2-}–H_2O

In addition, a particular study was made of the system Na^+–Ca^{2+}–Cl^-–CH_3COO^-–H_2O, given the importance of acetates in some museum contexts.

The model was successfully developed using the molality-based thermodynamic approach of Pitzer. However, serious problems were encountered towards the end of the contract when testing the model. A numerical algorithm is used to determine the equilibrium composition that is required by the user. It was discovered that the combined model and algorithm was numerically unstable for some input conditions and produced incorrect results. The only way to overcome the problem was to reparameterise the model in terms of mole-fractions rather than molalities — a task which required several man-months of unanticipated effort. It was not possible, in the time available, to reparameterise the entire data set, and the decision was

made to restrict the new mole-fraction set to the salts most commonly encountered in conservation: Na^+–K^+–Mg^{2+}–Ca^{2+}–Cl^-–NO_3^-–SO_4^{2-}–H_2O, but excluding mixtures containing both Ca^{2+} and SO_4^{2-}. This still covers the majority of cases likely to be encountered in practice.

The mole-fraction model was linked to an expert system (ECOS) that facilitated its use by conservators and conservation scientists. In view of the unexpected switch from the molality based approach to mole fractions, it was not possible to refine the system to the extent that had originally been envisaged, and the system should be regarded as a prototype. Copies on diskette are available to *bona fide* researchers upon application to the project coordinator (`c.price@ucl.ac.uk`).

The system represents a major achievement, enabling the user to predict the equilibrium behaviour of salt mixtures in a way which was quite impossible at the outset of the project. The partners hope that it will be directly applicable to the conservation of the cultural heritage, and that it will also serve as a stimulus to further research in this important area.

2

Salt Damage in Porous Materials

Clifford Price

Institute of Archaeology, University College London

2.1 Introduction

Salts are widely recognised as a major contributor to the loss of the world's architectural heritage. They can also cause severe damage to artefacts in museums. Modern materials are equally at risk, and examples abound of damage to structures as diverse as bridge decks, railway sleepers, dams and runways. The damage is attributable to the growth of salt crystals within the porous structure of materials such as stone, mud brick, ceramics, mortar, concrete and plaster. Crystal growth can take place as a result of crystallisation from supersaturated solutions, of changes in hydration state, or (more rarely) of chemical reactions.

The salts may be derived from many sources, including sea-spray, soil water, cleaning materials, de-icing materials, and building materials. One of the most insidious sources is the reaction between acidic air pollutants and calcareous materials such as limestone and marble, leading, for example, to the formation of calcium sulfate.

Salt damage typically causes powdering and granular disaggregation of the surface. This in turn leads to gradual loss of the surface, with consequent loss of original detail, whether carved or painted. However, it can sometimes lead to such severe loss that structural collapse becomes inevitable.

2.2 Mechanisms of salt damage

Given the severity of the problem, it is surprising that the mechanisms of salt damage are not yet fully understood. Even Goudie & Viles (1997), in their monograph devoted specifically to salt damage, have relatively little to say about damage mechanisms *per se*. Some studies, such as that of Correns (1949) have been handed on from one publication to the next with little critical evaluation, until they have become the accepted wisdom, almost by default.

It is surprising, too, that little is known about the reasons why some crystals grow on the surface (efflorescence), causing relatively little damage, whilst others grow inside the pore structure (subflorescence) with the potential for much greater damage.

One of the most enduring reviews of the subject is that of Evans (1970). A more recent review, in addition to that of Goudie and Viles, is to be found in a paper by Rodriguez-Navarro & Doehne (1999).

One point on which there can be little doubt is that the driving force behind crystallisation damage is the free energy associated with a supersaturated solution. It is the release of this energy on crystallisation that provides forces of sufficient magnitude to break down stone and concrete. Scherer (1999) accepts that the supersaturation puts an upper limit on the stresses that can be imposed by growing crystals on the pore wall, but he argues that the stresses depend on other factors as well, including

the pore size, the interfacial energy between the pore wall and the crystal, and even the strength of the crystal itself.

2.3 Preventing damage through environmental control

In some instances, it may be possible to prevent salt damage by extracting the damaging salts from the artefact or monument in question. This approach is most likely to succeed with relatively small objects that can be brought into the laboratory for treatment, although even here it may not be possible to extract the salts without further damaging an already weakened surface, or triggering other decay mechanisms such as the expansion of clay minerals. In many other instances, salt removal is wholly impracticable, and preventive conservation through environmental control is the only viable option.

The research described in this report is based on the widely held premise that crystallisation damage and hydration damage are directly attributable to the associated increase in crystal volume. The aim of the research was to be able to predict crystal volumes in a given system under given environmental conditions, and thereby to predict 'safe' conditions that would minimise increases in total crystal volume. To do this, we need to first to understand the influence of salts on the vapour pressure of solutions.

2.3.1 The vapour pressure of aqueous salt solutions

When a salt dissolves in water, the vapour pressure of the water is reduced. This means that the relative humidity of air that is in equilibrium with the salt solution is reduced correspondingly, since relative humidity is defined by the expression

$$\mathrm{RH} = \frac{p}{p_0} \times 100\%$$

where p is the vapour pressure of the solution and p_0 is the vapour pressure of pure water at the same temperature.

The reduction in vapour pressure is attributable to two things. First, the very presence of the salt means that the proportion of water in the solution is less than in pure water (where the proportion is clearly 100%). Fewer water molecules are available to escape from the liquid surface and thereby give rise to the vapour pressure. Alternatively, one can imagine that the surface of the liquid is being partially blocked by the ions derived from the salt, and that the escape of water molecules is hindered as a result. This is the behaviour that underlies Raoult's law, which states that the vapour pressure of an individual component in a solution is proportional to its mole fraction. However, Raoult's law assumes that a molecule of that component will have just the same escaping tendency, whatever its surroundings. In the context of an aqueous salt solution, this means that a water molecule would be just as likely to escape from the surface if it were surrounded by other water molecules, as if it were surrounded by ions. Such ideal behaviour does not occur in practice, and this leads to the second and additional reason for the reduction in vapour pressure. Water molecules are polar, and are attracted to the electrostatic charge of the ions. They are thus even less inclined to escape from the surface of a solution, since the presence of the ions holds them back. (For analogy, consider the reduced number of people in a shopping centre during a major sporting event; many people prefer to stay at home, clustered around the television.)

Table 2.1: Equilibrium relative humidities at 20°C (%).

Salt	RH
calcium sulfate	99.96
potassium sulfate	98
sodium sulfate	95
magnesium sulfate	90
ammonium sulfate	81
potassium nitrate	94
sodium nitrate	75
ammonium nitrate	66
calcium nitrate	56
magnesium nitrate	53
potassium chloride	85
ammonium chloride	80
sodium chloride	75
magnesium chloride	34
calcium chloride	33

The reduction in vapour pressure that occurs when a single salt dissolves in water is relatively easily described: the higher the concentration of salt, the lower the vapour pressure of the solution (and hence the lower the relative humidity of air in equilibrium with that solution). However, there is a limit to the amount of salt that can be dissolved, for a saturated solution is reached eventually. There is a corresponding limit to the reduction in vapour pressure that can take place, and a saturated salt solution will have a characteristic vapour pressure, regardless of the amount of excess solid that may be present in the solution. The equivalent relative humidity is commonly referred to as the 'equilibrium relative humidity' or ERH.[1] Different salts have different ERHs, partly because of their differing solubilities and partly because of the differing strengths with which water is attracted to different ions. The ERH can be determined by direct measurement, and the measured ERHs of some common salts are given in Table 2.1. As a general rule, one may expect sparingly soluble salts (such as calcium sulfate) to have a high ERH and highly soluble salts (such as calcium chloride) to have a low ERH.

In the context of salt damage, the reduced vapour pressure of solutions may be viewed more conveniently from the perspective of the salt, rather than the water. Imagine a quantity of a pure salt, which is to be exposed to varying relative humidities. If the relative humidity is above the ERH, the salt will pick up water vapour from the air and dissolve. Given enough time, the resulting solution, which will not be saturated, will reach equilibrium at the specified relative humidity. If the relative humidity is now lowered, water will evaporate from the solution until equilibrium is regained. If the relative humidity is lowered to reach the ERH, enough water will have evaporated for the solution to have become saturated. Any further reduction will cause the loss

[1]The term 'equilibrium relative humidity' is potentially confusing, since air can be in equilibrium with a solution of any concentration. In some respects, the alternative term 'saturation relativity humidity' is to be preferred, though this too can lead to confusion: does the saturation refer to saturation vapour pressure (no) or to saturation of the solution (yes)?

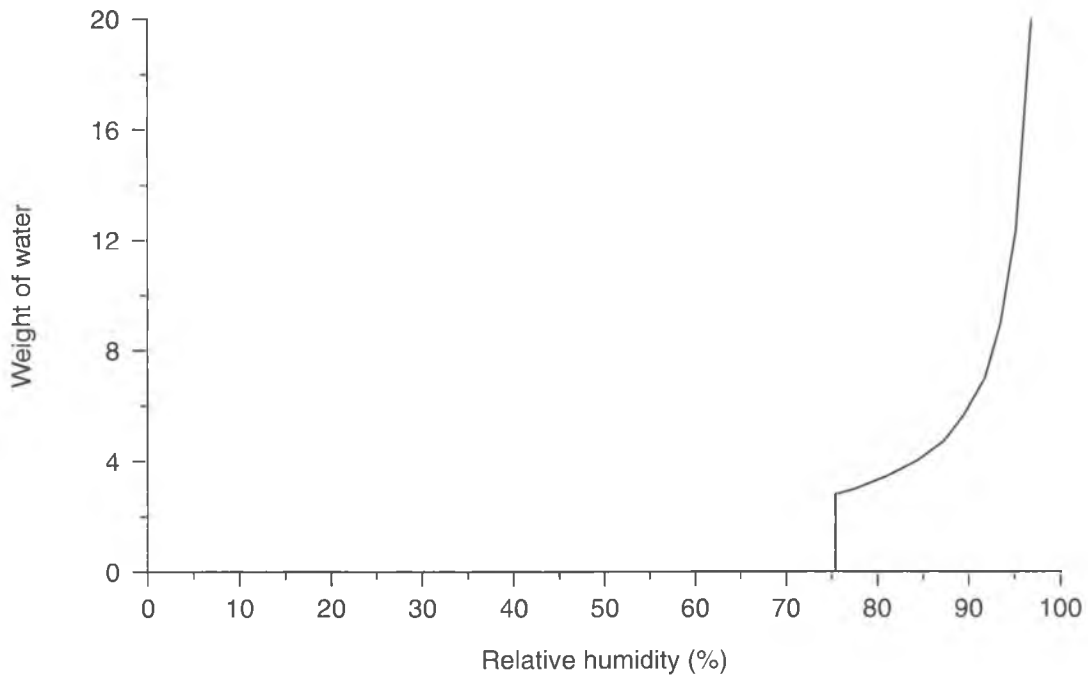

Figure 2.1: The weight of water taken up from the air by 1g sodium chloride. The vertical line represents a saturated solution with varying amounts of excess solid. The curved line represents non-saturated solutions.

of all the remaining water, and the entire quantity of salt will crystallise. At all RH values below the ERH, it is the solid salt that exists in equilibrium.

If the RH is then raised again, the salt will pick up water vapour from the air when the ERH is reached, forming a saturated solution. It will continue to do so as the RH is raised higher, the solution becoming ever more dilute.

This behaviour is depicted in Figs 2.1 and 2.2 for the case of sodium chloride (ERH 75% at 20°C), and a worked example is given in Price (1996).

The situation is slightly more complicated if the salt can exist in both anhydrous and hydrated forms. If such a salt is exposed to gradually increasing RH, conversion to the hydrate will take place at a particular RH, with the absorption of a set amount of water. No further absorption will take place until the ERH of the hydrate is reached, at which point the hydrate will start to dissolve. An example is given in Fig. 2.3, for the system $Na_2SO_4 + 10H_2O \leftrightharpoons Na_2SO_4 \cdot 10H_2O$.

It should now be clear how salt damage may be avoided. If the ambient RH is held permanently above or below the ERH, then no crystallisation or dissolution can occur. The salt will remain either permanently in the solid state, or permanently in solution, and crystallisation damage is averted. Similarly, provided the ambient RH is held within a range that excludes the RHs at which any hydration changes occur, then hydration damage is also avoided.

If only it were so easy. Whilst salt damage would still occur in situations where control of the ambient RH was impracticable, damage in museums, for example, could be avoided in a straightforward manner, and there would be no need for the research described in this report. Sadly, it is not so easy. Contamination with a single salt is rare, and it is usual for objects and monuments to be contaminated with a mixture of salts. Predicting the behaviour of salt mixtures is much more difficult.

What is needed, for any given combination of ions, is a means of determining which

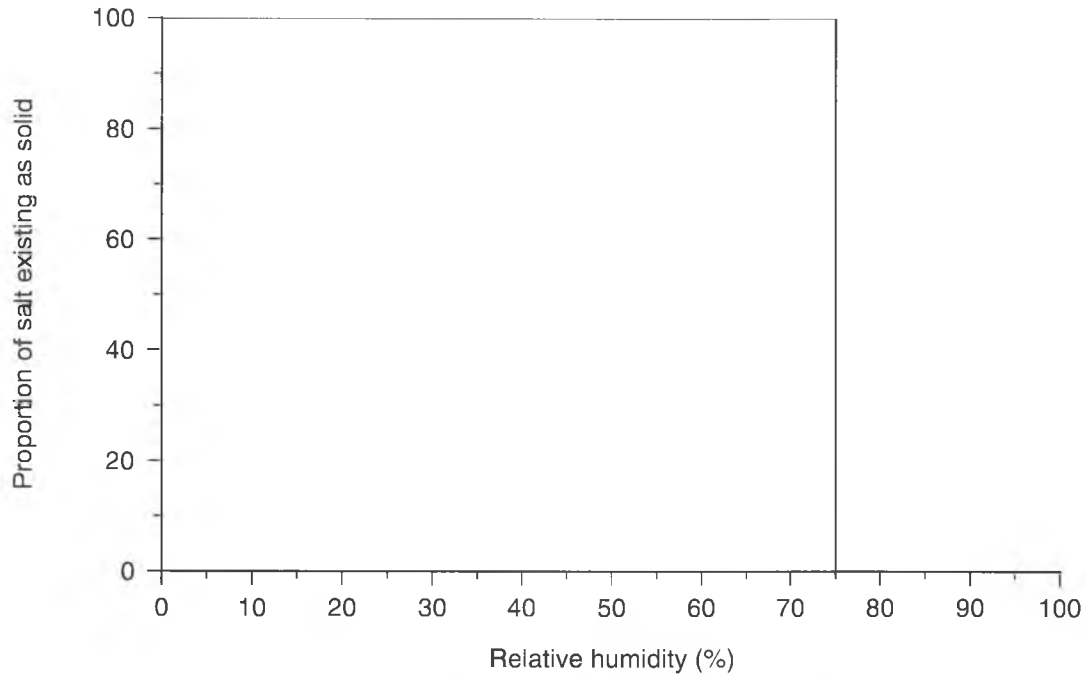

Figure 2.2: Proportion of sodium chloride existing in the solid state (%).

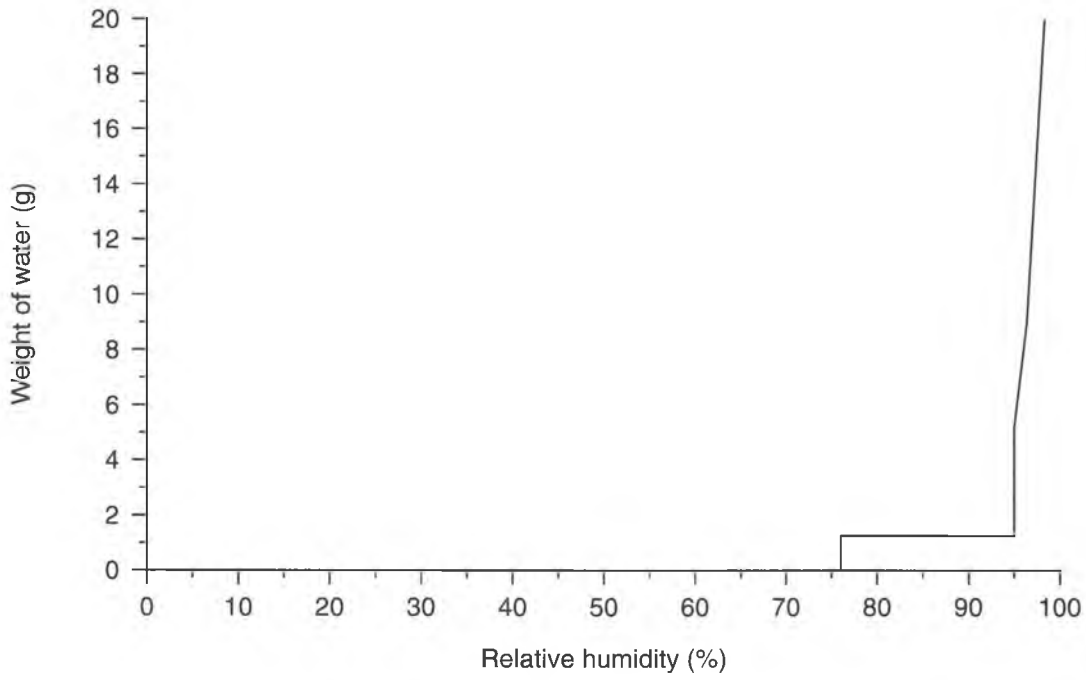

Figure 2.3: The weight of water picked up from the air by 1g sodium sulfate at 20°C. The hydrate is the stable form between 76 and 95% RH; above 95% (the ERH), the hydrate dissolves.

solid minerals will be present at any given relative humidity. Moreover, we need to know the volume occupied by those minerals. We should then be able to construct a curve, comparable to that of Fig. 2.2, which would indicate those ranges of relative humidity at which large volume increases occurred. By avoiding those ranges, damage due to crystal growth should be minimised, if not prevented altogether.

This was the fundamental objective of the research that is described in this report. Essentially, the issues are the same as those in the case of the single salt: the physical presence of ions restricting the escape of water molecules, and forces between ions and water molecules (whether between molecules and ions, between molecules and molecules, or between ions and ions) further reducing the vapour pressure and determining the point at which specific minerals crystallise out of solution. In the case of the single salt, the ERH could be determined experimentally; in the case of salt mixtures, the RH of air in equilibrium with any given system can also be measured experimentally, but it is wholly impracticable to make measurements on every possible combination that might ever be encountered. An alternative approach is required, based on modelling.

2.3.2 Predictive models

Attempts have been made over many years to model the behaviour of salt solutions. One of the earliest, and one of the most influential, was that of Debye & Hückel (1923). The model assumed that the solution was very dilute, and that all the ions were uniformly charged hard spheres of the same diameter. Deviations from ideal behaviour were attributed to long-range electrostatic attractions and repulsions between ions. Short-range interactions could be excluded on the grounds of high dilution. The model's predictions proved to be very reliable, its main limitation being that it applied only to what was sometimes uncharitably described as slightly contaminated distilled water. A further development was made in 1926 by Bjerrum, who introduced the concept of ion-pairs linked by short-range forces. In 1935, Guggenheim proposed that interactions that were not attributable to electrostatic forces could be described by a single ion-ion term for each existing ion combination (Fletcher 1993). His approach was developed further by Pitzer (1973), who allowed *inter alia* for short-range interactions between clumps of three ions. These refinements allowed the model to be applied to saturated solutions, which is essential for the prediction of crystallisation behaviour.

During the past decade the Pitzer model has achieved wide acceptance (see the review of Clegg & Whitfield 1991), and has been applied in a number of important areas in the chemistry of the natural environment, of which the equilibria of concentrated brines with deposited salts (Clegg & Whitfield 1991; Harvie *et al.* 1984; Spencer *et al.* 1990) and the solubility of atmospheric gases (Clegg & Brimblecombe 1990) are most similar to the salt-damage problem. The relevance of the model to the preventive conservation of salt-contaminated materials has been demonstrated by Price & Brimblecombe (1994), Steiger & Dannecker (1995) and Steiger & Zeunert (1996).

It is Pitzer's model that forms the basis for the research described in this report. The equations that constitute the model are formidable on first sight, and include a number of coefficients that represent the interactions between ions. The coefficients fall into two categories: single salt parameters (giving cation-anion interactions) and mixture parameters (a two-ion term for cation-cation or anion-anion interactions, and a three-ion term for interactions between two cations and an anion, or two anions and a cation). The parameters have to be determined experimentally (for example, by

measurement of solubility, vapour pressure and osmotic pressure), and the process of fitting the experimental data to the theoretical equations is known as parameterisation.

At the outset of the project, some parameters were available in the literature, but many more had to be determined in order to describe the range of salts likely to be encountered in monuments and museum artefacts. Some, but not all, of the necessary experimental data were obtainable from the literature, and a major programme of further measurements had to be undertaken by Steiger at the University of Hamburg (see Chapter 4). Evaluation of data and subsequent parameterisation was undertaken by Steiger and by Clegg, Brimblecombe and Reeves at the University of East Anglia (Chapters 5, 7 and 8).

2.3.3 Limitations

Whilst the Pitzer model provides a powerful tool for predicting the equilibrium behaviour of mixed salt solutions, there are some limitations that have to be taken into account in applying it to the prevention of salt damage. These fall into two categories: those relating to non-equilibrium conditions, and practical limitations of sampling and salt analysis.

Non-equilibrium conditions

The predictions of the Pitzer model, and consequently those of the ECOS program described in this report, assume that the whole of the salt system is in equilibrium with its surroundings at all times. However, this will not necessarily be the case in practice. For example, using humidity-controlled X-ray diffraction, Steiger *et al.* demonstrated that hydration of thenardite and crystallisation of the system Na^+–K^+–Mg^{2+}–NO_3^-–SO_4^{2-}–H_2O did not always occur under the predicted conditions. Further details are given in section 4.5.

One of the issues that needs to be addressed is the *rate* at which equilibrium is achieved. How fast will salt-contaminated masonry, or an object in a museum, respond to changes in ambient humidity? Will a wall-painting in a church, for example, be damaged by the humidity changes caused by the congregation attending a service? Are diurnal changes important? Or is it only seasonal changes that will have any major effect?

There is no doubt that phase transitions can take place within a matter of hours, or even minutes. This has been clearly demonstrated by the laboratory experiments of Charola & Weber (1992), Piqué *et al.* (1992) and Heritage (1995). It is less clear, however, how quickly the salts respond when they are constrained by the thermal and hygric mass of the porous matrix that surrounds them. Arnold & Zehnder (1991), for example, observed seasonal changes in the efflorescence occurring on wall paintings in the convent church of Müstair in Switzerland.

There are many factors contributing to the kinetics of crystal growth, including the composition of the salt mixture and the degree of disparity between the ambient conditions and equilibrium conditions Sawdy (1995), air movement Heritage (1995), and the characteristics of the porous matrix Piqué *et al.* (1992). It is an area that is attracting increasing levels of research, but the results are unlikely to influence the practical application of the ECOS program. ECOS will continue to predict optimal environmental conditions, irrespective of kinetics. If the rates of crystal growth prove to be slow in certain cases, then the object or monument in question will be more tolerant

to short-term fluctuations of temperature and RH than would otherwise have been the case. Appropriate environmental control becomes that much easier to achieve. On the other hand, Steiger's preliminary work (section 4.5), albeit under laboratory conditions, suggests that critical relative humidities predicted by the equilibrium model might be more realistically interpreted as upper limits.

A second non-equilibrium condition relates to the fractionation that may occur during the crystallisation process. When a porous material containing a mixed-salt solution starts to dry, the least soluble salts will crystallise first and may well be deposited at the interface between the solution and the surrounding air. The meniscus of the remaining salt solution may then recede further into the material, leaving behind the deposited crystals. These crystals are effectively removed from the salt solution, which is no longer properly described by the initial ionic concentrations.[2] A comparable problem arises during the wetting cycle. If the salt crystals are isolated from one another, they will not represent a single system, as assumed by the thermodynamic model. Instead, moisture will be picked up first by those crystals with the lowest ERH. The resulting solution may then spread to neighbouring crystals, which are thus gradually brought back into the system. The situation may become even more complicated when the ambient RH fluctuates within the range in which both liquid and solid are present.

This is an intractable problem that is not directly addressed by ECOS. Nonetheless, the program may be used to determine the ERHs of those minerals that are deposited during the drying cycle, and to investigate the behaviour of the systems that remain after the removal of the least soluble salts.

A third situation that may be difficult to describe with ECOS is the one presented by penetrating or rising dampness. Here, the moisture content of the system will not be attributable only to water vapour taken up from the air. The system may be further complicated by a steady supply of salts from the soil and, in some circumstances, by the loss of efflorescences from the surface of the wall. The interpretation of ECOS predictions will need to be undertaken judiciously under such circumstances, as will the implementation of environmental controls. A low ambient RH, deliberately maintained with the intention of avoiding crystallisation cycles, may simply serve to promote evaporation, thereby exacerbating the rising damp and causing an ever increasing deposition of salts.

Practical limitations

Any thermodynamic model of salt solutions assumes that the composition of the solution is known exactly. This may not be the case in practice, since full analysis of the soluble salts present in an object or monument is seldom practicable, and analytical techniques are seldom 100% accurate.

The problem of ionic imbalance in the analytical data is explicitly addressed by ECOS, and is described in Chapter 10. However, a further problem arises in ensuring that the samples taken for analysis are representative of the salt solution present in the porous material. This is, in part, a statistical problem, and sufficient samples must be taken from the object or (particularly) from the monument to ensure that they are representative of the whole. A more difficult problem arises in determining both how and when the samples should be taken.

[2] This will present a problem only in those cases where the crystals that are first deposited are redissolved under equilibrium conditions at lower RHs.

It is common practice for conservation scientists to scrape samples of efflorescence off the surface of a wall or an object, or to drill holes into the wall and analyse the resulting powder for soluble salts. Scraping off the efflorescence has the dual advantage of being simple and non-destructive, but there can be no assurance that the sample so obtained is in any way representative of the salts remaining in the wall. Indeed, it may be expected that the remaining salts, whether in solution or deposited as subflorescence, will differ markedly from the salt(s) that have effloresced (*cf.* the discussion of fractionation, above). Moreover, the efflorescence may be present at some times of year but not at others. Theoretically, one might argue that the appropriate sample should consist both of any efflorescence and of the soluble salts contained in the equivalent area of stone beneath it. But how deep should one drill? To what depth will the salts be affected by environmental conditions at the surface? Relatively little is known about the spatial distribution of salts within stone, and no firm answer can yet be given to these questions. Users of ECOS may wish to examine the sensitivity of its predictions to variations in the input data, as part of their overall appraisal of optimal environmental conditions.

2.4 References

ARNOLD, A. & K. ZEHNDER 1991. 'Monitoring wall paintings affected by soluble salts.' *In* S. Cather (ed.), *The Conservation of Wall Paintings*, pp. 103–136. Getty Conservation Institute, Los Angeles.

CHAROLA, A. E. & J. WEBER 1992. 'The hydration and deterioration mechanism of sodium sulfate.' *In* J. Delagado Rodrigues, F. Henriques & F. Telmo Jeremias (eds.), *7th International Congress on Deterioration and Conservation of Stone*, pp. 581–90. Laboratório Nacional de Engenharia Civil, Lisbon.

CLEGG, S. L. & P. BRIMBLECOMBE 1990. *In* D. C. Melchior & R. L. Bassett (eds.), *Chemical Modelling in Aqueous Systems II*, p. 58. American Chemical Society, Washington.

CLEGG, S. L. & M. WHITFIELD 1991. *In* K. S. Pitzer (ed.), *Activity Coefficients in Electrolyte Solutions*, pp. 279–434. CRC Press, Boca Raton.

CORRENS, C. W. 1949. 'Growth and dissolution of crystals under linear pressure.' *Discussions of the Faraday Society* 5: 267–271.

DEBYE, P. & E. HÜCKEL 1923. 'The theory of electrolytes I. Lowering of freezing point and related phenomena.' *Zeitschr. Physik* 24: 185–206.

EVANS, I. S. 1970. 'Salt crystallisation and rock weathering: a review.' *Revue du Géomorphologie Dynamique* 19: 155–177.

FLETCHER, P. 1993. *Chemical Thermodynamics for Earth Scientists.* Longman Scientific & Technical, Harlow.

GOUDIE, A. S. & H. VILES 1997. *Salt weathering hazards.* Wiley, Chichester.

HARVIE, C. E., N. MOLLER & J. H. WEARE 1984. *Geochim. Cosmochim. Acta* 48: 723–751.

HERITAGE, A. 1995. *Imaging dynamic processes in conservation; time- lapse video-microscopy and on-line date annotation.* Master's thesis, Conservation of Wall Painting Department, Courtauld Institute of Art, University of London.

PIQUÉ, F., L. DEI & E. FERRONI 1992. 'Physicochemical aspects of the deliquescence of calcium nitrate and its implications for wallpainting conservation.' *Studies in Conservation* 37: 217–227.

PITZER, K. S. 1973. 'Thermodynamics of electrolytes, I. Theoretical basis and general equations.' *J. Phys. Chem.* 77: 268–277.

PRICE, C. A. 1996. 'Salt damage in monuments, and means of control.' *In* J. Beavis. & K. Barker (eds.), *Science and Site: Evaluation and Conservation*, pp. 229–237. Bournemouth University School of Conservation Sciences, Bournemouth.

PRICE, C. A. & P. BRIMBLECOMBE 1994. 'Preventing salt damage in porous materials.' In *Preventive Conservation: Practice, Theory and Research*, pp. 90–93. International Institute for Conservation, London.

RODRIGUEZ-NAVARRO, C. & E. DOEHNE 1999. 'Salt weathering: influence of evaporation rate, supersaturation and crystallization pattern.' *Earth Surface Processes and Landforms* 24(9): 191–209.

SAWDY, A. 1995. *The kinetics of crystallisation and deliquescence of some soluble salts found in wall paintings.* Master's thesis, Conservation of Wall Painting Department, Courtauld Institute of Art, University of London.

SCHERER, G. W. 1999. 'Crystallization in pores.' *Cement and Concrete Research* 29: 1347–58.

SPENCER, R. J., N. MOLLER & J. H. WEARE 1990. *Geochim. et Cosmochim. Acta* 54: 575–590.

STEIGER, M. & W. DANNECKER 1995. *In* R. Snethlage (ed.), *Jahresberichte aus dem Forschungsprogramm Steinzerfall – Steinkonservierung Band 5 — 1993.* Ernst & Sohn, Berlin.

STEIGER, M. & A. ZEUNERT 1996. *In* J. Riederer (ed.), *Proc 8th Int Congress on Deterioration and Conservation of Stone*, pp. 535–544. Müller Druck und Verlag GmbH, Berlin.

$$K_{MX} = m_M^{\nu_M} \cdot m_X^{\nu_X} \cdot \gamma_M^{\nu_M} \cdot \gamma_X^{\nu_X} \cdot a_w^{z}$$

3

Pitzer Model of Electrolyte Solutions

S. L. Clegg and P. Brimblecombe

School of Environmental Studies, University of East Anglia

3.1 Thermodynamic relations

The central purpose of the model of the equilibrium crystallisation behaviour of mixed salt solutions is the determination of the solubility of each mineral phase concerned as a function of solution composition, relative humidity and temperature. For the hypothetic solid $M\nu_M X\nu_X \cdot z\mathrm{H_2O}$, consisting of ν_M cations M, ν_X anions X and z waters of crystallisation, the equilibrium constant governing solubility, termed the solubility product, K_{MX}, is denoted by:

$$\ln(K_{MX}) = \nu_M \ln(m_M) + \nu_X \ln(m_X) + \nu_M \ln(\gamma_M) + \nu_X \ln(\gamma_X) + z \ln(a_w) \tag{3.1}$$

where m_M and m_X are the ion molalities, γ_M and γ_X are the activity coefficients of the cation and anion, and a_w is the water activity of the solution.

Additionally, such a model needs to describe the relative humidity at which the mixed salt solution becomes saturated with respect to the various solids. This requires an understanding of the liquid-vapour phase equilibrium of the water. At equilibrium the chemical potential of liquid water, $\mu_{w,l}$ is equal to that of water vapour, $\mu_{w,v}$. Assuming ideal gas behaviour for the water vapour, this can be written as:

$$\mu_{w,l} = \mu^o_{w,l} + RT \ln(a_w) = \mu_{w,v} = \mu^o_{w,v} + RT \ln(p_w/p^o_w) \tag{3.2}$$

where R is the gas constant, T is the absolute temperature, and p_w and p^o_w are the partial pressure and saturated vapour pressure of water at temperature T. The quantities $\mu^o_{w,l}$ and $\mu^o_{w,v}$ are the standard chemical potential for water in the liquid and vapour phases respectively, and are thus equal, giving overall:

$$a_w = p_w/p^o_w = \mathrm{RH} \tag{3.3}$$

Thus, at equilibrium, the relative humidity (RH) equals the activity of liquid water (a_w), which in turn can related to another important solution property, the osmotic coefficient, via the following definition:

$$\ln(a_w) = -\phi(M_w/1000) \sum_i (m_i) \tag{3.4}$$

where M_w is the molecular mass of water and m_i is the molality of ion I.

From the preceding discussion it is apparent that the prediction of the solubility and vapour equilibria of mixed electrolyte solutions by the thermodynamic model requires knowledge of the activity coefficients of the ionic components together with either the activity coefficient of the water or the osmotic coefficient. Standard definitions and thermodynamic transformations can be used to derive these important quantities from the excess Gibbs free energy (G^{ex}) of the solution (*i.e.*, the Gibbs energy that is in excess of that due to an ideal solution of identical composition):

$$\ln(\gamma_i) = [\partial(G^{ex}/n_w RT)/\partial m_i]_{n_w}$$
$$\phi - 1 = -(G^{ex}/\partial n_w)_{n_i}/RT \sum_i m_i \tag{3.5}$$

where n_w is the number of kg of water and n_i is the number of moles of species I.

The basis of the thermodynamic model for the prediction of salt damage in porous materials is the Pitzer model of mixed electrolyte solutions. Central to the Pitzer model is an expression for G^{ex} in terms of ion molalities and empirically determined interaction parameters, from which can be obtained the activity coefficients of all solute species and the osmotic coefficient. Expressed in this way the equations for excess Gibbs energy (G^{ex}), activity coefficients γ_M and γ_X of arbitrary cation M and anion X, and the osmotic coefficient (ϕ) are:

$$\begin{aligned} G^{ex}/(n_w RT) = &-(4A_\phi I/1.2)\ln(1+1.2\sqrt{I}) \\ &+ \sum_c \sum_a m_c m_a (2B_{ca} + ZC^T_{ca}) \\ &+ \sum_{c<c'} \sum m_c m_{c'} [2\Phi_{cc'} + \sum_a m_a \psi_{cc'a}] \\ &+ \sum_{a<a'} \sum m_a m_{a'} [2\Phi_{aa'} + \sum_c m_c \psi_{caa'}] \end{aligned} \tag{3.6}$$

$$\begin{aligned} \ln(\gamma_M) = &\, z_M^2 F + \sum_a m_a (2B_{Ma} + ZC^T_{Ma}) + \sum_c m_c (2\Phi_{Mc} + \sum_a m_a \psi_{Mca}) \\ &+ \sum_{a<a'} \sum m_a m_{a'} \psi_{Maa'} + z_M \sum_c \sum_a m_c m_a C^T_{ca} \end{aligned} \tag{3.7}$$

$$\begin{aligned} \ln(\gamma_X) = &\, z_X^2 F + \sum_c m_c (2B_{cX} + ZC^T_{cX}) + \sum_a m_a (2\Phi_{Xa} + \sum_c m_c \psi_{Xac}) \\ &+ \sum_{c<c'} \sum m_c m_{c'} \psi_{Xcc'} + |z_X| \sum_c \sum_a m_c m_a C^T_{ca} \end{aligned} \tag{3.8}$$

$$\begin{aligned} \phi - 1 = &\, (2/\sum_i m_i)[-A_\phi I^{3/2}/(1+1.2\sqrt{I}) + \sum_c \sum_a m_c m_a (B^\phi_{ca} + ZC^{T\phi}_{ca}) \\ &+ \sum_{c<c'} \sum m_c m_{c'} (\Phi^\phi_{cc'} + \sum_a m_a \psi_{cc'a}) \\ &+ \sum_{a<a'} \sum m_a m_{a'} (\Phi^\phi_{aa'} + \sum_c m_c \psi_{aa'c})] \end{aligned} \tag{3.9}$$

Function F in equations 3.7 and 3.8 is given by:

$$\begin{aligned} F = &-A_\phi [\sqrt{I}/(1+1.2\sqrt{I}) + (2/1.2)\ln(1+1.2\sqrt{I})] \\ &+ \sum_c \sum_a m_c m_a (B'_{ca} + ZC^{T'}_{ca}/2) \\ &+ \sum_{c<c'} \sum m_c m_{c'} \Phi'_{cc'} + \sum_{a<a'} \sum m_a m_{a'} \Phi'_{aa'} \end{aligned} \tag{3.10}$$

In these equations the summations $c < c'$ and $a < a'$ are over all distinguishable pairs of cations (c) and anions (a) respectively. The Φ and ψ terms are ternary parameters representing two particle interactions (two non-identical cations or anions) and three particle interactions (two non-identical cations plus an anion, or two non-identical anions plus a cation). The A_ϕ term is the Debye-Hückel coefficient of Archer & Wang (1990). In the present model A_ϕ is obtained using a polynomial curve fit to the Archer and Wang values for temperatures >273.15K, and determined using an empirical extrapolation in the temperature range 234.15–273.15K (Clegg & Brimblecombe 1995). The above equations (3.6–3.10) contain the following functions:

$$Z = \sum_i m_i |z_i| \tag{3.11}$$

$$B_{ca} = \beta^{(0)}_{ca} + \beta^{(1)}_{ca} g(\alpha_{1_{ca}}\sqrt{I}) + \beta^{(2)}_{ca} g(\alpha_{2ca}\sqrt{I}) \tag{3.12}$$

$$B'_{ca} = \beta^{(1)}_{ca} g'(\alpha_{1_{ca}}\sqrt{I})/I + \beta^{(2)}_{ca} g'(\alpha_{2_{ca}}\sqrt{I})/I \tag{3.13}$$

$$B^{\phi}_{ca} = \beta^{(0)}_{ca} + \beta^{(1)}_{ca} \exp(-\alpha_{1_{ca}}\sqrt{I}) + \beta(2)_{ca} \exp(-\alpha_{2_{ca}}\sqrt{I}) \tag{3.14}$$

$$C^{T}_{ca} = C^{(0)}_{ca} + 4C^{(1)}_{ca} h(\omega_{ca}\sqrt{I}) \tag{3.15}$$

$$C^{T'}_{ca} = 4C^{(1)}_{ca} h'(\omega_{ca}\sqrt{I})/I \tag{3.16}$$

$$C^{T\phi}_{ca} = C^{(0)}_{ca} + C^{(1)}_{ca} \exp(-\omega_{ca}\sqrt{I}) \tag{3.17}$$

where z_i represents the charge of ion i. $\beta^{(0)}_{ca}$, $\beta^{(1)}_{ca}$, $C^{(0)}_{ca}$, and $C^{(1)}_{ca}$ are binary parameters representing the interaction between the cation and anion of a pure single salt — where $C^{(i)}_{ca} = C^{(i)\phi}_{ca}/(2|z_M z_X|^{1/2})$. Symbols α_1 and ω are arbitrary constants, which for most salts usually take the value 2.0 $\mathrm{kg}^{1/2}\mathrm{mol}^{-1/2}$ and 2.5$\mathrm{kg}^{1/2}\mathrm{mol}^{-1/2}$ respectively. The constant α_2 is only used for divalent-divalent salts such as $MgSO_4$ in order to account for the existence of strong ion pairing, for which the value 12.0$\mathrm{kg}^{1/2}\mathrm{mol}^{-1/2}$ is used, together with an adjusted value for the α_1 of 1.4$\mathrm{kg}^{1/2}\mathrm{mol}^{-1/2}$. The above also contain the functions $g(x)$ and $h(x)$, and their derivatives, which are given by the following functions:

$$g(x) = 2[1 - (1 + x)\exp(-x)]/x^2 \tag{3.18}$$

$$g'(x) = \exp(-x) - g(x) \tag{3.19}$$

$$h(x) = (6 - (6 + x(6 + 3x + x^2))\exp(-x))/x^4 \tag{3.20}$$

$$h'(x) = \exp(-x)/2 - 2h(x) \tag{3.21}$$

Other functions for the standard Pitzer model involve interactions between pairs of ions (i, j) of like sign:

$$\Phi_{ij} = \theta_{ij} + \theta^{E}_{ij}(I) \tag{3.22}$$

$$\Phi'_{ij} = \theta^{E'}_{ij}(I) \tag{3.23}$$

$$\Phi^{\phi}_{ij} = \theta_{ij} + \theta^{E}_{ij}(I) + I\theta^{E'}_{ij}(I) \tag{3.24}$$

The value of the unsymmetrical mixing term $\theta^{E}_{ij}(I)$ and its derivative are obtained from theory (Pitzer 1975) and are equal to zero where the charges on ions i and j are equal in magnitude.

The complete Pitzer model equations given above contain a number of empirical parameters that are not given by theory, but whose values are obtained by fitting to experimental data.

3.2 Pure aqueous solutions

The binary interaction parameters $\beta_{ca}^{(0)}$, $\beta_{ca}^{(1)}$, $\beta_{ca}^{(2)}$, $C_{ca}^{(0)}$, and $C_{ca}^{(1)}$, are obtained by fitting to thermodynamic data (actvities and osmotic coefficients) for pure aqueous solutions of single salts. Values of these parameters at 298.15K have previously been obtained for a large number of pure salts by direct fitting to osmotic coefficient and activities (see Pitzer 1991). Furthermore, the variation of the binary parameters with temperature can be obtained by fitting to relevant thermochemical data for the pure salt solutions, since enthalpy and heat capacity can be derived from the Gibbs energy by taking appropriate derivatives.

For the enthalpy, generally the apparent relative molal enthalpy ${}^{\phi}L$, we can make use of the well known Gibbs-Helmholtz equation, thus:

$$\begin{aligned} L &= -T^2[\partial G^{ex}/T)/\partial T]_{P,m} \\ {}^{\phi}L &= L/n_2 \end{aligned} \tag{3.25}$$

where L is the relative enthalpy, P is the pressure and n_2 is the number of moles of solute.

If the derivative indicated in equation 3.25 is applied to the equation for excess Gibbs energy 3.6, neglecting mixture terms because we are dealing with a single salt, we obtain:

$$\begin{aligned} {}^{\phi}L =& \nu|z_M z_X|(A_L/2b)\ln(1+b\sqrt{I}) \\ & - 2\nu_M\nu_X RT^2[mB_{MX}^L + m^2(\nu_M z_M)C_{MX}^L] \end{aligned} \tag{3.26}$$

where b is the constant from the extended Debye-Hückel Law, ν is the total stoichiometric number of ions in salt MX, and m the salt molality. The above equation also contains a variety of temperature derivatives:

$$A_L/RT = 4T(\partial A_\phi/\partial T)_P \tag{3.27}$$

and

$$\begin{aligned} B_{MX}^L &= (\partial B_{MX}/\partial T)_{P,I} \\ &= \beta^{(0)L} + \beta^{(1)L}g(\alpha_1\sqrt{I}) + \beta^{(2)L}g(\alpha_2\sqrt{I}) \end{aligned} \tag{3.28}$$

$$\beta^{(i)L} = (\partial\beta^{(i)}/\partial T)_P \qquad i = 0,1,2 \tag{3.29}$$

and similarly for C_{MX}

$$\begin{aligned} C_{MX}^L &= (\partial C_{MX}/\partial T)_{P,I} \\ &= C^{(0)L} + C^{(1)L}h(\omega\sqrt{I}) \end{aligned} \tag{3.30}$$

$$C^{(i)L} = (\partial C^{(i)}/\partial T)_P \qquad i = 0,1 \tag{3.31}$$

B_{MX}^L and C_{MX}^L can be obtained by fitting to experimental data for heats of dilution, or tabulated data for ${}^{\phi}L$. From these values equations 3.29 and 3.31 then yield the first temperature derivatives for the binary parameters. The second derivatives are readily obtainable from the apparent molal heat capacity, which is defined as:

$${}^{\phi}C_P = C_{P_2}^o + (\partial^{\phi}L/\partial T)_{P,m} \tag{3.32}$$

where $C^o_{P_2}$ is the infinite dilution heat capacity.

Performing the differentiation indicated above we obtain:

$$\begin{aligned} {}^{\phi}C_P = C^o_{P_2} &+ \nu|z_M z_X|(A_J/2b)\ln(1+b\sqrt{I}) \\ &- 2\nu_M\nu_X RT^2[mB^J_{MX} + m^2(\nu_M z_M)C^J_{MX}] \end{aligned} \tag{3.33}$$

where:

$$A_J = (\partial A_L/\partial T)_P \tag{3.34}$$

$$B^J_{MX} = (\partial^2 B_{MX}/\partial T^2)_{P,I} + (2/T)(\partial B_{MX}/\partial T)_{P,I} \tag{3.35}$$

$$C^J_{MX} = (\partial^2 C_{MX}/\partial T^2)_{P,I} + (2/T)(\partial C_{MX}/\partial T)_{P,I} \tag{3.36}$$

Fitting to apparent molal heat capacity data allows the determination of B^J_{MX} and C^J_{MX}, which combined with the first temperature derivatives derived from 3.29 and 3.29, permit the calculation of the second temperature derivatives of the binary parameters. These may be utilised in a Taylor expansion for the variation of the $\beta^{(i)}$ and $C^{(i)}$ over an extended temperature range:

$$\begin{aligned} P^{(i)}(T) = P^{(i)}_{298.15\mathrm{K}} &+ (\partial P^{(i)}/\partial T)(T-298.15) \\ &+ 1/2(\partial^2 P^{(i)}/\partial T^2)(T-298.15)^2 \\ &+ 1/6(\partial^3 P^{(i)}/\partial T^3)(T-298.15)^3 \\ &+ 1/24(\partial^4 P^{(i)}/\partial T^4)(T-298.15)^4 + \ldots \end{aligned} \tag{3.37}$$

where $P^{(i)}$ represents any $\beta^{(i)}$ or $C^{(i)}$.

3.3 Mixed aqueous solutions

The ternary interaction parameters θ_{ij} and $\psi_{ii'j}$ are here obtained by direct fitting to solubility data for ternary (three ion) salt mixtures over a range of temperatures. The form of the fitting equation adopted for this procedure is:

$$P(T) = a + b/T + cT \tag{3.38}$$

where $P(T)$ represents either θ_{ij} or $\psi_{ii'j}$ at arbitrary temperature T.

Ternary data other than solubility are neglected in the above fitting process, as the primary aim of the present model is the calculation of solubilities for mixed salt solutions. Data for quaternary (four ion) or higher mixtures are not required for the parameterisation of the model, as experience has shown that the modelling of the thermodynamic properties of multicomponent electrolyte mixtures only requires two or three particle interactions. An important feature of these ternary parameters is that the θ_{ij} parameter must be transferrable between all mixtures that contain a given pair of ions, i and j: the $\theta_{\mathrm{Na,K}}$ parameter, for example, having the same value in the Na–K–Cl ternary system as in Na–K-NO_3 and Na–K–SO_4. This is in contrast to the ψ_{ijk} parameter, which has a unique value for each ternary.

3.4 References

Archer, D. G. & P. Wang 1990. *J. Phys. Chem. Ref. Data* 19: 378–411.

Clegg, S. L. & P. Brimblecombe 1995. 'Application of a multicomponent thermodynamic model to activities and thermal properties of 0–40 mol kg^{-1} aqueous sulphuric acid from <200 K to 328 K.' *J. Chem. Eng. Data* 40: 43–64.

Pitzer, K. S. 1975. 'Thermodynamics of electrolytes V: effects of higher order electrostatic terms.' *J. Soln. Chem.* 4: 249–265.

Pitzer, K. S. 1991. *In* K. S. Pitzer (ed.), *Activity Coefficients in Electrolyte Solutions*, pp. 75–154. CRC Press, Boca Raton.

4
Data Compilation and Experimental Determinations

Michael Steiger, Roland Beyer, Joachim Dorn and Anke Zeunert
Institut für Anorganische und Angewandte Chemie, Universität Hamburg

4.1 Introduction

The Pitzer model is a semi-empirical model, *i.e.*, the form of the ion interaction equations arises from theoretical considerations while there remain empirical parameters which have to be determined from experimental data. Values of these parameters are obtained by fitting thermodynamic data of binary and common ion ternary data. These thermodynamic data are preferably taken from the published literature. In cases, however, where the data required are not available, additional measurements may be necessary. This chapter describes the compilation of literature data and the additional experimental work that was necessary to allow for the parameterisation of the Pitzer model including as many ions as possible. Additional experimental work using dynamic diffractometry was carried out to study phase equilibria and the kinetics of phase transformations.

4.2 Compilation of thermodynamic data

4.2.1 Water activities in binary solutions

A literature search on thermodynamic data for binary salt solutions revealed deficits of the data required for the parameterisation of the ion interaction model. Substantial gaps were found for nearly all of the organic salts relevant to the project, whilst the amount of data proved to be sufficient for the parameterisation of the inorganic salts (see Chapter 7). Hence, there was a need to perform new measurements of the water activity of single salt solutions of acetate, formates, and oxalates. These measurements are discussed below.

4.2.2 Salt solubilities in ternary systems

The thermodynamic model of mixed salt solutions requires the parameterisation of ternary interaction parameters (see Chapter 3). Different types of experimental data including solubility, vapour pressure, and freezing points may be used to fit the ternary parameters. Since the main objective of this project is the calculation of solubility equilibria in mixed solutions major emphasis was given to the compilation of existing solubility data in the literature. Based on this compilation gaps in the existing data and the extent of additional solubility measurements were identified.

Early during the course of the project the partners agreed upon the following priority list of ions to be included into the thermodynamic treatment of mixed salt systems:

priority 1: Na^+, K^+, Mg^{2+}, Ca^{2+}, Cl^-, NO_3^-, SO_4^{2-}
priority 2: priority 1 ions plus HCO_3^-, CO_3^{2-}, OH^-, NH_4^+, H^+
priority 3: priority 1 and 2 ions plus oxalate, acetate and formate

The ions of the priority 1 system are by far the most important constituents of salt systems in historic building materials and form a base set which has to be treated with high priority. It is expected that the priority 1 ions will be sufficient in most practical situations at historic monuments to adequately describe the crystallisation from mixed pore solutions. The ions of the priority 2 subset were selected as it is known that they are sometimes, though not always, present in historic stonework. Finally, much less is known about the relevance of the organic ions forming the priority 3 subsystem.

A literature compilation of solubility data including all inorganic and organic ions mentioned above was completed. Tables 4.1 and 4.2 provide a summary of the available solubility data. Though it cannot be ruled out that some sources of data have been overlooked, the final database can be regarded as being quite comprehensive. To a large extent the data were collected from existing compilations (*e.g.,* D'Ans 1933; Linke 1965; Silcock 1979). In many cases, however, it proved necessary to use the original sources of data to check for inconsistent or missing data, and typographic errors. Finally, the database was updated including the more recent literature. The references used to construct the literature database of solubilities are listed in the Appendix (Section 4.7 starting on page 38).

The concentrations given in the original sources were recalculated in units of molality. To test consistency and reliability of the literature data they were evaluated graphically and were checked for outliers, typographic errors *etc.* Individual data points were given preliminary weights. This procedure is illustrated in Figures 4.1 and 4.2. Based on solubility isotherms as those depicted in Figure 4.1 the data were first checked for gross outliers. Such outliers were then checked for typographic errors both in our data files and in the original tables. The assigned weights are based on the consistency of solubility isotherms at various temperatures (see Figure 4.1) and from plots similar to Figure 4.2 which depicts the temperature dependence of the univariant equilibria, hence the molalities of solutions saturated with two salts. The systems completed were passed to the University of East Anglia group where they were used to fit the ternary model parameters (see Chapter 7).

It can be seen from Tables 4.1 and 4.2 that the solubility database is essentially complete for the priority 1 systems. Also, in most systems the data are of sufficient quality and cover the whole temperature range of interest. Less data are available for some systems including nitrate and in some cases the available data do not extend to temperatures far from room temperature, or, the quality of the data suffers from inconsistencies and scatter making the assignment of weights sometimes difficult. However, there was only one priority 1 system, the Na^+–Ca^{2+}–NO_3^-–H_2O system, for which additional solubility measurements were deemed necessary. These measurements are discussed below.

Also, for most of the priority 2 systems the database is sufficient, considering the fact that some of the systems can be neglected because they are clearly not relevant to the properties of salt mixtures in stonework; *e.g.,* for obvious reasons, large concentrations of ammonium (NH_4^+) and carbonate/bicarbonate (CO_3^{2-}–HCO_3^-) can never be present at the same time.

It can be also seen from Tables 4.1 and 4.2, however, that there are substantial gaps in the solubility database regarding the organic (priority 3) salts. When planning this project it was expected that there would be a comparable amount of solubility

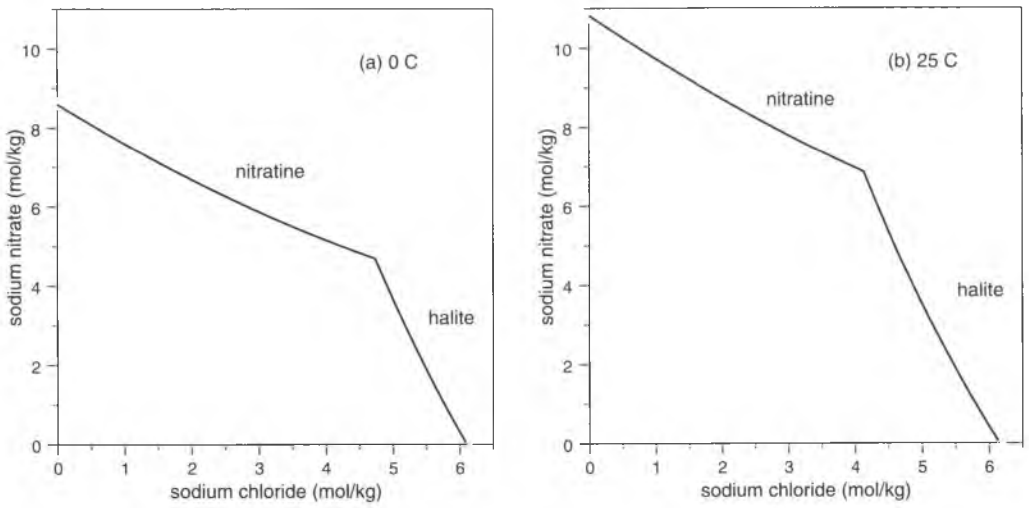

Figure 4.1: Solubilities in the Na^+–Cl^-–NO_3^-–H_2O system at 0°C and 25°C; symbols represent experimental values and have the following meanings: (•): solid phase nitratine ($NaNO_3$); (▼): solid phase halite (NaCl); (⧫): univariant equilibrium (solid phases nitratine-halite); closed symbols: data given full weight; open symbols: data given insignificant weight; curves are calculated solubilities using the Pitzer model.

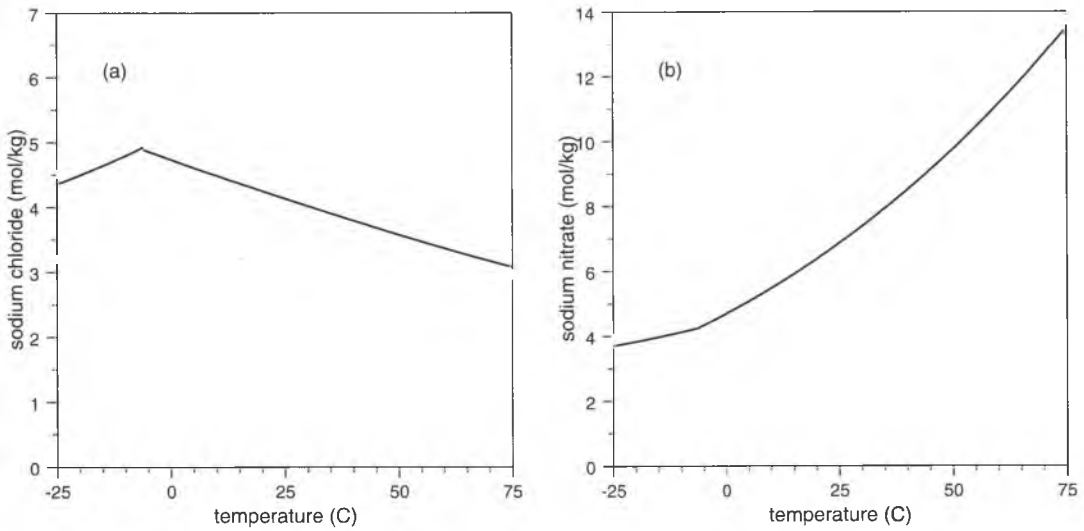

Figure 4.2: Univariant equilibria in the Na^+–Cl^-–NO_3^-–H_2O system: Corresponding molalities of NaCl and $NaNO_3$ in equilibrium with halite-nitratine (▼), hydrohalite ($NaCl \cdot 2H_2O$)-nitratine (•), halite-hydrohalite-nitratine (⧫), and ice-hydrohalite-nitratine (■); closed symbols: data given full weight; open symbols: data given insignificant weight; curves are calculated solubilities using the Pitzer model.

Table 4.1: The literature solubility database of ternary systems with common anion.

		Cl^-	NO_3^-	SO_4^{2-}	HCO_3^-	CO_3^{2-}	OH^-	$HCOO^-$	CH_3COO^-	$C_2O_4^{2-}$
Na^+	K^+	✓	✓	✓	✓	✓	✓	nd	nd	✓
	Mg^{2+}	✓	✓	✓	nd	✓	nd	nd	nd	✓
	Ca^{2+}	✓	✓	✓	nd	✓	✓	nd	nd	nd
	NH_4^+	✓	✓	✓	✓	✓		nd	nd	✓
	H^+	✓	✓	✓				✓	nd	nd
K^+	Mg^{2+}	✓	✓	✓	✓	nd	nd	nd	nd	nd
	Ca^{2+}	✓	✓	✓	nd	✓	nd	✓	nd	nd
	NH_4^+	✓	✓	✓	✓	nd		nd	nd	✓
	H^+	✓	✓	✓				nd	nd	✓
Mg^{2+}	Ca^{2+}	✓	✓	✓	✓	✓	✓	✓	nd	nd
	NH_4^+	✓	✓	✓		✓		nd	nd	✓
	H^+	✓	✓	✓				✓	nd	✓
Ca^{2+}	NH_4^+	nd	✓	✓	nd	nd		nd	nd	✓
	H^+	✓	✓	✓				nd	nd	✓
NH_4^+	H^+	✓	✓	✓				nd	nd	✓

Key: shaded cells: priority one systems; other cells: priority two and three; ✓: finished; nd: no data; empty cells: not relevant.

data available for the most common organic salts such as the acetates, formates, and oxalates. This was due to the fact that a similar solubility compilation is available (Stephen & Stephen 1964) as the ones mentioned above for the inorganic salts. As can be seen from Table 4.1, however, this expectation was too optimistic. At the same time it turned out that there is a substantial lack of thermodynamic data for the binary organic systems requiring additional vapour pressure measurements.

It ultimately became clear that it would be impossible to complete both, (1) the experimental work necessary to fill all gaps in the binary and ternary data, and, (2) the paramerisation work including all ions (requiring a huge number of ternary systems to be parameterised). Hence, the partners of this project decided to reduce the number of ions to be included into the final model and the following subsystems involving inorganic ions were selected as the multi-ion systems of most practical relevance.

1. Na^+–K^+–Mg^{2+}–Ca^{2+}–NH_4^+–Cl^-–NO_3^-–SO_4^{2-}–H_2O
2. Na^+–K^+–Cl^-–NO_3^-–SO_4^{2-}–HCO_3^-–H_2O
3. Na^+–K^+–Cl^-–NO_3^-–SO_4^{2-}–CO_3^{2-}–H_2O

Only a limited number of subsystems containing organic ions could be parameterised in this project. Hence, the most important subsystems had to be selected which might be relevant to the conservator. It is difficult, however, to identify the most important organic salts. Calcium oxalate crusts are commonly found on Italian marble and limestone monuments mainly as a result of biological activity (Del Monte *et al.* 1987). Due to its extremely low solubility, however, the presence of calcium oxalate does not influence the properties of the other salts. The question arises if other, more soluble oxalates might also be present in relevant concentrations. We therefore reevaluated the salt concentrations in more than 100 stone samples from several German monuments which were analyzed at IAAC some time ago. It was found, with no exception, that the molar calcium concentration was always significantly larger than the oxalate concentration. In many samples the oxalate concentration was below the detection limit (<50 mg/kg). It is, therefore, concluded that oxalate is present in stonework

Table 4.2: The literature solubility database of ternary systems with common cation.

		Na^+	K^+	Mg^{2+}	Ca^{2+}	NH_4^+	H^+
Cl^-	NO_3^-	✓	✓	✓	✓	✓	
	SO_4^{2-}	✓	✓	✓	✓	✓	
	HCO_3^-	✓	✓			✓	
	CO_3^{2-}	✓	✓	✓	✓	✓	
	OH^-	✓	✓	✓	✓		
	$HCOO^-$	nd	nd	nd	nd	nd	nd
	CH_3COO^-	nd	nd	nd	✓	nd	nd
	$C_2O_4^{2-}$	nd	nd	nd	nd	nd	nd
NO_3^-	SO_4^{2-}	✓	✓	✓	✓	✓	
	HCO_3^-	✓	✓	nd	nd	✓	
	CO_3^{2-}	✓	✓	nd	✓	nd	
	OH^-	✓	✓	✓	nd		
	$HCOO^-$	nd	nd	nd	nd	nd	nd
	CH_3COO^-	nd	nd	nd	nd	nd	nd
	$C_2O_4^{2-}$	✓	nd	nd	nd	nd	nd
SO_4^{2-}	HCO_3	✓	✓	✓	✓	✓	
	CO_3^{2-}	✓	✓		✓		
	OH^-	✓	✓	✓	✓		
	$HCOO^-$	nd	nd	nd	nd	nd	nd
	CH_3COO^-	nd	✓	nd	nd	nd	nd
	$C_2O_4^{2-}$	✓	nd	✓	✓	nd	nd
HCO_3^-	CO_3^{2-}	✓	✓	nd	✓		
	OH^-						
	$HCOO^-$	nd	nd	nd	nd	nd	nd
	CH_3COO^-	nd	nd	nd	nd	nd	nd
	$C_2O_4^{2-}$	nd	nd	nd	nd	nd	nd
CO_3^{2-}	OH^-	✓	✓	nd	nd		
	$HCOO^-$	nd	nd	nd	nd	nd	nd
	CH_3COO^-	nd	nd	nd	nd	nd	nd
	$C_2O_4^{2-}$	nd	nd	nd	nd	nd	nd
OH^-	CH_3COO^-	nd	nd	nd	nd	nd	nd
	CH_3COO^-	✓	nd	nd	nd	nd	nd
	$C_2O_4^{2-}$	nd	✓	nd	nd	nd	nd
$HCOO^-$	CH_3COO^-	nd	nd	nd	nd	nd	nd
	$C_2O_4^{2-}$	nd	nd	nd	nd	nd	✓
CH_3COO^-	$C_2O_4^{2-}$	nd	nd	nd	nd	nd	nd

Key: shaded cells: priority one systems; other cells: priority two and three; ✓: finished; nd: no data; empty cells: not relevant.

as practically insoluble calcium oxalate in most cases. Hence, salt systems containing oxalate were not included in the thermodynamic treatment of salt mixtures.

Much less is known about the concentrations of acetate (CH_3COO^-) and formate ($HCOO^-$) in stonework. Chemicals used for cleaning treatments are sometimes containing formic acid. The chemical reaction of these acids with the mineral constituents of the building materials leads to the formation and enrichment of formates (Zehnder & Arnold 1984). Acetic acid and formic acid emissions from the wood of museum storage and show cases were shown to be the cause for the formation of salt efflorescences on stone and metal artifacts. FitzHugh & Gettens (1971) report on the occurrence of calclacite efflorescences on calcareous materials, which was first characterised by Van Tassel (1958) as $CaCl_2{\cdot}Ca(OAc)_2{\cdot}10H_2O$. Tennent & Baird (1985) found different hydrates of calcium acetate and a calcium acetate formate hydrate on the surface of molluscs. Recently Gibson *et al.* (1997a,b) have found an unusual efflorescence on calcareous artifacts characterised as calcium nitrate chloride acetate hydrate, $CaCl_2{\cdot}3Ca(CH_3COO)_2{\cdot}2Ca(NO_3)_2{\cdot}14H_2O$.

As a reasonable first approach to understand the crystallisation properties of salt mixtures containing mixtures of organic and inorganic ions the Na^+–Ca^{2+}–Cl^-–CH_3COO^-–H_2O reciprocal system was selected. This system includes both the most common inorganic salt (sodium chloride) and the most important organic constituent of calcareous museum artefacts (calcium acetate). Hence, further solubility measurements focused on the ternary systems, Na^+–Ca^{2+}–CH_3COO^-–H_2O, Na^+–Cl^-–CH_3COO^-–H_2O, and Ca^{2+}–Cl^-–CH_3COO^-–H_2O.

4.3 Measurements of the water activity in electrolyte solutions

The chemical potential, $\mu_{w,l}$, of water in a liquid solution is expressed in terms of the standard state chemical potential,$\mu^o_{w,l}$, and the thermodynamic activity as:

$$\mu_{w,l} = \mu^o_{w,l} + RT \ln a_w \tag{4.1}$$

where R is the gas constant, T is the absolute temperature, and a_w is the water activity. At equilibrium the chemical potential of water in the vapour phase, $\mu_{w,v}$ equals that of the liquid phase, $\mu_{w,l}$, hence:

$$\mu_{w,v} = \mu^o_{w,v} + RT \ln(\frac{f_w}{f^o_w}) = \mu^o_{w,l} + RT \ln a_w = \mu_{w,l} \tag{4.2}$$

where f_w and f^o_w are the fugacities of the solution and of pure water, respectively. For many practical applications it is sufficient to assume ideal behaviour of water vapour, *i.e.*, the fugacities may be replaced by the water vapour pressures. We obtain for the water activity:

$$a_w = \frac{f_w}{f^o_w} \approx \frac{p_w}{p^o_w} = \mathrm{RH} \tag{4.3}$$

where p_w and p^o_w are the water vapour pressures above the solution and the saturation vapour pressure, respectively, and RH is the relative humidity. To determine the water activity of electrolyte solutions it is sufficient to measure the vapour pressure or the relative humidity above a solution of known composition at constant temperature directly. Indirect methods include the isopiestic technique (Rard & Platford 1991) requiring reference standard solutions of known vapour pressure.

A survey of the available sensors to measure vapour pressures directly revealed that the accuracy of standard humidity sensors is not sufficient for the major objective, *i.e.*, the parameterisation of ion interaction parameters. Capacitance gauges that measure the total pressure seemed to be more appropriate for that purpose and were applied here for the measurement of water activities of binary solutions of several organic salts. The use of standard humidity sensors, however, was also tested and they were applied to measure the relative humidities above mixed solutions to provide some data for model validation.

4.3.1 Direct vapour pressure measurements

A vapour pressure apparatus was built up consisting of a sample cell in a thermostated water bath and connected to a vacuum pump. Pressures were measured directly with a capacitance manometer (MKS Instruments, model Baratron 220). The quantity required for the determination of the ion interaction model parameters is the osmotic coefficient, ϕ, which for a binary salt solution is defined as:

$$\phi = -\frac{1000 \ln a_w}{M_w \nu m} \tag{4.4}$$

where M_w is the molecular is the molecular weight of water (18.01528 g/mol), ν is the total number of ions formed by complete dissociation of an electrolyte, and m is the molality. Correcting for the non-ideal behaviour of water vapour the water activities, a_w, and osmotic coefficients, ϕ, were calculated from the experimental vapour pressures according to Rard & Platford (1991).

To evaluate the accuracy of the technique vapour pressures over solutions of reference salts were measured whose water activities are known and tabulated for various temperatures. The overall uncertainty after careful calibration of the apparatus was about 0.2% in terms of the vapour pressure above NaCl solutions.

Due to solubility limitations no useful measurements could be made for aqueous calcium oxalate. Also, as a result of the limited solubility of sodium oxalate the uncertainties in the vapour pressure measurement resulted in unacceptable large uncertainties in the osmotic coefficients making it difficult to use the data for the determination of the binary model parameters. Due to the greater solubility of the acetates, formates, and potassium oxalate the osmotic coefficients are less scattered and the data may be directly used as input data for the model parameterisation. The vapour pressure measurements carried out in this project are summarised in Table 4.3.

Fig. 4.3 depicts the water activities at 25° of the alkali formates and acetates. The solubilities of the potassium salts allowed extension of the measurements to very high concentrations corresponding to water activities below 0.3. Fig. 4.4 depicts the water activities for the less soluble salts, *i.e.*, calcium acetate and formate, and the alkali oxalates. Due to the much lower concentrations in these solutions the water activities are considerably more scattered.

4.3.2 Measurement of relative humidity in equilibrium with saturated salt solutions

In addition to the direct vapour pressure measurements over single salt solutions attempts were also made to use standard RH and T sensors for the measurement of water activities. The accuracy of one of the sensors, a Testo 601 (Testotherm), was

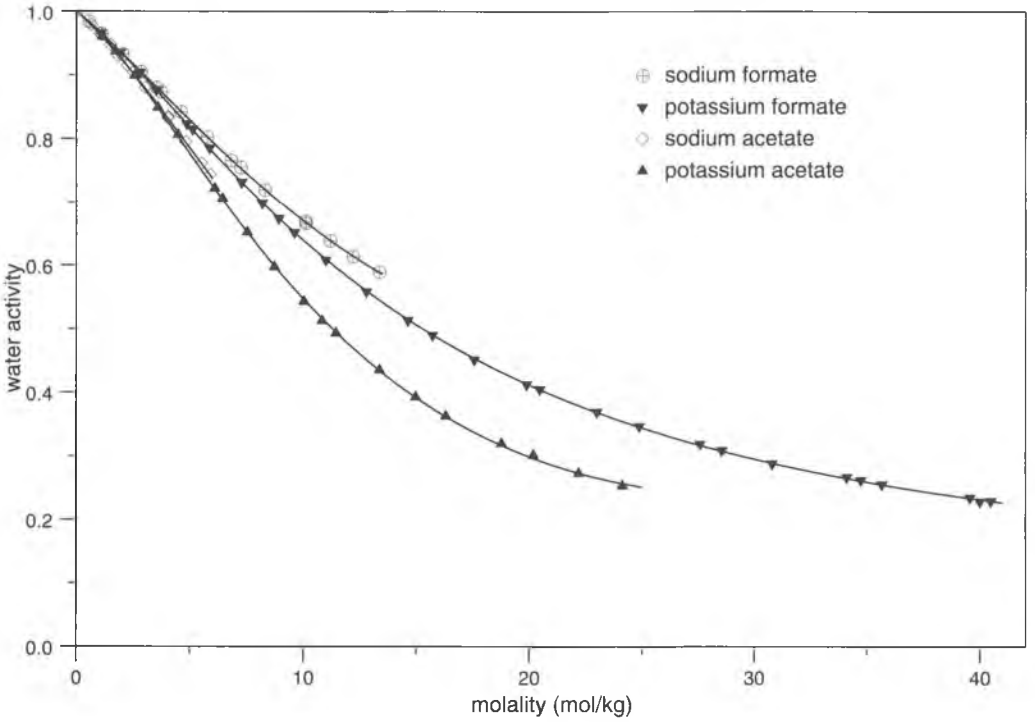

Figure 4.3: Water activities in solutions of $NaCH_3COO$, $NaHCOO$, KCH_3COO, and $KHCOO$ at 25°C.

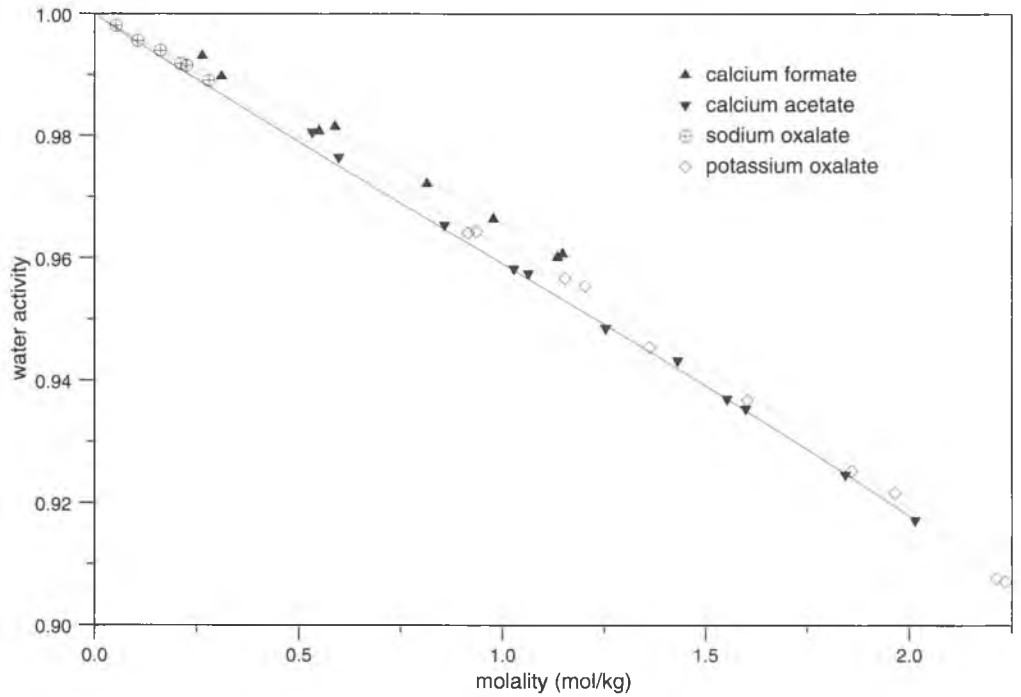

Figure 4.4: Water activities in solutions of $Ca(HCOO)_2$, $Ca(CH_3COO)_2$, $Na_2C_2O_4$ and $K_2C_2O_4$ at 25°C.

Table 4.3: Temperature range and molalities of vapour pressure measurements.

salt	molality range (mol/kg)	temperature range (°C)	N[(a)]
$NaCH_3COO$	0.65–6.47	5–35	83
KCH_3COO	1.13–24.1	5–35	127
$Ca(CH_3COO)_2$	0.53–2.01	5–35	77
$NaHCOO$	0.55–13.4	5–35	97
$KHCOO$	1.08–46.8	5–50	246
$Ca(HCOO)_2$	0.26–1.15	5–35	56
$Na_2C_2O_4$	0.05–0.08	5–33	35
$K_2C_2O_4$	0.92–2.24	5–35	57

(a) number of vapour pressure determinations.

tested using saturated solutions of LiCl and NaCl, and standard solutions of known water activity (Steinecker Elektronik GmbH). The results of these measurements are depicted in Fig. 4.5. Compared to the direct vapour pressure measurements the accuracy of the RH and T sensor is much lower and is not sufficient to obtain water activities or osmotic coefficients with the accuracy required for the determination of the binary model parameters. However, this type of measurements is much less time consuming than direct vapour pressure measurements and might be helpful for the model validation.

In order to test the use of RH sensors measurements over saturated salt solutions were carried out at 25°C using the Testo 601 and a Vaisala HMP230A sensor. Two systems with reciprocal salt pairs, $NaCl$–$Ca(NO_3)_2$–H_2O and $NaCl$–KNO_3–H_2O, respectively, were studied. Saturated solutions were prepared in a thermostated 250ml flask by adding an excess of one of the salts to a solution of the second salt. Temperature and RH above the solutions were continuously measured with the sensors which were connected to a PC. Equilibration times were such that T and RH reached constant values. The composition of the saturated solutions was measured using inductively coupled plasma emission spectrometry (ICP-AES) and ion chromatography (IC).

Results for the $NaCl$–KNO_3–H_2O system are shown in Fig. 4.5 and compared to calculated relative humidities using a preliminary parameterisation of the ion interaction model obtained at IAAC. Such comparisons provide a real test of the models predictive power since no systems containing more than three different ions were used for the model parameterisation. The prediction of saturation humidities using the equilibrium model requires the calculation of both, solubilities and water activities. Obviously there is very good agreement between the calculated and the experimental saturation humidities, preferably to within the combined experimental errors of the RH and the concentration measurements. Similar results were obtained for the solubility and the saturation humidity of $NaCl$ in $Ca(NO_3)_2$ solutions.

4.4 Solubility measurements

An isothermal technique was used for the solubility measurements. Saturated solutions were equilibrated in a constant temperature bath. The solid phases in equilibrium with the saturated solutions were characterised using X-ray diffraction (Siemens D5000 XRD). Cations present in the saturated solution were measured using induc-

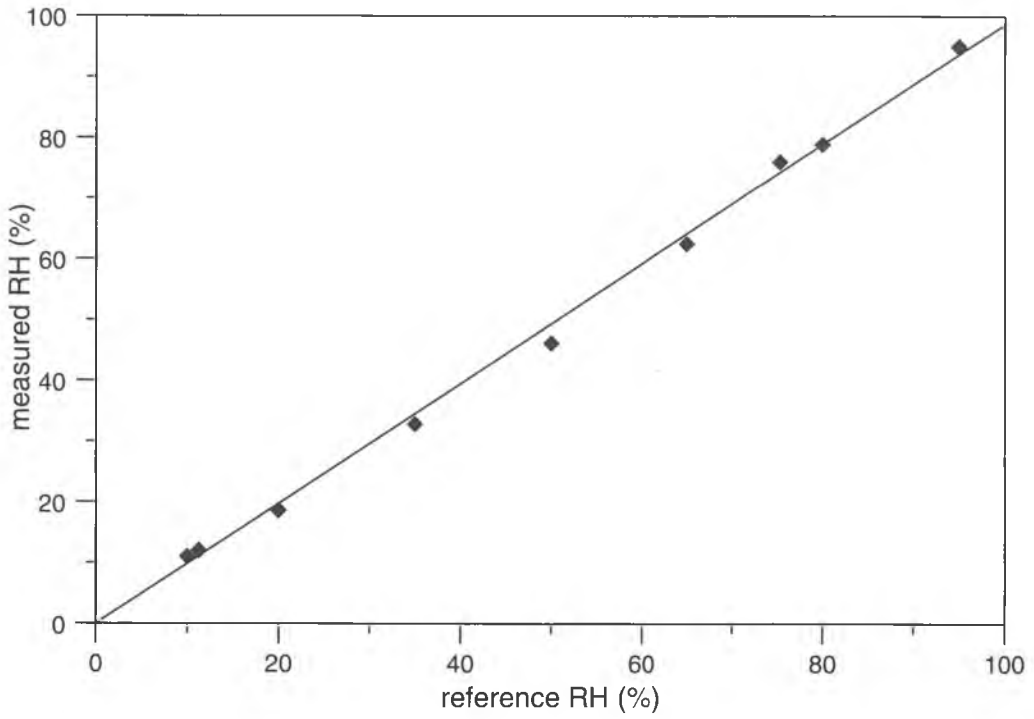

Figure 4.5: Response of the Testo 601 sensor.

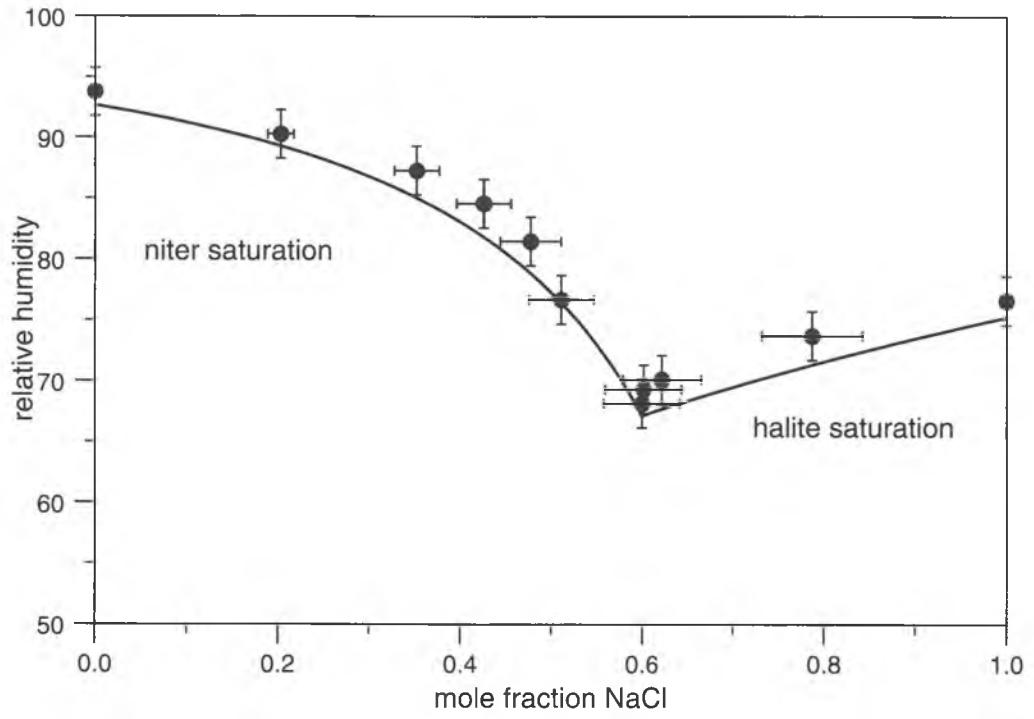

Figure 4.6: Calculated (solid lines) and experimental (symbols) saturation humidities of solutions saturated with niter (KNO_3) or halite (NaCl), respectively.

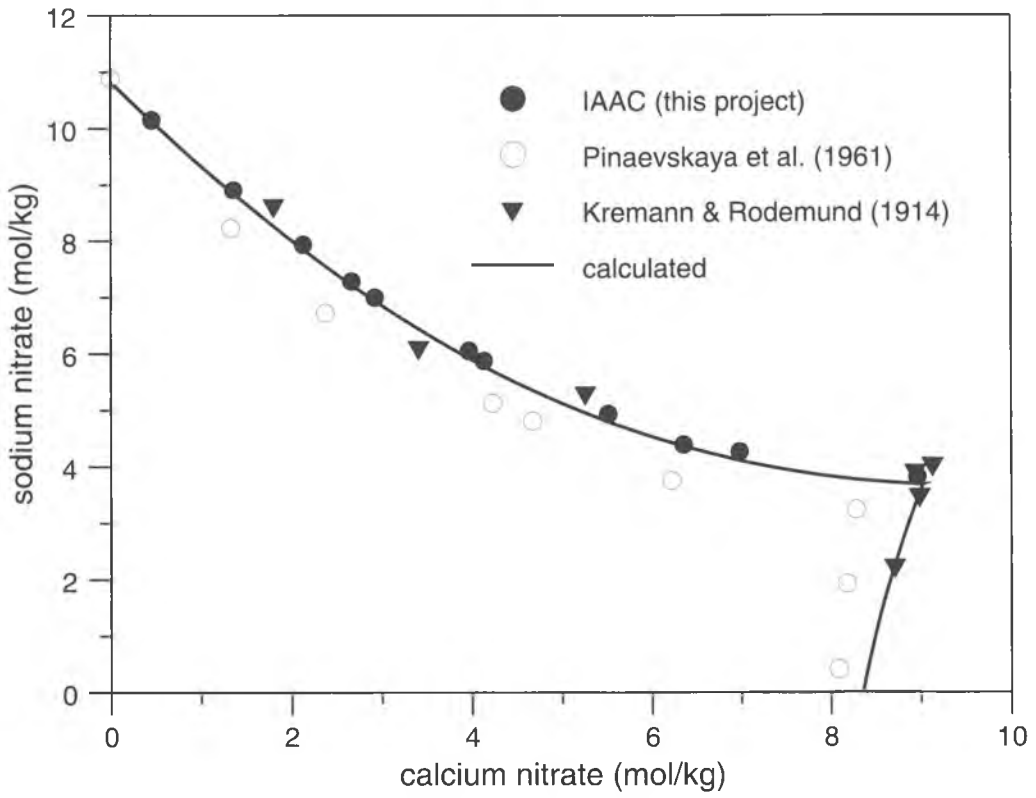

Figure 4.7: Experimental and calculated solubilities in the $NaNO_3$–$Ca(NO_3)_2$–H_2O system at 25°C.

tively coupled plasma emission spectrometry. Anions were analysed using either ion chromatography or potentiometric titrations, respectively.

It was already mentioned before that additional solubility measurements in the $NaNO_3$–$Ca(NO_3)_2$–H_2O system were necessary to remove obvious inconsistencies in the literature database. Measurements were carried out at 25°C. Our results are compared to the literature data in Fig. 4.7. It is obvious that the solubilities reported by Pinaevskaya *et al.* (1961) are in error, while the data of Kremann & Rodemund (1914), though scattered, seem to be more accurate. The additional measurements at 25°C, therefore, helped to assign weights to the solubilities at other temperatures, *e.g.*, all data of Pinaevskaya *et al.* (1961) were given zero weight.

Solubility measurements of the binary and ternary systems containing sodium, calcium, acetate and chloride required for the model parameterisation were carried out at 5, 25, and 50°C. Our experimental solubilities in the binary systems $NaCH_3COO$(aq) and $Ca(CH_3COO)_2$(aq) are compared to literature solubilities in Fig. 4.8 and Fig. 4.9, respectively. Also shown are freezing point data and calculated univariant curves which will be discussed in a later chapter. There is reasonable agreement between our sodium acetate solubilities and the literature data. Solubility data of calcium acetate are scarce and also contradictory, even regarding the nature of the stable solids. In agreement with Panzer (1962) and Saury *et al.* (1993) we have found the monohydrate, $Ca(CH_3COO)_2{\cdot}1H_2O$, and the hemihydrate, $Ca(CH_3COO)_2{\cdot}0.5H_2O$, as the stable solids. However, the solubilites are scattered and uncertainties remain regarding the transition temperature for the dehydration of the monohydrate and the

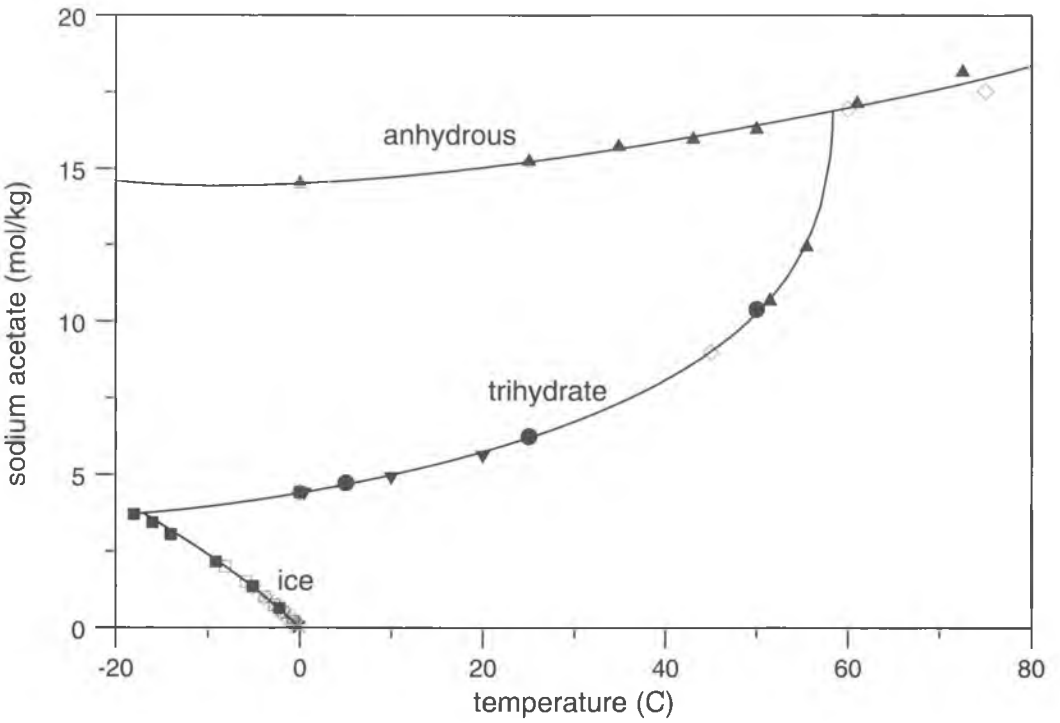

Figure 4.8: Experimental solubility and freezing point data and calculated univariant curves in the system $NaCH_3COO$–H_2O; symbols represent experimental values and have the following meanings: (•): this project; (▲): Green (1908); (▼): Morgan & Walker (1945); (◇): Dunningham (1912); (×): Scatchard & Prentiss (1934); (■): Guthrie (1876); (□): McBain *et al.* (1919).

formation of the hemihydrate.

Solubilities in the ternary systems were determined at 5, 25 and 50°C, respectively. As an example, Fig. 4.10 depicts the solubilities in the NaCl–$NaCH_3COO$–H_2O system at 5°C. No double salt was found in this system and $NaCH_3COO{\cdot}3H_2O$ is the only stable hydrate in the temperature range studied. Likewise, no double salt could be detected in the $NaCH_3COO$–$Ca(CH_3COO)_2$–H_2O system. The solubility diagrams of the $CaCl_2$–$Ca(CH_3COO)_2$–H_2O system are much more complicated due to the presence of double salts. Moreover, our data do not agree well with literature data of Stoilova & Staneva (1987) at 25°C and 50°C. We have no explanation for the discrepancies and preferred to use our own data for the parameterisation of this system. However, there are still uncertainties regarding the hydrates of calcium acetate and the nature of the double salts formed with calcium chloride requiring additional measurements.

4.5 *In situ* X-ray diffractometry

In order to study the phase changes causing damage to porous materials experimentally, in situ methods are highly desirable. Such techniques would be very helpful to investigate, both, the thermodynamics and the kinetics of phase transformation processes. In recent years the temperature controlled X-ray diffractometry (TXRD) became an increasingly important tool and was successfully applied in solid state chemistry (Epple 1994). In contrast, there are only few applications of humidity

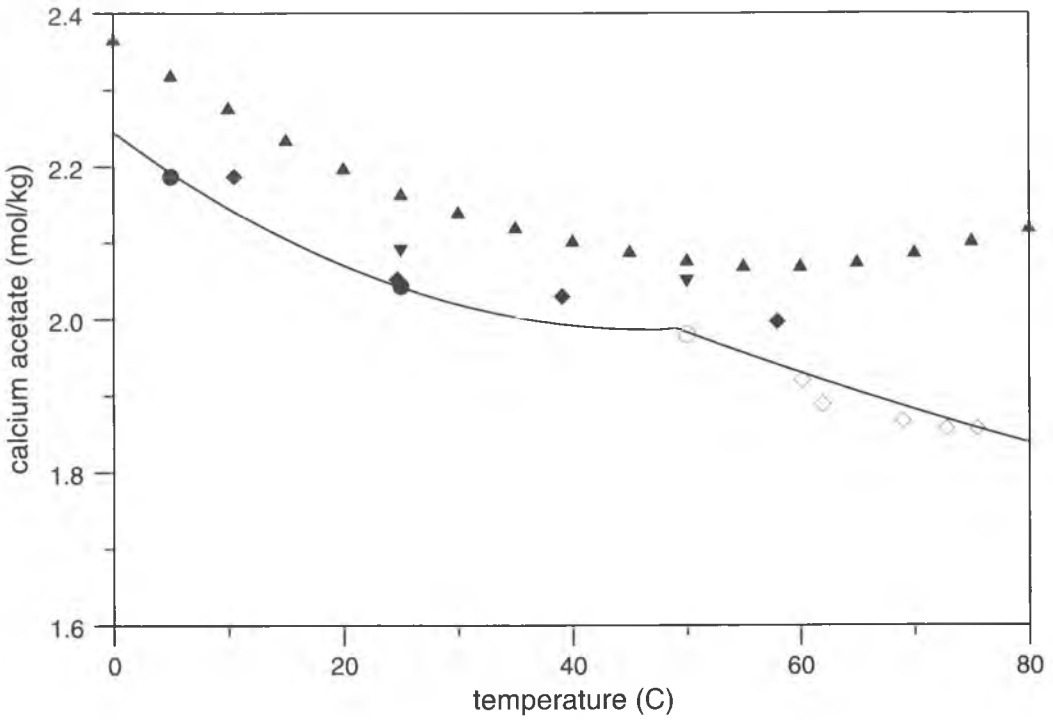

Figure 4.9: Experimental solubility and freezing point data and calculated univariant curves in the system $Ca(CH_3COO)_2$–H_2O; symbols represent experimental values and have the following meanings: (▲): Lumsden (1902), $Ca(CH_3COO)_2 \cdot 2H_2O$; (▼): Stoilova & Staneva (1987), $Ca(CH_3COO)_2 \cdot 2H_2O$; (*bullet*): this project, open symbol: $Ca(CH_3COO)_2 \cdot 0.5H_2O$, closed symbol: $Ca(CH_3COO)_2 \cdot 1H_2O$; (♦): Saury *et al.* (1993); open symbol: $Ca(CH_3COO)_2 \cdot 0.5H_2O$, closed symbol: $Ca(CH_3COO)_2 \cdot 1H_2O$.

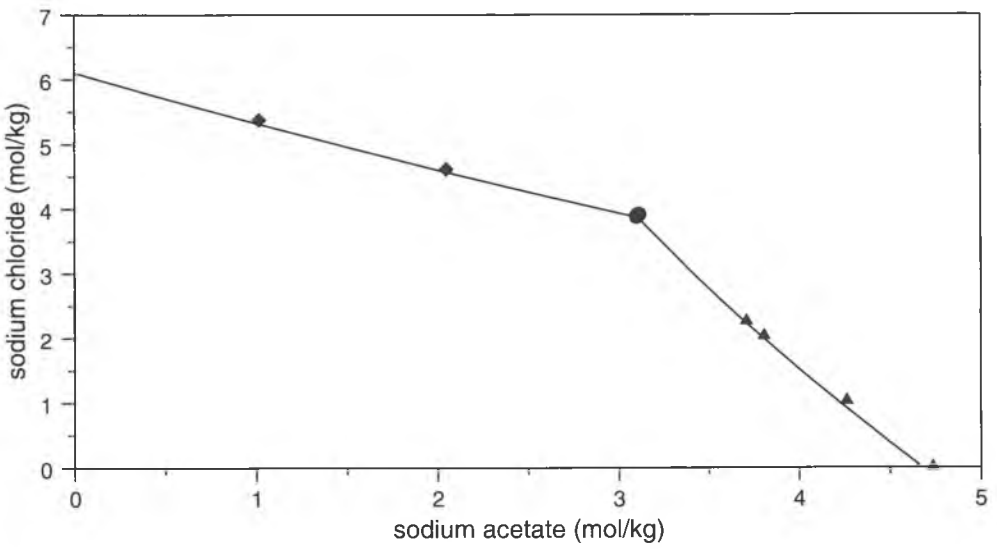

Figure 4.10: Solubilities in the Na^+–Cl^-–CH_3COO^-–H_2O system at 5°C; symbols represent experimental values and have the following meanings: (♦): solid phase halite (NaCl); (▲): solid phase sodium acetate trihydrate ($NaCH_3COO \cdot 3H_2O$); (•): univariant equilibrium (solid phases sodium acetate trihydrate and halite); curves are calculated solubilities using the Pitzer model.

Table 4.4: Examples for hydration equilibria and associated volume expansion.

lower hydrate	hydrated form	expansion
Na_2SO_4 (thenardite)	$Na_2SO_4 \cdot 10H_2O$ (mirabilite)	314%
$Na_2CO_3 \cdot H_2O$ (thermonatrite)	$Na_2CO_3 \cdot 10H_2O$ (natron)	257%
$MgSO_4 \cdot H_2O$ (kieserite)	$MgSO_4 \cdot 6H_2O$ (hexahydrite)	146%
$MgSO_4 \cdot 6H_2O$ (hexahydrite)	$MgSO_4 \cdot 7H_2O$ (epsomite)	10%

controlled X-ray diffraction (RHXRD) which would be extremely useful to study the phase changes relevant to damage of porous materials. RHXRD was first mentioned by Huxley & Kendrew (1953) who observed the shrinkage of proteins. Later applications include a study of the hydration-dehydration mechanism of oxalic acid (Gérard *et al.* 1967), the swelling of clay minerals (Watanabe & Sato 1988), and the deliquescence properties of ammonium nitrate sulfate double salts in atmospheric aerosols (Klaue & Dannecker 1994). In the present project we have used RHXRD to study the phase behaviour of pure salts and salt mixtures relevant to damage of porous materials.

The experimental set-up consists of a measurement chamber connected to the θ-circle of a Siemens D5000 X-ray diffractometer with a position sensitive detector (Steiger & Zeunert 1996). Temperature and relative humidity in the chamber are controlled by an external thermostat and a humidity generating system, respectively. Both, the measurement chamber and the humidity generator were designed and optimised in this project (Zeunert and Steiger, manuscript in preparation). A Vaisala humidity sensor (HMP 233) is used to measure the relative humidity in the chamber. The sensor is connected to the external humidity generator controlling the relative humidity in the chamber.

RHXRD measurements can be made in two different ways. First, it is possible to start with a solution containing the salts of interest. Stepwise decreases in the relative humidity then yield critical humidities of crystallisation or phase transformation and, finally, the identity of the crystalline solids after complete evaporation of water. Alternatively, it is possible to begin with a mixture of crystalline solids and determine the deliquescence humidities. A computer program was written to control the humidity scans. The software allows to define the starting and end point of the scan, the step size, and the equilibration times. Each successively recorded diffraction pattern is assigned to the respective relative humidity and temperature in the chamber. Any phase changes can be detected by the sudden appearance or disappearance of peaks.

4.5.1 RHXRD measurements in the system Na_2SO_4–H_2O

Several common salts can exist in different hydrated forms. The phase change from the lower hydrated (or anhydrous) form to the higher state of hydration causes an increase in volume. Due to this expansion hydration is considered as an important cause of damage. Table 4.4 lists examples of hydration-dehydration equilibria relevant to building materials. The hydration of thenardite (Na_2SO_4) and the formation of mirabilite ($Na_2SO_4 \cdot 10H_2O$) is generally assumed to be an important cause of damage.

The phase diagram of the system Na_2SO_4–H_2O is depicted in Fig. 4.11. At high relative humidities sodium sulfate can only exist as an aqueous solution. At temperatures above the transition temperature (32.4°C) thenardite (Na_2SO_4) crystallises out as the relative humidity drops below the deliquescence humidity (curve 1). At temperatures below 32.4°C mirabilite ($Na_2SO_4 \cdot 10H_2O$) is the stable solid in equilibrium

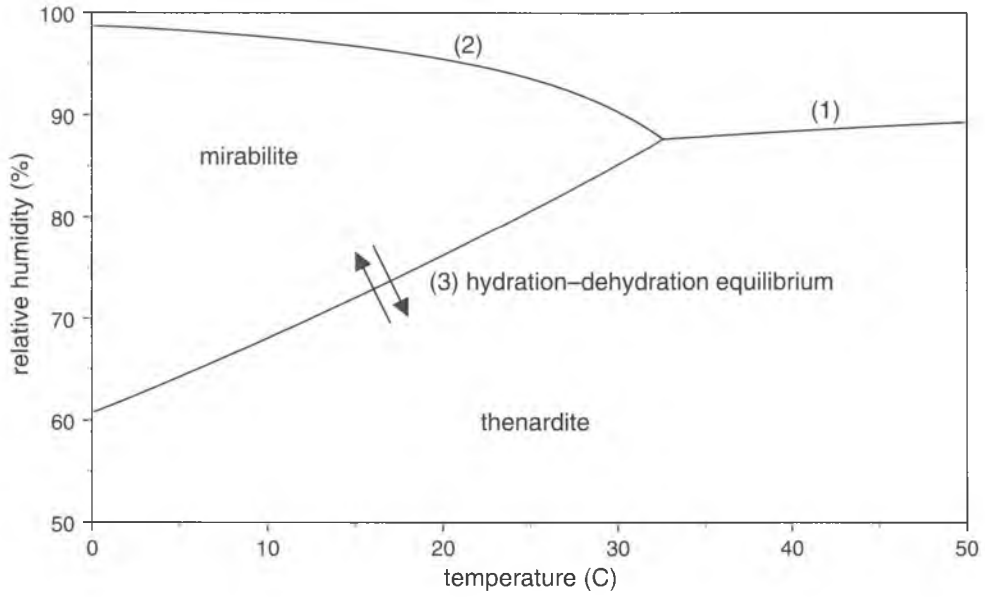

Figure 4.11: The Na_2SO_4–H_2O system from 0–50°C.

with a saturated sodium sulfate solution (curve 2). Finally, curve 3 represents the hydration-dehydration equilibrium according to:

$$Na_2SO_4 + 10H_2O(g) \rightleftharpoons Na_2SO_4 \cdot 10H_2O \tag{4.5}$$

Thenardite is the stable solid at low relative humidities, whilst mirabilite can only exist within a limited range of relative humidities at temperatures below 32.4°C. Hydration damage can occur if thenardite is hydrated due to changes in either temperature, or relative humidity, or both. XRD measurements under controlled conditions of temperature and relative humidity using the optimised instrument were carried out to study the hydration-dehydration behaviour of sodium sulfate. A successive scan of diffraction patterns of sodium sulfate at a constant temperature of 25°C and stepwise increasing the relative humidity is depicted in Fig. 4.12. The phase transition thenardite/mirabilite is observed at a relative humidity of 82±2.5% RH. Further increasing the relative humidity the deliquescence of mirabilite occurred at 91±2.5% RH. Both values agree with available thermodynamic data to within our stated experimental uncertainty.

Subsequently, the kinetics and reaction mechanisms of the hydration and dehydration reactions were studied in more detail. The temperature and humidity induced hydration and dehydration reactions were investigated. In both cases no amorphous intermediates could be observed. Hence, both reactions are obviously real solid state reactions. Intensity-time plots were used to gain further insight into the reaction mechanisms (Brown *et al.* 1980). It was found that each of the reactions studied was following a nucleation growth reaction mechanism. Details of these measurements will be presented elsewhere (Zeunert and Steiger, manuscript in preparation).

Some of the experiments revealed surprising results which could not be simply explained from equilibrium thermodynamics. For instance, in some cases the hydration of thenardite could not be observed, although the conditions were such that mirabilite would be the stable form. Also other authors noted that the hydration of thenardite in humid atmosphere is hindered (Charola & Weber 1992; Doehne 1994; Knacke &

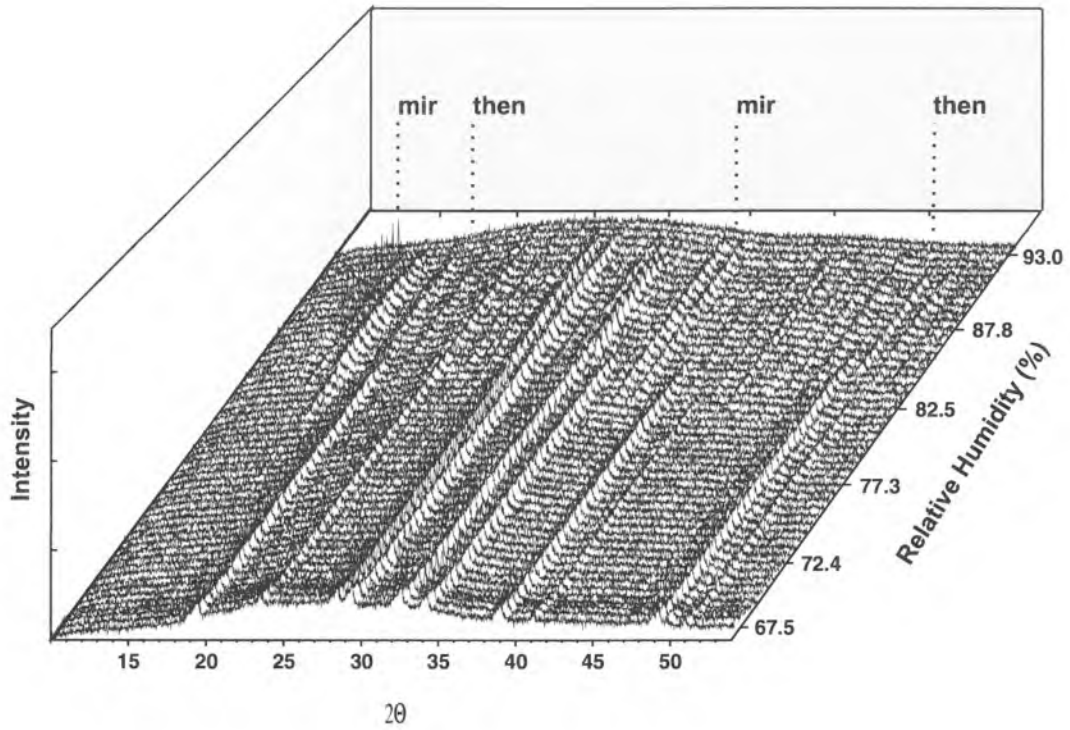

Figure 4.12: Diffraction patterns of sodium sulfate at 25°C with increasing relative humidity.

von Erdberg 1975). This effect is generally explained as kinetic hindrance due to the formation of a non-porous layer of the decahydrate blocking the hydration of the anhydrous salt. It is to be concluded that the hydration of thenardite is largely depending on both, the environmental conditions and the nature of the sample, *i.e.*, crystal sizes and the morphology of crystal aggregates. The situation might be even more complicated if sodium sulfate is present in a porous material. Any kinetic influences may be largely affected by the porosity and chemical composition of the material.

4.5.2 RHXRD measurements in the system Na^+–K^+–Mg^{2+}–NO_3^-–SO_4^{2-}–H_2O

As a final check of the performance of the RHXRD instrument measurements of the quinary system Na^+–K^+–Mg^{2+}–NO_3^-–SO_4^{2-}–H_2O were carried out. Experimental solubilities that could be used to construct the phase diagram of this system were not available. A solution containing these ions in a fixed composition was evaporated to dryness at different temperatures. The results of these experiments are summarised in Table 4.5.

At 25°C humberstonite, $K_3Na_7Mg_2(SO_4)_6(NO_3)_2{\cdot}6H_2O$, was found as the major constituent of the solid residue. This mineral is naturally occurring in the nitrate deposits of the Chilean Atacama desert (Mrose *et al.* 1970). However, no phase diagrams, nor solubility or other thermodynamic data are available for humberstonite. Therefore, this mineral could not be included in the thermodynamic model of this project. Other minerals that were detected at 25°C are nitratine, $NaNO_3$, and hexahydrite, $MgSO_4{\cdot}6H_2O$. According to the phase rule there must be a fourth mineral present, which most likely is niter, KNO_3. Due to interferences in the diffraction pattern, however, KNO_3 could not be detected. In theory the missing mineral could

Table 4.5: Salt minerals obtained after evaporation to dryness of a solution with composition (anion and cation eq. %, respectively): Na^+: 50%; K^+: 16%; Mg^{2+}: 34%; NO^{3-}: 33%; $SO_4{}^{2-}$: 67%.

10°C (39%)[a]	25°C (49%)[a]	50°C (n.d.)[b]
KNO_3	KNO_3[c]	KNO_3
$NaNO_3$	$NaNO_3$	$NaNO_3$
$MgSO_4{\cdot}6H_2O$	$MgSO_4{\cdot}6H_2O$	Na_2SO_4
$Mg(NO_3)_2{\cdot}6H_2O$[c]	$K_3Na_7Mg_2(SO_4)_6(NO_3)_2{\cdot}6H_2O$	$Na_{12}Mg_7(SO_4)_{13}{\cdot}15H_2O$

(a) crystallisation humidity.

(b) not determined.

(c) detection uncertain but likely present.

also be nitromagnesite, $Mg(NO_3)_2{\cdot}6H_2O$.

The temperature range of stable existence of humberstonite is obviously limited. The mineral could not be detected at 10°C, nor at 50°C. At 10°C no double salt was found at all. Nitratine, niter, and hexahydrite were identified at 10°C. Nitromagnesite is probably the fourth mineral. The identification in the X-ray pattern was uncertain, however.

In all experiments the successive crystallisation of salt minerals that would be expected from equilibrium thermodynamics could not be observed. In contrast, all minerals were crystallising at the same time and at very low relative humidities. Obviously the evaporating solution reaches a considerable level of supersaturation before the onset of crystallisation. The critical supersaturation is reached at very low relative humidities and all minerals precipitate at the same time. This implies that critical relative humidities as predicted by an equilibrium model might be more realistically interpreted as an upper limit of critical humidities. Future investigations will have to focus on the possibility of supersaturation in porous building materials and the resulting deviation from equilibrium.

4.6 References

Brown, W. E., D. Dollimore & A. K. Galway 1980. *In* C. H. Bamford & C. H. K. Tipper (eds.), *Comprehensive Chemical Kinetics 22: Reactions in the Solid State*. Elsevier, Amsterdam.

Charola, A. E. & J. Weber 1992. 'The hydration and deterioration mechanism of sodium sulfate.' *In* J. Delagado Rodrigues, F. Henriques & F. Telmo Jeremias (eds.), *7th International Congress on Deterioration and Conservation of Stone*, pp. 581–90. Laboratório Nacional de Engenharia Civil, Lisbon.

D'Ans, J. 1933. *Die Lösungsgleichgewichte der Systeme der Salze ozeanischer Salzablagerungen*. Verlagsgesellschaft für Ackerbau, Berlin.

Del Monte, M., C. Sabbioni & G. Zappia 1987. *Sci. Total Environ.* 67: 17–39.

Doehne, E. 1994. *In* V. Fassina, H. Ott & F. Zezza (eds.), *The conservation of monuments in the Mediterranean Basin. Proceedings 3rd International Symposium*, pp. 143–150. Venice.

Dunningham, A. C. 1912. *J. Chem. Soc.* 101: 431–444.

Epple, M. 1994. *J. Therm. Anal.* 42: 559–593.

FitzHugh, E. W. & R. J. Gettens 1971. *In* R. Brill (ed.), *Science and Archaeology*, pp. 91–102. MIT Press, Cambridge, Mass.

Gérard, N., G. A. Watelle-Marion & A. Thrierr-Sorel 1967. *Bull. Soc. Chem.* 5: 1788–1793.

Gibson, L. T., B. G. Cooksey, D. Littlejohn & N. H. Tennent 1997a. *Anal. Chim. Acta* 337: 151–164.

Gibson, L. T., B. G. Cooksey, D. Littlejohn & N. H. Tennent 1997b. *Anal. Chim. Acta* 337: 253–264.

Green, W. F. 1908. *J. Phys. Chem.* 12: 655–660.

Guthrie, F. 1876. *Phil. Mag.* 2(5): 211–225.

Huxley, H. E. & J. C. Kendrew 1953. *Acta Cryst.* 6: 76–80.

Klaue, B. & W. Dannecker 1994. *J. Aerosol. Sci.* 25: S297–S289.

Knacke, O. & R. von Erdberg 1975. *Ber. Bunsenges. Phys. Chem.* 79: 653–657.

Kremann, R. & H. Rodemund 1914. 'Über einige doppelte Umsetzungen des als Nebenprodukt des Leblanc'schen Sodaverfahrens abfallenden Calciumthiosulfates vom Standpunkte des Massenwirkungsgesetzes und der Phasenlehre.' *Monatshefte f. Chem.* 35: 1061–1113.

Linke, W. F. 1965. *Solubilities. Inorganic and Metal-Organic Compounds.* American Chemical Society, Washington D.C.

Lumsden, J. S. 1902. *J. Chem. Soc.* 81: 350–362.

McBain, J. W., M. E. Laing & A. F. Titley 1919. *J. Chem. Soc.* 119: 1279–1300.

Morgan, R. A. & K. R. Walker 1945. *Ind. Eng. Chem.* 37: 1186–1189.

Mrose, M. E., J. J. Fahey & G. E. Ericksen 1970. *Am. Mineral.* 55: 1518–1533.

Panzer, J. 1962. *J. Chem. Eng. Data* 7: 140–142.

Pinaevskaya, E. N., N. L. Antoshkina & G. G. Guseva 1961. 'Investigation of the aqueous reciprocal system of sodium and calcium chromates and nitrates.' *J. Appl. Chem. USSR* 34: 1642–1656.

Rard, J. A. & R. F. Platford 1991. *In* K. S. Pitzer (ed.), *Activity Coefficients in Electrolyte Solutions*, pp. 209–277. CRC Press, Boca Raton.

Saury, C., R. Boistelle, F. Dalemat & J. Bruggeman 1993. *J. Chem. Eng. Data* 38: 56–59.

Scatchard, G. & S. S. Prentiss 1934. *J. Am. Chem. Soc.* 56: 807–811.

Silcock, H. L. 1979. *Solubilities of inorganic and organic compounds. Volume 3. Ternary and multicomponent systems of inorganic substances.* Pergamon Press, Oxford.

Steiger, M. & A. Zeunert 1996. *In* J. Riederer (ed.), *Proc 8th Int Congress on Deterioration and Conservation of Stone*, pp. 535–544. Müller Druck und Verlag GmbH, Berlin.

Stephen, H. & T. Stephen 1964. *Solubilities of inorganic and organic compounds. Volume II. Ternary systems.* Pergamon Press, Oxford.

Stoilova, D. & D. Staneva 1987. *Izv. Po. Chim. (Sofija)* 20: 285–290.

Tennent, N. H. & T. Baird 1985. *Studies in Conservation* 30: 73–85.

Van Tassel 1958. *Acta Cryst.* 11: 745–746.

Watanabe, T. & T. Sato 1988. *Clay Science* 7: 129–138.

Zehnder, K. & A. Arnold 1984. *Studies in Conservation* 29: 32–34.

4.7 Appendix — References for solubility database

4.7.1 Existing compilations

D'Ans, J. 1933. *Die Lösungsgleichgewichte der Systeme der Salze ozeanischer Salzablagerungen.* Verlagsgesellschaft für Ackerbau, Berlin.

Linke, W. F. 1965. *Solubilities. Inorganic and Metal-Organic Compounds.* American Chemical Society, Washington D.C.

Silcock, H. L. 1979. *Solubilities of inorganic and organic compounds. Volume 3. Ternary and multicomponent systems of inorganic substances.* Pergamon Press, Oxford.

Stephen, H. & T. Stephen 1964. *Solubilities of inorganic and organic compounds. Volume II. Ternary systems.* Pergamon Press, Oxford.

4.7.2 References

Agaev, A. I., A. A. Mamedov & F. A. Mamedov 1976. 'The K, Mg//Cl, NO_3+H_2O system at −30°, −20°, −10° and 0°C.' *Russ. J. Inorg. Chem.* 21: 1850–1855.

Assarsson, G. O. 1950a. 'Equilibria in aqueous systems containing K^+, Na^+, Ca^{+2}, Mg^{+2} and Cl^-. I. The ternary system $CaCl_2$–KCl–H_2O.' *J. Am. Chem. Soc.* 72: 1433–1436.

Assarsson, G. O. 1950b. 'Equilibria in aqueous systems containing K^+, Na^+, Ca^{+2}, Mg^{+2} and Cl^-. II. The quaternary system $CaCl_2$–KCl–$NaCl$–H_2O.' *J. Am. Chem. Soc.* 72: 1437–1441.

Assarsson, G. O. 1950c. 'Equilibria in aqueous systems containing K^+, Na^+, Ca^{+2}, Mg^{+2} and Cl^-. III. The ternary system $CaCl_2$–$MgCl_2$–H_2O.' *J. Am. Chem. Soc.* 72: 1442–1444.

Autenrieht, H. & G. Braune 1960. 'Weitere Untersuchungen im stabilen und metastabilen Gebiet des reziproken Salzpaares Na_2Cl_2+$MgSO_4$+H_2O bei Sättigung an NaCl.' *Kali + Steinsalz* 3: 85–97.

Babenko, A. M. & A. M. Andrianov 1981. '$KHCO_3$–KNO_3–H_2O system.' *Russ. J. Inorg. Chem.* 26: 261–264.

Barbaudy, J. 1923. 'Note sur l'équilibre eau — chlorure de potassium — nitrate de potassium, nitrate de calcium et chlorure de calcium.' *Rec. Trav. Chim.* 42: 638–642.

Benrath, A. 1928. 'Über das reziproke Salzpaar $MgSO_4$–$Na_2(NO_3)_2$–H_2O. I.' *Z. Anorg. Chem.* 170: 257–287.

Benrath, A. 1943. 'Über die Löslichkeit von Salzen und Salzgemischen bei Temperaturen oberhalb von 100°. V.' *Z. Anorg. Chem.* 252: 86–94.

Benrath, A. & H. Benrath 1929. 'Das reziproke Salzpaar $MgSO_4$+$K_2(NO_3)_2$= $Mg(NO_3)_2$+K_2SO_4. I.' *Z. Anorg. Chem.* 184: 359–368.

Benrath, A. & H. Benrath 1930. 'Das reziproke Salzpaar $MgSO_4$+$K_2(NO_3)_2$= $Mg(NO_3)_2$+K_2SO_4. II.' *Z. Anorg. Chem.* 189: 72–81.

Benrath, A. & H. Schackmann 1934. 'Über scheinbare Mischkristalle. I.' *Z. Anorg. Allg. Chem.* 218: 139–145.

Benrath, A. & A. Sichelschmidt 1931. 'Das reziproke Salzpaar $MgSO_4$+ $K_2(NO_3)_2$=$Mg(NO_3)_2$+K_2SO_4. III.' *Z. Anorg. Chem.* 197: 113 128.

Bergmann, A. G. & L. V. Opredelenkova 1969. 'Solubility polytherms of the calcium nitrate-potassium nitrate-water and calcium nitrate-potassium chloride-water ternary systems.' *Russ. J. Inorg. Chem.* 14: 1144–1146.

Bergmann, A. G. & L. F. Shulyak 1973. 'The KNO_3–$NaNO_3$–H_2O system.' *Russ. J. Inorg. Chem.* 18: 731–734.

Bodländer, G. 1891b. 'Über die Löslichkeit von Salzgemischen in Wasser.' *Z. Phys. Chem.* 7: 358–366.

Bogoyavlenskii, P. S. & E. D. Gashpar 1973. 'The $KHCO_3$–KNO_3–H_2O system at 0°, 25°, and 40°C.' *Russ. J. Inorg. Chem.* 18: 1662–1663.

Caspari, W. A. 1924. 'The system sodium carbonate-sodium sulphate-water.' *J. Chem. Soc.* 125: 2381–2387.

Chrétien, A. 1929. 'Étude du système quaternaire. Eau, nitrate de sodium, chlorure de sodium, sulfate de sodium.' *Ann. Chim.* 12: 9–155.

Clarke, L. & E. P. Partridge 1934. 'Potassium sulfate from syngenite by high-temperature extraction with water.' *Ind. Eng. Chem.* 26: 897–903.

Cornec, E. & H. Krombach 1929. 'Contribution a l'étude des équilibres entre l'eau, les nitrates, les chlorures et les sulfates de sodium et de potassium.' *Ann. Chim.* 12: 203–295.

Cornec, E. & H. Krombach 1932. 'Équlibres entre le chlorure de potassium, le chlorure de sodium et l'eau depuis −23° jusqu'a +190°.' *Ann. Chim.* 18: 5–31.

D'Ans, J. 1933. *Die Lösungsgleichgewichte der Systeme der Salze ozeanischer Salzablagerungen.* Verlagsgesellschaft für Ackerbau, Berlin.

Dejewska, B. 1992. 'The distribution coefficient of isomorphous admixtures for KCl–KBr–H_2O, K_2SO_4–$(NH_4)_2SO_4$–H_2O and KNO_3–NH_4NO_3–H_2O systems at 298K.' *Cryst. Res. Technol.* 27: 385–394.

Denman, W. L. 1961. 'Maximum re-use of cooling water based on gypsum content and stability.' *Ind. Eng. Chem.* 53: 817–822.

Ehret, W. F. 1932. 'Ternary systems $CaCl_2$–$Ca(NO_3)_2$–H_2O(25°), $CaCl_2$-$Ca(ClO_3)_2$–H_2O(25°), $SrCl_2$–$Sr(NO_3)_2$–H_2O(25°), KNO_3–$Pb(NO_3)_2$–H_2O(0°).' *J. Am. Chem. Soc.* 54: 3126–3134.

Emons, H. H., D. Dümke & M. Förtsch 1966. 'Untersuchungen an Systemen aus Salzen und gemischten Lösungsmitteln. II. Die Systeme Natriumchlorid bzw. Kaliumchlorid, Methanol – Wasser und Natriumchlorid - Kaliumchlorid – Methanol – Wasser.' *Wiss. Z. Techn. Hochschule Chem. "Carl Schorlemmer" Leuna Merseburg* 8: 195–200.

Emons, H. H. & H. Röser 1967. 'Die Beeinflussung der Systeme Kaliumsulfat- bzw. Natriumsulfat-Alkohol-Wasser durch Zusatz von Natrium- oder Kaliumchlorid.' *Z. Anorg. Allg. Chem.* 353: 135–147.

Emons, H. H., H. Röser & E. Roschke 1970. 'Das Verhalten des reziproken Salzpaares $Na_2SO_4+2KCl=K_2SO_4+2NaCl$ in Methanol-Wasser-Mischungen.' *Z. Anorg. Allg. Chem.* 375: 281–290.

Erdös, E. & Z. Jiru 1960. 'Solubility of electrolytes. V. The quinary system potassium sulfate-potassium chloride-potassium nitrate-potassium bromate-water.' *Coll. Czech. Chem. Commun.* 25: 1720–1728.

Euler, H. 1904. 'Über Löslichkeitserniedrigungen.' *Z. Phys. Chem.* 49: 303–316.

Fedotieff, P. P. 1904. 'Der Ammoniaksodaprozess vom Standpunkte der Phasenlehre.' *Z. Phys. Chem.* 49: 162–188.

Flatt, R. & P. Bocherens 1962. 'Sur le système ternaire Ca^{++}–K^+–NO_3^-–H_2O.' *Helv. Chim. Acta* 45: 187–195.

Flatt, R., G. Brunisholz & R. Muhlethaler 1961. 'Contribution à l'étude du système quinaire Ca^{++}–NH_4^+–H^+–NO_3^-–PO_4^-–H_2O. XX. La polytherme de saturation du système ternaire Ca^{++}–NH_4^+–NO_3–H_2O de 0° à 75°.' *Helv. Chim. Acta* 44: 1582–1595.

Flatt, R. & P. Fritz 1950. 'Contribution á l'étude dy système quinaire Ca^{++}–NH_4^+–H^+–NO_3^-–PO_4^-–H_2O. II. Les système ternaires limites Ca^{++}–H^+–NO_3^-–H_2O, NH_4^+–H^+–NO_3^-–H_2O et Ca^{++}–NH_4^+–NO_3^-–H_2O à 25°.' *Helv. Chim. Acta* 33: 2045–2056.

Foote, H. W. 1925. 'The system sodium nitrate-sodium-sulphate-water, and the minerals darapskite and nitroglauberite.' *Am. J. Sci.* 9: 441–447.

Frolov, A. A., V. T. Orlova & I. N. Lepeshkov 1992. 'Solubility polytherm of the system $Ca(NO_3)_2$–$Mg(NO_3)_2$–H_2O.' *Inorg. Mat.* 28: 1040–1042.

Frowein, F. 1928. 'Das System $K_2/Ca/Na_2/(NO_3)_2/H_2O$.' *Z. Anorg. Chem.* 169: 336–344.

Frowein, F. & E. von Mühlendahl 1926. 'Die Lösungen des doppelt-ternären Salzgemisches $(K_2/Mg/Na_2)((NO_3)_2/Cl_2)$ und ihre Bedeutung für die Technik.' *Z. Angew. Chem.* 39: 1488–1500.

Galushkina, R. A. & A. G. Bergmann 1962. 'Polythermal diagram of the KNO_3–K_2SO_4–H_2O system.' *Russ. J. Inorg. Chem.* 7: 1165–1167.

Galushkina, R. A. & A. G. Bergmann 1973. 'Solubility polytherms of the K_2SO_4–$(NH_4)_2SO_4$–H_2O and KNO_3–$(NH_4)_2SO_4$–H_2O systems.' *Russ. J. Inorg. Chem.* 18: 133–135.

Hamid, M. A. 1926. 'Heterogeneous equilibria between the sulphates and nitrates of sodium and potassium and their aqueous solutions. Part I. The ternary systems.' *J. Chem. Soc.* 128: 199–205.

Hill, A. E. 1934. 'Ternary systems. XIX. Calcium sulfate, potassium sulfate and water.' *J. Am. Chem. Soc.* 56: 1071–1078.

Hill, A. E. & F. W. Miller 1927. 'Ternary systems. IV. Potassium carbonate, sodium carbonate and water.' *J. Am. Chem. Soc.* 49: 669–686.

Hill, A. E. & S. Moskowitz 1929. 'Ternary systems. VIII. Potassium carbonate, potassium sulfate and water at 25°.' *J. Am. Chem. Soc.* 51: 2396–2398.

Hill, A. E. & S. B. Smith 1929. 'Equilibrium between the carbonates and bicarbonates of sodium and potassium in aqueous solution at 25°.' *J. Am. Chem. Soc.* 51: 1626–1636.

Hill, A. E. & N. S. Yanick 1935. 'Ternary system. XX. Calcium sulfate, ammonium sulfate and water.' *J. Am. Chem. Soc.* 57: 645–651.

Holluta, J. & S. Mautner 1927. 'Untersuchungen über die Löslichkeitsbeeinflussung starker Elektrolyte. I. Die gegenseitige Löslichkeitsbeeinflussung gleichioniger Alkalisalze. 1. Teil.' *Z. Phys. Chem.* 127: 455–475.

Igelsrud, I. & T. G. Thompson 1936. 'Equilibria in saturated solutions of salts occurring in sea water. I. The ternary system $MgCl_2$–KCl–H_2O, $MgCl_2$–$CaCl_2$–H_2O, $CaCl_2$–KCl–H_2O and $CaCl_2$–$NaCl$–H_2O at 0°.' *J. Am. Chem. Soc.* 58: 318–322.

Jackman, D. N. & A. Browne 1922. 'The 25°-Isotherms of the systems magnesium nitrate-sodium nitrate-water and magnesium sulphate-magnesium nitrate-water.' *J. Chem. Soc.* 121: 694–697.

Jänecke, E. 1911. 'Über die Bildung von Konversionssalpeter vom Standpunkt der Phasenlehre.' *Z. Anorg. Chem.* 71: 1–18.

Jänecke, E. 1929. 'Über das reziproke Salzpaar $2NH_4NO_3+K_2SO_4=2KNO_3+(NH_4)_2SO_4$ und seine wässerigen Lösungen.' *Z. Angew. Chem.* 42: 1169–1172.

Jänecke, E., H. Hamacher & E. Rahlfs 1932. 'Über das System KNO_3–NH_4NO_3–H_2O.' *Z. Anorg. Chem.* 206: 357–368.

Karakhanyan, S. S., E. A. Sayamian, J. P. Yeghiazarian, T. I. Karapetian & G. T. Mirzoyan 1987. 'A study of components interaction in $Na_2CO_3+Ca(NO_3)_2=CaCO_3+2NaNO_3$–$H_2O$ reversible system at 25°C.' *Arm. Khim. Zh.* 40: 214–221.

Kosterina, V. I., A. A. Ponizovskii, E. A. Konstantinova, V. T. Orlova & I. N. Leperhkov 1985. 'The KNO_3–$Ca(NO_3)_2$–H_2O system at 55°C.' *Russ. J. Inorg. Chem.* 30: 129–131.

Kremann, R. & H. Rodemund 1914. 'Über einige doppelte Umsetzungen des als Nebenprodukt des Leblanc'schen Sodaverfahrens abfallenden Calciumthiosulfates vom Standpunkte des Massenwirkungsgesetzes und der Phasenlehre.' *Monatshefte f. Chem.* 35: 1061–1113.

Kudryashova, O. S., L. P. Filippova, S. F. Kudryashov, T. A. Kulikova & E. N. Boyarintseva 1996. 'System K^+, NH_4^+ // NO_3^-, Cl^-–H_2O.' *Russ. J. Inorg. Chem.* 41: 1474–1488.

Lightfoot, W. J. & C. F. Prutton 1946. 'Equilibria in saturated solutions. I. The ternary systems $CaCl_2$–$MgCl_2$–H_2O, $CaCl_2$–KCl–H_2O, and $MgCl_2$–KCl–H_2O at 35°.' *J. Am. Chem. Soc.* 68: 1001–1002.

Lightfoot, W. J. & C. F. Prutton 1947. 'Equilibria in saturated solutions. II. The ternary systems $CaCl_2$–$MgCl_2$–H_2O, $CaCl_2$–KCl–H_2O and $MgCl_2$–KCl–H_2O at 75°.' *J. Am. Chem. Soc.* 69: 2098–2100.

Madgin, W. M. & D. A. Swales 1956. 'Solubilities in the system $CaSO_4$–NaCl–H_2O at 25° and 35°.' *J. Appl. Chem.* 6: 482–487.

Makin, A. V. 1959. 'A study of the system $NaNO_3$–Na_2SO_4–H_2O at 25°C.' *Russ. J. Inorg. Chem.* 4: 538–542.

Mamedov, F. A., S. M. Novruzov & M. M. Ramazanzade 1988. 'Potassium chloride - potassium nitrate - water ternary system at 50°.' *Azerb. Khim. Zh.* pp. 92–95.

Massink, A. 1916. 'Doppelsalzbildung zwischen Nitraten und Sulfaten in wässeriger Lösung.' *Z. Phys. Chem.* 92: 351–380.

Meyer, T. A., C. F. Prutton & W. J. Lightfoot 1949. 'Equilibria in saturated salt solutions. V. The quinary system $CaCl_2$–$MgCl_2$–KCl–NaCl–H_2O at 35°.' *J. Am. Chem. Soc.* 71: 1236–1237.

Meyerhoffer, W. & A. P. Saunders 1899a. 'Über reziproke Salzpaare II. Die Gleichgewichtserscheinungen reziproker Salzpaare bei gleichzeitiger Anwesenheit eines Doppelsalzes. I. Teil.' *Z. Phys. Chem.* 28: 453–493.

Meyerhoffer, W. & A. P. Saunders 1899b. 'Über reziproke Salzpaare II. Die Gleichgewichtserscheinungen reziproker Salzpaare bei gleichzeitiger Anwesenheit eines Doppelsalzes. II. Teil.' *Z. Phys. Chem.* 31: 370–389.

Nikolajew, W. I. 1929. 'Die Verteilung starker Basen und starker Säuren in gesättigten wässrigen Lösungen.' *Z. Anorg. Allg. Chem.* 181: 249–279.

Perova, A. P. 1970. 'Crystallisation regions of schönite, leonite, and kainite in the Ca, K, Mg // Cl, SO_4–H_2O quinary system at 25° and 55°C.' *Russ. J. Inorg. Chem.* 15: 989–991.

Pilipchenko, V. N. & V. G. Shevchuk 1969. 'The $MgSO_4$–$(NH_4)_2SO_4$–Na_2SO_4–H_2O system at 50°C.' *Russ. J. Inorg. Chem.* 14: 430–432.

Pinaevskaya, E. N., N. L. Antoshkina & G. G. Guseva 1961. 'Investigation of the aqueous reciprocal system of sodium and calcium chromates and nitrates.' *J. Appl. Chem. USSR* 34: 1642–1656.

Poletaev, I. F. & L. V. Krasnenkova 1975. 'The Na^+, Rb^+ // NO_3^-, SO_4^{2-}–H_2O and Cs^+, Na^+ // NO_3^-, SO_4^{2-}–H_2O systems at 25° and 75°C.' *Russ. J. Inorg. Chem.* 20: 1250–1252.

Prutton, C. F. & O. F. Tower 1932. 'The system calcium chloride-magnesium chloride-water at 0, −15 and −30°.' *J. Am. Chem. Soc.* 54: 3040–3047.

Reinders, W. 1915. 'Die reziproken Salzpaare $KCl+NaNO_3=KNO_3+NaCl$ und die Bereitung von Konversionssalpeter.' *Z. Anorg. Chem.* 93: 202–212.

Saslawsky, A. J. & J. L. Ettinger 1935. 'Gemeinsame Löslichkeit der Aluminium-, Natrium, Kalium- und Eisennitrate im Wasser in Gegenwart von Salpetersäure.' *Z. Anorg. Allg. Chem.* 223: 277–287.

Schröder, W. 1929a. 'Über das reziproke Salzpaar $MgSO_4$–$Na_2(NO_3)_2$–H_2O. II.' *Z. Anorg. Chem.* 177: 71–85.

Schröder, W. 1929b. 'Über das reziproke Salzpaar $MgSO_4$–$Na_2(NO_3)_2$–H_2O. III.' *Z. Anorg. Chem.* 184: 63–76.

Schröder, W. 1930. 'Über das reziproke Salzpaar $MgSO_4$–$Na_2(NO_3)_2$–H_2O. V.' *Z. Anorg. Chem.* 185: 153–166.

Seidell, A. 1902. 'Solubility of mixtures of sodium sulphate and sodium chloride.' *Am. Chem. J.* 27: 52–62.

Seidell, A. & J. G. Smith 1904. 'The solubility of calcium sulphate in solutions of nitrates.' *J. Phys. Chem.* 8: 493–499.

Shevchuk, V. G. & R. A. Avarina 1965. 'The Li_2SO_4–$MgSO_4$–$(NH_4)_2SO_4$–H_2O system at 25°.' *Russ. J. Inorg. Chem.* 10: 1531–1532.

Shevchuk, V. G. & L. L. Kost' 1964. 'Equilibrium in the Cs_2SO_4–$MgSO_4$–H_2O and $(NH_4)_2SO_4$–$MgSO_4$–H_2O systems at 35°.' *Russ. J. Inorg. Chem.* 9: 235–237.

Shevchuk, V. G. & V. I. Omelyan 1990. 'The KNO_3–$Mg(NO_3)_2$–$Yb(NO_3)_3$–H_2O system at 25°C.' *Russ. J. Inorg. Chem.* 35: 420–421.

Shevchuk, V. G. & V. N. Pilipchenko 1968a. 'The $MgSO_4$–$(NH_4)_2SO_4$–Na_2SO_4–H_2O system at 0°C.' *Russ. J. Inorg. Chem.* 13: 1045–1047.

Shevchuk, V. G. & V. N. Pilipchenko 1968b. 'The $MgSO_4$–$(NH_4)_2SO_4$–Na_2SO_4–H_2O system at 25°C.' *Russ. J. Inorg. Chem.* 13: 1479–1480.

Shevchuk, V. G., V. N. Pilipchenko & V. N. Yukhimets 1969. 'The $MgSO_4$–$(NH_4)_2SO_4$–Na_2SO_4–H_2O system at 75°C.' *Russ. J. Inorg. Chem.* 14: 870–871.

Sieverts, A. & E. L. Müller 1931. 'Das reziproke Salzpaar $MgCl_2$, $Na_2(NO_3)_2$, H_2O. II.' *Z. Anorg. Chem.* 200: 305–320.

Sieverts, A. & H. Müller 1930. 'Das reziproke Salzpaar $MgCl_2$, $Na_2(NO_3)_2$, H_2O. I.' *Z. Anorg. Chem.* 189: 241–257.

Simková, H. & E. Erdös 1959. 'The solubility of electrolytes. III. The quaternary system sodium nitrate – sodium nitrite – sodium chloride – water.' *Coll. Czech. Chem. Commun.* 24: 694–699.

Smith, G. M. & T. R. Ball 1917. 'Heterogeneous equilibria between aqueous and metallic solutions. The interaction of mixed salt solutions and liquid amalgams. A study of the ionization relations of sodium and potassium chlorides and sulfates in mixtures.' *Am. Chem. J.* 39: 179–218.

Timoshenko, Y. M. 1986. 'The $NaNO_3$–KNO_3–NH_4NO_3–H_2O system at 25°C.' *Russ. J. Inorg. Chem.* 31: 1843–1844.

Timoshenko, Y. M. & I. N. Chekmareva 1989. 'The $NaNO_3$–NH_4NO_3–$Mg(NO_3)_2$–H_2O system at 25°C.' *Russ. J. Inorg. Chem.* 34: 1551–1552.

van't Hoff, J. H. 1905. 'Zur Bildung der ozeanischen Salzablagerungen.' *Z. Anorg. Chem.* 47: 244–280.

Vereshchagina, V. I., V. N. Derkacheva, L. F. Shulyak & L. V. Zolotareva 1973. '35°C solubility isotherms of the ternary aqueous systems based on potassium and calcium nitrates and chlorides.' *Russ. J. Inorg. Chem.* 18: 266–268.

Vereshchagina, V. I., L. V. Zolotareva & L. F. Shulyak 1969. 'The $CaCl_2$–$Ca(NO_3)_2$–$(KCl)_2$–$(KNO_3)_2$–H_2O system at 60°C.' *Russ. J. Inorg. Chem.* 14: 1787–1790.

Yakimov, M. A., E. I. Guzhavina & M. S. Lazeeva 1969. 'Solution-vapour equilibrium in calcium (cadmium) nitrate-alkali metal nitrate-water systems.' *Russ. J. Inorg. Chem.* 14: 1011–1014.

Yanat'eva, O. K. & V. T. Orlova 1959. 'Glaserite in the K, Na, Mg// Cl, SO_4–H_2O system at 0°C.' *Russ. J. Inorg. Chem.* 4: 861–864.

Yarym-Agaev, N. L., F. M. Klyashtornaya & V. Y. Rudin 1964. 'The aqueous system of potassium and sodium nitrates and chlorides: solubility isotherm of the salts at 75°.' *Russ. J. Inorg. Chem.* 9: 1423–1425.

Zhang, Y. & M. Muhammed 1989. 'Solubility of calcium sulfate dihydrate in nitric acid solutions containing calcium nitrate and phosphoric acid.' *J. Chem. Eng. Data* 34: 121–124.

5

A Thermodynamic Model of the Na^+–Ca^{2+}–Cl^-–CH_3COO^-–H_2O System

Michael Steiger, Roland Beyer, and Joachim Dorn

Institut für Anorganische und Angewandte Chemie, Universität Hamburg

5.1 Introduction

Calcium acetate has been frequently found as a major constituent of salt efflorescences on calcareous artifacts in wooden show cases in museums (*e.g.*, FitzHugh & Gettens 1971; Tennent & Baird 1985). Several different minerals containing calcium acetate have been identified, *i.e.*, different hydrated forms of calcium acetate and several double salts with calcium chloride and calcium formate. Gibson *et al.* (1997a,b) have recently found an unusual efflorescence characterised as calcium nitrate chloride acetate hydrate, $CaCl_2{\cdot}3Ca(OAc)_2{\cdot}2Ca(NO_3)_2{\cdot}14H_2O$. In order to understand the conditions for the formation of these minerals, solubility diagrams including a number of organic and inorganic salts are required. Major ions to be considered should preferably include Na^+, Ca^{2+}, Cl^-, NO_3^-, $HCOO^-$, and CH_3COO^-.

Unfortunately, the experimental data required for the parameterisation of these systems are not yet available. As has been pointed out before (Chapter 4), even the relevant data for the binary systems organic salt-water are lacking. Though, the vapour pressure measurements carried out in this project (Chapter 4) are sufficient for the parameterisation of the binary systems, there is still a lack of data for ternary mixtures. A complete parameterisation of complex salt mixtures containing the ions mentioned before is therefore not yet possible. As a reasonable first approach to understand the crystallisation properties of salt mixtures containing mixtures of organic and inorganic ions the Na^+–Ca^{2+}–Cl^-–CH_3COO^-–H_2O reciprocal system was selected. This system includes, both, the most common inorganic salt (sodium chloride), and the most important organic salt found in efflorescences on calcareous museum artifacts (calcium acetate).

This chapter provides a brief summary of the parameterisation of the Pitzer model equations for the Na^+–Ca^{2+}–Cl^-–CH_3COO^-–H_2O system. A more detailed description of the data evaluation and fitting procedure is provided elsewhere (manuscript in preparation).

5.2 Model parameterisation

To predict the crystallisation properties of mixed salt solutions the solubilities of mineral phases in the mixed system are required. In addition, the critical relative humidities at which a mixed solution becomes saturated with respect to one or more solid phases need to be known. A detailed description of the basic thermodynamic relations and the Pitzer model equations (Pitzer 1973, 1991) for electrolyte solutions is provided in Chapter 3. In the present treatment, a slightly different form of the equations was used.

The concentrations in the four binary systems for which a complete set of parameters is required to treat the Na^+–Ca^{2+}–Cl^-–CH_3COO^-–H_2O system extend to very high concentrations. Several extended forms of the Pitzer equations can be found in the literature to accurately reproduce experimental data of very concentrated solutions. The form of the equations described in Chapter 3 apply an ionic strength dependent third virial coefficient as suggested by Archer (1991). Here, we included the $\beta^{(2)}$ parameter in the expression for the second virial coefficient (*cf.* Chapter 3). Originally, the $\beta^{(2)}$ term was introduced by Pitzer & Mayorga (1974) for the treatment of the bivalent metal sulfates in order to avoid the explicit calculation of association equilibria. Later the $\beta^{(2)}$ term was used by Kodýtek & Dolejš (1986) to enhance the numerical flexibility by a slight adjustment of the original ionic strength dependence of B_{MX}. Including the $\beta^{(2)}$ term did also significantly improve the fits for aqueous $NaCl$, $CaCl_2$, and $NaCH_3COO$.

There are four binary systems for which a complete set of parameters is required to treat the Na^+–Ca^{2+}–Cl^-–CH_3COO^-–H_2O system. The equation used for $NaCl$(aq) is based on the very careful evaluation of the existing thermodynamic data by Archer (1992). His equation was used to generate a dataset of osmotic and activity coefficients which were fitted to the present set of equations, thus, adding the $\beta^{(2)}$ term instead of the ionic strength dependent third virial coefficient. The available data of thermodynamic properties of aqueous calcium chloride extend to very high concentrations. Attempts to represent the very complex behaviour of $CaCl_2$(aq) were found to be extremely difficult and the usual treatment fails at higher concentrations. Various approaches were used to establish equations valid to higher concentrations including extensions of the conventional Pitzer equations. The present treatment is largely based on osmotic and activity coefficients generated with existing equations (Holmes *et al.* 1994, 1997; Pitzer & Oakes 1994) and additional experimental data at subzero temperatures (Gibbard & Fong 1975; Oakes *et al.* 1990). These data can be reproduced with sufficient accuracy using a rather simple extension of the ionic strength dependence of the second virial coefficient by including a $\beta^{(2)}$ and a $\beta^{(3)}$ term.

There is a reasonable database of thermodynamic properties of aqueous sodium acetate including isopiestic vapour pressures, freezing and boiling temperatures, and thermal data (heats of dilution and heats of solution, heat capacities). These data were used along with our own vapour pressure data in one global fit to determine the binary interaction parameters of $NaCH_3COO$(aq). Much less thermodynamic data are available for aqueous calcium acetate. In fact, the properties of $Ca(CH_3COO)_2$(aq) at near ambient temperatures are largely determined by our own vapour pressure measurements. Due to solubility limitations the molality range does not extend above 2 mol kg^{-1} and the experimental data could be reproduced to within experimental error without inclusion of the $\beta^{(2)}$ term.

The calculation of mineral solubilities requires an expression for the temperature dependence of the thermodynamic solubility product, *i.e.*, the equilibrium constants of the dissolution reactions of the minerals. Given a salt mineral of general composition

$$M_{\nu_M} X_{\nu_X} \cdot \nu_0 H_2O \tag{5.1}$$

consisting of ν_M positive ions, M, of charge z_M, ν_X negative ions, X, of charge z_X and ν_0 molecules of water the equilibrium constant of the dissolution reaction:

$$M_{\nu_M} X_{\nu_X} \cdot \nu_0 H_2O \rightleftharpoons \nu_m M^{z_M} + \nu_X M^{z_X} + \nu_0 H_2O \tag{5.2}$$

Table 5.1: Salt minerals in the Na^+–Ca^{2+}–Cl^-–CH_3COO^-–H_2O system.

sodium acetate	$NaCH_3COO$
sodium acetate trihydrate	$NaCH_3COO{\cdot}3H_2O$
calcium acetate hemihydrate	$Ca(CH_3COO)_2{\cdot}0.5H_2O$
calcium acetate monohydrate	$Ca(CH_3COO)_2{\cdot}1H_2O$
halite	$NaCl$
hydrohalite	$NaCl{\cdot}2H_2O$
sinjarite	$CaCl2{\cdot}2H_2O$
calcium chloride tertahydrate	$CaCl_2{\cdot}4H_2O$
antarcticite	$CaCl_2{\cdot}6H_2O$
calclacite	$CaCl_2{\cdot}Ca(CH_3COO)_2{\cdot}10H_2O$

is given by:

$$\ln K = \nu_M \ln m_M + \nu_X \ln m_X + \nu_M \ln \gamma_M + \nu_X \ln \gamma_X + \nu_0 \ln a_w \tag{5.3}$$

where γ_M and γ_X represent the ion activity coefficients, and a_w is the water activity. Available experimental solubilities were used along with calculated activity coefficients and water activities at saturation molality to determine the values of the equilibrium constants, K, of the salt minerals listed in Table 5.1 at various temperatures. Subsequently, the univariant equilibria in the four binary systems were calculated using, both, the ion interaction parameters and the equilibrium constants. Calculated univariant curves for the chloride binary systems are depicted in Figs. 5.1 and 5.2, respectively. There is a large number of high quality experimental freezing point and solubility data available for these systems. The binary model parameterisation yields excellent fits to these data. The corresponding univariant curves for the acetate salts are shown in Chapter 4 (Figs. 4.8 and 4.9). Due to the scatter in the experimental solubility data, particularly in the instance of calcium acetate, there remains some uncertainty as discussed in Chapter 4.

Once the binary model parameters are known, the ternary parameters may be obtained from fits of appropriate equations to experimental solubilities in ternary systems with a common anion or cation, respectively. The ternary parameters θ and ψ account for the ion interactions in mixed electrolyte solutions (*cf.* Chapter 3). The parameters θ_{ij} account for interactions between pairs of ions of like sign. The parameters ψ_{ijk} are the third virial coefficient mixing parameters. They account for interactions between triplets of ions, *i.e.,* two different cations and an anion, or, two different anions and a cation, respectively. Values of the ternary mixing parameters, θ_{ij} and ψ_{ijk}, are obtained by fitting to experimental data, preferably solubilities. The logarithm of the solubility product for a mineral in a ternary solution containing three ions, i, j, and k, may be expressed as:

$$\ln K = \ln K_0 + R_1(m_i, m_j, m_k)\theta_{ij} + R_2(m_i, m_j, m_k)\psi_{ijk} \tag{5.4}$$

where $\ln K_0$ is the solubility product that is calculated if all terms in the equations for $\ln \gamma$ and $\ln a_w$ (eqs. 3.7 to 3.9) involving θ_{ij} and ψ_{ijk} are omitted. Hence, $R_1(m_i, m_j, m_k)$ and $R_2(m_i, m_j, m_k)$ are expressions involving all terms in θ_{ij} and ψ_{ijk}, where i and j refer to ions with charges of like sign, and k of opposite sign, respectively.

Experimental solubilities in the four ternary systems were used to determine the ternary interaction parameters. Solubilities in the $NaCl$–$CaCl_2$–H_2O system were

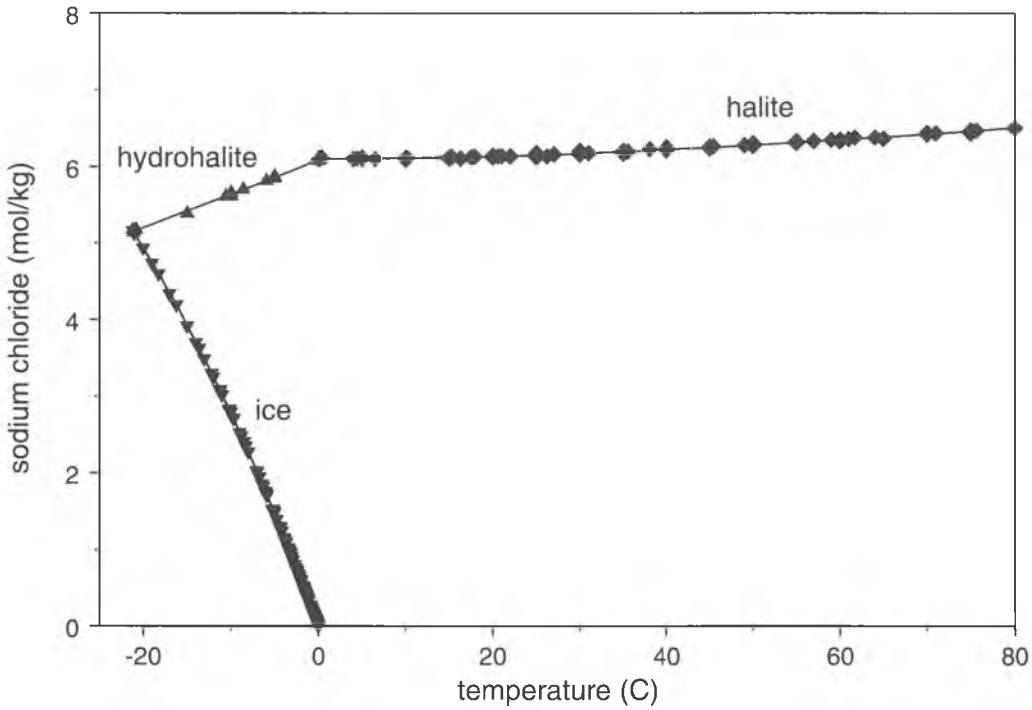

Figure 5.1: Experimental solubility and freezing point data and calculated univariant curves in the system $NaCl$–H_2O.

taken from the literature, whilst for the remaining ternaries we used our own solubility data. It was found that the temperature dependence of the mixing parameters could be neglected in the narrow temperature range relevant to this study (5–50°C). In general, there is good agreement between the measured and the calculated solubilities in the ternary systems. A typical example, the calculated and experimental solubilities in the Na^+–Ca^{2+}–CH_3COO^-–H_2O system at 5°C, may be found in Chapter 4 (Fig. 4.10).

5.3 Model results

Once that all binary and ternary interaction parameters and the equilibrium constants have been determined, the model can be used to calculate the equilibrium relative humidities, solubilities and crystallisation sequences for mixtures of any composition in the Na^+–Ca^{2+}–Cl^-–CH_3COO^-–H_2O reciprocal system. As an example, we have carried out some calculations for solutions containing $NaCl$ and $Ca(CH_3COO)_2$. Fig. 5.3 depicts the calculated solubilities at 25°C. Each point on the solubility curves represents the composition of a saturated solution with respect to one solid phase, either calcium acetate monohydrate or halite. There are no other stable solids in the $NaCl$–$Ca(CH_3COO)_2$–H_2O system at 25°C. The intersection of the two solubility curves represents the isothermal invariant equilibrium at 25°C giving the composition of the solution saturated with respect to both solids.

The crystallisation behaviour for different mixing ratios of the two salts can be simply derived from the solubility diagram. The crystallisation path of a dilute solution of composition A, an equimolar mixture of the two salts, is illustrated in Fig. 5.3. Decreasing the relative humidity, RH, would lead to the evaporation of water and the solution would become more concentrated (line AB). At point B the solution is

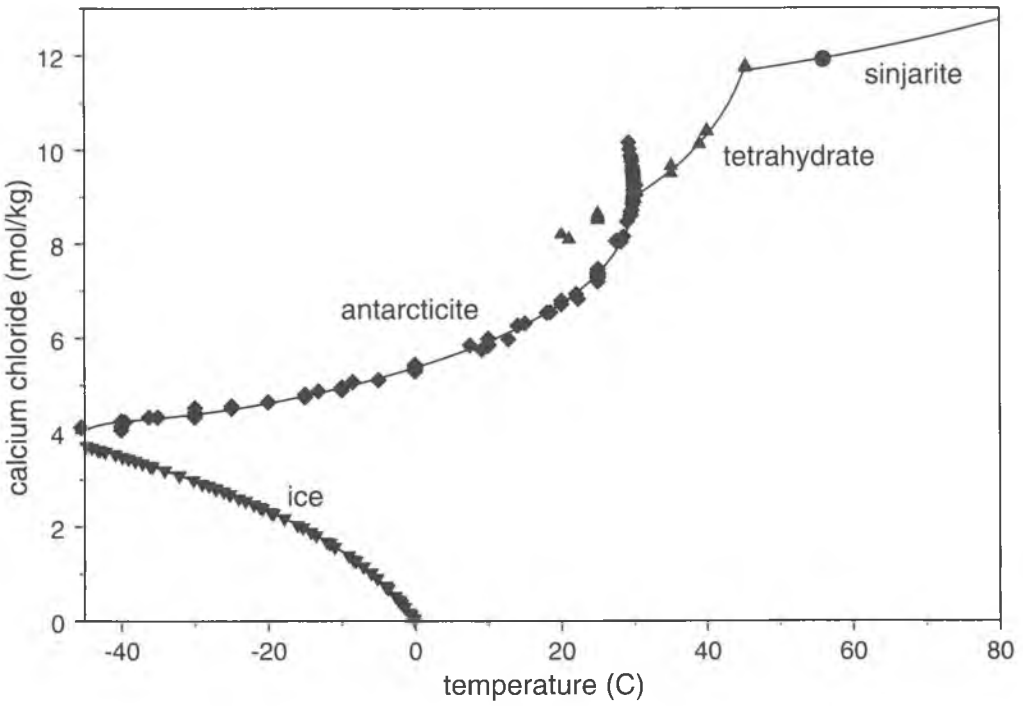

Figure 5.2: Experimental solubility and freezing point data and calculated univariant curves in the system $CaCl_2$–H_2O.

saturated with respect to $Ca(CH_3COO)_2{\cdot}1H_2O$, which would start to precipitate as the relative humidity is further decreased. The composition of the remaining solution then changes along the line BE. At point E any further removal of water would cause the simultaneous crystallisation of both, $Ca(CH_3COO)_2{\cdot}1H_2O$ and NaCl, and evaporation to complete dryness. The crystallisation humidities, *i.e.*, the critical humidity below which one solid starts to crystallise out, are shown in Fig. 5.4. They show the usual behaviour for mixtures of two salts.

Depending on the mixing ratio one of the two salts, $Ca(CH_3COO)_2{\cdot}1H_2O$ or NaCl, starts to crystallise out at a lower RH than the respective pure salt. The intersection of the two branches of the saturation humidity curve represents the drying point of the system. In contrast to a single salt, crystallisation of one solid from a mixture does not occur at a specific value but rather across a range of relative humidities. This is further illustrated by the crystallisation sequence of an equimolar mixture of the two salts as depicted in Fig. 5.5.

The crystallisation of calcium acetate monohydrate starts as the relative humidity drops below 86.0%. This value is considerably lower than the saturation humidity of pure calcium acetate at the same temperature (91.6%). As the relative humidity further decreases, more and more $Ca(CH_3COO)_2{\cdot}1H_2O$ crystallises out. Finally, at a relative humidity of 73.0% the solution is also saturated with halite. About 88% of the total calcium acetate in the mixture is now present as crystalline monohydrate, whilst all sodium chloride is still present as a concentrated solution. Any further decrease in the relative humidity, however, causes evaporation to dryness and the crystallisation of all sodium chloride and the remaining calcium acetate at the same time.

A similar calculation of the crystallisation behaviour is possible for any mixture composition in the Na^+–Ca^{2+}–Cl^-–CH_3COO^-–H_2O system and at temperatures

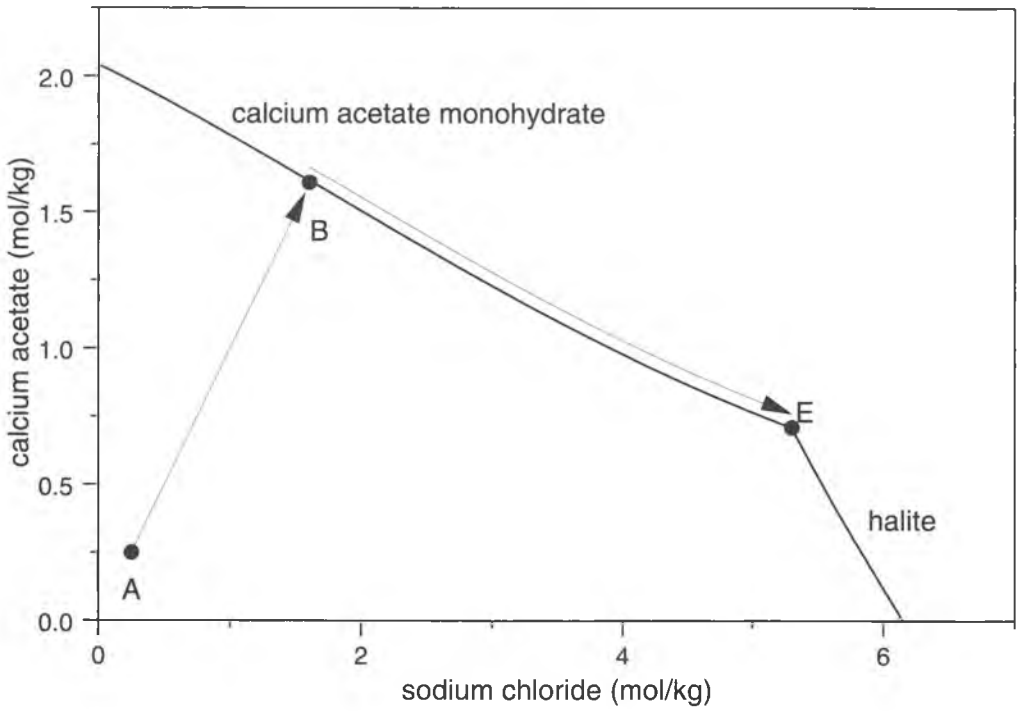

Figure 5.3: Solubilities in the system $NaCl–Ca(CH_3COO)_2–H_2O$ at 25°C.

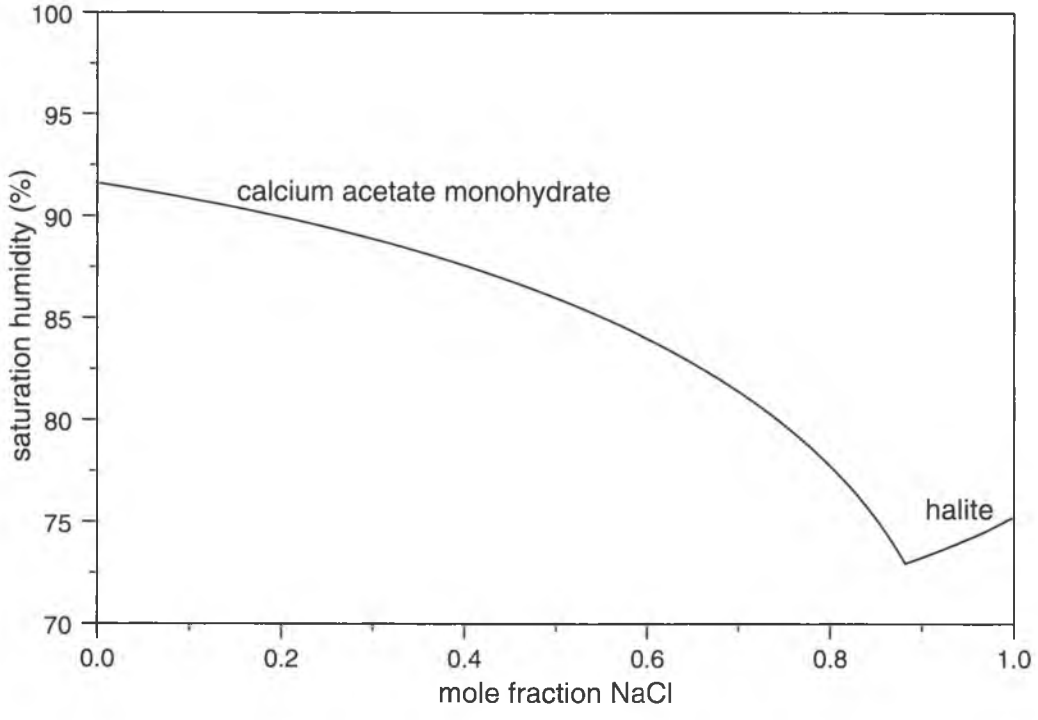

Figure 5.4: Saturation humidities in the system $NaCl–Ca(CH_3COO)_2–H_2O$ at 25°C.

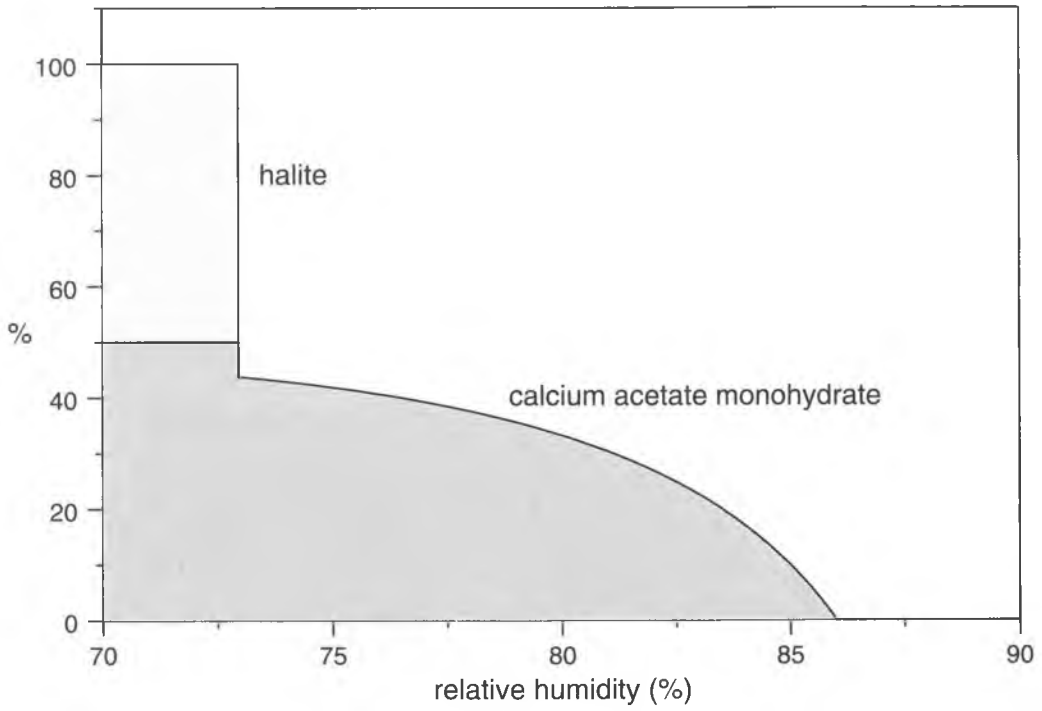

Figure 5.5: Crystallisation sequence of equimolar mixture of NaCl and $Ca(CH_3COO)_2$ at 25°C.

from about 5°C to 50°C. The extension of this model including more ions, *e.g.*, nitrate and formate, will have to be the subject of future research.

5.4 References

ARCHER, D. G. 1991. *J. Phys. Chem. Ref. Data* 20: 509–555.

ARCHER, D. G. 1992. *J. Phys. Chem. Ref. Data* 21: 793–829.

FITZHUGH, E. W. & R. J. GETTENS 1971. *In* R. Brill (ed.), *Science and Archaeology*, pp. 91–102. MIT Press, Cambridge, Mass.

GIBBARD, H. F. & S. L. FONG 1975. *J. Solution Chem.* 4: 863–872.

GIBSON, L. T., B. G. COOKSEY, D. LITTLEJOHN & N. H. TENNENT 1997a. *Anal. Chim. Acta* 337: 151–164.

GIBSON, L. T., B. G. COOKSEY, D. LITTLEJOHN & N. H. TENNENT 1997b. *Anal. Chim. Acta* 337: 253–264.

HOLMES, H. F., R. H. BUSEY, J. M. SIMONSON & R. E. MESMER 1994. *J. Chem. Thermodyn.* 26: 271–298.

HOLMES, H. F., J. M. SIMONSON & R. E. MESMER 1997. *J. Chem. Thermodyn.* 29: 1363–1373.

KODÝTEK, V. & V. DOLEJŠ 1986. *Z. Phys. Chem. Leipzig* 267: 743–746.

Oakes, C. S., R. J. Bodnar & J. M. Simonson 1990. *Geochim. Cosmochim. Acta* 54: 603–610.

Pitzer, K. S. 1973. 'Thermodynamics of electrolytes, I. Theoretical basis and general equations.' *J. Phys. Chem.* 77: 268–277.

Pitzer, K. S. 1991. *In* K. S. Pitzer (ed.), *Activity Coefficients in Electrolyte Solutions*, pp. 75–154. CRC Press, Boca Raton.

Pitzer, K. S. & G. Mayorga 1974. *J. Solution Chem.* 3: 539–546.

Pitzer, K. S. & C. S. Oakes 1994. *J. Chem. Eng. Data* 39: 553–559.

Tennent, N. H. & T. Baird 1985. *Studies in Conservation* 30: 73–85.

6
Total Volumes of Crystalline Solids and Salt Solutions

Michael Steiger
Institut für Anorganische und Angewandte Chemie, Universität Hamburg

6.1 Introduction

The total volume of interstitial salts and pore solutions is an important quantity required for studies of salt damage to porous materials. The calculation of total volumes requires both, the assembly of a database of mineral densities, or crystal volumes, and an appropriate model to calculate the densities of aqueous electrolyte solutions.

The Pitzer ion interaction approach is a set of equations to calculate thermodynamic properties of aqueous electrolyte solutions. The model was introduced more than twenty years ago (Pitzer 1973) and, since then, found wide acceptance and was applied in a number of research areas (*e.g.*, Clegg & Whitfield 1991; Harvie & Weare 1980). Applied to pore solutions in porous building materials the model can be used to predict the relevant phase changes. The ion interaction approach is also suitable to calculate the density of pore solution (Monnin 1989; Pitzer 1991; Rogers & Pitzer 1982) which are required to calculate the total volumes of pore solutions and interstitial salts. This chapter presents the database of molar volumes of salt minerals as it is used by ECOS. Also, a brief summary of the parameterisation and validation of the Pitzer model for the densities of mixed solutions is summarised.

6.2 Molar volumes of salt minerals

The database of molar volumes, V_M, of salt minerals is listed in Tables 6.1 and 6.2. Most of the data were collected from existing compilations (Broul *et al.* 1981; JCPDS 1991; Lide 1995; Robie *et al.* 1978). There are only few data of the thermal expansion of salt minerals. However, existing data show that the changes in volume in the temperature range of interest do probably not exceed 0.5%. Hence, for the purpose of this project this relatively minor effect of temperature on the molar volumes of salt minerals was neglected.

For some minerals no molar volume data are available. In these cases the molar volumes had to be estimated. For example, no volume data of some hydrated salts were found in the literature. In these cases, the volumes were estimated assuming that the contribution of each molecule of water is approximately the same. This approach is illustrated in Fig. 6.1 for the various hydrous forms of $MgCl_2{\cdot}nH_2O$ and $Mg(NO_3)_2{\cdot}nH_2O$, respectively. The plots of the tabulated molar volumes versus the number of hydration waters show a linear trend. Hence, the missing volumes for $MgCl_2{\cdot}8H_2O$ and $Mg(NO_3)_2{\cdot}9H_2O$ were estimated from the linear fits shown in Fig. 6.1.

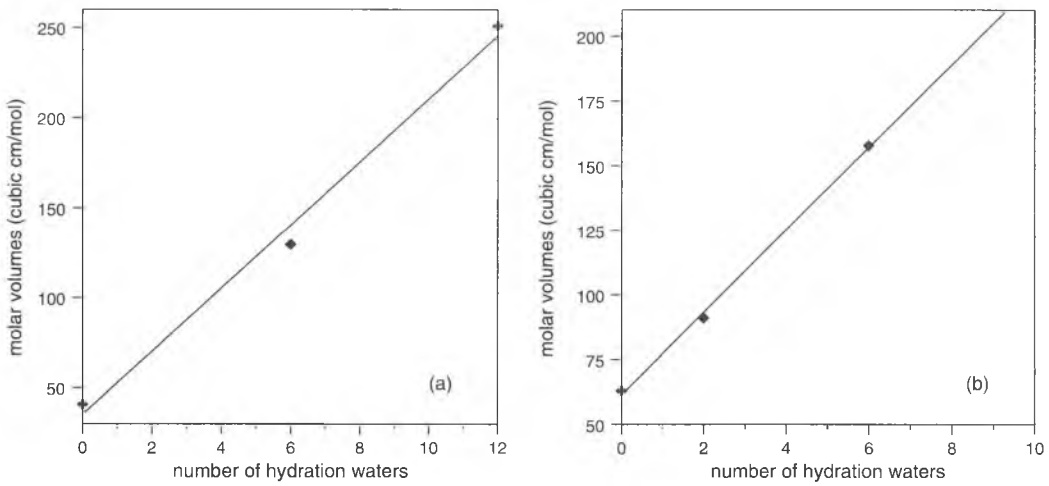

Figure 6.1: Molar volumes of (a) $MgCl_2 \cdot nH_2O$ and (b) $Mg(NO_3)_2 \cdot nH_2O$. Symbols represent tabulated data from sources given in Tables 6.1 and 6.2, lines are best linear fits to these data.

Missing volumes of double salts were simply calculated as the appropriate sum of the molar volumes of two single salts. For example, the molar volume of labile salt, $2Na_2SO_4 \cdot CaSO_4 \cdot 2H_2O$, was calculated as the stoichiometric sum of the volumes of thenardite, Na_2SO_4, and gypsum, $CaSO_4 \cdot 2H_2O$. Hence:

$$V_M(\text{labile salt}) = 2V_M(\text{thenardite}) + V_M(\text{gypsum}) \tag{6.1}$$

Molar volumes of hydrated double salts the composition of which could not be simply reproduced as the sum of two single salts were approximately calculated including the molar volume of ice. For example, the molar volume of ammonium pentasalt, $5CaSO_4 \cdot (NH_4)_2SO_4 \cdot 2H_2O$, was calculated from the molar volumes of anhydrite, $CaSO_4$, mascagnite, $(NH_4)2SO_4$, and ice, respectively. In order to test this simple approach molar volumes for a number of double salts were calculated and compared to tabulated values. The results are depicted in Fig. 6.2. It can be seen that the agreement is sufficient for the purpose of the present project.

6.3 The Pitzer model equations for the volume properties

There are several comprehensive reviews of the particular form of the Pitzer equations used to calculate the volumetric properties of multiple-solute electrolyte solutions (Krumgalz *et al.* 1995; Monnin 1989). Briefly, the total volume, V, of an electrolyte solution is given as:

$$V = 1000\nu_W + \sum_i m_i \overline{V}_i^\circ + V^{ex} \tag{6.2}$$

where ν_W is the specific volume of water; m_i and $\overline{V}_i^\circ$ are the molalities and partial molal volumes at infinite dilution of the ions, i, in solution; V^{ex} is the excess volume of the mixed solution. For binary solutions it is more convenient to use the apparent molal volume, ${}^\phi V_{MX}$, which is defined as:

$${}^\phi V_{MX} = \frac{V - 1000\nu_W}{m} = \overline{V}_{MX}^\circ + \frac{V^{ex}}{m} \tag{6.3}$$

Table 6.1: Molar volumes, V_M, of single salt minerals; units are $cm^3\ mol^{-1}$.

	formula	mineral name	V_M	ref.[a]
1	H_2O	ice	19.65	(1)
2	$NaCl$	halite	27.02	(1)
3	$NaCl{\cdot}2H_2O$	hydrohalite	43.64	(1)
4	$NaNO_3$	nitratine	37.60	(1)
5	Na_2SO_4	thenardite	53.11	(1)
6	$Na_2SO_4{\cdot}0H_2O$	mirabilite	219.8	(1)
7	$NaHCO_3$	nahcolite	37.99	(2)
8	$Na_2CO_3{\cdot}H_2O$	thermonatrite	55.11	(3)
9	$Na_2CO_3{\cdot}7H_2O$	sodium carbonate heptahydrate	153.7	(2)
10	$Na_2CO_3{\cdot}10H_2O$	natron	196.0	(2)
11	KCl	sylvite	37.52	(1)
12	KNO_3	niter	48.04	(1)
13	K_2SO_4	arcanite	65.50	(1)
14	$K_2SO_4{\cdot}H_2O$	potassium sulfate hydrate	74.24	(4)
15	$KHCO_3$	kalicinite	46.14	(2)
16	$K_2CO_3{\cdot}3/2H_2O$	potassium carbonate hydrate	76.67	(2)
17	$K_2CO_3{\cdot}6H_2O$	potassium carbonate hexahydrate	126	(5)
18	$MgCl_2{\cdot}6H_2O$	bischofite	129.6	(2)
19	$MgCl_2{\cdot}8H_2O$	magnesium chloride octahydrate	176	(5)
20	$MgCl_2{\cdot}12H_2O$	magnesium chloride dodecahydrate	251.1	(4)
21	$Mg(NO_3)_2{\cdot}2H_2O$	magnesium nitrate dihydrate	90.99	(2)
22	$Mg(NO_3)_2{\cdot}6H_2O$	nitromagnesite	157.7	(2)
23	$Mg(NO_3)2.9H_2O$	magnesium hydrate enneahydrate	205	(5)
24	$MgSO_4{\cdot}1H_2O$	kieserite	53.85	(2)
25	$MgSO_4{\cdot}4H_2O$	leonhardtite	95.87	(3)
26	$MgSO_4{\cdot}6H_2O$	hexahydrite	132.6	(3)
27	$MgSO_4{\cdot}7H_2O$	epsomite	146.8	(3)
28	$CaCl_2{\cdot}2H_2O$	sinjarite	79.47	(3)
29	$CaCl_2{\cdot}4H_2O$	calcium chloride tetrahydrate	100.2	(2)
30	$CaCl_2{\cdot}6H_2O$	antarcticite	128.0	(2)
31	$Ca(NO_3)_2{\cdot}2H_2O$	calcium nitrate dihydrate	100.1	(2)
32	$Ca(NO_3)_2{\cdot}3H_2O$	calcium nitrate trihydrate	115.0	(2)
33	$Ca(NO_3)_2{\cdot}4H_2O$	nitrocalcite	129.8	(2)
34	$Ca(NO_3)_2$	calcium nitrate	66.09	(1)
35	$CaSO_4$	anhydrite	45.94	(1)
36	$CaSO_4{\cdot}1/2H_2O$	bassanite	55.04	(2)
37	$CaSO_4{\cdot}2H_2O$	gypsum	74.69	(1)
38	NH_4Cl	salammoniac	35.06	(1)
39	NH_4NO_3	ammonia niter	46.49	(1)
40	$(NH_4)_2SO_4$	mascagnite	74.68	(1)

(a) References: (1) Robie *et al.* (1978); (2) Broul *et al.* (1981); (3) Lide (1995); (4) JCPDS (1991); (5) estimated (see text).

Table 6.2: Molar volumes, V_M, of double salts; units are $cm^3\ mol^{-1}$.

	formula	mineral name	V_M	ref.[a]
41	$NaNO_3{\cdot}Na_2SO_4{\cdot}H_2O$	darapskite	111.4	(4)
42	$Na_2SO_4{\cdot}3K_2SO_4$	glaserite (aphtitalite)	246.2	(4)
43	$Na_2SO_4{\cdot}MgSO_4{\cdot}4H_2O$	bloedite (astrakanite)	150.0	(4)
44	$Na_2SO_4{\cdot}CaSO_4$	glauberite	100.1	(4)
45	$2Na_2SO_4{\cdot}CaSO_4{\cdot}2H_2O$	labile salt	181	(5)
46	$NaSO_4{\cdot}(NH_4)2SO_4{\cdot}4H_2O$	sodium ammonium sulfate tetrahydrate	110.4	(5)
47	$KCl{\cdot}MgCl_2{\cdot}6H_2O$	carnallite	173.7	(4)
48	$KCl{\cdot}CaCl_2$	chlorocalcite (baeumlerite)	81.02	(4)
49	$KNO_3{\cdot}5Ca(NO_3)_2{\cdot}10H_2O$	potassium pentacalcium nitrate decahydrate	548	(5)
50	$KNO_3{\cdot}Ca(NO_3)_2{\cdot}3H_2O$	potassium calcium nitrate decahydrate	163	(5)
51	$K_2SO_4{\cdot}MgSO_4{\cdot}4H_2O$	leonite	166.7	(4)
52	$K_2SO_4{\cdot}MgSO_4{\cdot}6H_2O$	schoenite (picromerite)	198.4	(4)
53	$K_2SO_4{\cdot}CaSO_4{\cdot}H_2O$	syngenite	127.8	(3)
54	$K_2SO_4{\cdot}5CaSO_4{\cdot}H_2O$	pentasalt (görgeite)	304	(5)
55	$2MgCl_2{\cdot}CaCl_2{\cdot}12H_2O$	tachhydrite	309.9	(4)
56	$MgCl_2{\cdot}NH_4Cl{\cdot}6H_2O$	ammonium carnallite	175.3	(4)
57	$5Mg(NO_3)_2{\cdot}2NH_4NO_3{\cdot}30H_2O$	ammonium magnesium nitrate hydrate (5:2)	881	(5)
58	$5Mg(NO_3)_2{\cdot}NH_4NO_3{\cdot}30H_2O$	ammonium magnesium nitrate hydrate (5:1)	835	(5)
59	$MgSO_4{\cdot}(NH_4)_2SO_4{\cdot}6H_2O$	boussingaultite	209.3	(2)
60	$CaCl_2{\cdot}Ca(NO_3)_2{\cdot}4H_2O$	calcium chloride nitrate tetrahydrate	173	(5)
61	$NH_4NO_3{\cdot}Ca(NO_3)_2$	ammonium calcium nitrate	113	(5)
62	$NH_4NO_3{\cdot}Ca(NO_3)_2{\cdot}2H_2O$	ammonium calcium nitrate dihydrate	147	(5)
63	$NH_4NO_3{\cdot}Ca(NO_3)_2{\cdot}3H_2O$	ammonium calcium nitrate trihydrate	162	(5)
64	$NH_4NO_3{\cdot}5Ca(NO_3)_2{\cdot}10H_2O$	ammonium pentacalcium nitrate decahydrate	547	(5)
65	$2CaSO_4{\cdot}(NH_4)_2SO_4$	ammonium calcium sulfate	168.7	(4)
66	$5CaSO_4{\cdot}(NH_4)_2SO_4{\cdot}H_2O$	ammonium pentasalt	324	(5)
67	$CaSO_4{\cdot}(NH_4)_2SO_4{\cdot}H_2O$	koktaite (ammonium syngenite)	137.0	(4)
68	$3NH_4NO_3{\cdot}(NH_4)_2SO_4$	ammonium nitrate sulfate (3:1)	220.4	(4)
69	$2NH_4NO_3{\cdot}(NH_4)_2SO_4$	ammonium nitrate sulfate (2:1)	168	(5)
70	$(Na,K)_2CO_3{\cdot}6H_2O$	solid solution	142.1	(3)
71	$K_2SO_4{\cdot}(NH_4)_2SO_4$	solid solution	140	(5)

(a) References: (1) Robie *et al.* (1978); (2) Broul *et al.* (1981); (3) Lide (1995); (4) JCPDS (1991); (5) estimated (see text).

V^{ex} is related to the excess Gibbs energy, G^{ex} (see Chapter 3), by:

$$V^{ex} = \left(\frac{\partial G^{ex}}{\partial P}\right)_{T,m} \tag{6.4}$$

yielding:

$$^{\phi}V_{MX} = \overline{V}^{\circ}_{MX} + \nu|z_M z_X|\frac{A_v}{2b}\ln(1+bI^{1/2}) + 2RT\nu_M\nu_X(mB^V_{MX} + \nu_M z_M m^2 C^V_{MX}) \tag{6.5}$$

Here, the same notation is used as in Chapter 3. Hence, A_V is the Debye-Hückel parameter for the volume (Archer & Wang 1990). Also:

$$B^V_{MX} = \left(\frac{\partial B_{MX}}{\partial P}\right)_{T,I} = \beta^{(0)V}_{MX} + \beta^{(1)V}_{MX} g(\alpha_1, I^{1/2}) + \beta^{(2)V}_{MX} g(\alpha_2, I^{1/2}) \tag{6.6}$$

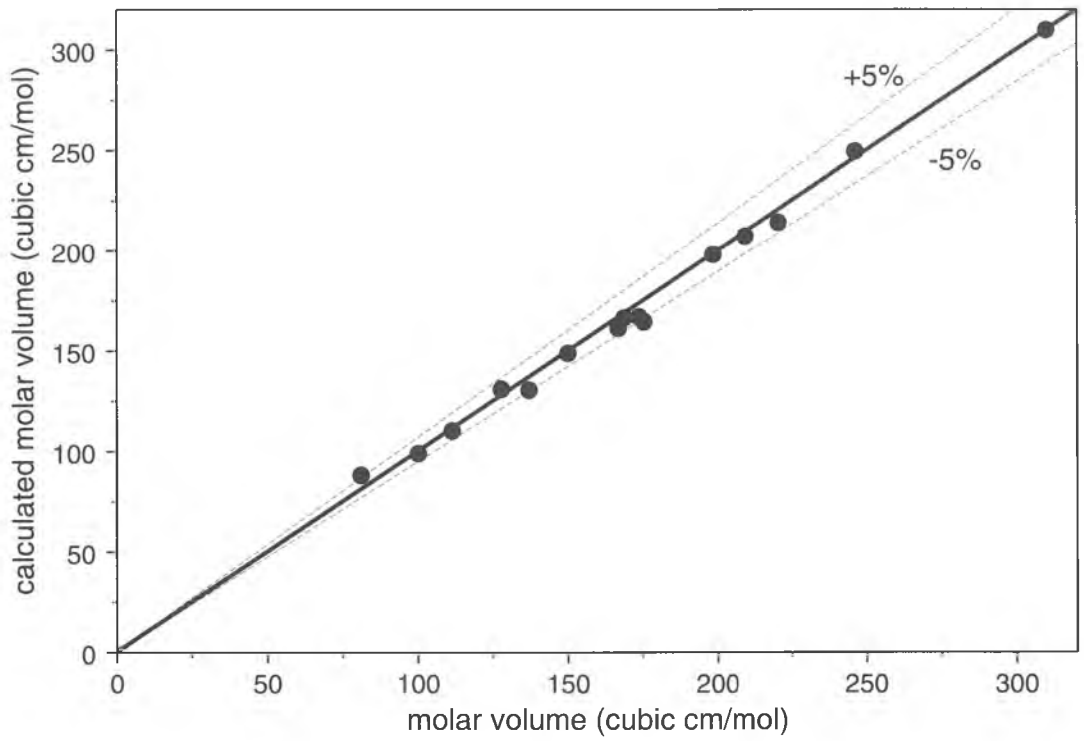

Figure 6.2: Calculated *v.* tabulated molar volumes of some double salts.

with:

$$\beta_{MX}^{(i)V} = \left(\frac{\partial \beta_{MX}^{(i)V}}{\partial P}\right)_T, i = 0, 1, 2 \tag{6.7}$$

and:

$$C_{MX}^{V} = \left(\frac{\partial C_{MX}}{\partial P}\right)_T \tag{6.8}$$

The function g is the same as already given in Chapter 3. Apparent molal volumes can be calculated from solution densities by using:

$$^{\phi}V = \frac{1000(\rho_0 - \rho)}{m\rho\rho_0} + \frac{M}{\rho} \tag{6.9}$$

where ρ and ρ_0 are the densities of the solution and of pure water, respectively, and M is the molecular weight of the solute. Hence, fitting experimental densities, converted to $^{\phi}V$, yield an isothermal set of volumetric interaction parameters, $\overline{V}^{\circ}_{MX}$, $\beta_{MX}^{(0)V}$, $\beta_{MX}^{(1)V}$, $\beta_{MX}^{(2)V}$ and C_{MX}^{V}. For reasons of consistency it is preferable to compute values of all parameters from the same set of experimental data, rather than using tabulated values of $\overline{V}^{\circ}_{MX}$ from existing compilations.

An important restriction arises from the additivity principle (Millero 1972) according to which $\overline{V}^{\circ}_{MX}$ for a single electrolyte is given as the sum of its ionic components:

$$\overline{V}^{\circ}_{MX} = \nu_M \overline{V}^{\circ}_{M} + \nu_x \overline{V}^{\circ}_{X} \tag{6.10}$$

It follows from equation 6.10 that the values of $\overline{V}^{\circ}_{MX}$ for different electrolytes are not independent. In order to obtain a consistent set of volumetric interaction parameters

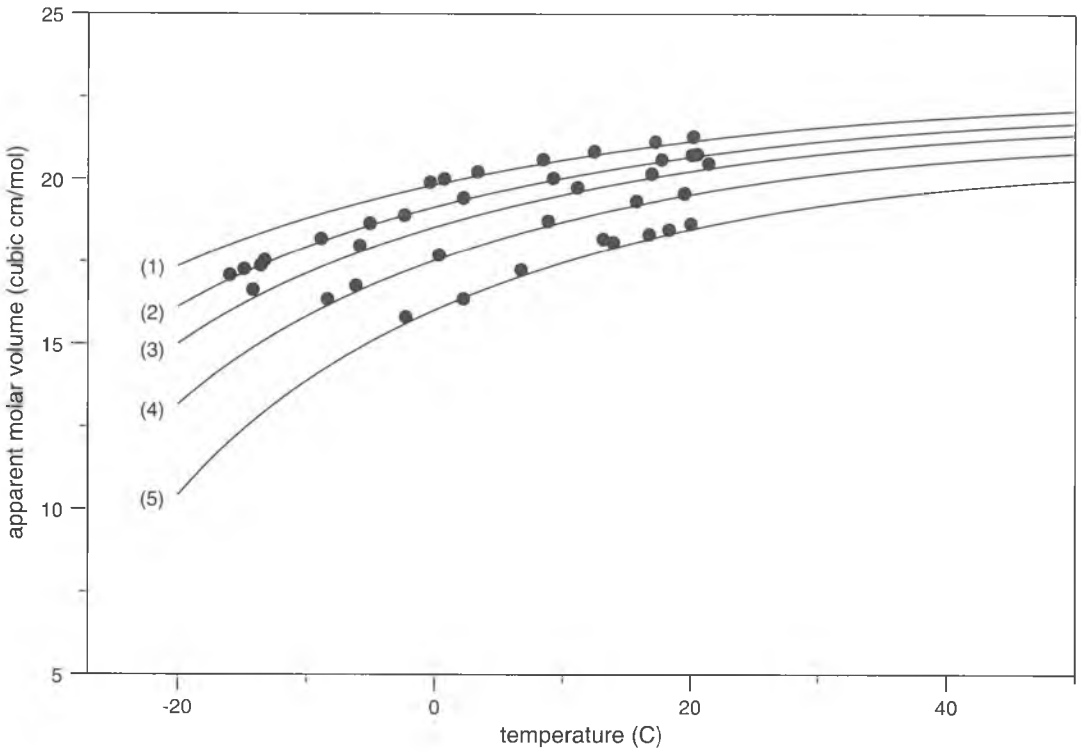

Figure 6.3: Apparent molar volumes of NaCl at molalities (1): 6.0 mol kg^{-1}, (2): 4.9 mol kg^{-1}, (3): 4.0 mol kg^{-1}, (4): 2.8 mol kg^{-1}, (5): 1.4 mol kg^{-1}, respectively; symbols represent experimental values of Koch (1924); lines are calculated values using the equation given by Archer (1992).

it is necessary to split the $\overline{V}^{\circ}_{MX}$ into ionic contributions. Here, the approach for the splitting of the $\overline{V}^{\circ}_{MX}$, based on the convention that $\overline{V}^{\circ}_{H^+} = 0$, suggested by Krumgalz *et al.* (1996) was used.

In the beginning of this study it was hoped that existing correlating equations for as many salts as possible could be incorporated into the present set of equations. However, it turned out that only the equation for the thermodynamic properties of NaCl(aq) given by Archer (1992) could be used directly. Though no experimental volumetric measurements at subzero temperatures were included in his parameterisation it was found that the equation does extrapolate reasonably well to subzero temperatures, as can be seen from Fig. 6.3. The calculated ${}^{\phi}V_{\mathrm{NaCl}}$ agree with the experimental data at low temperatures (Koch 1924) to within the experimental error which can be estimated from the deviations at temperatures above 273K where the model equation is an excellent representation of the most accurate experimental data presently available.

A database of solution densities or apparent molar volumes, respectively, was constructed for the following electrolytes: $NaNO_3$, Na_2SO_4, KCl, KNO_3, K_2SO_4, $MgCl_2$, $Mg(NO_3)_2$, $MgSO_4$, $MgCl_2$, and $Mg(NO_3)_2$. Due to solubility limitations the apparent molal volume of aqueous $CaSO_4$ can be represented with sufficient accuracy by only considering the apparent volume at infinite dilution and neglecting the parameters $\beta^{(i)V}_{MX}$ and C^{V}_{MX}. Hence, experimental data for $CaSO_4$(aq) were not considered. The literature database consists of about 130 literature sources including all relevant sources to about the end of 1996. In some cases where there are no, or only very few, high quality data available from the more recent literature very old measurements or

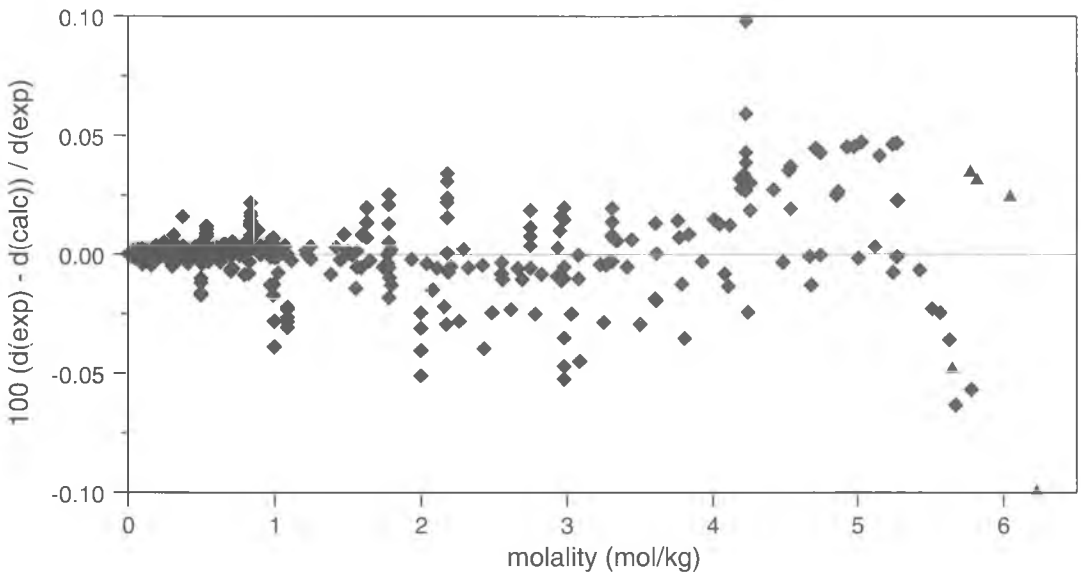

Figure 6.4: Percentage deviation of calculated densities, d(calc), from experimental densities, d(exp), in binary solutions of $MgCl_2$(aq); symbols have the following meanings: (♦): unsaturated solutions; (▲): saturated solutions.

the smoothed densities tabulated in existing compilations (*e.g.,* ICT 1928) had to be used.

Apparent molal volumes were calculated from the experimental densities using equation 6.9. The densities of water, ρ_0, were calculated using the expression given by Kell (1977). The resulting database of apparent molal volumes was checked for consistency and preliminary weights and estimated uncertainties were assigned to the individual data points. The experimental molal volumes, ${}^{\phi}V_{MX}$, thus obtained were then fitted to equation 6.5 using an empirical expression to represent the temperature dependence of the volumetric interaction parameters. A more detailed description of the data evaluation and model parameterisation is provided elsewhere (Steiger, manuscript in preparation). As an example, Fig. 6.4 depicts a comparison of the experimental and the calculated densities of $MgCl_2$(aq) covering the temperature range from −24°C to 55°C. It can be seen that the model equations using the recommended parameters are a very good representation of the experimental densities.

In theory, the application of the ion interaction approach to multicomponent mixtures requires additional mixing terms, θ^v_{ij} and ψ^v_{ijk}, in the expression for V^{ex} (Krumgalz *et al.* 1995). The mixing parameters can be calculated from experimental density data for ternary solutions with a common ion. The equations become considerably more complicated if mixing terms are included. For the system Na^+–K^+–Mg^{2+}–Ca^{2+}–Cl^-–$NO_3{}^-$–$SO_4{}^{2-}$–H_2O, the complete parameterisation requires the calculation of 9 θ^v_{ij} and 27 ψ^v_{ijk} parameters, respectively. Experimental data of sufficient accuracy are not available for all of the 27 ternary systems. Monnin (1989) has pointed out that the values of the mixing parameters are very sensitive to the quality of the ternary data sometimes leading to ambiguous results. He concluded that effects of the mixing parameters were in the range of the experimental uncertainty in most cases. Krumgalz *et al.* (1995) have also found that most of the available experimental data are not sufficiently reliable to allow for the determination of mixing parameters. They were only able to calculate mixing parameters for the system NaCl–KCl–H_2O. Also, for unsymmetrical mixtures (*e.g.,* Na^+–Mg^{2+}) the binary parameters $\beta^{(i)V}_{MX}$ and C^V_{MX}

enter the mixing equations (Connaughton *et al.* 1989; Krumgalz *et al.* 1995), thus, further complicating the determination of the mixing parameters. Hence, for the present study, it was decided to neglect the mixing parameters.

In order to check the model's ability to predict the densities of multicomponent mixtures, test calculations were carried out using the binary interaction parameters only. There are only very few high quality experimental data of multicomponent electrolyte solutions. Here, we used the data of Krumgalz *et al.* (1992). Using the present model parameterisation the calculated densities of solutions containing four salts (NaCl, KCl, $MgCl_2$, $CaCl_2$) agreed with the experimental densities to within a maximum deviation of 0.019%. The average deviation amounts to 0.012% which is in the same order of magnitude than typical deviations for single salts (*cf.* Fig. 6.4). Hence, there is excellent agreement between the calculated and the experimental densities without inclusion of the ternary interaction parameters.

A more rigorous test of the model is illustrated in Fig. 6.5. Solubilities and densities of the saturated solutions in the Na^+–Cl^-–NO_3^-–H_2O system at different temperatures were both calculated using the ion interaction model. Again there is excellent agreement with the experimental data. The calculated densities of solutions saturated with respect to nitratine and halite agree with the available experimental data to within the expected experimental uncertainty. Similar results were also obtained for other ternary systems. It is concluded that, for the purpose of this project, it is sufficient to neglect the ternary interaction parameters for the volumetric properties. The final model parameterisation as included in the ECOS code allows for a very satisfactory treatment of concentrated mixed salt solutions and can be used to model the total volumes of pore solutions in building materials.

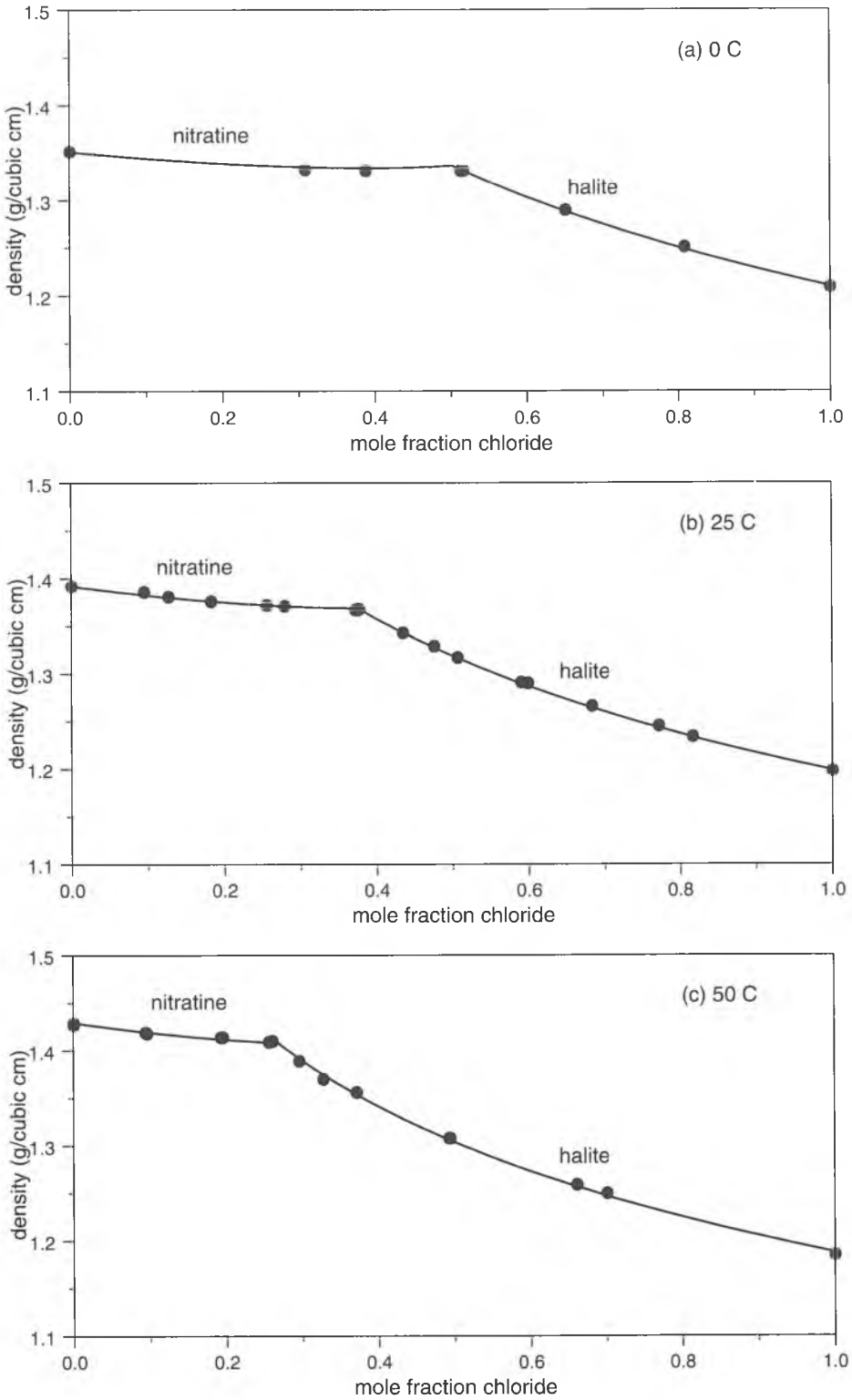

Figure 6.5: Densities of saturated solutions in the Na^+–Cl^-–NO_3^-–H_2O system at 0°C, 25°C, and 50°C; symbols represent experimental solubilities and densities of Cornec & Krombach (1929), Chrétien (1929), Sieverts & Müller (1930), and Cornec & Chrétien (1924) (the latter data taken from Silcock 1979, Table 3067); curves represent both calculated solubilities and densities using the Pitzer model.

6.4 References

Archer, D. G. 1992. *J. Phys. Chem. Ref. Data* 21: 793–829.

Archer, D. G. & P. Wang 1990. *J. Phys. Chem. Ref. Data* 19: 378–411.

Broul, M., J. Nývlt & O. Söhnel 1981. *Solubility in inorganic two-component systems.* Elsevier, Amsterdam.

Chrétien, A. 1929. 'Étude du système quaternaire. Eau, nitrate de sodium, chlorure de sodium, sulfate de sodium.' *Ann. Chim.* 12: 9–155.

Clegg, S. L. & M. Whitfield 1991. *In* K. S. Pitzer (ed.), *Activity Coefficients in Electrolyte Solutions*, pp. 279–434. CRC Press, Boca Raton.

Connaughton, L. M., F. J. Millero & K. S. Pitzer 1989. *J. Solution Chem.* 18: 1007–1017.

Cornec, E. & A. Chrétien 1924. *Caliche* 6: 358–369.

Cornec, E. & H. Krombach 1929. 'Contribution a l'étude des équilibres entre l'eau, les nitrates, les chlorures et les sulfates de sodium et de potassium.' *Ann. Chim.* 12: 203–295.

Harvie, C. E. & J. H. Weare 1980. *Geochim. Cosmochim. Acta* 44: 981–997.

ICT 1928. *International Critical Tables, Vol.* McGraw-Hill, New York.

JCPDS 1991. *JCPDS-Powder Diffraction File 2 (PDF-2), compiled by the Joint Committee on Powder Diffraction Standards (JCPDS).* JCPDS, Swarthmore, Pennsylvania, USA.

Kell, G. S. 1977. *J. Phys. Chem. Ref. Data* 6: 1109–1131.

Koch, W. 1924. *Z. ges. Kälte-Ind.* 31: 105–108.

Krumgalz, B. S., I. A. Malester, I. J. Ostrich & F. J. Millero 1992. *J. Solution Chem.* 21: 635–649.

Krumgalz, B. S., R. Pogorelsky & K. S. Pitzer 1995. *J. Solution Chem.* 24: 1025–1038.

Krumgalz, B. S., R. Pogorelsky & K. S. Pitzer 1996. *J. Phys. Chem. Ref. Data* 25: 663–689.

Lide, D. R. 1995. *CRC Handbook of Chemistry and Physics.* CRC Press, Boca Raton.

Millero, F. J. 1972. *In* R. A. Horne (ed.), *Water and Aqueous Solutions. Structure, Thermodynamics, and Transport Processes*, pp. 519–564. Wiley-Interscience, New York.

Monnin, C. 1989. *Geochim. Cosmochim. Acta* 53: 1177–1188.

Pitzer, K. S. 1973. 'Thermodynamics of electrolytes, I. Theoretical basis and general equations.' *J. Phys. Chem.* 77: 268–277.

Pitzer, K. S. 1991. *In* K. S. Pitzer (ed.), *Activity Coefficients in Electrolyte Solutions*, pp. 75–154. CRC Press, Boca Raton.

Robie, R. A., B. S. Hemingway & J. A. Fisher 1978. *US. Geol. Survey Bull.* p. 1452.

Rogers, P. S. Z. & K. S. Pitzer 1982. *J. Phys. Chem. Ref. Data* 11: 15–81.

Sieverts, A. & H. Müller 1930. 'Das reziproke Salzpaar $MgCl_2$, $Na_2(NO_3)_2$, H_2O. I.' *Z. Anorg. Chem.* 189: 241–257.

Silcock, H. L. 1979. *Solubilities of inorganic and organic compounds. Volume 3. Ternary and multicomponent systems of inorganic substances.* Pergamon Press, Oxford.

7

Data Evaluation and Molality-Based Parameterisation

N. J. Reeves, S. L. Clegg and P. Brimblecombe
School of Environmental Studies, University of East Anglia

7.1 Methodology

7.1.1 Binary parameters

For a pure single salt the Pitzer model equations for excess Gibbs energy, ionic activity and osmotic coefficients (3.6–3.9) consist of the Debye-Hückel term, plus expressions involving binary interaction parameters only. For most salts this leaves only four unknown parameters which have to be obtained by fitting to experimental data: $\beta^{(0)}$, $\beta^{(1)}$, $C^{(0)}$ and $C^{(1)}$ — the exception being divalent-divalent salts such as $MgSO_4$ which require an additional $\beta^{(2)}$ term.

For the three systems that were the main subject of this study, there are a total of 21 binary interactions for which parameters are required. For most of these binaries, parameterisations have already been published in the literature for the temperature range of interest in this study (−40°C to 50°C) (see section 7.4). For these binaries, the existing parameterisations were checked to see if they gave an adequate representation of the osmotic coefficient at the freezing point of the pure salt solution (Klotz & Rosenberg 1972), data for which were obtained from the compilation of Seidell (presented in Linke 1965). However, for seven of the binary salts, most notably the nitrates and the soluble salts $CaCl_2$ and NH_4Cl, parameters were redetermined in this study, either because no previously published parameterisations were available over the whole temperature range of interest, or because the existing parameters were deemed inadequate.

The binary systems for which parameters were fitted in this study are summarised in Table 7.1 along with the literature sources for the experimental data used in the parameter determination. In general, the methodology adopted for each binary parameter, $P^{(i)}$, was to obtain the value of $P^{(i)}_{298.15\mathrm{K}}$ by fitting to osmotic coefficient data at 25°C (298.15K). The fitting was performed in all cases using the generalised non-linear least squares fitting algorithm E04FDF (Numerical Algorithms Group 1991).

Higher order terms in the Taylor expansion for $P^{(i)}(T)$ were obtained by fitting to apparent relative molal enthalpy (${}^{\phi}L$) and apparent molal heat capacity (${}^{\phi}C_P$) data at 25°C. This yielded the first and second temperature derivatives of the parameters (*i.e.*, $\partial P^{(i)}/\partial T$ and $\partial^2 P^{(i)}/\partial T^2$) via equations 3.28–3.38. For each of the binary salts, the parameter expressions thus obtained were tested to see if they correctly reproduced the osmotic coefficient at the freezing point of the salt solutions. If agreement was acceptable for a particular salt then the Taylor expansion was truncated to the second order terms only. In the case of $CaCl_2$, however, third (for all $P^{(i)}$) and even fourth temperature derivatives (for $C^{(0)}$ and $C^{(1)}$ only) were found to be necessary in order to adequately account for the freezing point data. These higher order terms were

obtained by fitting to heat capacity data at 0–50°C and by fitting to the freezing point depression curve itself.

The final element of the parameterisation process for the binary salt solutions is the determination of expressions for the thermodynamic solubility product (as a function of temperature) for each mineral phase that saturates over the temperature range of interest to this study. This is contingent on having already obtained accurate expressions for the binary interaction parameters. The general fitting expression for the equilibrium constant (K_{MX}) governing the solubility of salt MX at arbitrary temperature $T(K)$ is given by:

$$\ln[K(T)] = \ln[K(T_r)] + \left(\frac{\Delta_r H^0}{R}\right)\left(\frac{1}{T_r} - \frac{1}{T}\right) + \left(\frac{\Delta a}{R}\right)\left(\frac{T_r}{T} - 1 + \ln\left(\frac{T}{T_r}\right)\right) + \left(\frac{\Delta b}{2R}\right)\left(T_r\left(\frac{T_r}{T-1}\right) + T - T_r\right) \quad (7.1)$$

where $T_r(K)$ is a reference temperature (here taken as 298.15K) and $\Delta_r H^0$ is the enthalpy change for the reaction. The symbols Δa and Δb are constants appearing in the empirical expression for heat capacity change for the reaction (*i.e.*, $\Delta_r C_p^0 = \Delta a + \Delta bT$).

The four constants $\ln[K(T)]$, $\Delta_r H^0$, Δa and Δb are obtained by fitting to the product of the model calculated activity product. Solubilities are taken from the extensive review of experimental measurements tabulated by Seidell (in Linke 1965). In practice, not all of these parameters were found necessary to obtain a fit to the solubility data actually used. This is related to the degree of linearity of the solubility curve, and to the temperature range of the data — the smaller the temperature range the fewer the coefficients fitted so as to avoid fitting errors at the end-points of the data. For most salts Δb, and often Δa are given the value zero (see Table 7.3).

The pure single salts of calcium sulfate were the sole exception to the methodology described above, as these were necessarily parameterised using ternary data rather than pure salt data. This was done because of the exceptionally low aqueous solubility of these salts, and because of the lack of thermodynamic measurements for the pure salt solutions. The solubility product for $CaSO_4{\cdot}1/2H_2O$ was obtained using data for the Ca–Cl–SO_4 ternary, whilst the equilibrium constants for $CaSO_4$ and $CaSO_4{\cdot}2H_2O$ were obtained during the fitting for the Na–Cl–SO_4 system.

7.1.2 Ternary parameters

For an aqueous solution of mixed salts the Pitzer model equations consist of the usual Debye-Hückel and binary interaction parameter terms, plus additional terms involving mixture parameters. If the binary parameters are known for the components of a given ternary (three ion) system, then there are two unknown Pitzer model parameters — $\theta_{cc'}$ and $\psi_{cc'a}$ for a system consisting of two cations (c and c') and one anion (a), and analogously $\theta_{aa'}$ and $\psi_{aa'c}$ for a system consisting of two anions (a and a') and one cation (c).

For the majority of ternary systems examined in this study values of the mixture parameters at 25°C are available from the literature. However, expressions for the temperature variation of these ternary parameters are either not available, or the expressions are not adequate for the temperature range of interest here. Consequently, for most ternaries the mixture parameters were rederived.

The mixture parameters were fitted to solubility data over a range of temperatures using the general expression for the temperature variation of a parameter given

Table 7.1: Literature sources for binary parameter fitting data.

Salt	Data type	$t(°C)$	Molality range	Source
$CaCl_2$	ϕ	25	0–10.771	[1]
	${}^{\phi}L$	25	0–12.0	[2]
	${}^{\phi}C_P$	0–50	0–11.0	[2]
	freezing point	0–(−51.2)	0–3.97	[3]
NH_4Cl	ϕ	25	0–7.405	[4]
	${}^{\phi}L$	25	0–7.929	[5]
	${}^{\phi}C_P$	25	0–7.4008	[5]
$NaNO_3$	ϕ	25	0–10.830	[4]
	${}^{\phi}L$	25	0–6.0	[5]
	${}^{\phi}C_P$	25	0	[5],[6-10]
KNO_3	ϕ	25	0–3.500	[4]
	${}^{\phi}L$	25	0–3.7004	[5]
	${}^{\phi}C_P$	25	0–3.7004	[5],[7],[8]
$Mg(NO_3)_2$	ϕ	25	0–5.0	[12]
	${}^{\phi}L$	25	0–4.513	[13]
	${}^{\phi}C_P$	25	0–7.605	[14-16][a]
$Ca(NO_3)_2$	ϕ	25	0–20.0	[12]
	${}^{\phi}L$	25	0–19.55	[17]
	${}^{\phi}C_P$	25	0–7.605	[14-16][a]
NH_4NO_3	ϕ	25	0–40.0[b]	[18]
	${}^{\phi}L$	25	0–40.0[b]	[5, 19]
	${}^{\phi}C_P$	25	0–40.0[b]	[5, 20-22]

(a) datasets for $Mg(NO_3)_2$ and $Ca(NO_3)_2$ combined
concentration range limited to $0.0 \leq m \leq 40.0$

Key to Table 1: [1] Rard & Clegg (1997); [2] Ananthaswamy & Atkinson (1985); [3] Garvin *et al.* (1987); [4] Hamer & Wu (1972); [5] Parker (1965); [6] Epikhin & Stakhanova (1967); [7] Enea *et al.* (1977); [8] Randall & Rossini (1929); [9] Roux *et al.* (1977); [10] Puchkov *et al.* (1973); [11] Seidell (1965) cited in Linke (1965); [12] Lobo & Quaresma (1981); [13] Ewing *et al.* (1934); [14] Spitzer *et al.* (1979); [15] Drakin *et al.* (1967); [16] Tomus *et al.* (1995); [17] Ewing & Rogers (1933); [18] Venderzee *et al.* (1980); [19] Roux *et al.* (1977); [20] Epikhin *et al.* (1977); [21] Sorina *et al.* (1977); [22] Gladushko *et al.* (1985).

previously (equation 3.38). The minimum number of coefficients necessary to obtain a good fit to the solubility data were used, with values for both θ_{ij} and ψ_{ijk} being fitted simultaneously. Where appropriate, the values of the mixture parameters at 25°C were fixed to published values. This was done in order to reduce the number of fitting parameters, and in order to maintain maximum compatibility with previously published work. The two-coefficient and three-coefficient expressions for a parameter at arbitrary temperature T, $P(T)$, now become:

$$\begin{cases} P(T) = a + [T_r(P(T_r) - a)]/T & i.e.,\ b = T_r(P(T_r) - a) \\ P(T) = a + b/T + [(1/T_r)(P(T_r) - a - b/T_r)]T & i.e.,\ c = (1/T_r)(P(T_r) - a - b/T_r) \end{cases} \tag{7.2}$$

where T_r is a reference temperature (here 298.15K) and a and b are fitting constants (*cf.* equation 3.38).

The fitting process for the mixture terms is complicated by the requirement that the θ_{ij} parameter must be transferable between all mixtures containing ions i and j. Thus, it was often necessary to determine a compromise expression for this parameter that was appropriate to all ternary systems that contain the given combination of ions, and then redetermine expressions for ψ_{ijk} for each of these affected ternaries that were compatible with the new value for the two ion parameter.

In addition to obtaining the temperature functions for θ_{ij} and ψ_{ijk}, the fitting procedure for the ternary systems often involved the determination of the thermodynamic solubility product for the double salts that are often encountered in these salt mixtures. This was done simultaneously with the fitting for θ_{ij} and ψ_{ijk}, and using the same general methodology and temperature function as used for the single salt case (equation 7.1).

The presence of more than one double salt in the dataset for a ternary mixture necessitated the overall determination of a relatively large number of parameters. Reduction of the number of parameters was achieved by fitting the parameters for the 25°C data first, giving the values of $P(T_r)$ (equation 7.2) for θ_{ij} and ψ_{ijk}, as well as giving values for $\ln[K(T_r)]$ (equation 7.1) for the solid phases. This reduced the number of fitting terms when the solubility data for temperatures other than 25°C were examined. In addition, for double salts with relatively few datapoints it was often desirable to parameterise the θ_{ij} and ψ_{ijk} expressions, and equilibrium constants for the major double compounds, before proceeding to the minor solid phases.

The various solid phases found in ternaries containing both NH_4 and K were not parameterised according to the method just described. The double compounds and solid solutions formed in the NH_4–K–Cl system were not fitted as individual phases, but were apportioned to either the NH_4Cl or KCl branch of the solubility isotherms. This not only simplified the fitting process considerably, but produced the best fit to the data. An analogous procedure was adopted for the NH_4–K–NO_3 ternary.

The NH_4–K–SO_4 ternary, however, was far more problematic, containing a continuous series of solid solutions usually given as $(K,NH_4)_2SO_4$. It was not possible to distinguish separate $(NH_4)_2SO_4$ and K_2SO_4 branches for these isotherms, and the data was badly scattered and not internally consistent at temperatures below 25°C. Analysis showed that the composition of the solid solution could not be regarded as being constant as the concentration of the components was varied. The solid solution was finally fitted by assuming that it had a continuously varying composition dependent upon the NH_4:K ratio of the solution, and that the logarithm of the solubility product of the solid solution was given by a weighted sum of the $\ln[K(T)]$ terms for $(NH_4)_2SO_4$ and K_2SO_4 (see equation 7.1 and note (a) to Table 7.6).

7.2 Results

7.2.1 Binary parameters

The binary interaction parameters for the seven pure salts parameterised in this study are summarised in Table 7.2. For most of these salts the second temperature derivative was found to be the highest term necessary in the expression for the temperature variation of the parameters (equation 3.37). The exception to this was $CaCl_2$, for which third and fourth derivatives were found necessary in order to obtain a good fit to the experimental data used. For each of these salts an α value of $2.0 kg^{1/2} mol^{-1/2}$ was employed. The binary parameters for the remaining 14 pure salt systems that this study is concerned with were taken directly from the literature. The values for

Table 7.2: Fitted Pitzer model parameters $P^{(i)}$, for single salts parameterised in this study.

Salt	$P^{(i)}$	$P^{(i)}298.15K$	$\partial P^{(i)}/\partial T$	$\partial^2 P^{(i)}/\partial T^2$	$\partial^3 P^{(i)}/\partial T^3$	$\partial^4 P^{(i)}/\partial T^4$	ω
$CaCl_2$	$\beta^{(0)}$	0.6378	-0.4558×10^{-3}	-0.2196×10^{-4}	0.2428×10^{-6}		1.1
	$\beta^{(1)}$	0.9738	0.4450×10^{-2}	0.6457×10^{-4}	-0.1081×10^{-5}		
	$C^{(0)}$	-0.9836×10^{-2}	-0.3738×10^{-4}	0.9887×10^{-6}	-0.8733×10^{-8}	-0.3312×10^{-9}	
	$C^{(1)}$	-0.4485	0.9678×10^{-3}	0.7668×10^{-5}	0.4750×10^{-6}	-0.1674×10^{-7}	
NH_4Cl	$\beta^{(0)}$	0.526×10^{-1}	0.2855×10^{-3}	-0.4442×10^{-7}			2.5
	$\beta^{(1)}$	0.2083	0.1053×10^{-2}	-0.1841×10^{-5}			
	$C^{(0)}$	-0.1507×10^{-2}	-0.1388×10^{-4}	-0.2032×10^{-6}			
	$C^{(1)}$	-0.1780×10^{-1}	-0.5730×10^{-3}	-0.4895×10^{-4}			
$NaNO_3$	$\beta^{(0)}$	0.326497×10^{-2}	0.566007×10^{-3}	-0.291693×10^{-5}			2.5
	$\beta^{(1)}$	0.198281	0.289951×10^{-2}	-0.102655×10^{-3}			
	$C^{(0)}$	-0.730000×10^{-5}	-0.252166×10^{-4}	0.131872×10^{-6}			
	$C^{(1)}$	0.978300×10^{-2}	0.352506×10^{-2}	-0.840595×10^{-4}			
KNO_3	$\beta^{(0)}$	-0.966911×10^{-1}	0.660283×10^{-3}	-0.412930×10^{-4}			2.5
	$\beta^{(1)}$	0.930104×10^{-1}	0.577723×10^{-2}	-0.938940×10^{-4}			
	$C^{(0)}$	0.495295×10^{-2}	-0.130900×10^{-4}	0.31698×10^{-5}			
	$C^{(1)}$	0.6152335×10^{-1}	0.363413×10^{-2}	0.788410×10^{-4}			
$Mg(NO_3)_2$	$\beta^{(0)}$	0.3138	0.4161×10^{-3}	0.1084×10^{-4}			2.5
	$\beta^{(1)}$	0.1413×10^{1}	0.5852×10^{-2}	-0.4921×10^{-4}			
	$C^{(0)}$	-0.1423×10^{-2}	-0.4275×10^{-4}	-0.1861×10^{-5}			
	$C^{(1)}$	0.6835	0.1434×10^{-2}	-0.3020×10^{-3}			
$Ca(NO_3)_2$	$\beta^{(0)}$	0.13	-0.2535×10^{-3}	-0.12870×10^{-4}			1.5
	$\beta^{(1)}$	0.1634×10^{1}	0.9096×10^{-2}	-0.99776×10^{-4}			
	$C^{(0)}$	-0.9984×10^{-3}	0.1346×10^{-5}	0.46177×10^{-6}			
	$C^{(1)}$	0.1571	0.489×10^{-2}	-0.26846×10^{-4}			
NH_4NO_3	$\beta^{(0)}$	-0.830505×10^{-2}	-0.263928×10^{-4}	0.39258×10^{-6}			1.5
	$\beta^{(1)}$	0.224455	0.411504×10^{-2}	-0.788695×10^{-4}			
	$C^{(0)}$	0.236303×10^{-4}	0.241720×10^{-5}	-0.184619×10^{-7}			
	$C^{(1)}$	-0.295538×10^{-1}	0.142159×10^{-2}	-0.180449×10^{-4}			

these parameters are summarised in Section 7.4, together with the literature source for the parameterisation.

The fitting expressions determined for the thermodynamic solubility products of the 36 solid phases that saturate in the pure salt solutions are summarised in Table 7.3. Also included in Table 7.3 are the equilibrium constants determined for $CaSO_4$, $CaSO_4 \cdot 1/2H_2O$ and $CaSO_4 \cdot 2H_2O$, which were actually obtained during the fitting of the ternary solution data, but which are included here because they are pure single salts.

Table 7.3: Fitted equilibrium constants (see equation 7.1) and temperature range (ΔT) of solubility data for pure single salts parameterised in this study.

solid	$\ln K(T_r)$	$\Delta_r H(J\text{mol}^{-1})$	$\Delta a(J\text{mol}^{-1}K^{-1})$	$\Delta b(J\text{mol}^{-1}K^{-2})$	ΔT
NaCl	0.366063×10^{1}	0.426370×10^{4}	-0.128671×10^{3}		0–80
$NaCl{\cdot}2H_2O$	0.346088×10^{1}	0.116180×10^{5}	-0.333741×10^{3}		−22–0
$NaNO_3$	0.249997×10^{1}	0.175607×10^{5}	-0.299647×10^{3}		−18–75
Na_2SO_4	−0.730042	-0.217569×10^{4}	-0.259713×10^{3}		35–80
$Na_2SO_4{\cdot}10H_2O$	-0.285475×10^{1}	0.783782×10^{5}			0–32
$NaHCO_3$	−0.896778	0.204270×10^{5}			−2–100
$Na_2CO_3{\cdot}H_2O$	0.100650×10^{1}	0.277872×10^{5}	-0.133458×10^{4}		30–80
$Na_2CO_3{\cdot}7H_2O$	-0.100186×10^{1}	0.495925×10^{5}			0–34
$Na_2CO_3{\cdot}10H_2O$	-0.182826×10^{1}	0.727390×10^{5}	0.701146×10^{3}		−2–33
KCl	0.206958×10^{1}	0.177844×10^{5}	-0.161469×10^{3}		−11–60
KNO_3	−0.219874	0.170019×10^{5}	-0.767447×10^{5}	0.259251×10^{3}	−3–90
K_2SO_4	-0.412499×10^{1}	0.238633×10^{5}	-0.357141×10^{3}		0–80
$K_2SO_4{\cdot}H_2O$	-0.295264×10^{1}	0.117199×10^{6}	0.454003×10^{4}		0–10
$KHCO_3$	0.671705	0.120398×10^{5}	-0.299391×10^{3}		−6–70
$K_2CO_3{\cdot}3/2H_2O$	0.703953×10^{1}	0.333019×10^{4}			−6–50
$K_2CO_3{\cdot}6H_2O$	0.431538×10^{1}	0.143964×10^{5}			−37– − 6
$MgCl_2{\cdot}6H_2O$	0.105393×10^{2}	-0.2111643×10^{5}	-0.855832×10^{2}		−3–80
$MgCl_2{\cdot}8H_2O$	0.105659×10^{2}	0.518904×10^{5}	0.126550×10^{4}		−17– − 3
$MgCl_2{\cdot}12H_2O$	0.741323×10^{1}	0.310905×10^{5}			−33– − 16
$Mg(NO_3)_2{\cdot}2H_2O$	0.162997×10^{2}	0.172158×10^{6}	-0.126644×10^{5}		55–80
$Mg(NO_3)_2{\cdot}6H_2O$	0.687432×10^{1}	0.154259×10^{5}	0.721859×10^{4}	-0.262417×10^{2}	−33–80
$Mg(NO_3)_2{\cdot}9H_2O$	0.613087×10^{1}	0.294724×10^{5}			−32– − 15
$MgSO_4{\cdot}H_2O$	0.5701	-0.5611×10^{5}			25–75
$MgSO_4{\cdot}4H_2O$	-0.3261×10^{1}	-0.1031×10^{2}			35–75
$MgSO_4{\cdot}6H_2O$	-0.387036×10^{1}	0.803729×10^{4}	-0.153114×10^{3}		48–69
$MgSO_4{\cdot}7H_2O$	-0.424080×10^{1}	0.122176×10^{5}	0.101536×10^{3}		−4–48
$CaCl_2{\cdot}2H_2O$	0.164082×10^{2}	-0.956111×10^{5}			39–50
$CaCl_2{\cdot}4H_2O$	0.121860×10^{2}	-0.146745×10^{5}	0.114865×10^{6}	-0.383494×10^{3}	16–41
$CaCl_2{\cdot}6H_2O$	0.905481×10^{1}	0.172060×10^{5}	0.118010×10^{3}		−50–29
$Ca(NO_3)_2{\cdot}2H_2O$	0.125702×10^{2}	-0.324487×10^{5}	0.316147×10^{4}		25–60
$Ca(NO_3)_2{\cdot}3H_2O$	0.808363×10^{1}	0.200415×10^{5}			49–75
$Ca(NO_3)_2{\cdot}4H_2O$	0.638352×10^{1}	0.899262×10^{4}			40–50
$Ca(NO_3)_2$	0.451680×10^{1}	0.290667×10^{5}	-0.190704×10^{3}		−29–48
$CaSO_4$[(a)]	-0.9449×10^{1}	-0.2708×10^{5}			50–110
$CaSO_4{\cdot}1/2H_2O$[(b)]	-0.1073×10^{2}				55
$CaSO_4{\cdot}2H_2O$[(a)]	-0.1020×10^{2}	-0.1907×10^{4}			0–75
NH_4Cl	0.286540×10^{1}	0.157597×10^{5}	0.311431×10^{4}	-0.112145×10^{2}	−16–100
NH_4NO_3	0.256771×10^{1}	0.271545×10^{5}	-0.372734×10^{2}		−15–32
$(NH_4)2SO_4$	0.174034×10^{-2}	0.495242×10^{4}	-0.197544×10^{3}		−19–50

(a) determined in the Na–Ca–SO_4 ternary
(b) determined in the Na–Cl–SO_4 ternary

7.2.2 Ternary Parameters

The fitted mixture parameters for the 58 ternary systems parameterised in this study, together with the fitted solubility products for the double salts that saturate in these solutions are summarised on the following pages.

Key to Tables 7.4 and 7.5: [1] Silcock (1979); [2] Reinders (1915); [3] Uyeda (1909); [4] Cornec & Krombach (1932); [5] Meyer *et al.* (1949); [6] Emons *et al.* (1966); [7] Frowein & von Mühlendahl (1926); [8] Yarym-Agaev *et al.* (1964); [9] Kornec & Krombach (1929); [10] Timoshenko (1986); [11] Saslawsky & Ettinger (1935); [12] Saslawsky & Ettinger (1935); [13] Jänecke (1911); [14] Emons *et al.* (1970); [15] Meyerhoffer & Saunders (1899a); [16] Meyerhoffer & Saunders (1899b); [17] Yanat'eva & Orlova (1959); [18] Hamid (1926); [19] Smith & Ball (1917); [20] Hill & Smith (1929); [21] Hill & Miller (1927); [22] Sieverts & Müller (1930); [23] Sieverts & Müller (1931); [24] Jackman & Browne (1922); [25] Benrath (1928); [26] Schröder (1929a); [27] Schröder (1930); [28] Timoshenko & Chekmareva (1989); [29] Karakhanyan *et al.* (1987); [30] Frowein (1928); [31] Kremann & Rodemund (1914); [32] Benrath & Schackmann (1934); [33] Mazzotto (1891); [34] Hara *et al.* (1991); [35] Rengade (1922a); [36] Rengade (1922b); [37] Toporescu (1922a); [38] Toporescu (1922b); [39] Krause (1927); [40] Bergmann & Shulyak (1972); [41] Shpunt (1946); [42] Gmelin (n.d.); [43] Nakamura (1982); [44] Timoshenko (1979); [45] Kirgintsev & Luk'yanov (1963); [46] Sborgi *et al.* (1924); [47] Sborgi *et al.* (1924); [48] Sborgi & Bovalini (1924); [49] Levi (1924); [50] Filippov *et al.* (1987); [51] Filippov & Charykova (1989); [52] Kotlyar-Shapirov & Kirgintsev (1973); [53] Agaev *et al.* (1976); [54] Lightfoot & Prutton (1946); [55] Lightfoot & Prutton (1947); [56] Igelsrud & Thompson (1936); [57] Benrath & Benrath (1929); [58] Benrath & Benrath (1930); [59] Benrath & Sichelschmidt (1931); [60] Shevchuk & Omelyan (1990); [61] Frowein & von Mühlendahl (1926); [62] Agaev *et al.* (1976); [63] Perova (1970); [64] Vereshchagina *et al.* (1969); [65] Vereshchagina *et al.* (1973); [66] Barbaudy (1923); [67] Igelsrud & Thompson (1936); [68] Assarsson (1950a); [69] Assarsson (1950b); [70] Flatt & Bocherens (1962); [71] Kosterina *et al.* (1985); [72] Vereshchagina *et al.* (1973); [73] Vereshchagina *et al.* (1969); [74] Yakimov *et al.* (1969); [75] Bergmann & Opredelenkova (1969); [76] Hill (1934); [77] Clarke & Partridge (1934); [78] Cameron & Breazeale (1904); [79] Barre (1909); [80] van Veldhuizen (1929); [81] D'Ans (1933); [82] Kudryashova *et al.* (1996); [83] Dejewska (1992); [84] Jänecke *et al.* (1932); [85] Galushkina & Bergmann (1973); [86] Jänecke (1929); [87] Assarsson (1950a); [88] Prutton & Tower (1932); [89] Spencer *et al.* (1990); [90] Frolov *et al.* (1992); [91] Denman (1961); [92] Shevchuk & Kost' (1964); [93] Shevchuk & Pilipchenko (1968a); [94] Shevchuk & Pilipchenko (1968b); [95] Pilipchenko & Shevchuk (1969); [96] Shevchuk *et al.* (1969); [97] Shevchuk & Avarina (1965); [98] Flatt & Fritz (1950); [99] Flatt *et al.* (1961); [100] Hill & Yanick (1935); [101] Chrétien (1929); [102] Nikolajew (1929); [103] Simková & Erdös (1959); [104] Bodländer (1891b); [105] Benrath & Braun (1940); [106] Mazzotto (1891); [107] Nikolajew (1929); [108] Holluta & Mautner (1927); [109] Bodländer (1891a); [110] Mamedov *et al.* (1988); [111] Ehret (1932); [112] Emons & Röser (1967); [113] Blarez (1891); [114] Koch (1841); [115] Debler (1913); [116] Wollner (1913); [117] Jänecke & Erdmann (1920); [118] Erdös & Jiru (1960); [119] Blasdale, cited in [81]; [120] Tilden & Shenstone (1885); [121] Lunge (1885); [122] Dolique & Pauc (1946); [123] Mulder (1864, Part III, 188); [128] Hill & Loucks (1937); [125] Fedotieff (1904); [126] Makin (1959); [127] Massink (1916); [128] Foote (1925); [129] Poletaev & Krasnenkova (1975); [130] Euler (1904); [131] Benrath (1943); [132] Galushkina & Bergmann (1962); [133] Schröder (1929b); [134] Jackman & Browne (1922); [135] Seidell & Smith (1904); [136] Zhang & Muhammed (1989); [137] Fedotieff & Koltunoff (1914); [138] Babenko & Andrianov (1981); [139] Bogoyavlenskii & Gashpar (1973); [140] Caspari (1924); [141] Hill & Moskowitz (1929).

Table 7.4: Fitted model parameters for common anion ternaries: $a(\theta_{ij})$, $b(\theta_{ij})$, $c(\theta_{ij})$, and $a(\psi_{ijk})$, $b(\psi_{ijk})$, $c(\psi_{ijk})$ are the coefficients for the temperature expressions for θ_{ij} and ψ_{ijk} respectively (equation 3.38), ΔT is the temperature range of the experimental data fitted.

i	j	k	$a(\theta_{ij})$	$b(\theta_{ij})$	$c(\theta_{ij})$	$a(\psi_{ijk})$	$a(\psi_{ijk})$	$a(\psi_{ijk})$	ΔT	Source
Na	K	Cl	-0.7291×10^{-2}			0.3627×10^{-2}	-0.1891×10^{1}		−13–70	1–6
		NO_3	-0.7291×10^{-2}			0.9127	-0.1329×10^{3}	-0.1589×10^{-2}	−19–80	1–3, 7–13
		SO_4	-0.7291×10^{-2}			0.333×10^{-2}	-0.2431×10^{1}		−3–75	1, 9, 7–13
		HCO_3	-0.7291×10^{-2}			-0.3×10^{-2}			0–50	1, 20
		CO_3	-0.7291×10^{-2}			0.3×10^{-2}			−37–75	1, 21
Na	Mg	Cl	0.7×10^{-1}			0.9613	-0.321×10^{3}		0–55	1
		NO_3	0.7×10^{-1}			0.1937×10^{-1}	-0.6317×10^{2}		0–70	1, 22–28
		SO_4	0.7×10^{-1}			0.1263	-0.4252×10^{2}		0–50	1
Na	Ca	Cl	0.1875	-0.3503×10^{2}		0.2709	-0.2794×10^{2}	-0.6044×10^{-3}	−35–70	1
		NO_3	0.1875	-0.3503×10^{2}		0.5683×10^{-1}	-0.1198×10^{2}	-0.8102×10^{-4}	0–75	1, 29–32
		SO_4	0.1875	-0.3503×10^{2}		-0.1689×10^{-1}			0–75	1
Na	NH_4	Cl	0.8997×10^{-1}	-0.1043×10^{2}		0.2289	-0.1775×10^{2}	-0.5785×10^{-3}	-25–80	1, 33–39
		NO_3	0.8997×10^{-1}	-0.1043×10^{2}		-0.4947×10^{-1}	0.6149×10^{1}	0.9549×10^{-4}	−25–75	1, 40–45
		SO_4	0.8997×10^{-1}	-0.1043×10^{2}		0.499	−0.1499		−21–70	1, 46–52
K	Mg	Cl	0.0			0.5188×10^{-1}	-0.233×10^{2}		−13–75	1, 53–56
		NO_3	0.0			0.1107	-0.4372×10^{2}		0–75	1, 57–62
		SO_4	0.0			-0.6379×10^{-1}	-0.3292×10^{2}		−5–66	1, 57–59, 63
K	Ca	Cl	0.1156			−0.1066	0.2475×10^{2}		−13–55	1, 64–69
		NO_3	0.1156			0.1883×10^{1}	-0.286×10^{3}	-0.3218×10^{-2}	0–35	1, 30, 66, 70–75
		SO_4	0.1156			-0.7376×10^{1}	0.745×10^{5}		0–60	1, 76–81
K	NH_4	Cl	0.5545×10^{-2}	0.2557×10^{1}		-0.108×10^{-1}	0.3295×10^{1}		−13–75	1, 82
		NO_3	0.5545×10^{-2}	0.2557×10^{1}		-0.4728×10^{-2}			−15–70	1, 82–84
		SO_4	0.5545×10^{-2}	0.2557×10^{1}		0.4765×10^{-2}	-0.5404×10^{1}		0–60	1, 82, 85–86
Mg	Ca	Cl	0.536	−0.8522	-0.1765×10^{-3}	-0.8287×10^{-1}	0.9438×10^{1}	0.2013×10^{-3}	−30–75	1, 54–55, 67, 87–89
		NO_3	0.536	−0.8522	-0.1765×10^{-3}	0.2216×10^{1}	-0.3014×10^{3}	-0.4154×10^{-2}	−30–55	1, 90
		SO_4	0.536	−0.8522	-0.1765×10^{-3}	0.2679	0.5586×10^{2}		25–55	1, 91
Mg	NH_4	Cl	-0.5345×10^{1}	0.1557×10^{3}		0.6488×10^{1}	-0.1115×10^{4}	-0.9121×10^{-2}	3.5–60	1
		NO_3	-0.5345×10^{1}	0.1557×10^{3}					25	1
		SO_4	-0.5345×10^{1}	0.1557×10^{3}		0.1228×10^{2}	0.1678×10^{4}	-0.1721×10^{-1}	0–75	1, 92–97
Ca	NH_4	Cl	no data			no data			no data	no data
		NO_3	0.5117	-0.1732×10^{3}		0.1259×10^{-1}	0.4107×10^{1}		0–70	1, 98–99
		SO_4	0.5117	-0.1732×10^{3}		−0.1284	0.4340×10^{2}		5–70	1, 100

Table 7.5: Fitted model parameters for common cation ternaries: $a(\theta_{ij})$, $b(\theta_{ij})$, $c(\theta_{ij})$, and $a(\psi_{ijk})$, $b(\psi_{ijk})$, $c(\psi_{ijk})$ are the coefficients for the temperature expressions for θ_{ij} and ψ_{ijk} respectively (equation 3.38), ΔT is the temperature range of the experimental data fitted.

i	j	k	$a(\theta_{ij})$	$b(\theta_{ij})$	$c(\theta_{ij})$	$a(\psi_{ijk})$	$a(\psi_{ijk})$	$a(\psi_{ijk})$	ΔT	Source
Cl	NO_3	Na	−0.4121	0.1276×10^{3}		0.2163	-0.4541×10^{2}	-0.234×10^{-3}	−25–75	1–3, 7, 9, 13, 22, 23, 101–104
		K	−0.4121	0.1276×10^{3}		0.1414×10^{1}	-0.226×10^{3}	-0.2229×10^{-2}	−12–75	1–3, 7, 8, 13, 53, 66, 72, 73, 82, 105–110
		Mg	−0.4121	0.1276×10^{3}		0.9607	-0.1631×10^{3}	-0.1397×10^{-2}	-30–75	7, 22, 23, 53
		Ca	−0.4121	0.1276×10^{3}		0.3022×10^{1}	-0.4943×10^{3}	-0.4582×10^{-2}	25–60	66, 72, 73, 111
		NH_4	−0.4121	0.1276×10^{3}		0.58778	-0.9435×10^{2}	-0.9071×10^{-3}	−22–80	1, 33–36
Cl	SO_4	Na	0.5099	-0.1461×10^{3}		−0.311	0.6928×10^{2}	0.2684×10^{-3}	−22–109	1, 101
		K	0.5099	-0.1461×10^{3}		−0.2157	0.6638		−11–70	1, 14, 15, 106, 112–118
		Mg	0.5099	-0.1461×10^{3}		−0.4155	0.9602×10^{2}	0.2858×10^{-3}	0–75	1, 81, 119
		Ca	0.5099	-0.1461×10^{3}		-0.601×10^{1}	0.8973×10^{3}	0.976×10^{-2}	15–55	1, 80, 91, 120, 121
		NH_4	0.5099	-0.1461×10^{3}		−0.269	0.4347×10^{2}	0.4153×10^{-3}	−23–80	1, 122–124
Cl	HCO_3	Na	0.0359			−0.0143			−21–60	1, 125
		K	0.0359			0.0			10–40	1
Cl	CO_3	Na	−0.02			0.0085			−21–109	1
		K	−0.02			0.004			0–70	1
NO_3	SO_4	Na	0.2309	-0.1149×10^{2}	-0.3199×10^{-3}	0.1928×10^{-1}	-0.7056×10^{1}		−18–75	18, 25–27, 101, 126–129
		K	0.2309	-0.1149×10^{2}	-0.3199×10^{-3}	−0.1971	0.5912×10^{2}		−3–70	1, 18, 118, 127, 130–132
		Mg	0.2309	-0.1149×10^{2}	-0.3199×10^{-3}	−0.2551	0.3808×10^{2}	0.3972×10^{-3}	0–75	25, 26, 58, 133, 134
		Ca	0.2309	-0.1149×10^{2}	-0.3199×10^{-3}	-0.4039×10^{-2}			25	135, 136
		NH_4	0.2309	-0.1149×10^{2}	-0.3199×10^{-3}	0.5378×10^{-1}	-0.1142×10^{2}	-0.6692×10^{2}	0–70	1
NO_3	HCO_3	Na	-0.1417×10^{-1}			0.4972×10^{-2}			0–30	137
		K	-0.1417×10^{-1}			-0.1821×10^{-1}	0.8961×10^{1}		−6–40	138, 139
NO_3	CO_3	Na	0.8378×10^{-1}			0.4819×10^{-3}			0–30	29, 32
		K	0.8378×10^{-1}			-0.2401×10^{1}	0.7118×10^{3}		−6–40	1
SO_4	HCO_3	Na	0.01			−0.005			−3–50	1
		K	0.01			0.0			25–50	1
SO_4	CO_3	Na	0.02			−0.005			−3–75	1, 140
		K	0.02			−0.009			0–70	1, 141

Table 7.6: Fitted equilibrium constants (see equation 7.1) and temperature range (ΔT) of solubility data for double salts parameterised in this study.

solid	$\ln K(Tr)$	$\Delta_r H(J mol^{-1})$	$\Delta a(J mol^{-1} K^{-1})$	$\Delta b(J mol^{-1} K^{-2})$	ΔT
$CaCl_2 \cdot Ca(NO_3)2 \cdot 4H_2O$	0.2104×10^2	0.2442×10^6	-0.1215×10^5		25–60
$KCl \cdot CaCl_2$	0.1517×10^2	-0.7265×10^5			38–55
$KNO_3 \cdot 5Ca(NO_3)2 \cdot 10H_2O$	0.2468×10^2	0.183×10^6			35–55
$KNO_3 \cdot Ca(NO_3)2 \cdot 3H_2O2O$	0.2755×10^1	-0.2117×10^5	-0.6035×10^4		0–50
$K_2SO_4 \cdot 5CaSO_4 \cdot H_2O$	-0.5646×10^2	-0.6488×10^5			35-60
$K_2SO_4 \cdot CaSO_4 \cdot H_2O$	-0.1687×10^2	0.1742×10^5			0–60
$KCl \cdot MgCl_2 \cdot 6H_2O$	0.1128×10^2	0.1152×10^5	-0.1379×10^4		−20–75
$K_2SO_4 \cdot MgSO_4 \cdot 4H_2O$	-0.8971×10^1	0.7812×10^4			45–66
$K_2SO_4 \cdot MgSO_4 \cdot 6H_2O$	0.9963×10^1	-0.1779×10^4	-0.1719×10^5	0.5853×10^3	−5–50
$2MgCl_2 \cdot CaCl_2 \cdot 12H_2O$	0.3950×10^2	-0.1030×10^6	-0.5904×10^3		25–75
$MgCl_2.NH_4Cl \cdot 6H_2O$	0.1011×10^2	-0.7049×10^4	-0.1246×10^4		3.6-60
$5Mg(NO_3)2 \cdot 2NH_4NO_3 \cdot 30H_2O$	0.3761×10^2				25
$5Mg(NO_3)2 \cdot NH_4NO_3 \cdot 30H_2O$	0.366×10^2				25
$CaSO_4 \cdot Na_2SO_4$	-0.1157×10^2	-0.2638×10^5	-0.2665×10^3		25–100
$CaSO_4 \cdot 2Na_2SO_4 \cdot 2H_2O$	-0.1242×10^2	-0.4239×10^5	0.5344×10^3		25–75
$Na_2SO_4 \cdot 3K_2SO_4$	-0.1743×10^2	0.7975×10^5	0.9346×10^4	-0.3446×10^2	−3–75
$Na_2SO_4 \cdot MgSO_4 \cdot 4H_2O$	-0.536×10^1	0.1393×10^4	-0.1059×10^4		25–50
$NaNO_3 \cdot Na_2SO_4 \cdot H_2O$	0.918	0.2484×10^5	-0.5877×10^3		13–72
$NH_4NO_3 \cdot Ca(NO_3)_2$	0.1033×10^2	0.1073×10^6			40–75
$NH_4NO_3 \cdot Ca(NO_3)_2 \cdot 2H_2O$	0.9202×10^1	0.4425×10^5			10–40
$NH_4NO_3 \cdot Ca(NO_3)_2 \cdot 3H_2O$	0.7519×10^1	0.6198×10^5			0–35
$NH_4NO_3 \cdot 5Ca(NO_3)_2 \cdot 10H_2O$	0.3573×10^2	0.1461×10^6			10–75
$2CaSO_4 \cdot (NH_4)2SO_4$	-0.2058×10^2				50–75
$5CaSO_4 \cdot (NH_4)_2SO_4 \cdot H_2O$	-0.5065×10^2	-0.1929×10^6	0.1102×10^5		25–75
$CaSO_4 \cdot (NH_4)_2SO_4 \cdot H_2O$	-0.10908×10^2	-0.6374×10^4			25–75
$(NH_4 \cdot K)_2SO_4$	see note (a)				25–60
$(NH_4)_2SO_4 \cdot MgSO_4 \cdot 6H_2O$	-0.1071×10^2	0.1678×10^5	-0.3020×10^4		25–75
$(NH_4)_2SO_4 \cdot Na_2SO_4 \cdot 4H_2O$	-0.3935×10^1	0.499×10^5	0.6091×10^4	-0.2255×10^2	−19–99
$(NH_4)_2SO_4 \cdot 3NH_4NO_3$	0.6901×10^1	0.7462×10^5	-0.6336×10^3		0–70
$(NH_4)_2SO_4 \cdot 2NH_4NO_3$	0.4607×10^1	0.5474×10^5	-0.3974×10^3		0 –70

(a) solid of continuously varying composition; equilibrium constant given by:

$\ln K[\text{solid solution}] = f \ln K[(NH_4)_2SO_4] + (1 - f) \ln K[K_2SO_4]$

where

$f = (-0.6195 + 0.0044T) X_A^{(12.75 - -0.0342T)}$, and $X_A = mNH_4/(mNH_4 + mK)$

7.3 Conclusion

The prediction of the deterioration of porous materials containing complex salt solutions requires a thermodynamic model appropriate to the conditions found in pore water. With this aim in mind, Pitzer model interaction parameters have either been adopted from the literature, or determined by fitting to experimental solubilities for the following multi-ion systems (with the exception of Ca–NH_4–Cl for which no solubility data were found):

1. Na–K–Ca–Mg–NH_4–Cl–NO_3–SO_4–H_2O ($\Delta T \sim -20$–$70°C$)
2. Na–K–Cl–NO_3–SO_4–HCO_3–H_2O ($\Delta T \sim -20$–$70°C$)
3. Na–K–Cl–NO_3–SO_4–CO_3–H_2O ($\Delta T \sim -20$–$70°C$).

The parameterisation of these systems has been performed for as much of the temperature range $-40°C$ to $50°C$ as was allowed by the available solubility data. For the vast majority of salts parameterised in this study, the solubility data included in the fitting process covered the entire solubility range up to saturation — the exception being NH_4NO_3 for which data above a concentration of 40.0 mol kg^{-1} were necessarily neglected. The emphasis upon including data up to saturation was to ensure that the fully parameterised model was optimised to the prediction of the solubilities of the mineral phases in pore water.

The range of ions included in this parameterisation was not as comprehensive as originally anticipated for the model. This was mainly due to lack of available experimental solubility data for the formates, acetates and oxalates. However, the solubility measurements from the project partners in IAAC did allow the parameterisation of the multi-ion system Na–Ca–Cl–CH_3COO–H_2O (Chapter 5). The combined model will thus facilitate the prediction of salt solubility in the majority of salt mixtures of interest to the conservator.

7.4 Binary interaction parameters adopted from literature sources

7.4.1 Na_2SO_4 model parameters

Source: Holmes & Mesmer (1986)
Fitting range: 273–498K
$\alpha = 1.4$

$$
\begin{aligned}
T_r &= 298.15\text{K} \\
\beta^{(0)} &= -1.727 \times 10^{-2} \\
&\quad + 1.7828 \times 10^{-3}(T_r - T_r^2/T) \\
&\quad + 9.133 \times 10^{-6}(T^2 + 2T_r^3/T - 3T_r^2) \\
&\quad + (-6.552)(\log(T/T_r) + T_r/T - 1) \\
&\quad + (-96.9)(1/(680 - T) + (T_r^2 - 680T)/(T(680 - T_r)^2)) \\
\beta^{(1)} &= 7.534 \times 10^{-1} \\
&\quad + 5.61 \times 10^{-3}(T_r - T_r^2/T)
\end{aligned}
$$

$$+ (-5.7513 \times 10^{-4})(T_2 + 2T_r^3/T - 3T_r^2)$$
$$+ 1.11068(T + T_r^2/T - 2T_r)$$
$$+ (-378.8)(\log(T/T_r) + T_r/T - 1)$$
$$+ 1861.3(1/(680 - T) + (T_r^2 - 680T)/(T(680 - T_r)^2))$$

$$C^{\phi(0)} = 1.1745 \times 10^{-2}$$
$$+ (-3.3038 \times 10^{-4})(T_r - T_r^2/T)$$
$$+ 1.85794 \times 10^{-5}(T_2 + 2T_r^3/T - 3Tr2)$$
$$+ (-3.92 \times 10^{-2})(T + T_r^2/T - 2T_r)$$
$$+ 14.213(\log(T/T_r) + T_r/T - 1)$$
$$+ (-24.95)(1/(680 - T) + (T_r^2 - 680T)/(T(680 - T_r)^2))$$

$$C^{\phi(1)} = 0.0$$

7.4.2 Na_2CO_3 model parameters

Source: Monnin & Schott (1984)
$\alpha = 2.0$

$$T_r = 298.15\text{K}$$

$$\beta^{(0)} = 0.0362 + 1.79 \times 10^{-3}(T - T_r) + 0.5(-4.22 \times 10^{-5})(T - T_r)^2$$
$$\beta^{(1)} = 1.51 + 2.05 \times 10^{-3}(T - T_r) + 0.5(-16.8 \times 10^{-5})(T - T_r)^2$$
$$C^{\phi(0)} = 0.0052$$
$$C^{\phi(1)} = 0.0$$

7.4.3 $NaHCO_3$ model parameters

Source: Monnin & Schott (1984)
$\alpha = 2.0$

$$T_r = 298.15$$

$$\beta^{(0)} = 0.028 + 10^{-3}(T - T_r) - 0.5(2.6 \times 10^{-5})(T - T_r)^2$$
$$\beta^{(1)} = 0.044 + 1.1 \times 10^{-3}(T - T_r) - 0.5(4.3 \times 10^{-5})(T - T_r)^2$$
$$C^{\phi(0)} = 0.0$$
$$C^{\phi(1)} = 0.0$$

7.4.4 NaOH model parameters

Source: Monnin & Schott (1984)
$\alpha = 2.0$

$$T_r = 298.15\text{K}$$

$$\beta^{(0)} = 0.0864 + 0.7 \times 10^{-3}(T - T_r) + 0.5(-2 \times 10^{-5})(T - T_r)^2$$
$$\beta^{(1)} = 0.253 + 0.134 \times 10^{-3}(T - T_r) + 0.5(-2.1 \times 10^{-5})(T - T_r)^2$$
$$C^{\phi(0)} = 0.0044 - 0.1894 \times 10^{-3}(T - T_r) + 0.5(0.29 \times 10^{-5})(T - T_r)^2$$
$$C^{(1)} = 0.0$$

7.4.5 KCl model parameters

Source: Holmes & Mesmer (1983)
Fitting range: 273–523K at 1 bar
$\alpha = 2.0$

$$T_r = 298.15\text{K}$$

$$\begin{aligned}\beta^{(0)} &= 4.808 \times 10^{-2} \\ &+ (-758.48)(1/T - 1/T_r) \\ &+ (-4.7062)\log(T/T_r) \\ &+ 1.0072 \times 10^{-2}(T - T_r) \\ &+ (-3.7599 \times 10^{-6})(T^2 - T_r^2)\end{aligned}$$

$$\begin{aligned}\beta^{(1)} &= 4.76 \times 10^{-2} \\ &+ 303.9(1/T - 1/T_r) \\ &+ 1.066\log(T/T_r) \\ &+ 4.70 \times 10^{-2}\log(T - 260)\end{aligned}$$

$$\begin{aligned}C^{\phi(0)} &= -7.88 \times 10^{-4} \\ &+ 91.27(1/T - 1/T_r) \\ &+ 5.8643 \times 10^{-1}\log(T/T_r) \\ &+ (-1.298 \times 10^{-3})(T - T_r) \\ &+ 4.9567 \times 10^{-7}(T_2 - T_r^2)\end{aligned}$$

$$C^{\phi(1)} = 0.0$$

7.4.6 K_2SO_4 model parameters

Source: Holmes & Mesmer (1986)
Fitting range: 273–498K at 1 bar
$\alpha = 1.4$

$$T_r = 298.15\text{K}$$

$$\begin{aligned}\beta^{(0)} &= 0.0 \\ &+ 7.476 \times 10^{-4}(T_r - T_r^2/T) \\ &+ 4.265 \times 10^{-3}(T + T_r^2/T - 2T_r) \\ &+ (-3.088)(\log(T/T_r) + T_r/T - 1)\end{aligned}$$

$$\beta^{(1)} = 6.179 \times 10^{-1}$$
$$+ 6.85 \times 10^{-3}(T_r - T_r^2/T)$$
$$+ 5.576 \times 10^{-5}(T_2 + 2T_r^3/T - 3T_r^2)$$
$$+ (-5.841 \times 10^{-2})(T + T_r^2/T - 2T_r)$$
$$+ (-0.9)(1/(T - 263) + (263T - T_r^2)/(T(T_r - 263)^2))$$

$$C^{\phi(0)} = 9.1547 \times 10^{-3} + (-1.81 \times 10^{-4})(T + T_r^2/T - 2T_r)$$

$$C^{\phi(1)} = 0.0$$

7.4.7 K_2CO_3 model parameters

Source: Harvie *et al.* (1984)
$\alpha = 2.0$

$$\beta^{(0)} = 0.1488$$
$$\beta^{(1)} = 1.43$$
$$C^{\phi(0)} = -0.0015$$
$$C^{\phi(1)} = 0.0$$

7.4.8 $KHCO_3$ model parameters

Source: Harvie *et al.* (1984)
$\alpha = 2.0$

$$\beta^{(0)} = 0.0296$$
$$\beta^{(1)} = -0.013$$
$$C^{\phi(0)} = -0.008$$
$$C^{\phi(1)} = 0.0$$

7.4.9 KOH model parameters

Source: Harvie *et al.* (1984)
$\alpha = 2.0$

$$\beta^{(0)} = 0.1298$$
$$\beta^{(1)} = 0.320$$
$$C^{\phi(0)} = 0.0041$$
$$C^{\phi(1)} = 0.0$$

7.4.10 $MgCl_2$ model parameters

Source: de Lima & Pitzer (1983)
Fitting range: 298–473K at 1 bar
$\alpha = 2.0$

$$\beta^{(0)} = 5.76066 \times 10^{-1} + (-9.31654 \times 10^{-4})T + 5.93915 \times 10^{-7}T^2$$
$$\beta^{(1)} = 2.60135 + (-1.09438 \times 10^{-2})T + 2.60169 \times 10^{-5}T^2$$
$$C^{\phi(0)} = 5.9532 \times 10^{-2} + (-2.49949 \times 10^{-4})T + 2.41831 \times 10^{-7}T^2$$
$$C^{(1)} = 0.0$$

7.4.11 $MgSO_4$ model parameters

Source: Phutela & Pitzer (1986)
Fitting range: 273–498K at 1 bar
$\alpha_1 = 1.4$
$\alpha_2 = 12.0$

$$T_r = 298\text{K}$$

$$\begin{aligned}\beta^{(0)} &= 2.1499 \times 10^{-1} \\ &+ (-1.0282)(T/2 + T_r^2/2T - T_r) \\ &+ 8.479 \times 10^{-3}(T^2/6 + T_r^3/3T - T_r^2/2) \\ &+ (-2.33667 \times 10^{-5})(T^3/12 + T_r^4/4T - T_r^3/3) \\ &+ 2.1575 \times 10^{-8}(T^4/20 + T_r^5/5T - T_r^4/4) \\ &+ 6.8402 \times 10^{-4}(T_r - T_r^2/T)\end{aligned}$$

$$\begin{aligned}\beta^{(1)} &= 3.3646 \\ &+ (-2.9596 \times 10^{-1})(T/2 + T_r^2/2T - T_r) \\ &+ 9.4564 \times 10^{-4}(T^2/6 + T_r^3/3T - T_r^2/2) \\ &+ 1.1028 \times 10^{-2}(T_r - T_r^2/T)\end{aligned}$$

$$\begin{aligned}\beta^{(2)} &= -32.743 \\ &+ (-1.3764 \times 10^{-1})(T/2 + T_r^2/2T - T_r) \\ &+ 1.2121 \times 10^{-1}(T^2/6 + T_r^3/3T - T_r^2/2) \\ &+ (-2.7642 \times 10^{-4})(T^3/12 + T_r^4/4T - T_r^3/3) \\ &+ (-2.1515 \times 10^{-1})(T_r - T_r^2/T)\end{aligned}$$

$$\begin{aligned}C &= 6.993 \times 10^{-3} \\ &+ 1.0541 \times 10^{-1}(T/2 + T_r^2/2T - T_r) \\ &+ (-8.9316 \times 10^{-4})(T^2/6 + T_r^3/3T - T_r^2/2) \\ &+ 2.51 \times 10^{-6}(T^3/12 + T_r^4/4T - T_r^3/3) \\ &+ (-2.3436 \times 10^{-9})(T^4/20 + T_r^5/5T - T_r^4/4) \\ &+ (-8.7899 \times 10^{-5})(T_r - T_r^2/T)\end{aligned}$$

$$C^{\phi(0)} = 4C$$

$$C^{\phi(1)} = 0.0$$

7.4.12 $CaSO_4$ model parameters

Source: Moller (1987)
$\alpha_1 = 1.4$
$\alpha_2 = 12.0$

$$T_r = 298\text{K}$$

$$\beta^{(0)} = 0.15$$

$$\beta^{(1)} = 3.0$$

$$\beta^{(2)} = -129.399287 + 4.00431027 \times 10^{-1}(T)$$

$$C^{\phi(0)} = 0.0$$

$$C^{\phi(1)} = 0.0$$

7.4.13 $(NH_4)_2SO_4$ model parameters

Source: Clegg *et al.* (1996)
Fitting range: 298K to approx. 383K at 1 bar
$\alpha = 2.0$
$\omega = 2.5$
Note: expressions below are built up from the parameter values at 25°C (P) and with first ($P1$), second ($P2$), and third ($P3$) temperature differentials also at 25°C:

$$\begin{aligned} P(T) &= P \\ &+ (P1 - P2T_r - 0.5P3TT_r)(T - T_r) \\ &+ 0.5P2(T^2 - T_r^2) \\ &+ (1/6)P3(T^3 - T_r^3) \end{aligned}$$

$$\begin{aligned} \beta^{(0)} &= 0.0374028 \\ &+ (0.347309 \times 10^{-3} - (-0.571929 \times 10^{-5})T_r - 0.5(0.0)TT_r)(T - T_r) \\ &+ 0.5(-0.571929 \times 10^{-5})(T^2 - T_r^2) \\ &+ (1/2)(0.0)(T^3 - T_r^3) \end{aligned}$$

$$\begin{aligned} \beta^{(1)} &= 0.534514 \\ &+ (0.462287 \times 10^{-2} - (-0.216307 \times 10^{-3})T_r - 0.5(-0.162030 \times 10^{-5})TT_r)(T - T_r) \\ &+ 0.5(-0.216307 \times 10^{-3})(T^2 - T_r^2) \\ &+ (1/6)(-0.162030 \times 10^{-5})(T^3 - T_r^3) \end{aligned}$$

$$\begin{aligned} C^{\phi(0)} &= -0.615514 \times 10^{-3} \\ &+ (-0.387711 \times 10^{-4} - (0.474881 \times 10^{-6})T_r - 0.5(0.555927 \times 10^{-8})TT_r)(T - T_r) \end{aligned}$$

$$+ 0.5(0.474881 \times 10^{-6})(T^2 - T_2^r)$$
$$+ (1/6)(0.555927 \times 10^{-8})(T^3 - T_3^r)$$

$$C^{\phi(1)} = 0.464606$$
$$+ (0.227143 \times 10^{-1} - (0.0)T_r - 0.5(0.0)TT_r)(T - T_r)$$
$$+ 0.5(0.0)(T^2 - T_r^2)$$
$$+ (1/6)(0.0)(T^3 - T_r^3)$$

7.4.14 Fortran Pseudocode for NaCl model parameters

Source: Archer (1992).

First the Archer model parameters, for $\beta^{(0)}$...

```
      DATA (BX(1,J),J=1,24)/0.242408292826506D0,0.D0,
     > -0.162683350691532D0,1.38092472558595D0,0.D0,0.D0,
     > -67.2829389568145D0,0.D0,0.625057580755179D0,-21.2229227815693D0,
     > 81.8424235648693D0,-1.59406444547912D0,0.D0,0.D0,
     > 28.6950512789644D0,-44.3370250373270D0,1.92540008303069D0,
     > -32.7614200872551D0,0.D0,0.D0,30.9810098813807D0,
     > 2.46955572958185D0,-0.725462987197141D0,10.1525038212526D0/
```

now $\beta^{(1)}$...

```
      DATA (BX(2,J),J=1,24)/ -1.90196616618343D0,5.45706235080812D0,
     >  0.D0,-40.5376417191367D0,0.D0,0.D0,485.065273169753D0,
     > -0.661657744698137D0,0.D0,0.D0,242.206192927009D0,0.D0,
     > -99.0388993875343D0,0.D0,0.D0,-59.5815563506284D0,8*0.D0/
```

now $C^{(0)}$...

```
      DATA (BX(3,J),J=1,24)/ 0.D0,-0.0412678780636594D0,
     >  0.0193288071168756D0,-0.338020294958017D0,0.D0,
     >  0.0426735015911910D0,4.14522615601883D0,-0.00296587329276653D0,
     >  0.D0,1.39697497853107D0,-3.80140519885645D0,0.06622025084D0,
     >  0.D0,-16.8888941636379D0,-2.49300473562086D0,3.14339757137651D0,
     >  0.D0,2.79586652877114D0,5*0.D0,-0.502708980699711D0/
```

now $C^{(1)}$...

```
      DATA (BX(4,J),J=1,24)/0.78898797421857D0,-3.67121085194744D0,
     >  1.12604294979204D0,0.D0,0.D0,-10.1089172644722D0,17*0.D0,
     >  16.6503495528290D0/

** 250-533K ** <100 MPa ** ARCHER EXTENDED MODEL
 NB: Pressure 'PR' comes in as bars, but Archer
works in MPa, hence change below.
 ***********************************************
```

set reference temperature ($T_0 = 1\text{K}$), reference pressure ($P_0 = 1.0\text{MPa}$) and convert pressure ($PR = 1.0\text{Bars}$) into MPa:

```
      P0 = 1.D0
      PR = 1.D0 / 10.D0
      T0 = 1.D0

      DO 1 I=1,4
        DP1 = BX(I,1) + BX(I,2)*T/(1000.D0*T0)
     >    + BX(I,3)*(T/(500.D0*T0))**2
     >    + BX(I,4)*T0/(T-200.D0) + BX(I,5)*T0/T
     >    + BX(I,6)*100.D0*(T0/(T-200.D0))**2
     >    + BX(I,7)*200.D0*(T0/T)**2 + BX(I,8)*(T/(500.D0*T0))**3
     >    + BX(I,9)*SQRT(T0/(650.D0-T))
     >    + BX(I,10)*1.D-5*(PR/P0)
     >    + BX(I,11)*2.D-4*(PR/P0)*(T0/(T-225.D0))
     >    + BX(I,12)*1.D2*(PR/P0)*(T0/(650.D0-T))**3
     >    + BX(I,13)*1.D-5*(PR/P0)*(T/(500.D0*T0))
     >    + BX(I,14)*2.D-4*(PR/P0)*(T0/(650.D0-T))

        DP2 = BX(I,15)*1.D-7*(PR/P0)**2
     >    + BX(I,16)*2.D-6*(PR/P0)**2*(T0/(T-225.D0))
     >    + BX(I,17)*(PR/P0)**2*(T0/(650.D0-T))**3
     >    + BX(I,18)*1.D-7*(PR/P0)**2*(T/(500.D0*T0))
     >    + BX(I,19)*1.D-7*(PR/P0)**2*(T/(500.D0*T0))**2
     >    + BX(I,20)*4.D-2*(PR/P0)*(T0/(T-225.D0))**2
     >    + BX(I,21)*1.D-5*(PR/P0)*(T/(500.D0*T0))**2
     >    + BX(I,22)*2.D-8*(PR/P0)**3*(T0/(T-225.D0))
     >    + BX(I,23)*1.D-2*(PR/P0)**3*(T0/(650.D0-T))**3
     >    + BX(I,24)*200.D0*(T0/(650.D0-T))**3

      IF(I.EQ.1) THEN
        β(0) = DP1+DP2
      ELSEIF(I.EQ.2) THEN
        β(1) = DP1+DP2
      ELSEIF(I.EQ.3) THEN
        C(0) = DP1+DP2
```

...convert C to C^{ϕ}:

```
      Cφ(0) = C(0) * 2.D0
      ELSEIF(I.EQ.4) THEN
      C(1) = DP1+DP2
```

...convert C to C^{ϕ}:

```
      Cφ(1) = C(1) * 2.D0
      ENDIF
      CONTINUE
```

7.5 Predicted solubility diagrams at 25°C for the ternary systems parameterised in this study

Solubility diagrams for each of the ternary salt systems are reproduced in this section. Solubility curves were calculated separately for each mineral phase that saturates in the ternary solutions at 25°C. In general, the procedure adopted was to take the experimental compositions of one of the ternary components as being fixed (represented by the ordinate in the following diagrams), and then to perform a one-dimensional (vertical) minimisation to obtain the concentration of the other ternary component using the model calculated activities and the mineral solubility product. The one-dimensional minimisation was performed using the golden-section method (Press 1992). For some salt mixtures discontinuities occur in the calculated solubilities at very high ionic strengths. These are due to the inability of the molality-based model described in Chapter 3 to represent the thermodynamic properties adequately. Chapter 8 describes the alternative model that is used in ECOS to overcome these problems.

An exception to the above methodology is the NH_4K–Cl ternary, which contains a number of solid solutions. In this case, the various crystalline phases were assigned to either the KCl or NH_4Cl branch of the isotherm, and the solubility curve calculated as if they were pure KCl or pure NH_4Cl. The solid solutions present in the NH_4–K–NO_3 ternary were treated analogously.

In all of the following diagrams the experimental solubility data are represented as points, whilst the model calculated solubility curve is shown as a solid line.

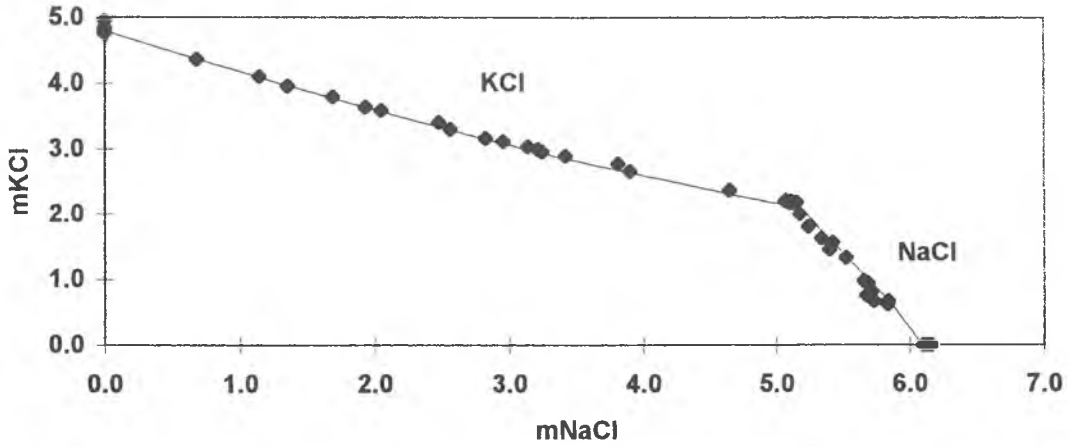

Figure 7.1: Solubility diagram for Na–K–Cl at 25°C.

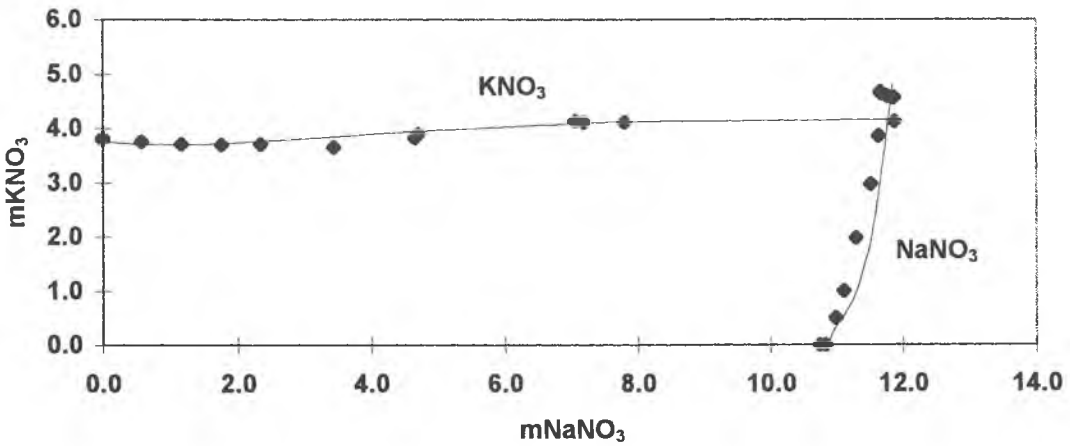

Figure 7.2: Solubility diagram for Na–K–NO_3 at 25°C.

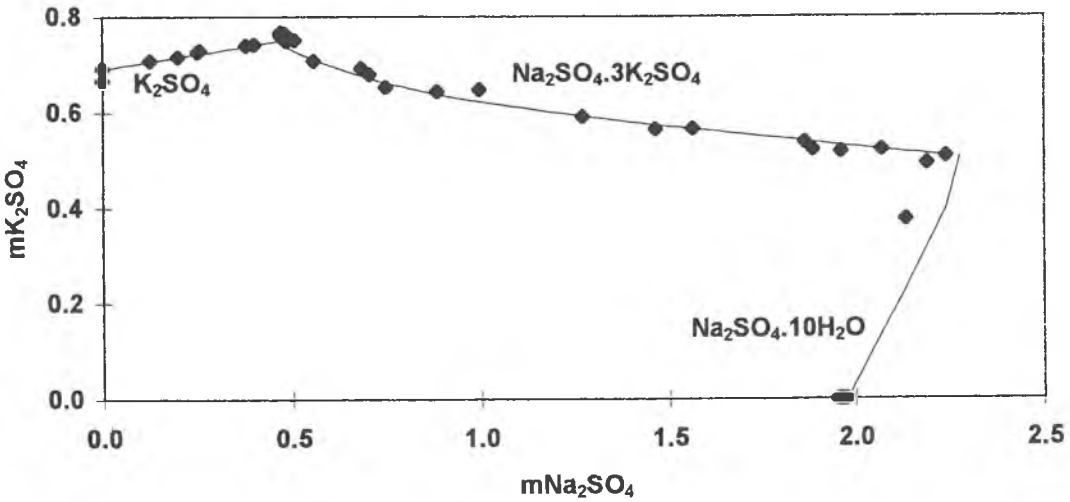

Figure 7.3: Solubility diagram for Na–K–SO_4 at 25°C.

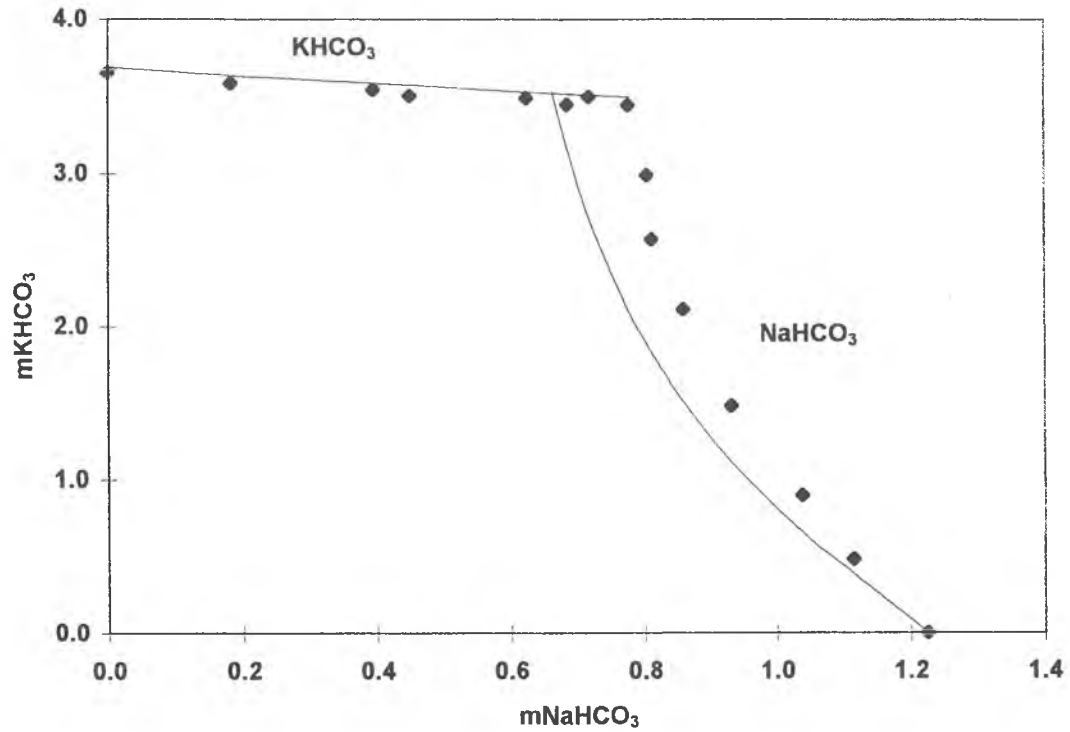

Figure 7.4: Solubility diagram for Na–K–HCO_3 at 25°C.

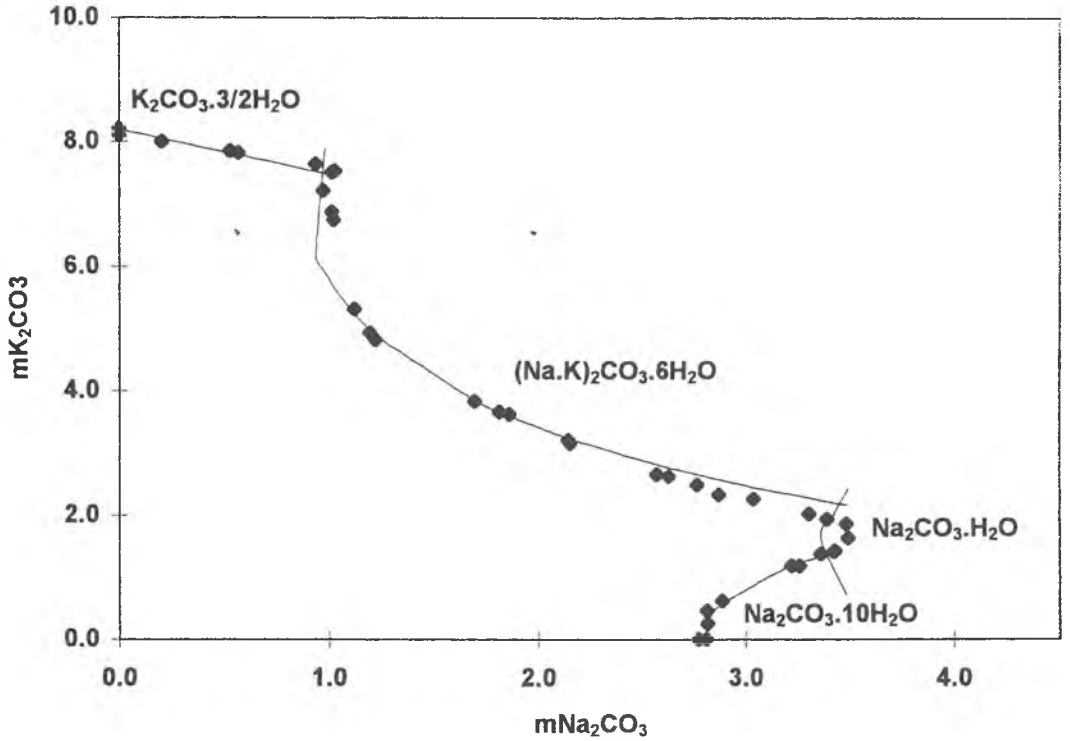

Figure 7.5: Solubility diagram for Na–K–CO_3 at 25°C.

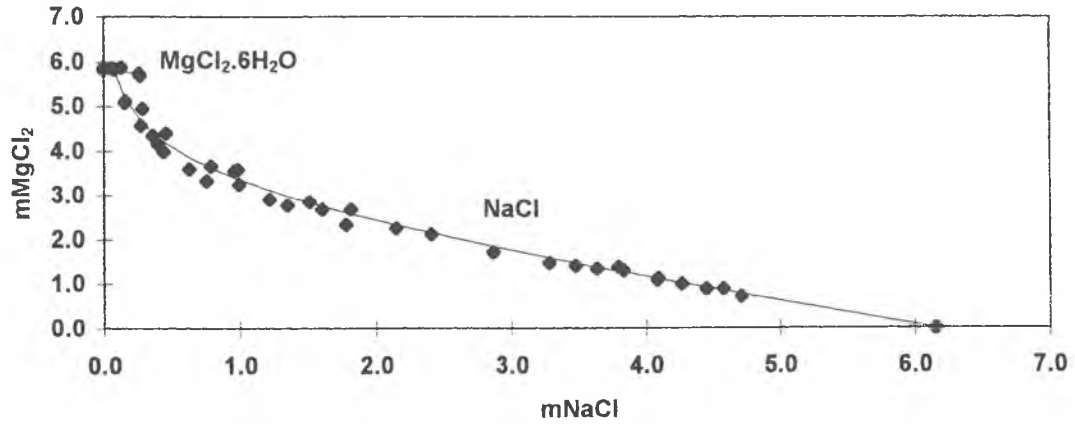

Figure 7.6: Solubility diagram for Na–Mg–Cl at 25°C.

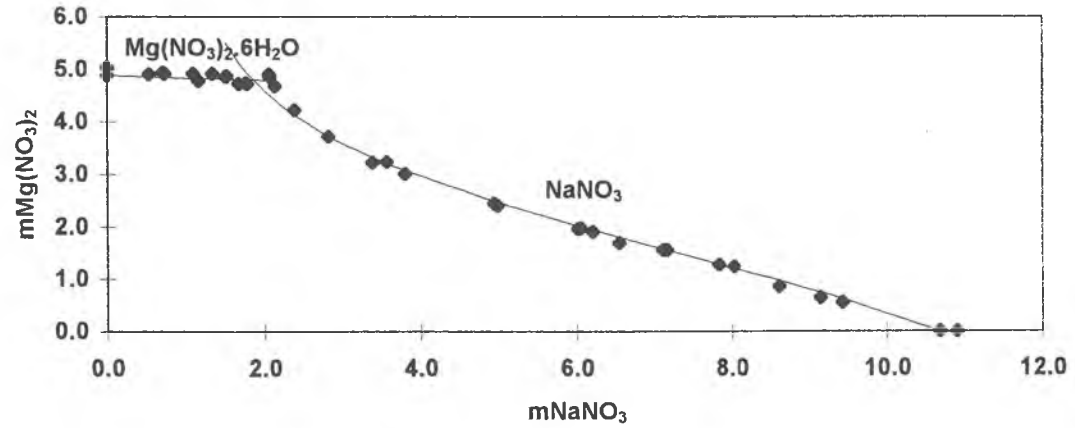

Figure 7.7: Solubility diagram for Na–Mg–NO_3 at 25°C.

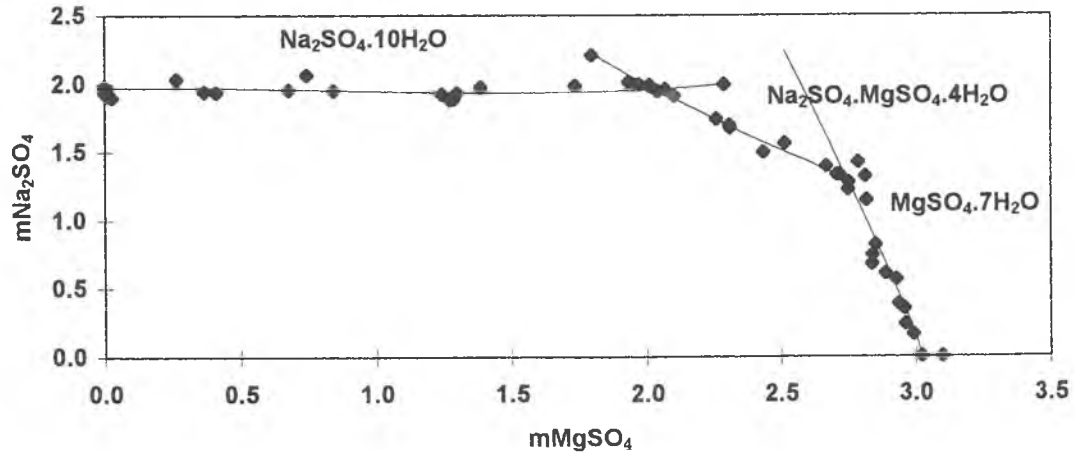

Figure 7.8: Solubility diagram for Na–Mg–SO_4 at 25°C.

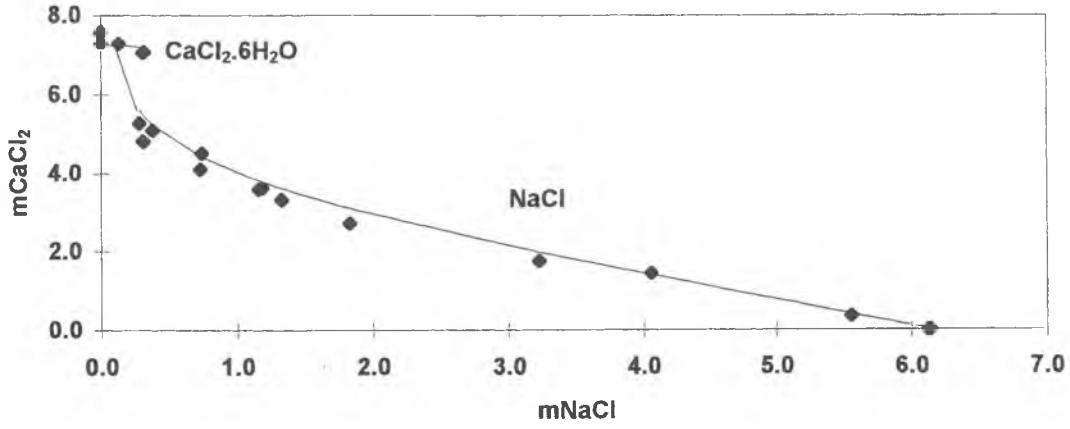

Figure 7.9: Solubility diagram for Na–Ca–Cl at 25°C.

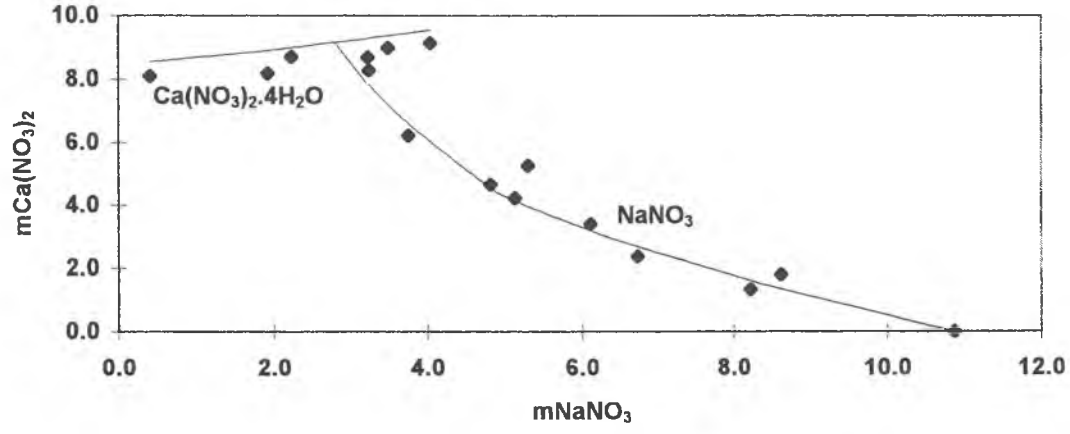

Figure 7.10: Solubility diagram for Na–Ca–NO_3 at 25°C.

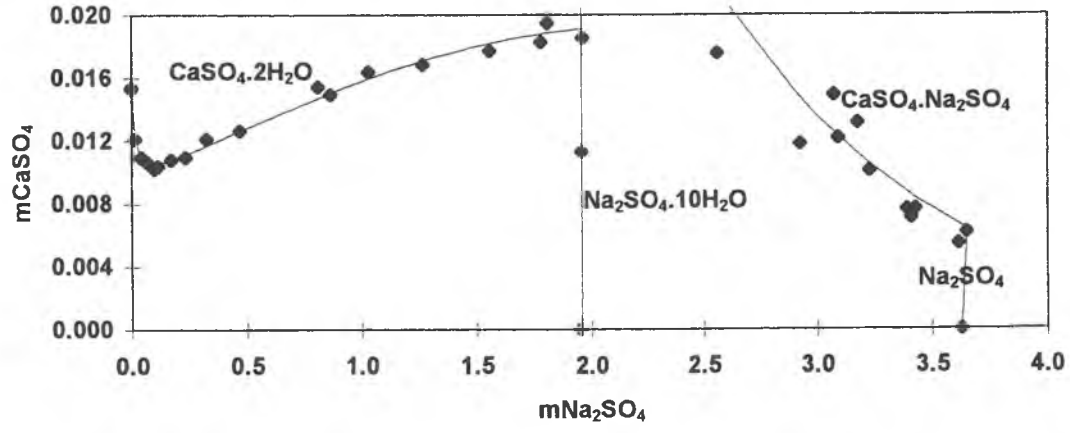

Figure 7.11: Solubility diagram for Na–Ca–SO_4 at 25°C.

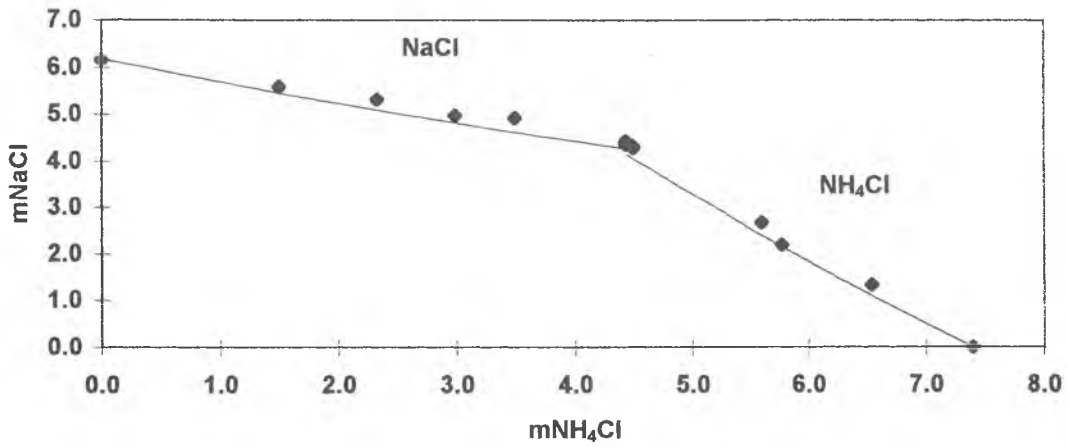

Figure 7.12: Solubility diagram for NH_4–Na–Cl at 25°C.

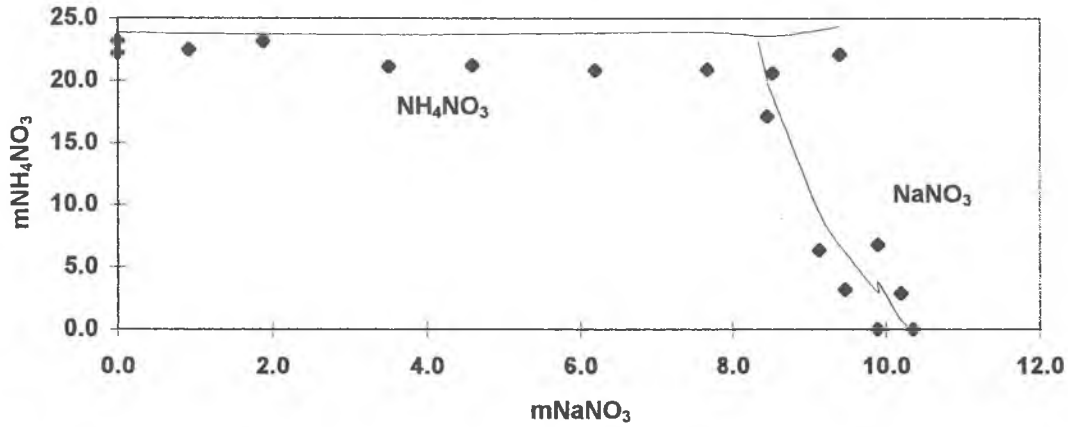

Figure 7.13: Solubility diagram for NH_4–Na–NO_3 at 25°C.

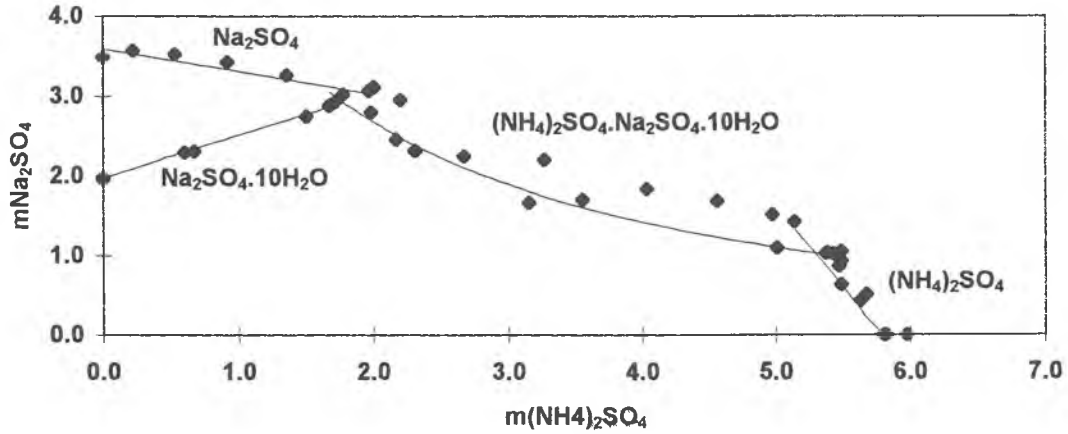

Figure 7.14: Solubility diagram for NH_4–Na–SO_4 at 25°C.

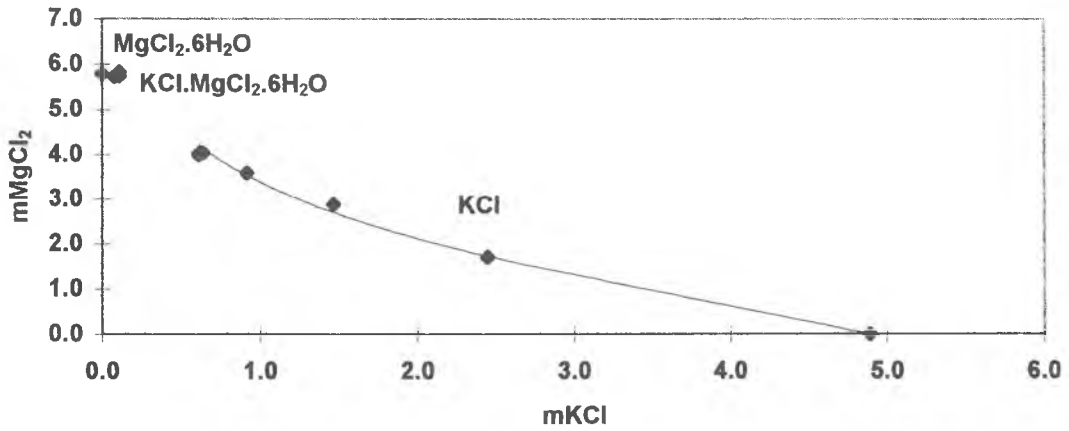

Figure 7.15: Solubility diagram for K–Mg–Cl at 25°C.

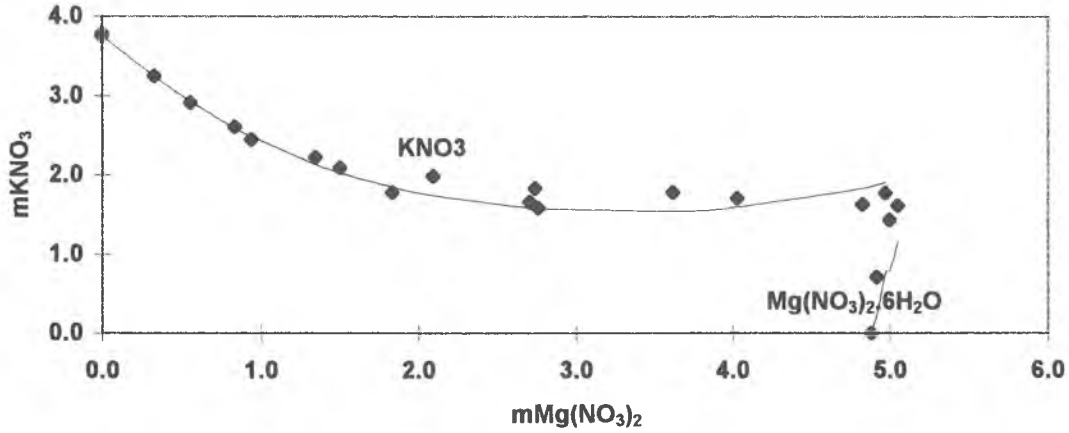

Figure 7.16: Solubility diagram for K–Mg–NO_3 at 25°C.

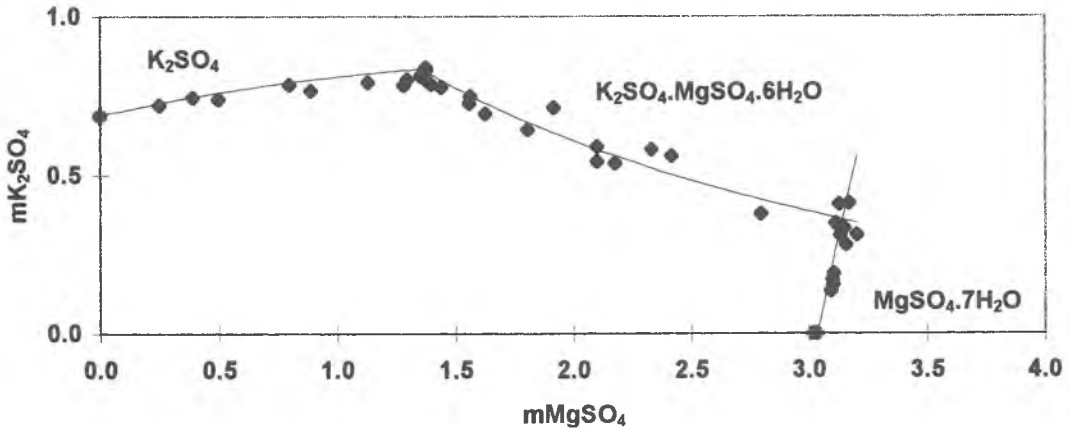

Figure 7.17: Solubility diagram for K–Mg–SO_4 at 25°C.

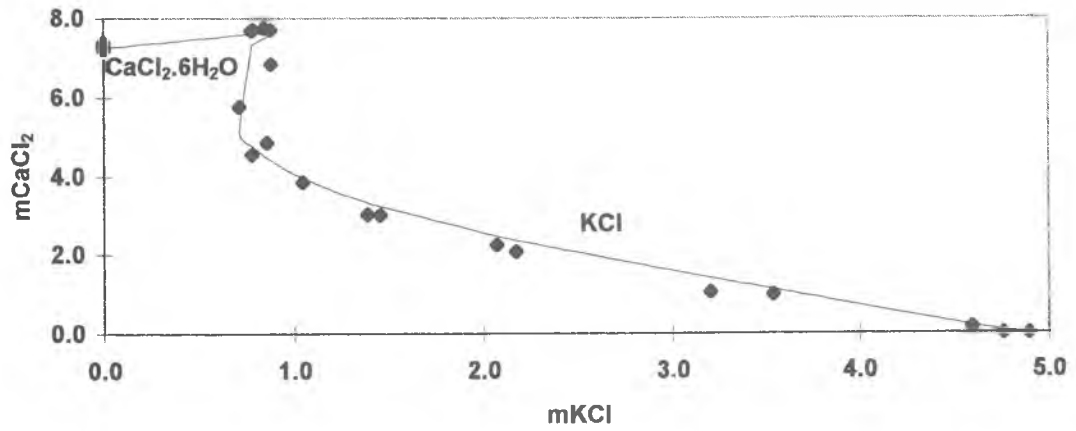

Figure 7.18: Solubility diagram for K–Ca–Cl at 25°C.

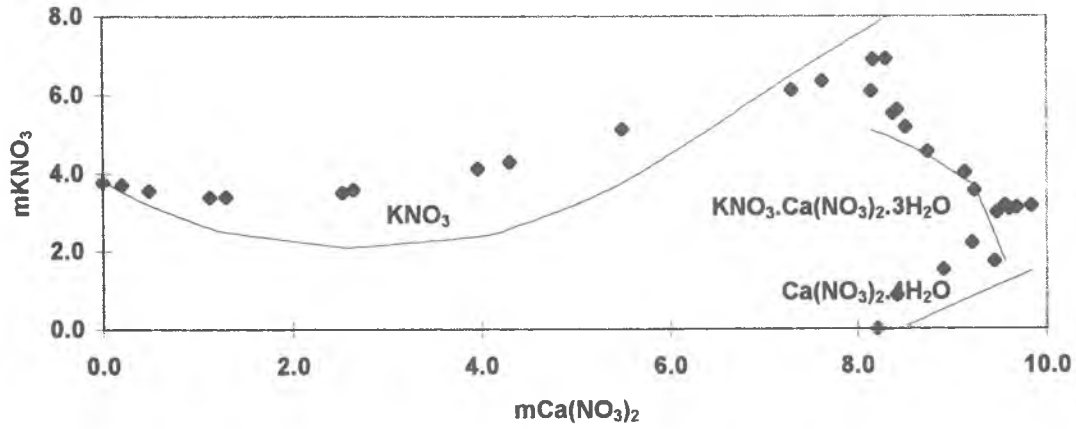

Figure 7.19: Solubility diagram for K–Ca–NO_3 at 25°C.

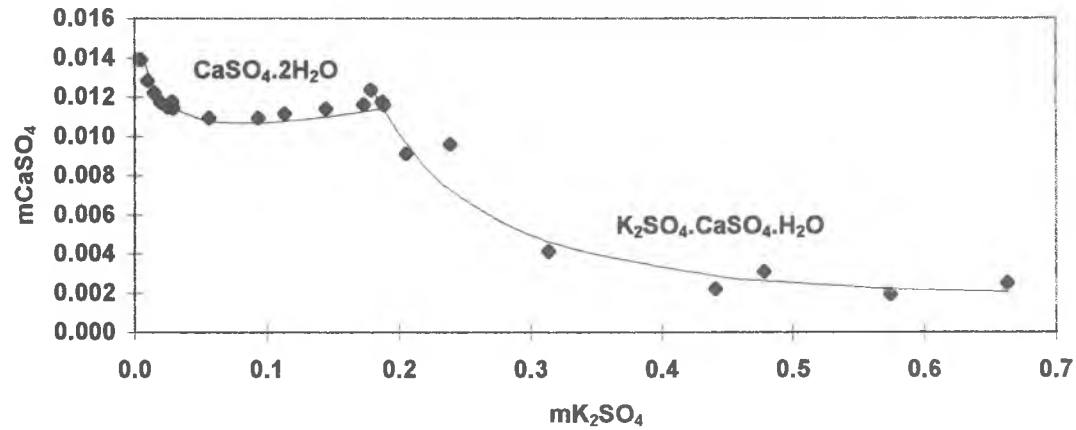

Figure 7.20: Solubility diagram for K–Ca–SO_4 at 25°C.

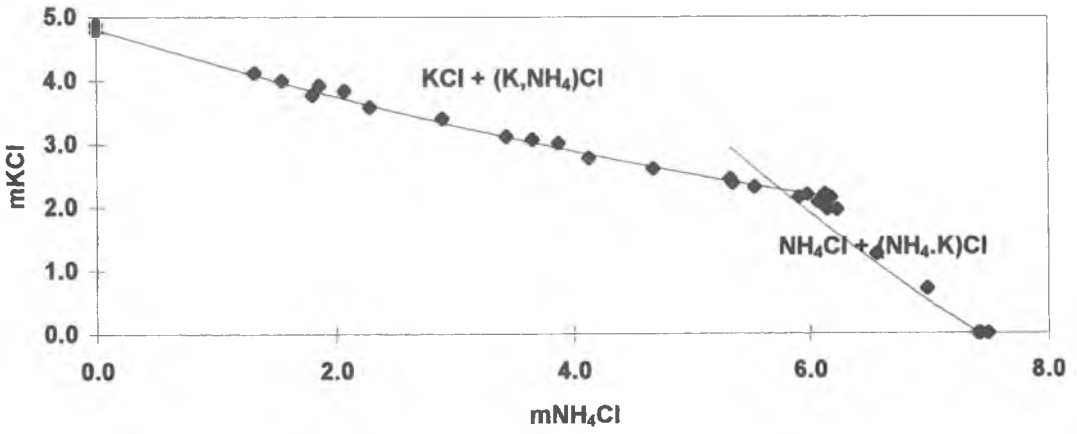

Figure 7.21: Solubility diagram for K–NH_4–Cl at 25°C.

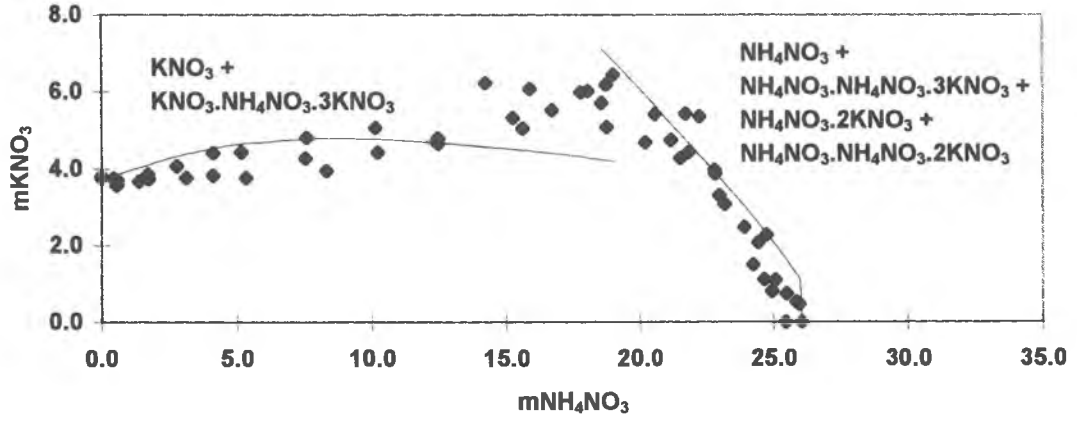

Figure 7.22: Solubility diagram for K–NH_4–NO_3 at 25°C.

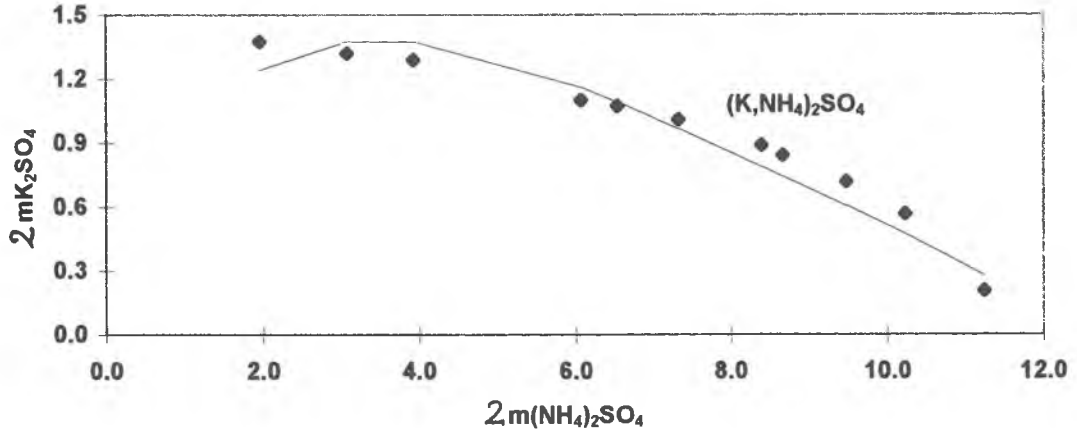

Figure 7.23: Solubility diagram for K–NH_4–SO_4 at 25°C.

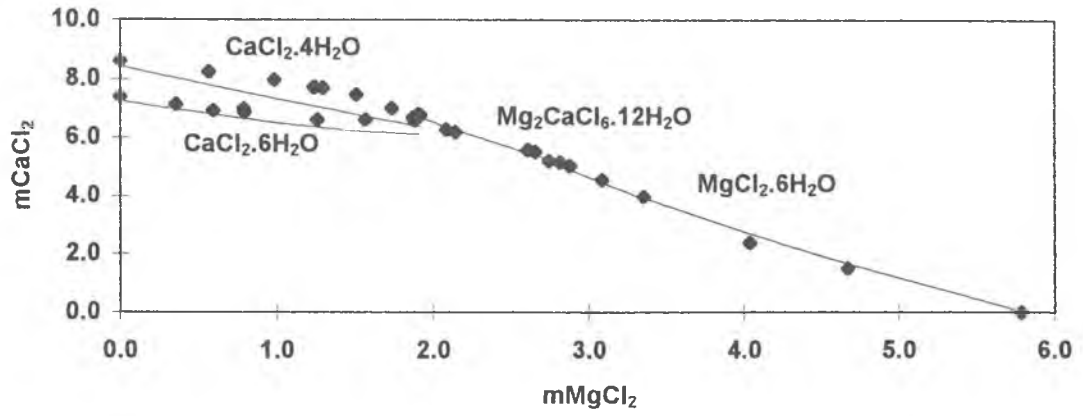

Figure 7.24: Solubility diagram for Mg–Ca–Cl at 25°C.

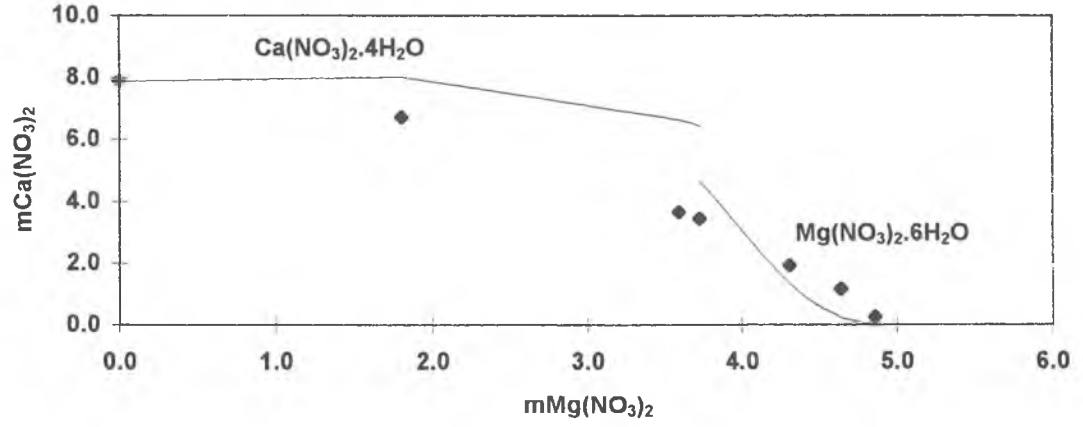

Figure 7.25: Solubility diagram for Mg–Ca–NO_3 at 25°C.

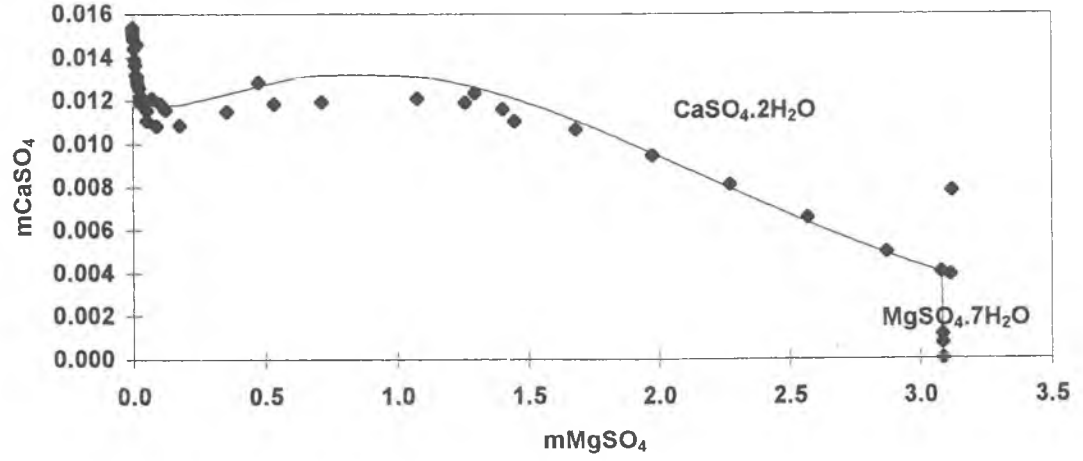

Figure 7.26: Solubility diagram for Mg–Ca–SO_4 at 25°C.

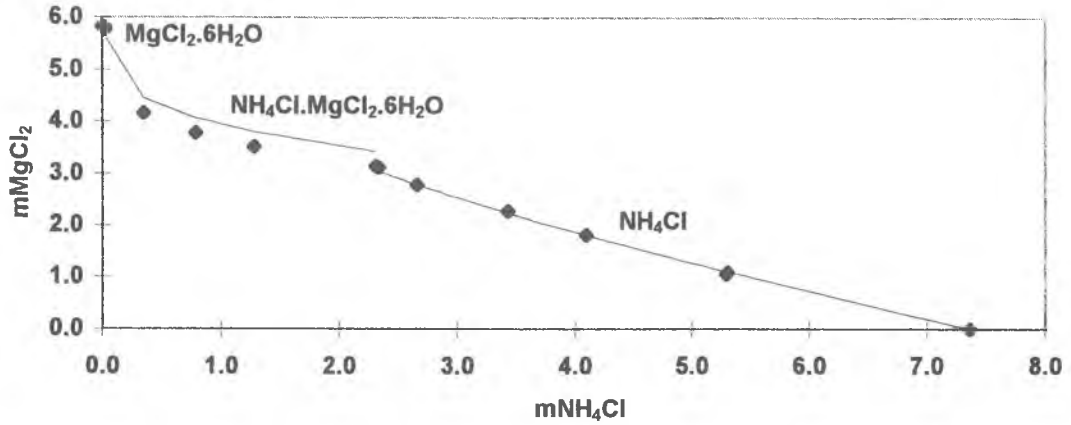

Figure 7.27: Solubility diagram for NH_4–Mg–Cl at 25°C.

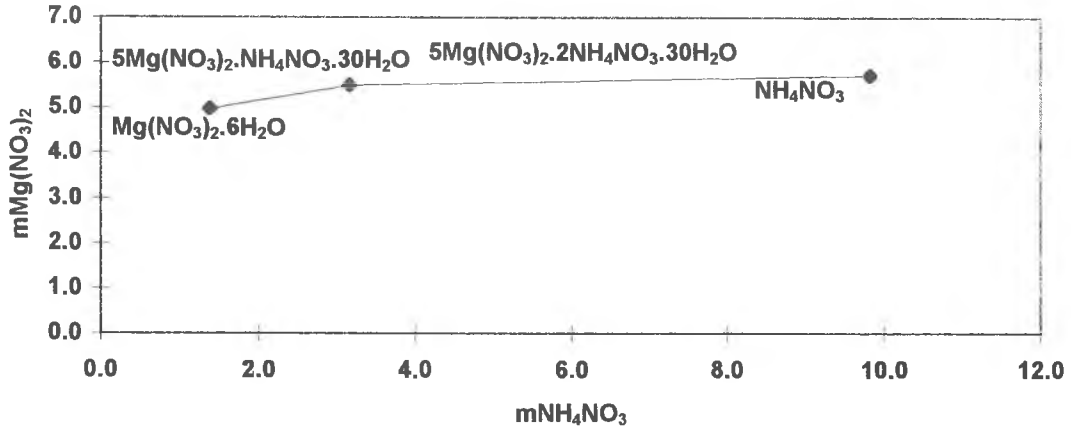

Figure 7.28: Solubility diagram for Mg–NH_4–NO_3 at 25°C.

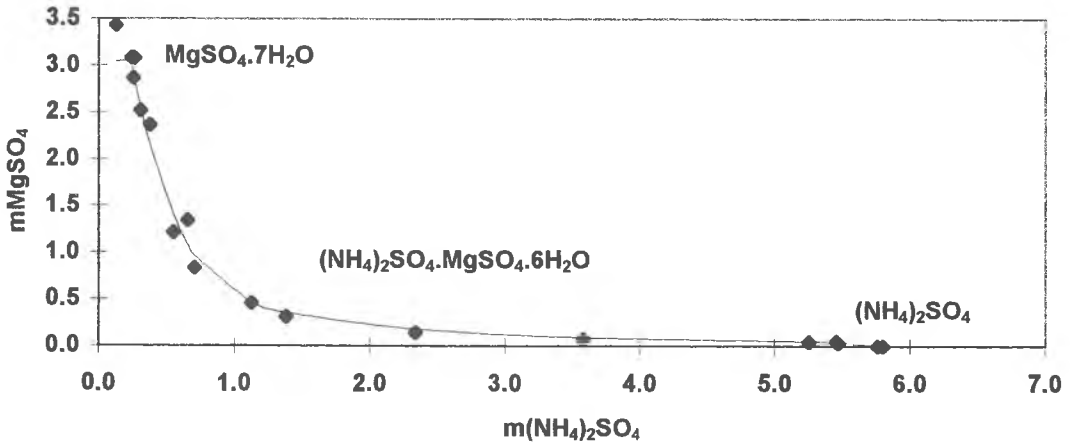

Figure 7.29: Solubility diagram for NH_4–Mg–SO_4 at 25°C.

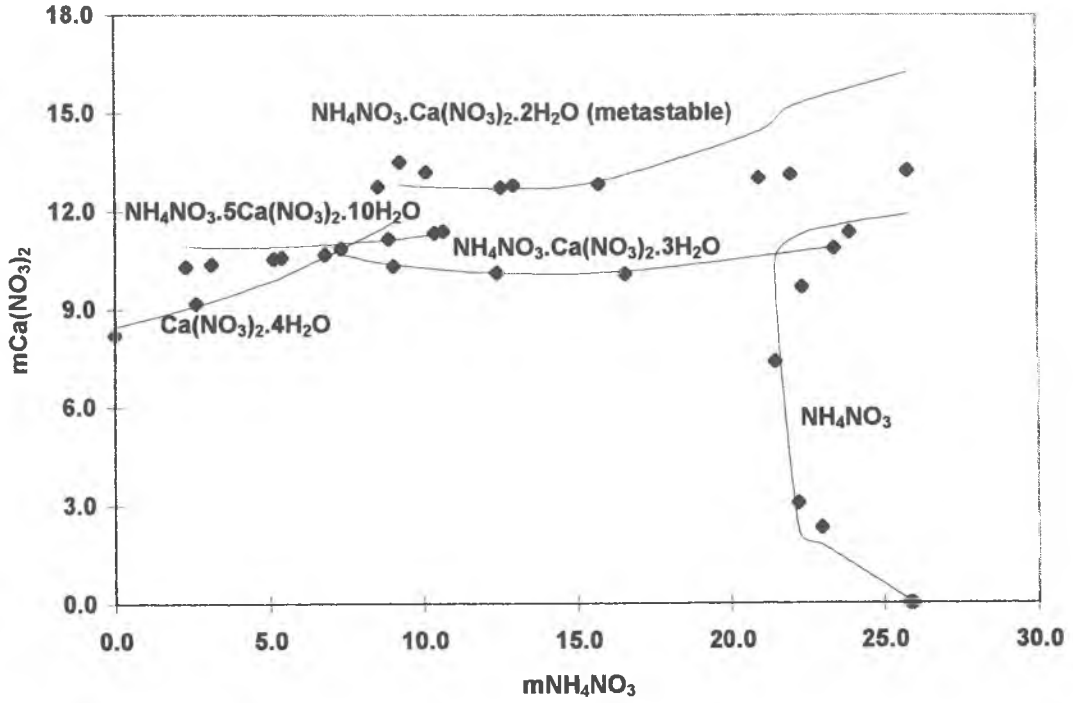

Figure 7.30: Solubility diagram for NH_4–Ca–NO_3 at 25°C.

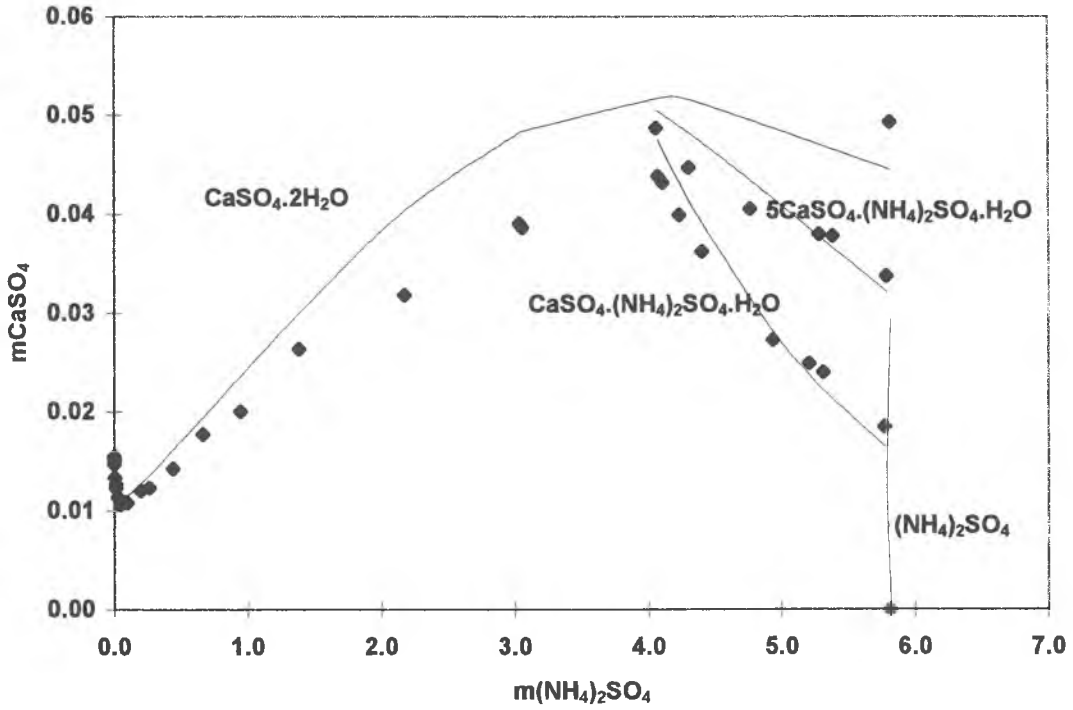

Figure 7.31: Solubility diagram for NH_4–Ca–SO_4 at 25°C.

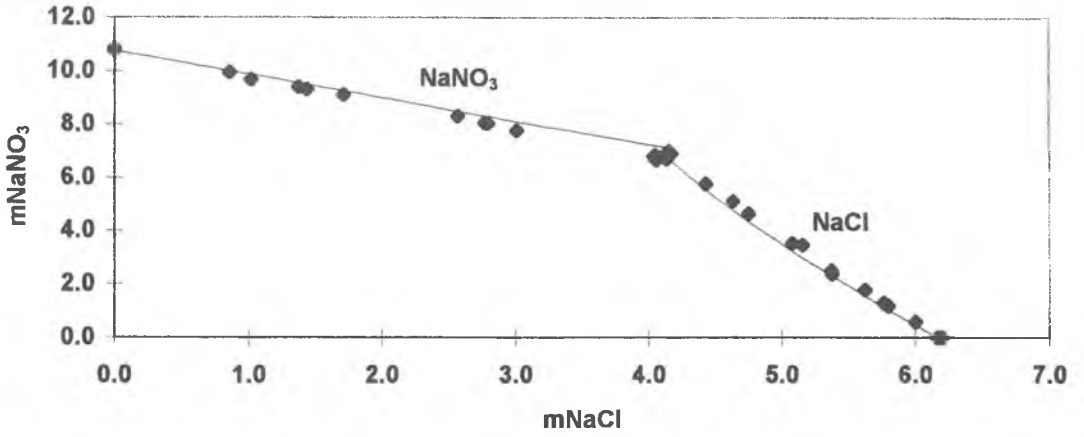

Figure 7.32: Solubility diagram for Na–Cl–NO_3 at 25°C.

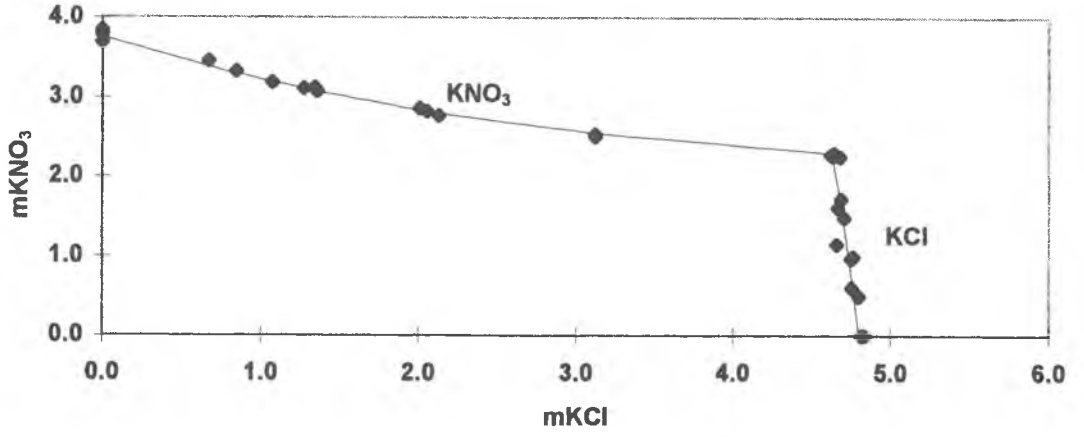

Figure 7.33: Solubility diagram for K–Cl–NO_3 at 25°C.

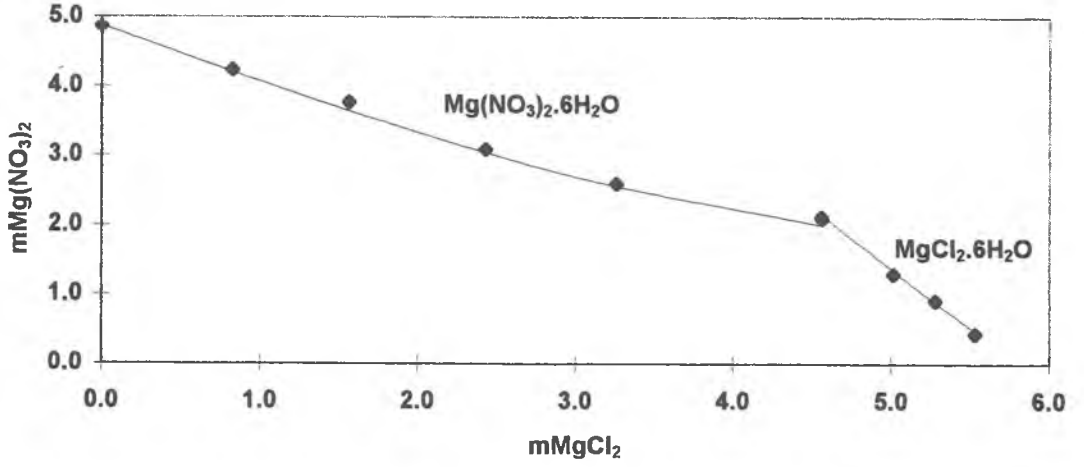

Figure 7.34: Solubility diagram for Mg–Cl–NO_3 at 25°C.

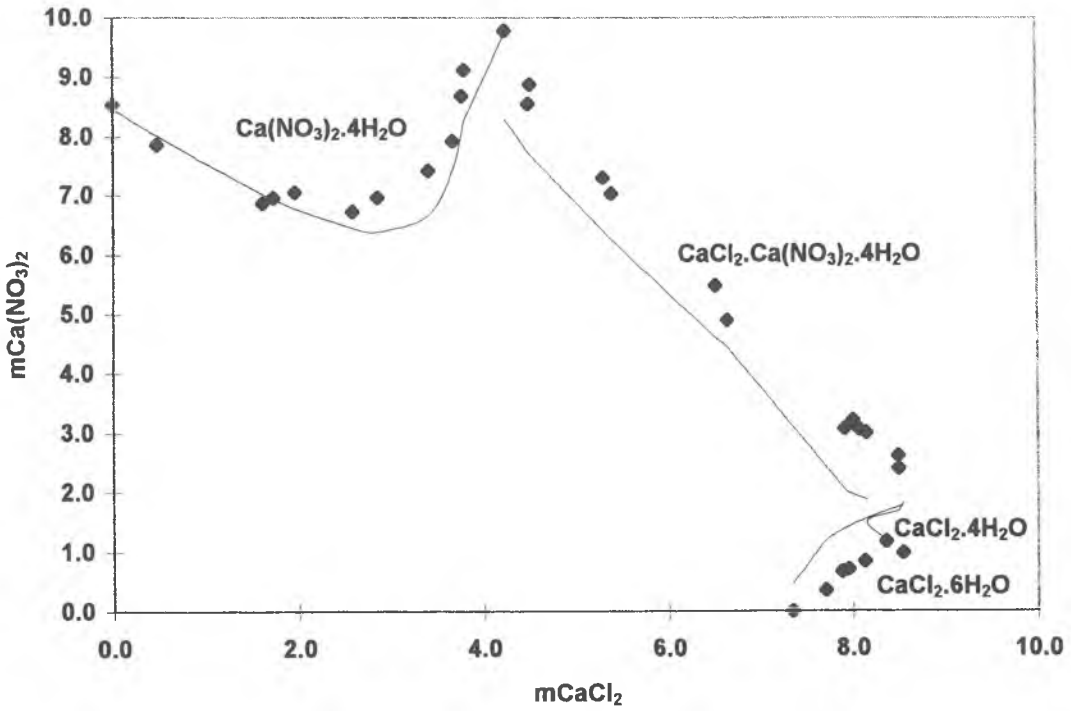

Figure 7.35: Solubility diagram for Ca–Cl–NO_3 at 25°C.

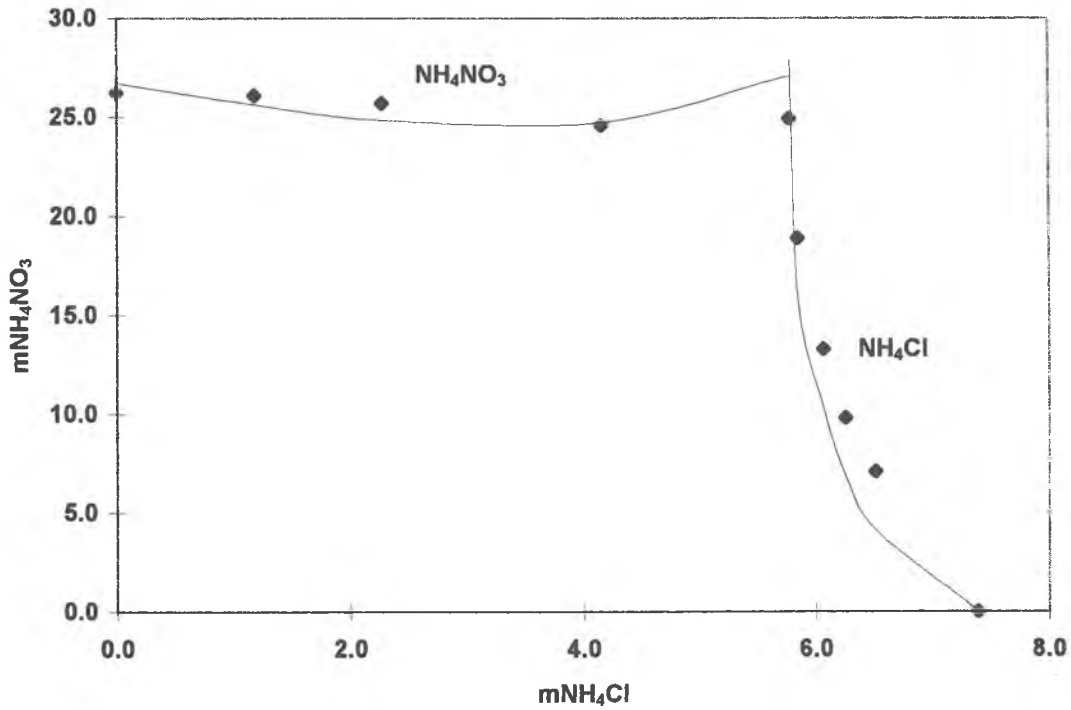

Figure 7.36: Solubility diagram for NH_4–Cl–NO_3 at 25°C.

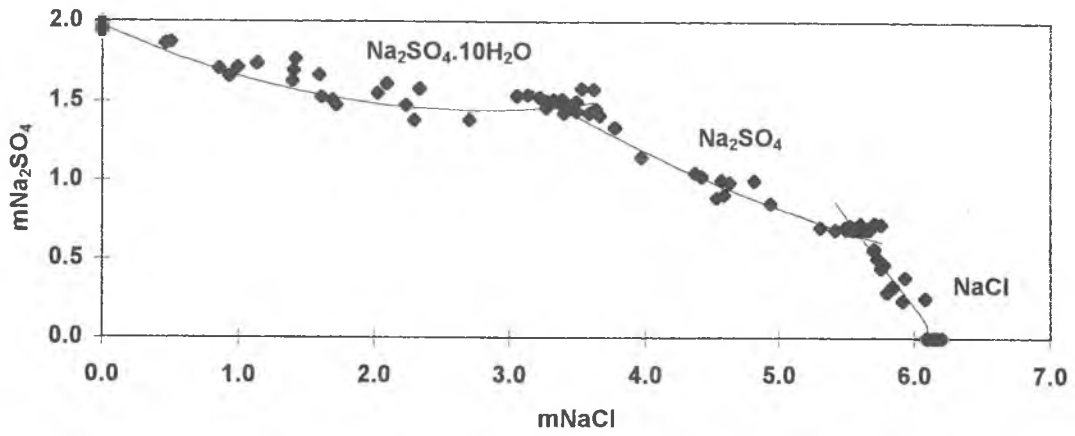

Figure 7.37: Solubility diagram for Na–Cl–SO_4 at 25°C.

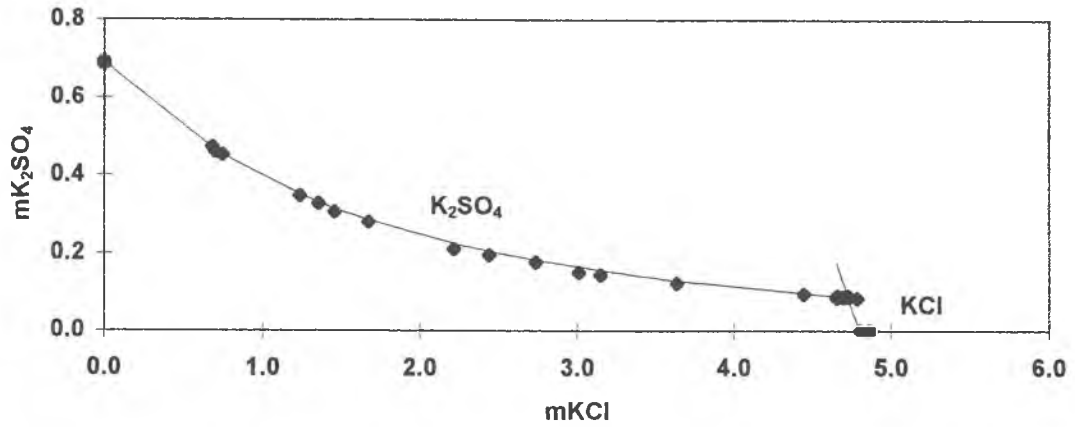

Figure 7.38: Solubility diagram for K–Cl–SO_4 at 25°C.

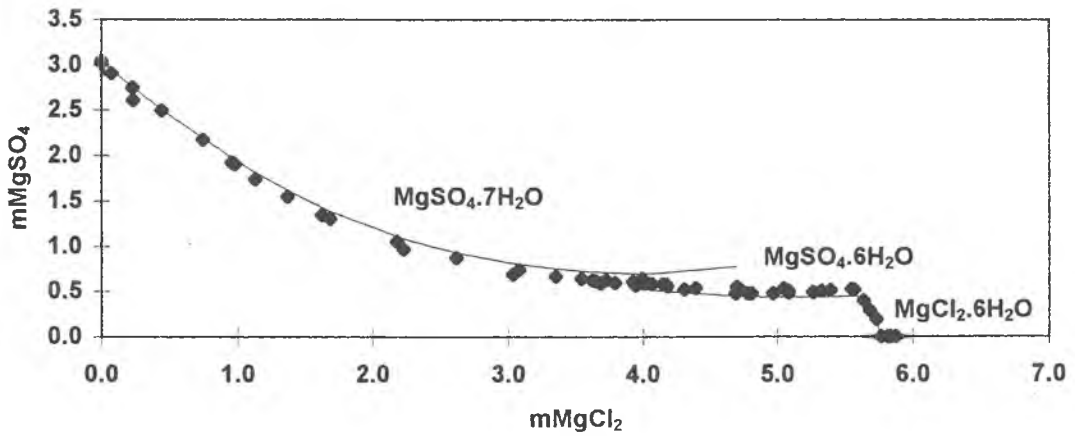

Figure 7.39: Solubility diagram for Mg–Cl–SO_4 at 25°C.

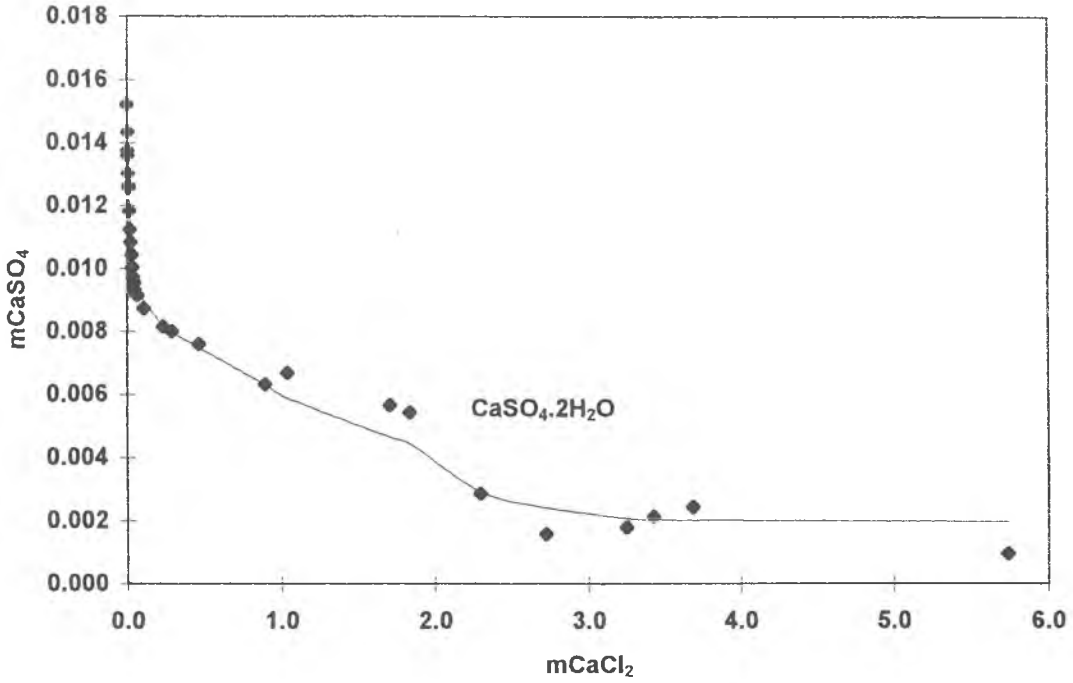

Figure 7.40: Solubility diagram for Ca–Cl–SO_4 at 25°C.

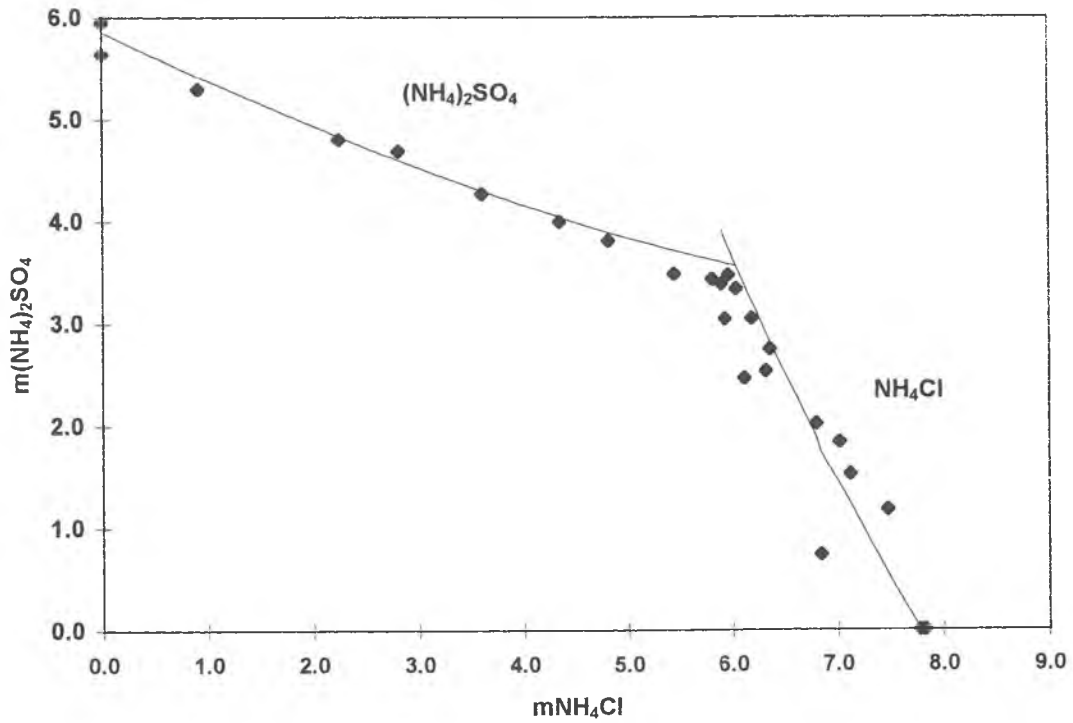

Figure 7.41: Solubility diagram for NH_4–Cl–SO_4 at 25°C.

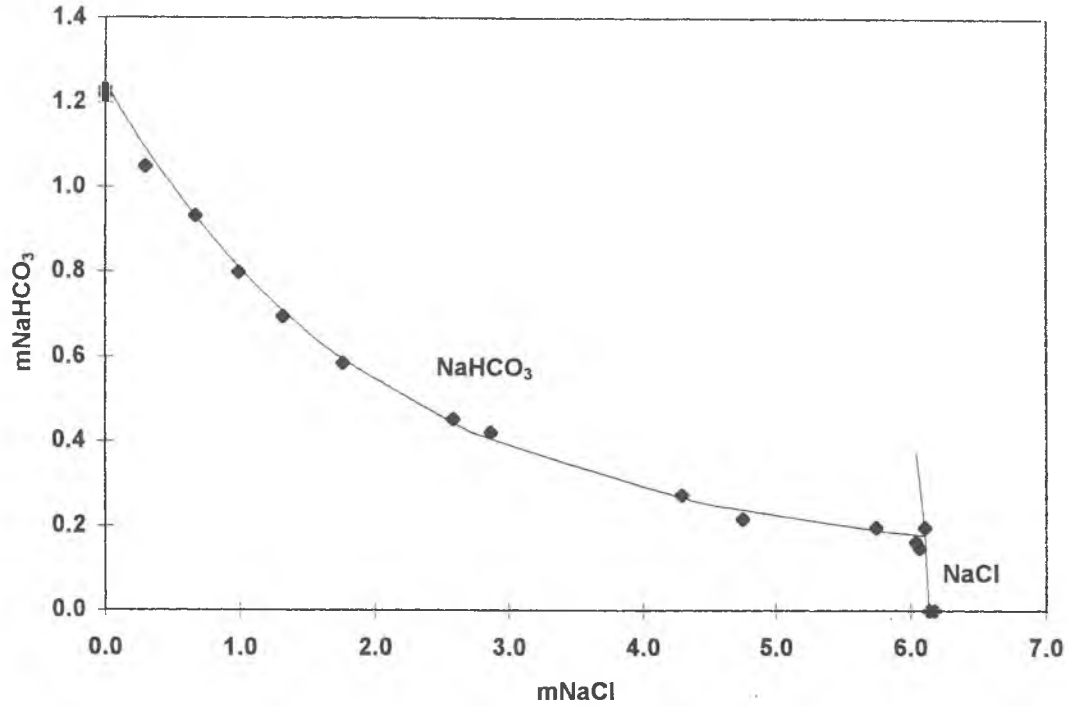

Figure 7.42: Solubility diagram for Na–Cl–HCO_3 at 25°C.

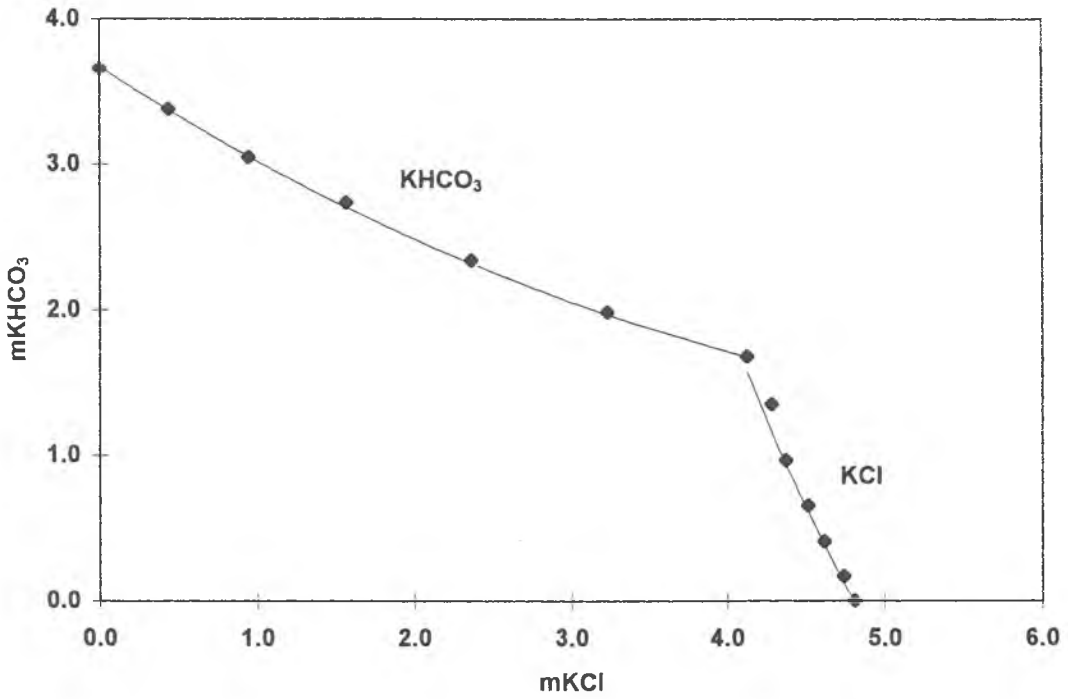

Figure 7.43: Solubility diagram for K–Cl–HCO_3 at 25°C.

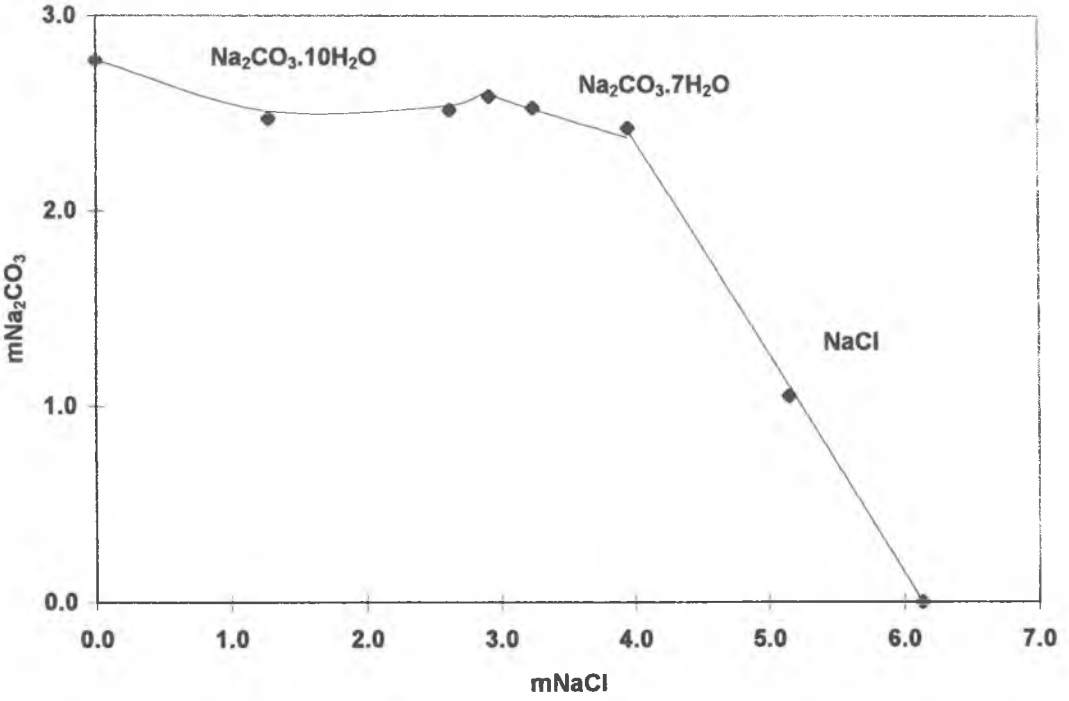

Figure 7.44: Solubility diagram for Na–Cl–CO_3 at 25°C.

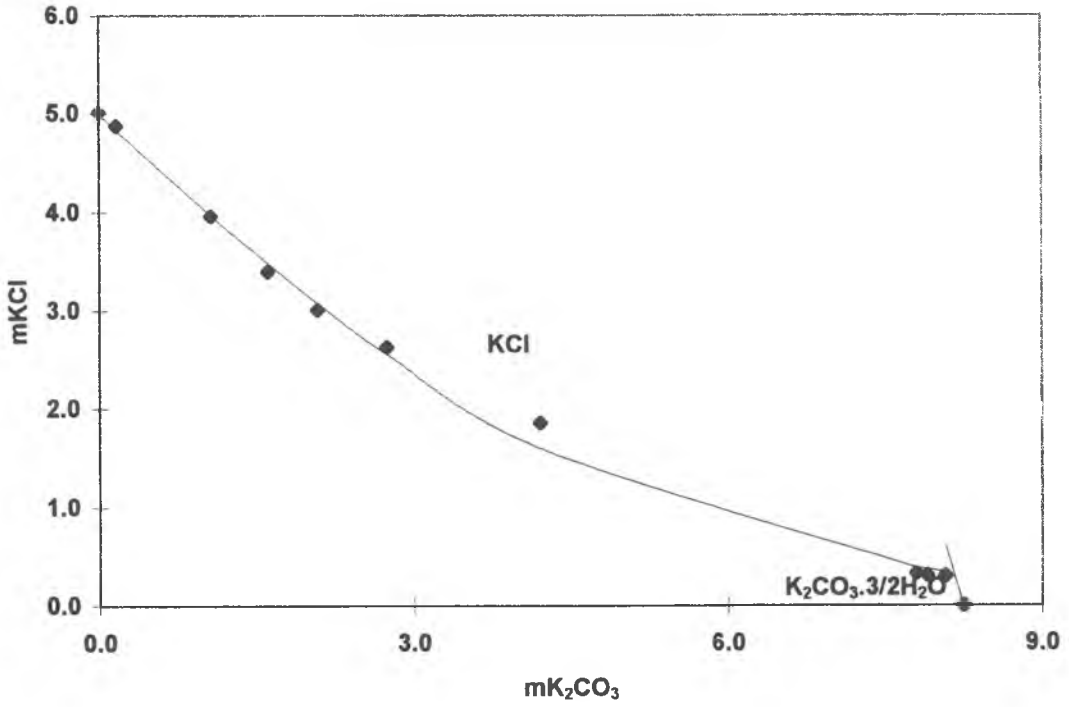

Figure 7.45: Solubility diagram for K–Cl–CO_3 at 25°C.

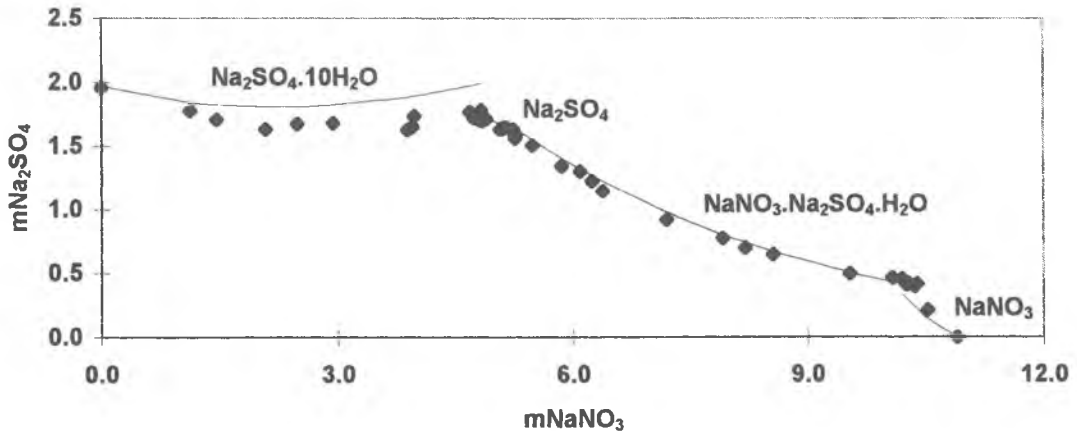

Figure 7.46: Solubility diagram for Na–NO_3–SO_4 at 25°C.

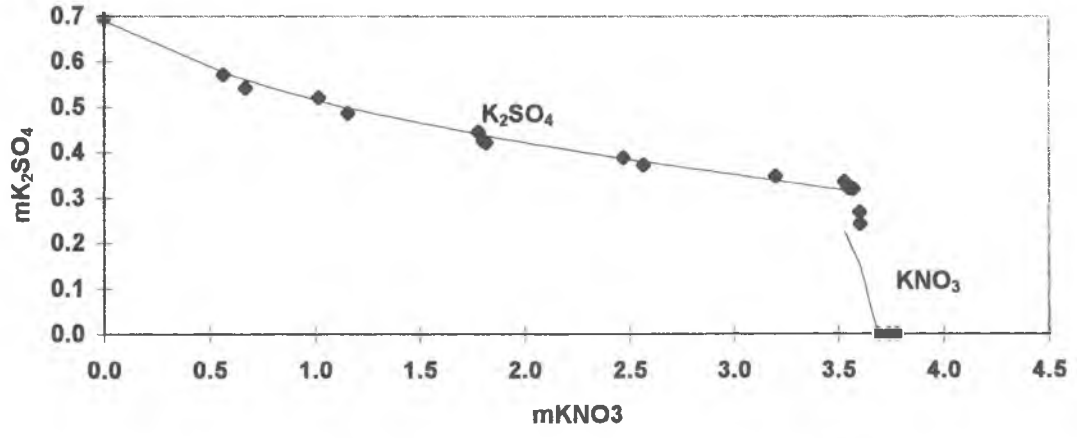

Figure 7.47: Solubility diagram for K–NO_3–SO_4 at 25°C.

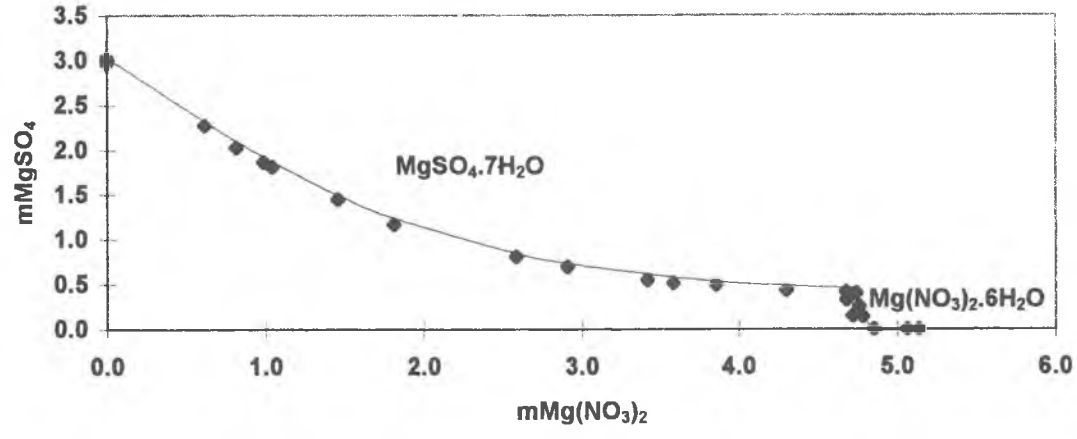

Figure 7.48: Solubility diagram for Mg–NO_3–SO_4 at 25°C.

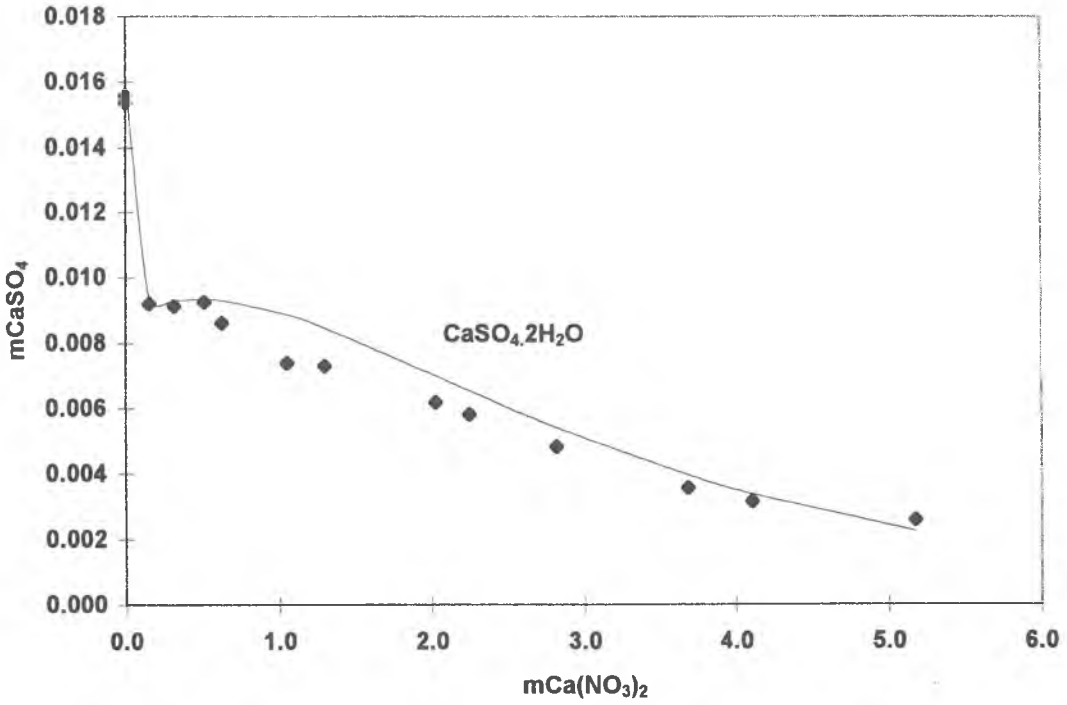

Figure 7.49: Solubility diagram for Ca–NO_3–SO_4 at 25°C.

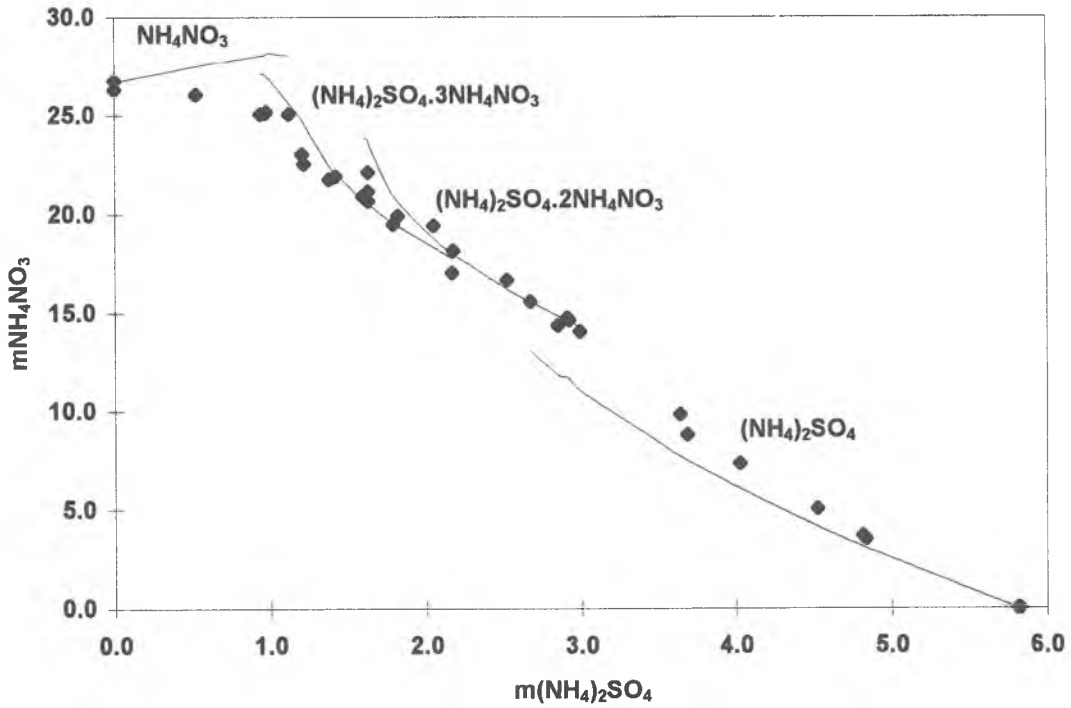

Figure 7.50: Solubility diagram for NH_4–NO_3–SO_4 at 25°C.

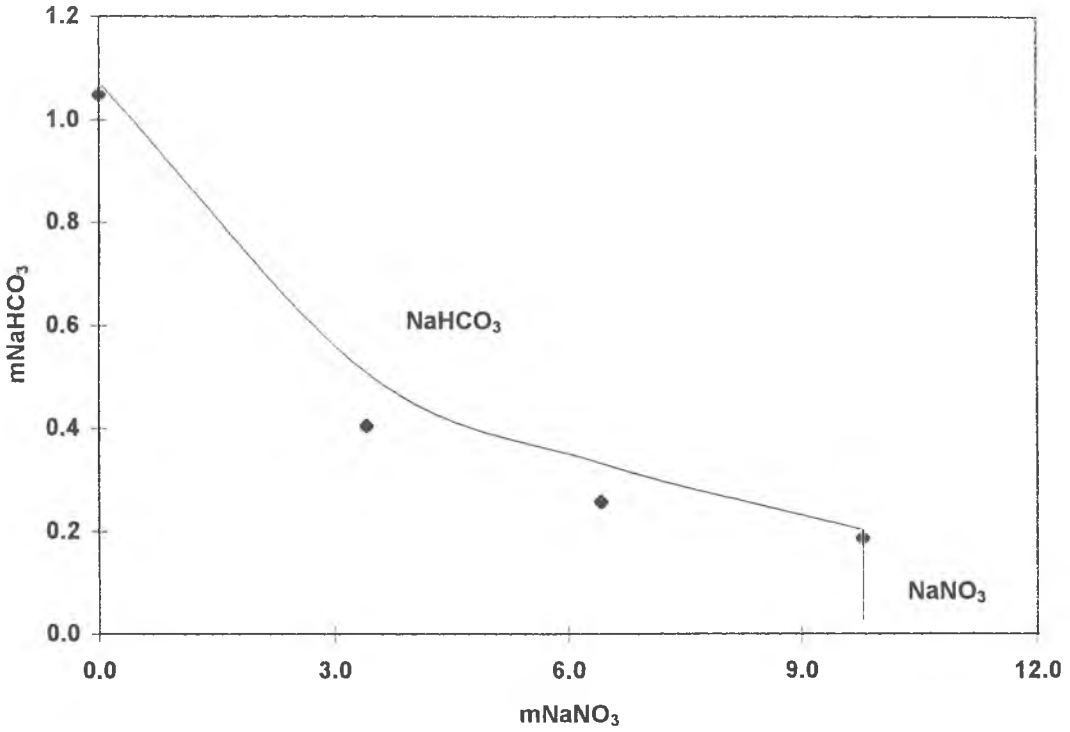

Figure 7.51: Solubility diagram for Na–NO_3–HCO_3 at 25°C.

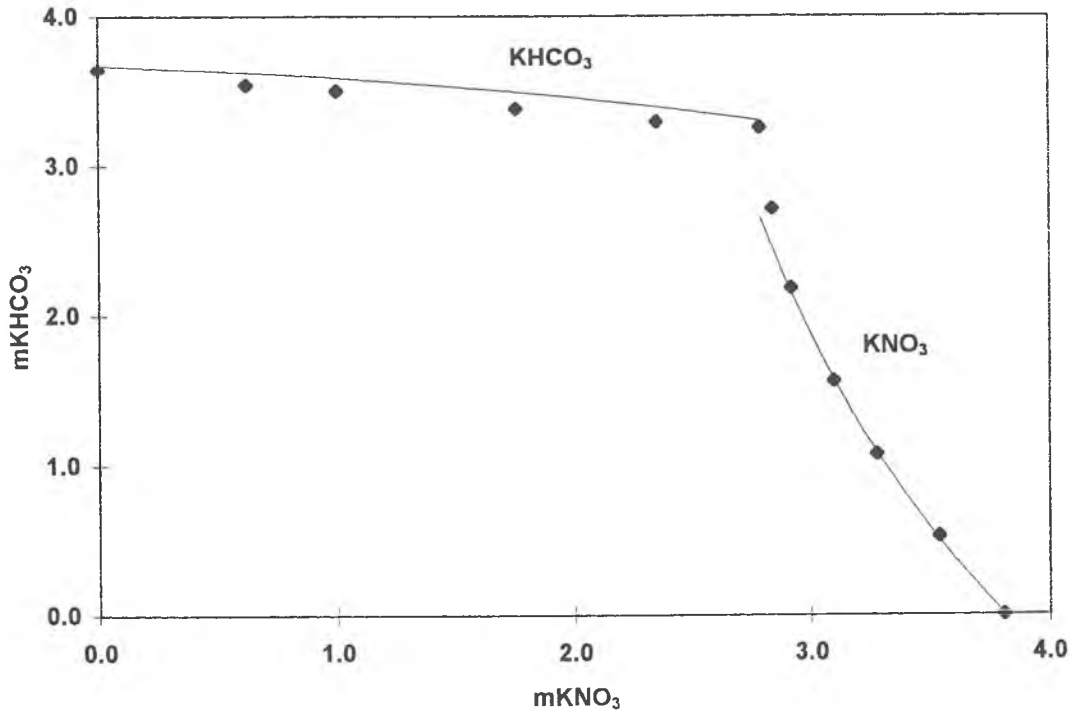

Figure 7.52: Solubility diagram for K–NO_3–HCO_3 at 25°C.

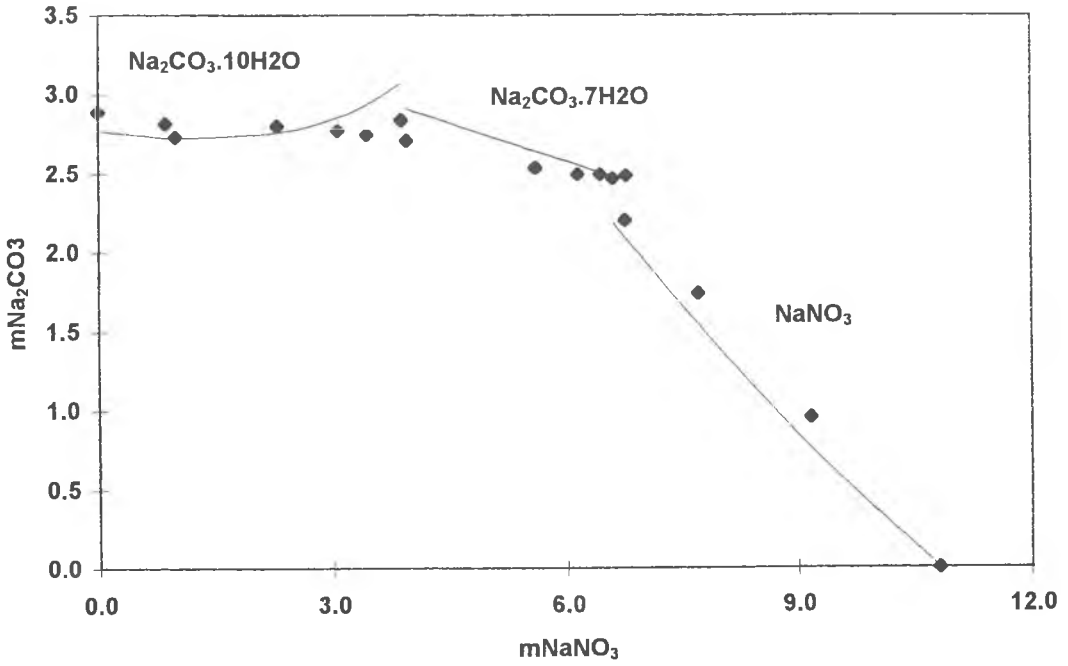

Figure 7.53: Solubility diagram for Na–NO_3–CO_3 at 25°C.

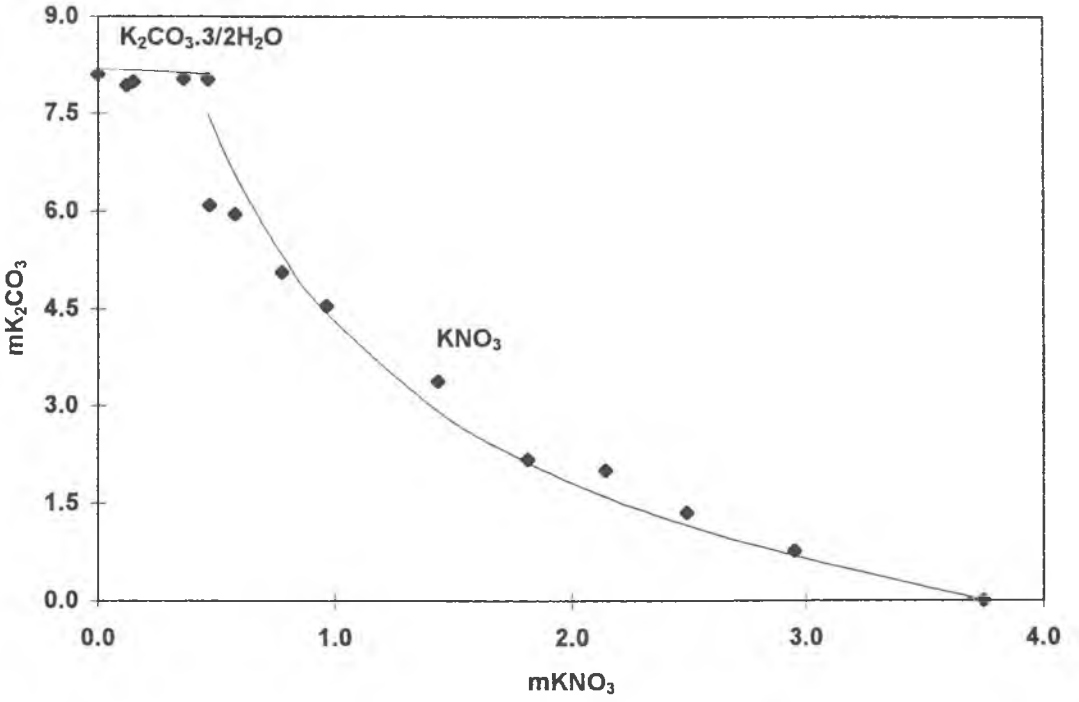

Figure 7.54: Solubility diagram for K–NO_3–CO_3 at 25°C.

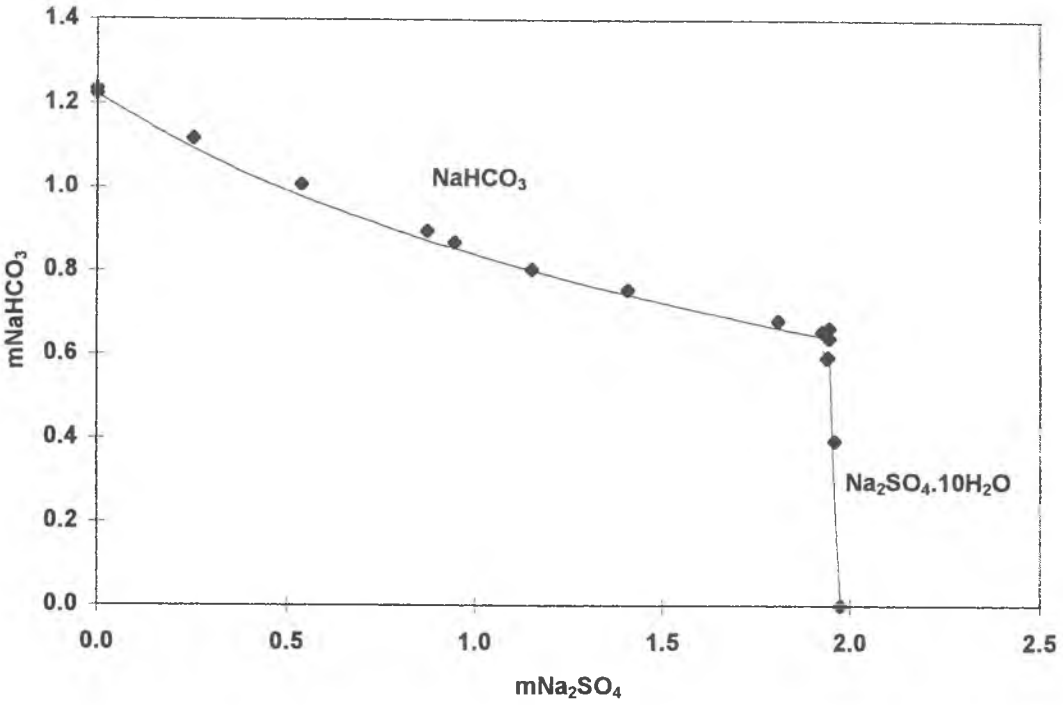

Figure 7.55: Solubility diagram for Na–SO_4–HCO_3 at 25°C.

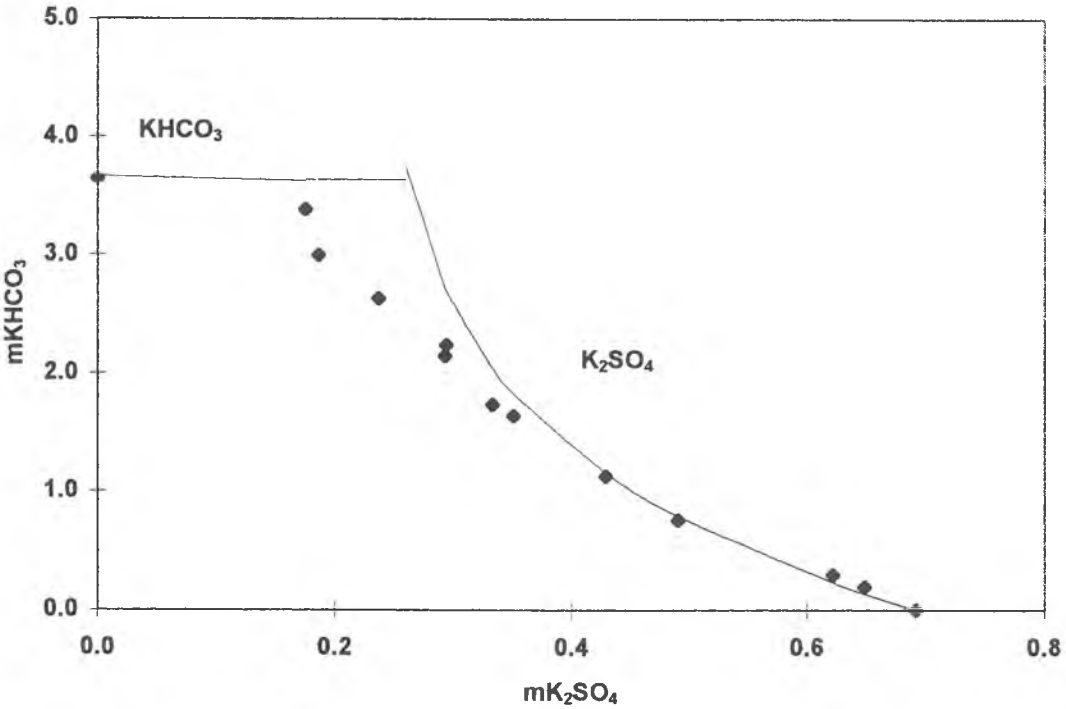

Figure 7.56: Solubility diagram for K–SO_4–HCO_3 at 25°C.

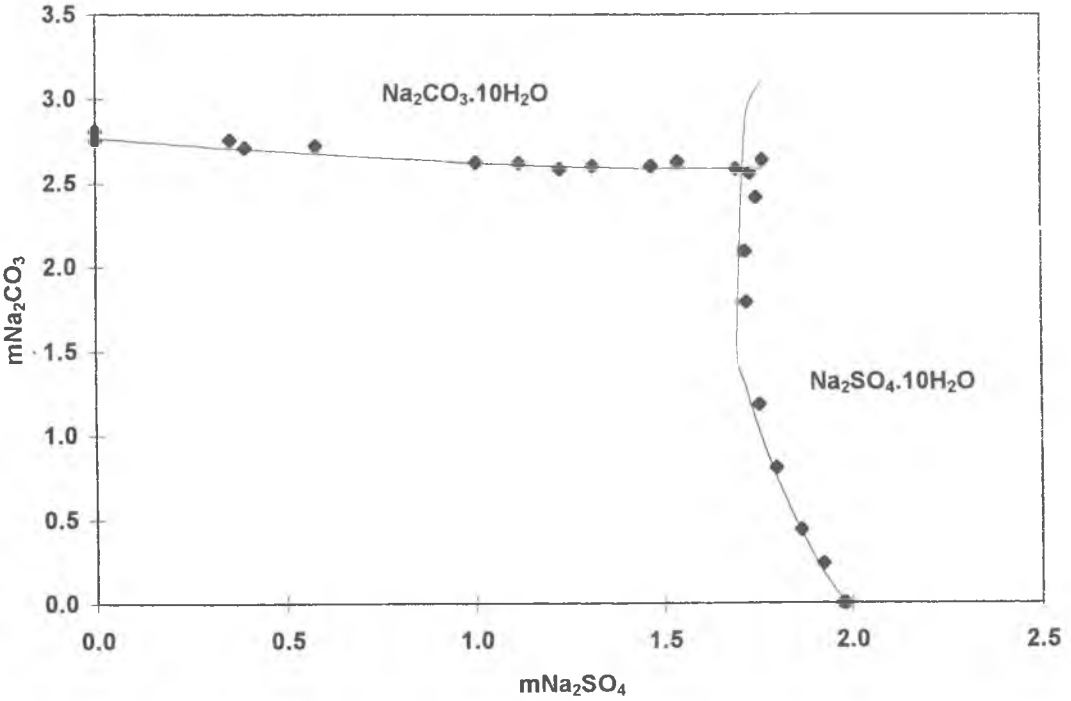

Figure 7.57: Solubility diagram for Na–SO_4–CO_3 at 25°C.

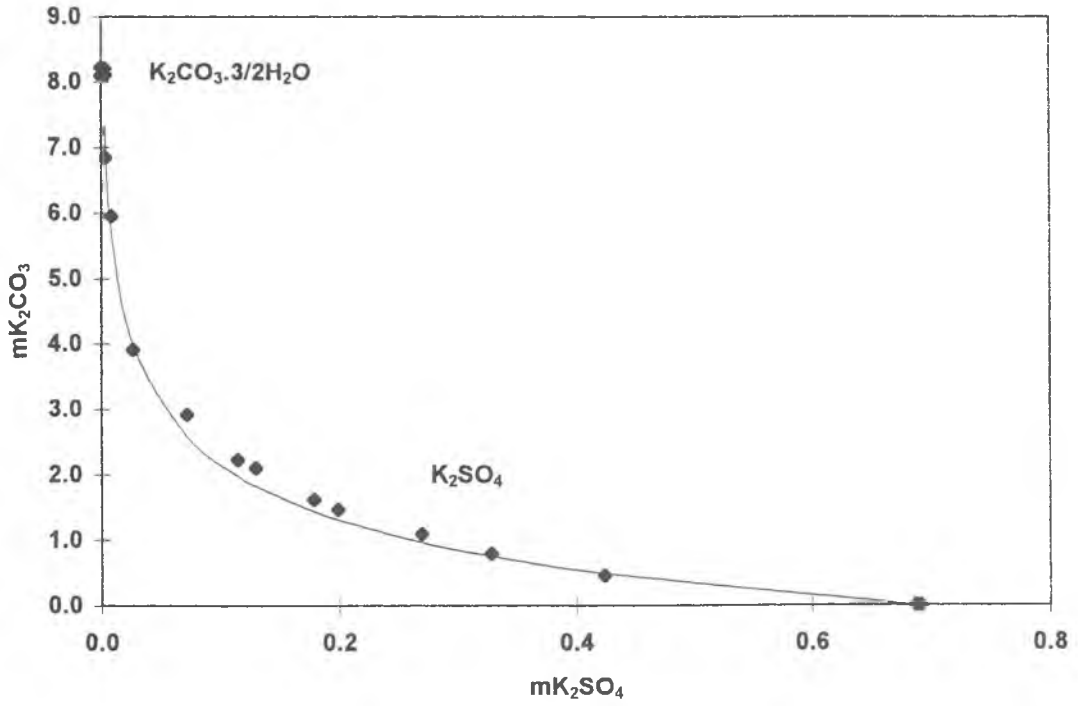

Figure 7.58: Solubility diagram for K–SO_4–CO_3 at 25°C.

7.6 References

Agaev, A. I., A. A. Mamedov & F. A. Mamedov 1976. 'The K, Mg//Cl, NO_3+H_2O system at −30°, −20°, −10° and 0°C.' *Russ. J. Inorg. Chem.* 21: 1850–1855.

Ananthaswamy, J. & G. Atkinson 1985. *J. Chem. Eng. Data* 30: 120.

Archer, D. G. 1992. *J. Phys. Chem. Ref. Data* 21: 793–829.

Assarsson, G. O. 1950a. 'Equilibria in aqueous systems containing K^+, Na^+, Ca^{+2}, Mg^{+2} and Cl^-. I. The ternary system $CaCl_2$–KCl–H_2O.' *J. Am. Chem. Soc.* 72: 1433–1436.

Assarsson, G. O. 1950b. 'Equilibria in aqueous systems containing K^+, Na^+, Ca^{+2}, Mg^{+2} and Cl^-. II. The quaternary system $CaCl_2$-KCl–$NaCl$–H_2O.' *J. Am. Chem. Soc.* 72: 1437–1441.

Babenko, A. M. & A. M. Andrianov 1981. '$KHCO_3$–KNO_3–H_2O system.' *Russ. J. Inorg. Chem.* 26: 261–264.

Barbaudy, J. 1923. 'Note sur l'équilibre eau — chlorure de potassium — nitrate de potassium, nitrate de calcium et chlorure de calcium.' *Rec. Trav. Chim.* 42: 638–642.

Barre 1909. *Compt. Rend.* 148: 1604–1606.

Benrath & Braun 1940. *Z. Anorg. Allg. Chem.* 244: 348–358.

Benrath, A. 1928. 'Über das reziproke Salzpaar $MgSO_4$–$Na_2(NO_3)_2$–H_2O. I.' *Z. Anorg. Chem.* 170: 257–287.

Benrath, A. 1943. 'Über die Löslichkeit von Salzen und Salzgemischen bei Temperaturen oberhalb von 100°. V.' *Z. Anorg. Chem.* 252: 86–94.

Benrath, A. & H. Benrath 1929. 'Das reziproke Salzpaar $MgSO_4$+$K_2(NO_3)_2$= $Mg(NO_3)_2$+K_2SO_4. I.' *Z. Anorg. Chem.* 184: 359–368.

Benrath, A. & H. Benrath 1930. 'Das reziproke Salzpaar $MgSO_4$+$K_2(NO_3)_2$= $Mg(NO_3)_2$+K_2SO_4. II.' *Z. Anorg. Chem.* 189: 72–81.

Benrath, A. & H. Schackmann 1934. 'Über scheinbare Mischkristalle. I.' *Z. Anorg. Allg. Chem.* 218: 139–145.

Benrath, A. & A. Sichelschmidt 1931. 'Das reziproke Salzpaar $MgSO_4$+ $K_2(NO_3)_2$=$Mg(NO_3)_2$+K_2SO_4. III.' *Z. Anorg. Chem.* 197: 113–128.

Bergmann, A. G. & L. V. Opredelenkova 1969. 'Solubility polytherms of the calcium nitrate-potassium nitrate-water and calcium nitrate-potassium chloride-water ternary systems.' *Russ. J. Inorg. Chem.* 14: 1144–1146.

Bergmann, A. G. & L. F. Shulyak 1972. *Russ. J. Inorg. Chem.* 17(4): 593–596.

Blarez 1891. *Compt. Rend.* 112: 939–42.

Bodländer, G. 1891a. *Z. Phys. Chem.* 7: 308–366.

Bodländer, G. 1891b. 'Über die Löslichkeit von Salzgemischen in Wasser.' *Z. Phys. Chem.* 7: 358–366.

Bogoyavlenskii, P. S. & E. D. Gashpar 1973. 'The $KHCO_3$–KNO_3–H_2O system at 0°, 25°, and 40°C.' *Russ. J. Inorg. Chem.* 18: 1662–1663.

Cameron & Breazeale 1904. *J. Phys. Chem.* 8: 335–340.

Caspari, W. A. 1924. 'The system sodium carbonate-sodium sulphate-water.' *J. Chem. Soc.* 125: 2381–2387.

Chrétien, A. 1929. 'Étude du système quaternaire. Eau, nitrate de sodium, chlorure de sodium, sulfate de sodium.' *Ann. Chim.* 12: 9–155.

Clarke, L. & E. P. Partridge 1934. 'Potassium sulfate from syngenite by high-temperature extraction with water.' *Ind. Eng. Chem.* 26: 897–903.

Clegg, S., S. Milioto & D. A. Palmer 1996. *J. Chem. Eng. Data* 41(3): 455–467.

Cornec, E. & H. Krombach 1932. 'Équlibres entre le chlorure de potassium, le chlorure de sodium et l'eau depuis −23° jusqu'a +190°.' *Ann. Chim.* 18: 5–31.

D'Ans, J. 1933. *Die Lösungsgleichgewichte der Systeme der Salze ozeanischer Salzablagerungen.* Verlagsgesellschaft für Ackerbau, Berlin.

de Lima, M. C. P. & K. S. Pitzer 1983. *J. Solution Chem.* 12: 187–199.

Debler 1913. *Dissertation.* Erlangen.

Dejewska, B. 1992. 'The distribution coefficient of isomorphous admixtures for KCl–KBr–H_2O, K_2SO_4–$(NH_4)_2SO_4$–H_2O and KNO_3–NH_4NO_3–H_2O systems at 298K.' *Cryst. Res. Technol.* 27: 385–394.

Denman, W. L. 1961. 'Maximum re-use of cooling water based on gypsum content and stability.' *Ind. Eng. Chem.* 53: 817–822.

Dolique, R. & M. Pauc 1946. *Trav. Soc. Pharm.* 6: 56–59, 86–92.

Drakin, S. I., L. V. Lantukhova & M. K. Karapet'yants 1967. *Russ. J. Phys. Chem.* 41(1): 50–53.

Ehret, W. F. 1932. 'Ternary systems $CaCl_2$–$Ca(NO_3)_2$–$H_2O(25°)$, $CaCl_2$-$Ca(ClO_3)_2$–$H_2O(25°)$, $SrCl_2$–$Sr(NO_3)_2$–$H_2O(25°)$, KNO_3–$Pb(NO_3)_2$–$H_2O(0°)$.' *J. Am. Chem. Soc.* 54: 3126–3134.

Emons, H. H., D. Dümke & M. Förtsch 1966. 'Untersuchungen an Systemen aus Salzen und gemischten Lösungsmitteln. II. Die Systeme Natriumchlorid bzw. Kaliumchlorid, Methanol – Wasser und Natriumchlorid - Kaliumchlorid – Methanol – Wasser.' *Wiss. Z. Techn. Hochschule Chem. "Carl Schorlemmer" Leuna Merseburg* 8: 195–200.

Emons, H. H. & H. Röser 1967. 'Die Beeinflussung der Systeme Kaliumsulfat- bzw. Natriumsulfat-Alkohol-Wasser durch Zusatz von Natrium- oder Kaliumchlorid.' *Z. Anorg. Allg. Chem.* 353: 135–147.

Emons, H. H., H. Röser & E. Roschke 1970. 'Das Verhalten des reziproken Salzpaares Na_2SO_4+2KCl=K_2SO_4+2NaCl in Methanol-Wasser-Mischungen.' *Z. Anorg. Allg. Chem.* 375: 281–290.

Enea, O., P. P. Singh, E. M. Woolley, K. G. McCurdy & L. G. Hepler 1977. *J. Chem. Thermodynamics* 9: 731–734.

Epikhin, Y. A., I. V. Bazlova & M. K. Karapet'yants 1977. *Russ. J. Phys. Chem.* 51: 676–677.

Epikhin, Y. A. & M. Stakhanova 1967. *Russ. J. Phys. Chem.* 41(9): 1157–1160.

Erdös, E. & Z. Jiru 1960. 'Solubility of electrolytes. V. The quinary system potassium sulfate-potassium chloride-potassium nitrate-potassium bromate-water.' *Coll. Czech. Chem. Commun.* 25: 1720–1728.

Euler, H. 1904. 'Über Löslichkeitserniedrigungen.' *Z. Phys. Chem.* 49: 303–316.

Ewing, W. W., E. Klinger & J. D. Brandner 1934. *J. Am. Chem. Soc.* 56: 1053–1057.

Ewing, W. W. & A. N. Rogers 1933. *J. Am. Chem. Soc.* 55: 3603–3609.

Fedotieff, P. P. 1904. 'Der Ammoniaksodaprozess vom Standpunkte der Phasenlehre.' *Z. Phys. Chem.* 49: 162–188.

Filippov, V. K. & M. V. Charykova 1989. *Z. Phys. Chem.* 270: 49–57.

Filippov, V. K., M. V. Charykova & Y. M. Trofimov 1987. *Zh. Prikl. Khim.* 60: 257–262.

Flatt, R. & P. Bocherens 1962. 'Sur le système ternaire Ca^{++}–K^+–NO_3^-–H_2O.' *Helv. Chim. Acta* 45: 187–195.

Flatt, R., G. Brunisholz & R. Muhlethaler 1961. 'Contribution à l'étude du système quinaire Ca^{++}–NH_4^+–H^+–NO_3^-–PO_4^-–H_2O. XX. La polytherme de saturation du système ternaire Ca^{++}–NH_4^+–NO_3–H_2O de 0° à 75°.' *Helv. Chim. Acta* 44: 1582–1595.

Flatt, R. & P. Fritz 1950. 'Contribution á l'étude dy système quinaire Ca^{++}–NH_4^+–H^+–NO_3^-–PO_4^-–H_2O. II. Les système ternaires limites Ca^{++}–H^+–NO_3^-–H_2O, NH_4^+–H^+–NO_3^-–H_2O et Ca^{++}–NH_4^+–NO_3^-–H_2O à 25°.' *Helv. Chim. Acta* 33: 2045–2056.

Foote, H. W. 1925. 'The system sodium nitrate-sodium-sulphate-water, and the minerals darapskite and nitroglauberite.' *Am. J. Sci.* 9: 441–447.

Frolov, A. A., V. T. Orlova & I. N. Lepeshkov 1992. 'Solubility polytherm of the system $Ca(NO_3)_2$–$Mg(NO_3)_2$–H_2O.' *Inorg. Mat.* 28: 1040–1042.

Frowein, F. 1928. 'Das System K_2/Ca/Na_2/$(NO_3)_2$/H_2O.' *Z. Anorg. Chem.* 169: 336–344.

Frowein, F. & E. von Mühlendahl 1926. 'Die Lösungen des doppelt-ternären Salzgemisches (K_2/Mg/Na_2)($(NO_3)_2$/Cl_2) und ihre Bedeutung für die Technik.' *Z. Angew. Chem.* 39: 1488–1500.

Galushkina, R. A. & A. G. Bergmann 1962. 'Polythermal diagram of the KNO_3–K_2SO_4-H_2O system.' *Russ. J. Inorg. Chem.* 7: 1165–1167.

Galushkina, R. A. & A. G. Bergmann 1973. 'Solubility polytherms of the K_2SO_4–$(NH_4)_2SO_4$–H_2O and KNO_3–$(NH_4)_2SO_4$–H_2O systems.' *Russ. J. Inorg. Chem.* 18: 133–135.

Garvin, D., V. B. Parker & H. J. White 1987. *CODATA Thermodynamic Tables, Selections for Some Compounds of Calcium and Related Mixtures: A Prototype Set of Tables.* Hemisphere, Washington.

Gladushko, V. I., G. A. Bochenko, G. N. Prokof'eva, V. P. Privalko & J. Vinarcik 1985. *J. Inzh. Fiz. Zh.* 48: 90–91.

Gmelin n.d. *Handbook of Inorganic Chemistry, Ammonium (system 23), v2.* Springer Verlag.

Hamer, W. J. & Y. C. Wu 1972. *J. Phys. Chem. Ref. Data* 1(4): 1047–1099.

Hamid, M. A. 1926. 'Heterogeneous equilibria between the sulphates and nitrates of sodium and potassium and their aqueous solutions. Part I. The ternary systems.' *J. Chem. Soc.* 128: 199–205.

Hara, Y., N. Akiyoshi, N. Nawachi & H. Nakamura 1991. *Kogyo Kayaku* 52: 239–245.

Harvie, C. E., N. Moller & J. H. Weare 1984. *Geochim. Cosmochim. Acta* 48: 723–751.

Hill, A. E. 1934. 'Ternary systems. XIX. Calcium sulfate, potassium sulfate and water.' *J. Am. Chem. Soc.* 56: 1071–1078.

Hill, A. E. & C. M. Loucks 1937. *J. Am. Chem. Soc.* 56: 2094–2098.

Hill, A. E. & F. W. Miller 1927. 'Ternary systems. IV. Potassium carbonate, sodium carbonate and water.' *J. Am. Chem. Soc.* 49: 669–686.

Hill, A. E. & S. Moskowitz 1929. 'Ternary systems. VIII. Potassium carbonate, potassium sulfate and water at 25°.' *J. Am. Chem. Soc.* 51: 2396–2398.

Hill, A. E. & S. B. Smith 1929. 'Equilibrium between the carbonates and bicarbonates of sodium and potassium in aqueous solution at 25°.' *J. Am. Chem. Soc.* 51: 1626–1636.

Hill, A. E. & N. S. Yanick 1935. 'Ternary system. XX. Calcium sulfate, ammonium sulfate and water.' *J. Am. Chem. Soc.* 57: 645–651.

Holluta, J. & S. Mautner 1927. 'Untersuchungen über die Löslichkeitsbeeinflussung starker Elektrolyte. I. Die gegenseitige Löslichkeitsbeeinflussung gleichioniger Alkalisalze. 1. Teil.' *Z. Phys. Chem.* 127: 455–475.

Holmes, H. F. & R. E. Mesmer 1983. *J. Phys. Chem.* 87: 1242–1255.

Holmes, H. F. & R. E. Mesmer 1986. *J. Solution Chem.* 15: 495–518.

Igelsrud, I. & T. G. Thompson 1936. 'Equilibria in saturated solutions of salts occurring in sea water. I. The ternary system $MgCl_2$–KCl–H_2O, $MgCl_2$–$CaCl_2$–H_2O, $CaCl_2$–KCl–H_2O and $CaCl_2$–$NaCl$–H_2O at 0°.' *J. Am. Chem. Soc.* 58: 318–322.

Jackman, D. N. & A. Browne 1922. 'The 25°-Isotherms of the systems magnesium nitrate-sodium nitrate-water and magnesium sulphate-magnesium nitrate-water.' *J. Chem. Soc.* 121: 694–697.

Jänecke & Erdmann 1920. *Jahrb. d. Halleschen Verbandes* 2: 239–280.

Jänecke, E. 1911. 'Über die Bildung von Konversionssalpeter vom Standpunkt der Phasenlehre.' *Z. Anorg. Chem.* 71: 1–18.

Jänecke, E. 1929. 'Über das reziproke Salzpaar $2NH_4NO_3+K_2SO_4=2KNO_3+(NH_4)_2SO_4$ und seine wässerigen Lösungen.' *Z. Angew. Chem.* 42: 1169–1172.

Jänecke, E., H. Hamacher & E. Rahlfs 1932. 'Über das System KNO_3–NH_4NO_3–H_2O.' *Z. Anorg. Chem.* 206: 357–368.

Karakhanyan, S. S., E. A. Sayamian, J. P. Yeghiazarian, T. I. Karapetian & G. T. Mirzoyan 1987. 'A study of components interaction in $Na_2CO_3+Ca(NO_3)_2=CaCO_3+2NaNO_3$–$H_2O$ reversible system at 25°C.' *Arm. Khim. Zh.* 40: 214–221.

Kirgintsev, A. N. & A. V. Luk'yanov 1963. *Russ. J. Phys. Chem.* 37: 1501–1502.

Klotz, I. M. & R. M. Rosenberg 1972. *Chemical Thermodynamics, Basic Theory and Methods.* Benjamin/Cummings, Menlo Park, CA, 3rd edition.

Kornec & Krombach 1929. *Ann. Chim.* 12: 203–295.

Kosterina, V. I., A. A. Ponizovskii, E. A. Konstantinova, V. T. Orlova & I. N. Leperhkov 1985. 'The KNO_3–$Ca(NO_3)_2$–H_2O system at 55°C.' *Russ. J. Inorg. Chem.* 30: 129–131.

Kotlyar-Shapirov, G. S. & A. N. Kirgintsev 1973. *Dep. Publ. VINITI* pp. 5609–73.

Krause, A. 1927. *Przemysl chemiczny.* 11: 625–628.

Kremann, R. & H. Rodemund 1914. 'Über einige doppelte Umsetzungen des als Nebenprodukt des Leblanc'schen Sodaverfahrens abfallenden Calciumthiosulfates vom Standpunkte des Massenwirkungsgesetzes und der Phasenlehre.' *Monatshefte f. Chem.* 35: 1061–1113.

Kudryashova, O. S., L. P. Filippova, S. F. Kudryashov, T. A. Kulikova & E. N. Boyarintseva 1996. 'System K^+, NH_4^+ // NO_3^-, Cl^-–H_2O.' *Russ. J. Inorg. Chem.* 41: 1474–1488.

Levi, S. M. 1924. *Z. Physik. Chem.* 108: 411–430.

Lightfoot, W. J. & C. F. Prutton 1946. 'Equilibria in saturated solutions. I. The ternary systems $CaCl_2$–$MgCl_2$–H_2O, $CaCl_2$–KCl–H_2O, and $MgCl_2$–KCl–H_2O at 35°.' *J. Am. Chem. Soc.* 68: 1001–1002.

Lightfoot, W. J. & C. F. Prutton 1947. 'Equilibria in saturated solutions. II. The ternary systems $CaCl_2$–$MgCl_2$–H_2O, $CaCl_2$–KCl–H_2O and $MgCl_2$–KCl–H_2O at 75°.' *J. Am. Chem. Soc.* 69: 2098–2100.

Linke, W. F. 1965. *Solubilities. Inorganic and Metal-Organic Compounds.* American Chemical Society, Washington D.C.

Lobo, M. M. & J. L. Quaresma 1981. *Electrolyte Solutions: Literature Data on Thermodynamic and Transport Properties.* Coimbra, Portugal.

Lunge 1885. 'J. Soc. Chem. Ind.' *J. Soc. Chem. Ind.* 4: 31–32.

Makin, A. V. 1959. 'A study of the system $NaNO_3$–Na_2SO_4–H_2O at 25°C.' *Russ. J. Inorg. Chem.* 4: 538–542.

Mamedov, F. A., S. M. Novruzov & M. M. Ramazanzade 1988. 'Potassium chloride - potassium nitrate - water ternary system at 50°.' *Azerb. Khim. Zh.* pp. 92–95.

Massink, A. 1916. 'Doppelsalzbildung zwischen Nitraten und Sulfaten in wässeriger Lösung.' *Z. Phys. Chem.* 92: 351–380.

Mazzotto, D. 1891. *Nuovo Cimento* 29: 21–36.

Meyer, T. A., C. F. Prutton & W. J. Lightfoot 1949. 'Equilibria in saturated salt solutions. V. The quinary system $CaCl_2$–$MgCl_2$–KCl–NaCl–H_2O at 35°.' *J. Am. Chem. Soc.* 71: 1236–1237.

Meyerhoffer, W. & A. P. Saunders 1899a. 'Über reziproke Salzpaare II. Die Gleichgewichtserscheinungen reziproker Salzpaare bei gleichzeitiger Anwesenheit eines Doppelsalzes. I. Teil.' *Z. Phys. Chem.* 28: 453–493.

Meyerhoffer, W. & A. P. Saunders 1899b. 'Über reziproke Salzpaare II. Die Gleichgewichtserscheinungen reziproker Salzpaare bei gleichzeitiger Anwesenheit eines Doppelsalzes. II. Teil.' *Z. Phys. Chem.* 31: 370–389.

Moller, N. 1987. *Geochim. Cosmochim. Acta* 52: 821–837.

Monnin, C. & J. Schott 1984. *Geochim. Cosmochim. Acta* 48: 571–581.

Mulder, G. J. 1864. *Bijdragen tot de Geschiedenis van het Scheikundig Gebonden Water. Scheikundige Verhandelingen en Onderzoekingen.* Rotterdam.

Nakamura, H. 1982. *Kogyo Kayaku* 43(2): 63–69.

Nikolajew, W. I. 1929. 'Die Verteilung starker Basen und starker Säuren in gesättigten wässrigen Lösungen.' *Z. Anorg. Allg. Chem.* 181: 249–279.

Numerical Algorithms Group 1991. *FORTRAN Library Mk 15.* NAG, Oxford, release 1 edition.

Parker, V. B. 1965. *Report NSRDS – NBS.* U.S. Govt. Printing Office, Washington.

Perova, A. P. 1970. 'Crystallisation regions of schönite, leonite, and kainite in the Ca, K, Mg// Cl, SO_4–H_2O quinary system at 25° and 55°C.' *Russ. J. Inorg. Chem.* 15: 989–991.

Phutela, R. C. & K. S. Pitzer 1986. *J. Phys. Chem.* 90: 895–901.

Pilipchenko, V. N. & V. G. Shevchuk 1969. 'The $MgSO_4$–$(NH_4)_2SO_4$–Na_2SO_4–H_2O system at 50°C.' *Russ. J. Inorg. Chem.* 14: 430–432.

Poletaev, I. F. & L. V. Krasnenkova 1975. 'The Na^+, Rb^+ // NO_3^-, SO_4^{2-}–H_2O and Cs^+, Na^+ // NO_3^-, SO_4^{2-}–H_2O systems at 25° and 75°C.' *Russ. J. Inorg. Chem.* 20: 1250–1252.

Press, W. 1992. *Numerical recipes in FORTRAN: the art of scientific computing.* Cambridge University Press, Cambridge.

Prutton, C. F. & O. F. Tower 1932. 'The system calcium chloride-magnesium chloride-water at 0, −15 and −30°.' *J. Am. Chem. Soc.* 54: 3040–3047.

Puchkov, L. V. *et al.* 1973. *Zh. Prikl. Khim.* 46(2): 443–5.

Randall, M. & F. D. Rossini 1929. *J. Am. Chem. Soc.* 51(2): 322–345.

Rard, J. A. & S. L. Clegg 1997. *J. Chem. Eng. Data* 42(5): 819–849.

Reinders, W. 1915. 'Die reziproken Salzpaare KCl+$NaNO_3$=KNO_3+$NaCl$ und die Bereitung von Konversionssalpeter.' *Z. Anorg. Chem.* 93: 202–212.

Rengade, E. 1922a. *Chim. et Industr.* 7: 835–846.

Rengade, E. 1922b. *Chim. et Industr.* 7: 1090–1098.

Roux, A., G. M. Musbally, G. Perron, P. P. Singh, E. M. Woolley & L. G. Hepler 1977. *Can. J. Chem.* 56: 24–28.

Saslawsky, A. J. & J. L. Ettinger 1935. 'Gemeinsame Löslichkeit der Aluminium-, Natrium, Kalium- und Eisennitrate im Wasser in Gegenwart von Salpetersäure.' *Z. Anorg. Allg. Chem.* 223: 277–287.

Sborgi, U. & E. Bovalini 1924. *Gazz. Chim. Ital.* 54: 919–933.

Sborgi, U., E. Bovalini & M. Medici 1924. *Gazz. Chim. Ital.* 54: 934–945.

Schröder, W. 1929a. 'Über das reziproke Salzpaar $MgSO_4$–$Na_2(NO_3)_2$–H_2O. II.' *Z. Anorg. Chem.* 177: 71–85.

Schröder, W. 1929b. 'Über das reziproke Salzpaar $MgSO_4$–$Na_2(NO_3)_2$–H_2O. III.' *Z. Anorg. Chem.* 184: 63–76.

Schröder, W. 1930. 'Über das reziproke Salzpaar $MgSO_4$–$Na_2(NO_3)_2$–H_2O. V.' *Z. Anorg. Chem.* 185: 153–166.

Seidell, A. & J. G. Smith 1904. 'The solubility of calcium sulphate in solutions of nitrates.' *J. Phys. Chem.* 8: 493–499.

Shevchuk, V. G. & R. A. Avarina 1965. 'The Li_2SO_4–$MgSO_4$–$(NH_4)_2SO_4$–H_2O system at 25°.' *Russ. J. Inorg. Chem.* 10: 1531–1532.

Shevchuk, V. G. & L. L. Kost' 1964. 'Equilibrium in the Cs_2SO_4–$MgSO_4$–H_2O and $(NH_4)_2SO_4$–$MgSO_4$–H_2O systems at 35°.' *Russ. J. Inorg. Chem.* 9: 235–237.

Shevchuk, V. G. & V. I. Omelyan 1990. 'The KNO_3–$Mg(NO_3)_2$–$Yb(NO_3)_3$–H_2O system at 25°C.' *Russ. J. Inorg. Chem.* 35: 420–421.

Shevchuk, V. G. & V. N. Pilipchenko 1968a. 'The $MgSO_4$–$(NH_4)_2SO_4$–Na_2SO_4–H_2O system at 0°C.' *Russ. J. Inorg. Chem.* 13: 1045–1047.

Shevchuk, V. G. & V. N. Pilipchenko 1968b. 'The $MgSO_4$–$(NH_4)_2SO_4$–Na_2SO_4–H_2O system at 25°C.' *Russ. J. Inorg. Chem.* 13: 1479–1480.

Shevchuk, V. G., V. N. Pilipchenko & V. N. Yukhimets 1969. 'The $MgSO_4$–$(NH_4)_2SO_4$–Na_2SO_4–H_2O system at 75°C.' *Russ. J. Inorg. Chem.* 14: 870–871.

Shpunt, S. Y. 1946. *Zh. Prikl. Khim.* 19: 293–303.

Sieverts, A. & E. L. Müller 1931. 'Das reziproke Salzpaar $MgCl_2$, $Na_2(NO_3)_2$, H_2O. II.' *Z. Anorg. Chem.* 200: 305–320.

Sieverts, A. & H. Müller 1930. 'Das reziproke Salzpaar $MgCl_2$, $Na_2(NO_3)_2$, H_2O. I.' *Z. Anorg. Chem.* 189: 241–257.

Silcock, H. L. 1979. *Solubilities of inorganic and organic compounds. Volume 3. Ternary and multicomponent systems of inorganic substances.* Pergamon Press, Oxford.

Simková, H. & E. Erdös 1959. 'The solubility of electrolytes. III. The quaternary system sodium nitrate – sodium nitrite – sodium chloride – water.' *Coll. Czech. Chem. Commun.* 24: 694–699.

Smith, G. M. & T. R. Ball 1917. 'Heterogeneous equilibria between aqueous and metallic solutions. The interaction of mixed salt solutions and liquid amalgams. A study of the ionization relations of sodium and potassium chlorides and sulfates in mixtures.' *Am. Chem. J.* 39: 179–218.

Sorina, G. A., G. M. Kozlovskaya, Y. V. Tsekhanskaya, L. I. Bezlyudova & N. G. Shmakov 1977. *Zh. Fiz. Khim.* 51: 2099–2100.

Spencer, R. J., N. Moller & J. H. Weare 1990. *Geochim. et Cosmochim. Acta* 54: 575–590.

Spitzer, J. J., I. V. Olofsson, P. P. Singh & L. G. Hepler 1979. *J. Chem. Thermodynamics* 11: 233–238.

Tilden & Shenstone 1885. *Proc. Roy. Soc.* 38: 331–336.

Timoshenko, Y. M. 1979. *Issl. V. Obl. Khim. Prost. i Kompleks. Soedin. Nekotov. Met. Kazan.* pp. 164–168.

Timoshenko, Y. M. 1986. 'The $NaNO_3$–KNO_3–NH_4NO_3–H_2O system at 25°C.' *Russ. J. Inorg. Chem.* 31: 1843–1844.

Timoshenko, Y. M. & I. N. Chekmareva 1989. 'The $NaNO_3$–NH_4NO_3–$Mg(NO_3)_2$–H_2O system at 25°C.' *Russ. J. Inorg. Chem.* 34: 1551–1552.

Tomus, E. J., L. Istrate & M. Bulcu 1995. *Revue Roumaine de Chemie* 40(4): 315–318.

Toporescu, E. 1922a. *Comptes Rendus* 174: 870–873.

Toporescu, E. 1922b. *Comptes Rendus* 175: 268–270.

Uyeda 1909. *Mem. Coll. Sci. Eng., Kyoto Imperial University* 10(ii): 245–251.

van Veldhuizen 1929. *Proefschrift.* Utrecht.

Venderzee, C. E., D. H. Waugh & N. C. Haas 1980. *J. Chem. Themodynamics* 12: 21–25.

Vereshchagina, V. I., V. N. Derkacheva, L. F. Shulyak & L. V. Zolotareva 1973. '35°C solubility isotherms of the ternary aqueous systems based on potassium and calcium nitrates and chlorides.' *Russ. J. Inorg. Chem.* 18: 266–268.

Vereshchagina, V. I., L. V. Zolotareva & L. F. Shulyak 1969. 'The $CaCl_2$–$Ca(NO_3)_2$–$(KCl)_2$–$(KNO_3)_2$–H_2O system at 60°C.' *Russ. J. Inorg. Chem.* 14: 1787–1790.

Wollner 1913. *Dissertation.* Erlangen.

Yakimov, M. A., E. I. Guzhavina & M. S. Lazeeva 1969. 'Solution-vapour equilibrium in calcium (cadmium) nitrate-alkali metal nitrate-water systems.' *Russ. J. Inorg. Chem.* 14: 1011–1014.

Yanat'eva, O. K. & V. T. Orlova 1959. 'Glaserite in the K, Na, Mg// Cl, SO_4–H_2O system at 0°C.' *Russ. J. Inorg. Chem.* 4: 861–864.

Yarym-Agaev, N. L., F. M. Klyashtornaya & V. Y. Rudin 1964. 'The aqueous system of potassium and sodium nitrates and chlorides: solubility isotherm of the salts at 75°.' *Russ. J. Inorg. Chem.* 9: 1423–1425.

Zhang, Y. & M. Muhammed 1989. 'Solubility of calcium sulfate dihydrate in nitric acid solutions containing calcium nitrate and phosphoric acid.' *J. Chem. Eng. Data* 34: 121–124.

8

Model Parameterisation Based on Mole-Fractions

Simon Clegg and Peter Brimblecombe
University of East Anglia

8.1 Introduction

Chapter 7 describes the parameterisation of Pitzer's molality-based thermodynamic model for the system Na^+–K^+–Mg^{2+}–Ca^{2+}–NH^{4+}–Cl^-–NO_3^-–SO_4^{2-}–HCO_3^-–CO_3^{2-}–H_2O, from which salt solubilities can be calculated. Within the expert system, the model must be combined with a mathematical algorithm to determine the amounts of solids and liquid present for specified input conditions (composition, temperature, and relative humidity). During testing of the expert system it was determined that the combined model and algorithm were unstable for some input conditions and produced incorrect results. In most instances this was not because of limitations in the model parameterisation, but rather because the route that the algorithm takes to determine an answer can include physically unrealistic conditions outside the range of validity of the model.

It did not prove possible to modify the model parameterisation described in Chapter 7 to obtain complete reliability within the expert system. Accordingly, an alternative thermodynamic model was applied to a subset of the ionic system given above, containing the ions and salts most important to conservators. This is Na^+–K^+–Mg^{2+}–Ca^{2+}–Cl^-–NO_3^-–SO_4^{2-}–H_2O, but excluding mixtures containing both Ca^{2+} and SO_4^{2-}, as these ions would always tend to exist in solid form as gypsum. The parameterisation, which is the one included in the expert system presented as the output of this project, is described below.

8.2 Parameterisation of mole-fraction-based model

This model (Clegg *et al.* 1992, 1994, 1995) is similar in principle to the molality based equations used earlier and described in Chapter 3. Here, all ion concentrations are expressed as mole fractions, and interactions are described in terms of a series of parameters for binary (cation-anion) and ternary interactions (two ions of the same sign with one of opposite sign). The practical aspects of parameterisation are fully described in a recent application of the model by Clegg *et al.* (1998), and are essentially identical to those described in Chapter 7. An important characteristic of the mole-fraction-based model is that it extrapolates well to very high concentrations — which is necessary in order to give accurate results with the algorithm used in the expert system.

Coefficients for binary cation-anion interaction parameters are listed in Table 8.1. Each parameter P (B_{ca}, W_{ca}, U_{ca} or V_{ca}) is given at temperature T(K) by the equation:

$$P = p_1T^2/6 + p_2T/2 - p_6/T + p_7 + p_9T^3/3 \qquad (8.1)$$

Similarly, coefficients for each ternary parameter ($W_{ii'j}$, $Q_{1,ii'j}$) are listed in Table 8.2. Each interaction parameter P' is given by:

$$P' = q_1 + q_2(T - 298.15) + q_3(T - 298.15)^2 \tag{8.2}$$

8.3 Thermodynamic properties of salts and water

The expert system calculates the equilibrium state of an ion/water mixture by minimising the total Gibbs energy of the system (*e.g.*, Fletcher 1993), using a computer algorithm to obtain the final result by a sophisticated iterative technique. The molar Gibbs energy (in J mol^{-1}) of any component of the system (ion, salt, ice, liquid water or water vapour) is given by the following equation:

$$\begin{aligned} G(T) = GT/T_r - RT\{&H(1/T_r - 1/T)/R \\ &+ a_1(T_r/T - 1 + \ln(T/T_r))/R \\ &+ a_2(T_r(T_r/T - 1) + T - T_r)/2R \\ &+ a_3(2T_r^2(T_r/T - 1) + T^2 - T_r^2)/6R \\ &+ a_4(3T_r^3(T_r/T - 1) + T^3 - T_r^3)/12R\} \end{aligned} \tag{8.3}$$

where G (J mol^{-1}) is the Gibbs energy of formation at reference temperature T_r (generally 298.15K), and H is the corresponding enthalpy of formation. Coefficients $a_1 - a_4$ give the heat capacity (C_p) as a function of temperature T(K):

$$C_p = a_1 + a_2T + a_3T^2 + a_4T^3 \tag{8.4}$$

The following special expression is used for the Gibbs energy of water vapour below 0°C:

$$\begin{aligned} G(T) = -229685.737145T/T_r - RT\{&-242646.44281(1/T_r - 1/T)/R \\ &+ 33.269811(T_r/T - 1 + \ln(T/T_r))/R \\ &+ 0.00113261(T_r(T_r/T - 1) + T - T_r)/2R \\ &- 1.099821E - 5(2T_r^2(T_r/T - 1) + T^2 - T_r^2)/6R \\ &+ 3.573575E - 8(3T_r^3(T_r/T - 1) + T^3 - T_r^3)/12R\} \end{aligned} \tag{8.5}$$

where T_r is 273.15 K. The molar Gibbs energy of ice is:

$$\begin{aligned} G(T) = -2.41294330406D5T/T_r - RT\{&-293736.15(1/T_r - 1/T)/R \\ &+ 59.856189(T_r/T - 1 + \ln(T/T_r))/R \\ &- 0.57943577(T_r(T_r/T - 1) + T - T_r)/2R \\ &+ 0.002879618(2T_r^2(T_r/T - 1) + T^2 - T_r^2)/6R \\ &- 3.8444421E - 6(3T_r^3(T_r/T - 1) + T^3 - T_r^3)/12R\} \end{aligned} \tag{8.6}$$

where T_r is also 273.15K. Gibbs energies (G), enthalpies (H), and coefficients a_1 to a_4 are given for all species modelled using the mole fraction based equations in Tables 8.3–8.5.

Table 8.1: Mole fraction model parameters for binary interactions.

salt	prmtr.	P_1	P_2	P_6	P_7	P_9
NaCl	B	0.92410	-0.1432×10^{3}	0.11518×10^{7}	0.14824×10^{5}	-0.3726×10^{-3}
NaCl	W	−0.55695	0.8649×10^{2}	-0.69129×10^{6}	-0.89541×10^{4}	0.2246×10^{-3}
NaCl	U	-0.15188×10^{1}	0.2351×10^{3}	-0.18678×10^{7}	-0.24246×10^{5}	0.6140×10^{-3}
NaCl	V	0.11325×10^{1}	-0.1749×10^{3}	0.13880×10^{7}	0.18008×10^{5}	-0.4589×10^{-3}
$NaNO_3$	B	-0.47340×10^{-2}	0	0.43993×10^{5}	0.19609×10^{3}	0
$NaNO_3$	B2	-0.57730×10^{-2}	0	0.72941×10^{5}	0.35717×10^{3}	0
$NaNO_3$	W	-0.15070×10^{-3}	0	0.25688×10^{4}	0.11375×10^{2}	0
$NaNO_3$	U	0.10000×10^{-3}	0	0.68996×10^{3}	0.10992×10^{1}	0
$NaNO_3$	V	0.10000×10^{-3}	0	-0.26120×10^{3}	-0.46605×10^{1}	0
Na_2SO_4	B	-0.12950×10^{-1}	0	0.15045×10^{6}	0.74056×10^{3}	0
Na_2SO_4	W	0.17199×10^{-3}	0	0.23394×10^{4}	−0.79809	0
Na_2SO_4	U	-0.19671×10^{-3}	0	0.30997×10^{4}	0.50389×10^{1}	0
Na_2SO_4	V	-0.53000×10^{-3}	0	0.13572×10^{5}	0.54117×10^{2}	0
KCl	B	-0.15560×10^{-2}	0	0.23356×10^{5}	0.10967×10^{3}	0
KCl	W	0.65860×10^{-4}	0	-0.65648×10^{3}	-0.70596×10^{1}	0
KCl	U	-0.66880×10^{-4}	0	0.13724×10^{4}	0.16909×10^{1}	0
KCl	V	-0.11400×10^{-3}	0	0.15405×10^{4}	0.79698×10^{1}	0
KNO_3	B	-0.78480×10^{-2}	0	0.11179×10^{6}	0.48807×10^{3}	0
KNO_3	W	0.13990×10^{-3}	0	-0.10199×10^{4}	-0.73216×10^{1}	0
KNO_3	U	-0.13520×10^{-3}	0	0.23118×10^{4}	0.27839×10^{1}	0
KNO_3	V	-0.10000×10^{-3}	0	0.36391×10^{4}	0.16187×10^{2}	0
K_2SO_4	B	-0.13180×10^{-1}	0	0.17625×10^{6}	0.81392×10^{3}	0
K_2SO_4	W	0.60050×10^{-3}	0	-0.47270×10^{4}	-0.31668×10^{2}	0
K_2SO_4	U	-0.52730×10^{-3}	0	0.13189×10^{5}	0.42995×10^{2}	0
K_2SO_4	V	0.14700×10^{-2}	0	-0.21876×10^{5}	-0.95152×10^{2}	0
$CaCl_2$	B	0.73410×10^{-2}	0	-0.91167×10^{5}	-0.31728×10^{3}	0
$CaCl_2$	W	0.14060×10^{-3}	0	0.42701×10^{4}	0.29907	0
$CaCl_2$	U	-0.11670×10^{-3}	0	-0.44731×10^{3}	0.63117×10^{1}	0
$CaCl_2$	V	-0.32000×10^{-3}	0	0.13494×10^{5}	0.35001×10^{2}	0
$Ca(NO_3)_2$	B	-0.56070×10^{-2}	0	0.11953×10^{6}	0.59428×10^{3}	0
$Ca(NO_3)_2$	W	0.10640×10^{-3}	0	-0.26734×10^{3}	-0.69110×10^{1}	0
$Ca(NO_3)_2$	U	-0.10730×10^{-3}	0	0.36889×10^{3}	0.39880×10^{1}	0
$Ca(NO_3)_2$	V	-0.20000×10^{-3}	0	0.62116×10^{4}	0.19972×10^{2}	0
$MgCl_2$	B	0.64000×10^{-2}	0	-0.39829×10^{5}	-0.43007×10^{2}	0
$MgCl_2$	W	0.12670×10^{-3}	0	0.58055×10^{4}	-0.65755×10^{1}	0
$MgCl_2$	U	-0.13670×10^{-3}	0	0.33447×10^{4}	0.18534×10^{1}	0
$MgCl_2$	V	0.13250×10^{-3}	0	0.32741×10^{4}	−0.98169	0
$Mg(NO_3)_2$	B	-0.26410×10^{-2}	0	0.58232×10^{5}	0.36424×10^{3}	0
$Mg(NO_3)_2$	W	0.10840×10^{-3}	0	0.13269×10^{4}	-0.82756×10^{1}	0
$Mg(NO_3)_2$	U	-0.17340×10^{-4}	0	-0.24176×10^{3}	0.27880×10^{1}	0
$Mg(NO_3)_2$	V	-0.38000×10^{-3}	0	0.78018×10^{4}	0.21797×10^{2}	0
$MgSO_4$	B	-0.40183×10^{-1}	0.7234×10^{1}	0.11227×10^{6}	0.16589×10^{3}	0
$MgSO_4$	B2	-0.22071×10^{1}	0.1599×10^{4}	-0.53185×10^{8}	-0.38822×10^{6}	0
$MgSO_4$	W	0.61353×10^{-1}	-0.1845×10^{2}	0.29543×10^{6}	0.27859×10^{4}	0
$MgSO_4$	U	0.76286×10^{-1}	-0.2314×10^{2}	0.37422×10^{6}	0.35101×10^{4}	0
$MgSO_4$	V	0	0	0	0.20000×10^{2}	0

Table 8.2: Mole fraction model parameters for ternary interactions.

Ions	Parameter	q1	q2	q3
Na–NO_3–SO_4	W	−9.433	0.074416	0
Na–NO_3–SO_4	Q	7.679	−0.018868	0
Na–Cl–NO_3	W	−6.378	−0.07960	-0.3792×10^{-3}
Na–Cl–NO_3	Q	3.177	0.07701	0.6299×10^{-3}
Na–Cl–SO_4	W	−4.968	0.6673	0
Na–Cl–SO_4	Q	6.784	−0.3969	0
Ca–Cl–NO_3	W	6.922	−0.1599	0
Ca–Cl–NO_3	Q	−6.587	0.1398	0
Na–Mg–Cl	W	−30.0	0	0
Na–Mg–Cl	Q	12.41	0.002789	0
Na–Ca–Cl	W	−15.0	−1.727	0
Na–Ca–Cl	Q	11.15	1.114	-0.7092×10^{-3}
Mg–Ca–Cl	W	−40.0	0.4141	0.03566
Mg–Ca–Cl	Q	24.37	−0.4589	−0.02855
Na–Ca–NO_3	W	−11.8	0.04867	0
Na–Ca–NO_3	Q	7.984	0	0
Na–Mg–NO_3	W	−15.00	0.1714	0
Na–Mg–NO_3	Q	3.072	−0.1053	0
Mg–Cl–NO_3	W	2.327	0.2860	0
Mg–Cl–NO_3	Q	−1.541	−0.1770	0
Mg–Ca–NO_3	W	−20.0	0	0
Mg–Ca–NO_3	Q	8.274	−0.03116	0
Na–K–NO_3	W	−5.016	0.0413	0
Na–K–NO_3	Q	2.217	−0.02183	0
Na–K–Cl	W	−4.694	0.08069	0
Na–K–Cl	Q	2.047	−0.05429	0
Na–K–SO_4	W	−6.663	0.02374	0
Na–K–SO_4	Q	3.372	−0.004813	0
K–Ca–NO_3	W	−23.78	0.1672	0
K–Ca–NO_3	Q	10.56	−0.0379	0
Mg–NO_3–SO_4	W	−26.4	−0.6894	0
Mg–NO_3–SO_4	Q	9.173	0.4931	0
K–Cl–NO_3	W	−12.27	0.04944	0
K–Cl–NO_3	Q	7.541	−0.006654	0
K–Cl–SO_4	W	−18.23	−0.008112	0
K–Cl–SO_4	Q	−10.46	−0.01740	0
Na–Mg–SO_4	W	−26.34	−0.444	0
Na–Mg–SO_4	Q	5.076	0.3306	0
Mg–Cl–SO_4	W	−21.24	−0.8103	0
Mg–Cl–SO_4	Q	10.39	0.5403	0
K–Mg–SO_4	W	−80.0	−1.077	0
K–Mg–SO_4	Q	32.84	0.7349	0
K–Mg–Cl	W	−57.46	1.056	0
K–Mg–Cl	Q	20.0	−0.5716	0
K–Mg–NO_3	W	−40.00	0.4654	0
K–Mg–NO_3	Q	14.17	−0.2174	0
K–Ca–Cl	W	−25.0	−0.2436	0
K–Ca–Cl	Q	3.124	0.1757	0
K–NO_3–SO_4	W	−7.281	−0.3030	0
K–NO_3–SO_4	Q	−5.719	0.1686	0

Table 8.3: Thermodynamic quantities for ions and liquid water.

Species	G	H	a_1	a_2	a_3	a_4
Na^+	−261905	−240120	46.4	0.0	0.0	0.0
K^+	−283270	−252380	21.8	0.0	0.0	0.0
Mg^{2+}	−454800	−466850	4.2	0.0	0.0	0.0
Ca^{2+}	−553580	−542830	−2.9	0.0	0.0	0.0
Cl^-	−131228	−167159	−136.4	0.0	0.0	0.0
$NO_3{}^-$	−108740	−205000	−86.6	0.0	0.0	0.0
$SO_4{}^{2-}$	−744530	−909270	−293.	0.0	0.0	0.0
H_2O(l)	−237129	−285830	295.1612	−1.540498	2.7023×10^{-3}	0.0

Table 8.4: Thermodynamic quantities for salts and water vapour.

Salt	G	H
NaCl	-4.03986114402×10^5	-4.1131423×10^5
$NaCl\cdot2H_2O$	-8.78702358553×10^5	-9.90118×10^5
$NaNO_3$	-3.84441937988×10^5	-4.62978×10^5
Na_2SO_4	-1.29987585897×10^6	-1.3877352×10^6
$Na_2SO_4\cdot10H_2O$	-3.67646223968×10^6	-4.32762914×10^6
KCl	-4.29260301038×10^5	-4.368225×10^5
KNO_3	-4.12474865715×10^5	-4.9167865×10^5
K_2SO_4	-1.35098983177×10^6	-1.43699563×10^6
$K_2SO_4\cdot H_2O$	-1.58838291308×10^6	-1.72386631×10^6
$MgCl_2\cdot6H_2O$	-2.14341782871×10^6	-2.4954122×10^6
$MgCl_2\cdot8H_2O$	-2.62040423999×10^6	-3.09375135×10^6
$MgCl_2\cdot12H_2O$	-3.57361234478×10^6	-4.2630635×10^6
$Mg(NO_3)_2\cdot2H_2O$	-1.12532149786×10^6	-1.341033×10^6
$Mg(NO_3)_2\cdot6H_2O$	-2.10785786537×10^6	-2.6072077×10^6
$Mg(NO_3)_2\cdot9H_2O$	-2.81550070909×10^6	-3.5336633×10^6
$MgSO_4\cdot H_2O$	-1.45546541704×10^6	-1.6122451×10^6
$MgSO_4\cdot4H_2O$	-2.17573157761×10^6	-2.51782063×10^6
$MgSO_4\cdot6H_2O$	-2.6520007403×10^6	-3.1079352×10^6
$MgSO_4\cdot7H_2O$	-2.88964808631×10^6	-3.39284311×10^6
$CaCl_2\cdot2H_2O$	-1.27288384326×10^6	-1.36692×10^6
$CaCl_2\cdot4H_2O$	-1.76337872839×10^6	-2.02520736×10^6
$CaCl_2\cdot6H_2O$	-2.24618682477×10^6	-2.61946776×10^6
$Ca(NO_3)_2\cdot2H_2O$	-1.25425779541×10^6	-1.5312212×10^6
$Ca(NO_3)_2\cdot3H_2O$	-1.49601484938×10^6	-1.8276368×10^6
$Ca(NO_3)_2\cdot4H_2O$	-1.73799327255×10^6	-2.1240524×10^6
$Ca(NO_3)_2$	-7.80613828439×10^5	-9.3839×10^5
$NaNO_3\cdot Na_2SO_4\cdot H_2O$	-1.92374680059×10^6	-2.143876×10^6
$Na_2SO_4\cdot3K_2SO_4$	-5.3660027708×10^6	-5.71035×10^6
$Na_2SO_4\cdot MgSO_4\cdot4H_2O$	-3.4793741388×10^6	-3.89624×10^6
$KCl\cdot MgCl_2\cdot6H_2O$	-2.57745074301×10^6	-2.955597×10^6
$KCl\cdot CaCl_2$	-1.21029346829×10^6	-1.150787×10^6
$KNO_3\cdot5Ca(NO_3)_2\cdot10H_2O$	-6.7083871474×10^6	-8.13547×10^6
$KNO_3\cdot Ca(NO_3)_2\cdot3H_2O$	-1.80513211992×10^6	-2.1212×10^6
$K_2SO_4\cdot MgSO_4\cdot4H_2O$	-3.52988800525×10^6	-3.929681×10^6
$K_2SO_4\cdot MgSO_4\cdot6H_2O$	-4.00744299327×10^6	-4.54398×10^6
$2MgCl_2\cdot CaCl_2\cdot12H_2O$	-5.08843608047×10^6	-5.778644×10^6
$CaCl_2\cdot Ca(NO_3)_2\cdot4H_2O$	-2.53517025318×10^6	-2.940218×10^6
$CaCl_2\cdot4H_2O(\beta)$	-1.76160189726×10^6	-2.01744188×10^6
$CaCl_2\cdot4H_2O(\gamma)$	-1.76137748641×10^6	-2.01076259×10^6
$MgCa(NO_3)_4\cdot10H_2O$	-3.84824440416×10^6	-4.70866×10^6
H_2O(g) [0–100° C]	−228537.98	-2.4177239×10^5

Table 8.5: Thermodynamic quantities for salts and water vapour (cont.).

Salt	a_1	a_2	a_3	a_4
NaCl	43.058	0.0	0.0	0.0
$NaCl{\cdot}2H_2O$	832.3344	−3.080996	0.0054046	0.0
$NaNO_3$	104.198	0.0	0.0	0.0
Na_2SO_4	278.177	0.0	0.0	0.0
$Na_2SO_4{\cdot}10H_2O$	2751.412	−15.40498	0.027023	0.0
KCl	1.752	0.0	0.0	0.0
KNO_3	103.276	0.0	0.0	0.0
K_2SO_4	125.29	0.0	0.0	0.0
$K_2SO_4{\cdot}H_2O$	45.7612	−1.540498	0.0027023	0.0
$MgCl_2{\cdot}6H_2O$	1540.1228	−9.242988	0.0162138	0.0
$MgCl_2{\cdot}8H_2O$	2092.6896	−12.323984	0.0216184	0.0
$MgCl_2{\cdot}12H_2O$	3273.3344	−18.485976	0.0324276	0.0
$Mg(NO_3)_2{\cdot}2H_2O$	−1625.7976	−3.080996	0.0054046	0.0
$Mg(NO_3)_2{\cdot}6H_2O$	1601.9672	−9.242988	0.0162138	0.0
$Mg(NO_3)_2{\cdot}9H_2O$	1396.0508	−13.864482	0.0243207	0.0
$MgSO_4{\cdot}H_2O$	188.7612	−1.540498	0.0027023	0.0
$MgSO_4{\cdot}4H_2O$	891.8448	−6.161992	0.0108092	0.0
$MgSO_4{\cdot}6H_2O$	1946.8372	−9.242988	0.0162138	0.0
$MgSO_4{\cdot}7H_2O$	2029.0584	−10.783486	0.0189161	0.0
$CaCl_2{\cdot}2H_2O$	−1128.0776	−3.080996	0.0054046	0.0
$CaCl_2{\cdot}4H_2O$	242.2448	−6.161992	0.0108092	0.0
$CaCl_2{\cdot}6H_2O$	1116.0972	−9.242988	0.0162138	0.0
$Ca(NO_3)_2{\cdot}2H_2O$	414.2224	−3.080996	0.0054046	0.0
$Ca(NO_3)_2{\cdot}3H_2O$	709.3836	−4.621494	0.0081069	0.0
$Ca(NO_3)_2{\cdot}4H_2O$	1290.7458	−6.161992	0.0108092	0.0
$Ca(NO_3)_2$	−176.1	0.0	0.0	0.0
$NaNO_3{\cdot}Na_2SO_4{\cdot}H_2O$	607.3912	−1.540498	0.0027023	0.0
$Na_2SO_4{\cdot}3K_2SO_4$	−155.6	0.0	0.0	0.0
$Na_2SO_4{\cdot}MgSO_4{\cdot}4H_2O$	691.6448	−6.161992	0.0108092	0.0
$KCl{\cdot}MgCl_2{\cdot}6H_2O$	1387.7672	−9.242988	0.0162138	0.0
$KCl{\cdot}CaCl_2$	−390.3	0.0	0.0	0.0
$KNO_3{\cdot}5Ca(NO_3)_2{\cdot}10H_2O$	2006.312	−15.40498	0.027023	0.0
$KNO3.Ca(NO_3)_2{\cdot}3H_2O$	1090.9836	−4.621494	0.0081069	0.0
$K_2SO_4{\cdot}MgSO_4{\cdot}4H_2O$	642.4448	−6.161992	0.0108092	0.0
$K_2SO_4{\cdot}MgSO_4{\cdot}6H_2O$	1363.7672	−9.242988	0.0162138	0.0
$2MgCl_2{\cdot}CaCl_2{\cdot}12H_2O$	2729.0344	−18.485976	0.0324276	0.0
$CaCl_2{\cdot}Ca(NO_3)_2{\cdot}4H_2O$	728.8448	−6.161992	0.0108092	0.0
$CaCl_2{\cdot}4H_2O(beta)$	1763.7648	−6.161992	0.0108092	0.0
$CaCl_2{\cdot}4H_2O(\gamma)$	904.9448	−6.161992	0.0108092	0.0
$MgCa(NO_3)_4{\cdot}10H_2O$	2606.512	−15.40498	0.027023	0.0
H_2O(g) [0–100°C]	137.07248	−0.439385	-9.3701×10^{-4}	4.27758×10^{-6}

In chemical systems where there is a liquid component, there is also an 'activity' contribution to the total Gibbs energy for water and for all ions. For each species j this contribution to G is given by:

$$G_j = n_j \cdot RT \ln(x_j f_j^*) \tag{8.7}$$

where n_j is the number of moles of j in the liquid phase, x_j is its mole fraction, and $f^\star j$ is its activity coefficient. These activity coefficients are calculated using the mole-fraction-based thermodynamic model referred to above.

8.4 Testing the thermodynamic model and expert system

The thermodynamic model was coded in FORTRAN and included in a program with the algorithm code. This was tested by carrying out calculations for all possible combinations of ions, for relative humidities from 98% to 15%, and for temperatures between +50 and −30°C. No errors (*i.e.*, failure of the algorithm) were detected. The representation of measured salt solubilities by the present model are not shown here. However, it was found during the parameterisation process that the results were significantly better than obtained using the molality-based equations in many cases. This was particularly so for systems in which high concentrations were reached, for example calcium and magnesium chloride and nitrate mixtures.

8.5 Accuracy and reliability

How accurate are the results of the expert system calculations? This depends upon two factors:

1. *The accuracy and extent of salt solubility and other thermodynamic data used to parameterise the model.* In considering this, we need to look at the data for both pure aqueous (*i.e.*, single salt) solutions and ternary mixtures (solutions containing two anions and one cation or *vice versa*). The extent of thermodynamic measurements — yielding equilibrium relative humidities and ionic activities as functions of concentration and temperature — vary widely between different salts. As might be expected, aqueous NaCl has been extremely well studied, whereas measurements for salts such as $MgSO_4$ and $Mg(NO_3)_2$ are relatively sparse and limited chiefly to 25°C. This introduces uncertainties at the extremes of the temperature range (close to 50°C and below 0°C). Consequently, for both pure aqueous and mixed solutions the expert system will be most accurate for temperatures of about 15–35°C— that is, about 10°C either side of the thermodynamic standard temperature at which measurements are most often made.

   In the case of mixtures, the development of the thermodynamic model ideally requires salt solubility measurements for wide ranges of composition, and for temperatures covering the complete range of the model. This requirement of the model is most nearly met for solutions containing 'common' ions such as Na^+, Cl^- and $SO_4{}^{2-}$. Data are generally more sparse for $NO_3{}^-$ solutions. Limitations on the accuracy of the model due to lack of data (or inconsistent sets of measurements) are most likely to be related to mixed solution and not single salt properties. Users with interests in a particular salt mixture should compare the output of the model with original solubility measurements referenced in the attached final report.

2. *Limitations of the model.* The model is most accurate (to better than 1% in equilibrium relative humidity) for salts containing singly charged ions, for aqueous concentrations up to about 6 mol kg^{-1}. The most difficult salts to represent are Ca^{2+} and Mg^{2+} chlorides and nitrates, due to the high ionic strengths that can be attained in their aqueous solutions. The salts, and their mixtures, are highly soluble, and the results of the model at low relative humidities and temperatures far from 25°C should be interpreted with caution. In particular,

it is recommended that calculations for conditions close (in relative humidity, temperature and composition) to those of interest be carried out to check for variations in the predicted state of the system — particularly for the presence of different solids. Again, it is also sensible to compare with original measurements of salt solubilities where possible (see references in Chapter 7).

8.6 References

Clegg, S. L., P. Brimblecombe & A. S. Wexler 1998. 'A thermodynamic model of the system H–NH_4–SO_4–NO_3–H_2O at tropospheric temperatures.' *J. Phys. Chem.* A102: 2127–2154.

Clegg, S. L., K. S. Pitzer & P. Brimblecombe 1992. 'Thermodynamics of multicomponent, miscible, ionic solutions. II Mixtures including unsymmetrical electrolytes.' *J. Phys. Chem.* 96: 9470–9479.

Clegg, S. L., K. S. Pitzer & P. Brimblecombe 1994. 'Thermodynamics of multicomponent, miscible, ionic solutions. II Mixtures including unsymmetrical electrolytes.' *J. Phys. Chem.* 98: 1368f.

Clegg, S. L., K. S. Pitzer & P. Brimblecombe 1995. 'Thermodynamics of multicomponent, miscible, ionic solutions. II Mixtures including unsymmetrical electrolytes.' *J. Phys. Chem.* 99: 6755f.

Fletcher, P. 1993. *Chemical Thermodynamics for Earth Scientists.* Longman Scientific & Technical, Harlow.

9

The ECOS Program

Shaiba Mahmoud

Institute of Archaeology, University College London

9.1 Introduction

The computer program ECOS provides a user-friendly interface to the thermodynamic model, which would otherwise be inaccessible to many potential users. It utilises the mole-fraction parameterisation of the system Na^+–K^+–Mg^{2+}–Ca^{2+}–Cl^-–$NO_3{}^-$–$SO_4{}^{2-}$–H_2O, but excluding mixtures containing both Ca^{2+} and $SO_4{}^{2-}$, as described in the preceding chapters.

The process of diagnosing salt damage is an involved one. A combination of association, induction and mathematical reasoning is used to arrive at the right decision. These reasoning processes are realised in a series of different knowledge processing activities, resulting in a large complex activity. Therefore any attempt to apply Artificial Intelligence techniques to automate decision making in the conservation of salt damaged materials requires a thorough analysis of the different activities performed by conservators, to get a good insight into the goals structure and their problem solving activities. During the first two months of the project, a number of interviews were carried out with experts in the field, and visits were made to historical sites, where conservators were watched during their investigation of salt damaged monuments.

The process of conservation was divided into a number of sub-processes, and the knowledge processing activities in each of the sub-processes were identified. Activities were characterised by the problem they solved, the reasoning technique they employed, and the knowledge they used. This exercise laid the foundation for the planning of the architecture, the knowledge representation formalism and the reasoning techniques suitable for the proposed system.

The underlying assumption is that the conservation of salt-susceptible materials is a multi-step knowledge transformation process. It starts from a generalised knowledge at the lowest level of sub-processes and moves into a more specific sub-process at a higher level, and continues until a detailed definition of the problem under consideration is attained. This knowledge transformation process is achieved through a succession of knowledge applying and knowledge generating processes; knowledge is applied at one level to generate new knowledge that is required to move the conservation sub-process to the next level. This knowledge transformation process is sequential.

The following sub-processes have been identified:

1. Collection of site data (salts analysis data and environmental data),
2. Examination, processing of data and presentation of the inferred thermodynamics of the salt sample to determine its behaviour.

The resulting system structure is illustrated in Figure 9.1.

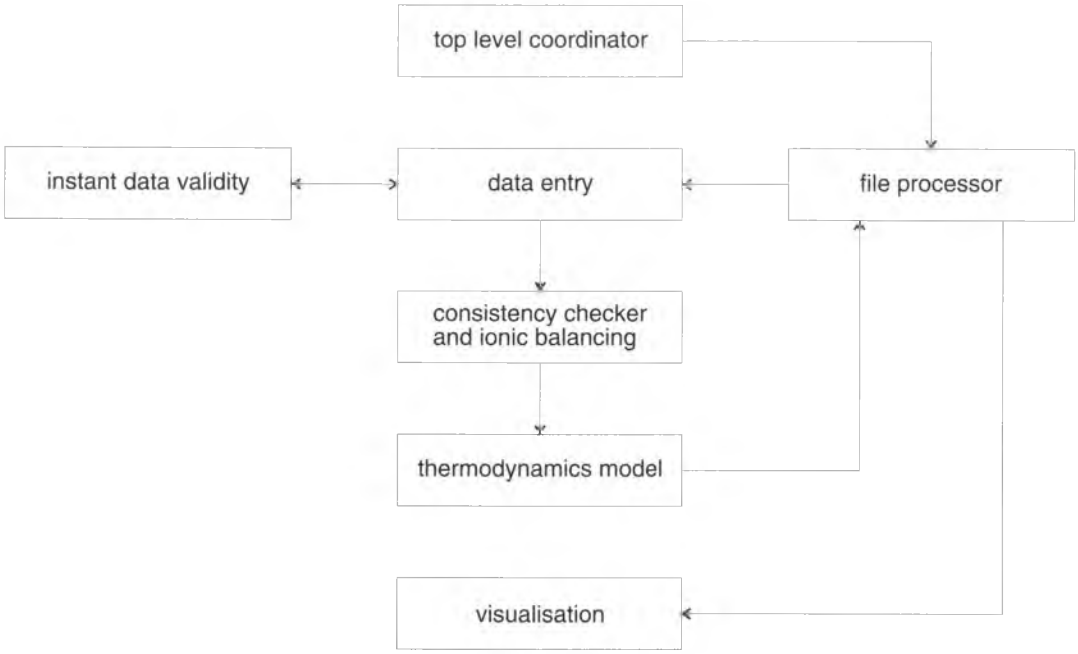

Figure 9.1: ECOS system structure.

9.2 Software choice

General purpose shells may offer the required knowledge representation formalism. but still they impose constraints on the application, because their design methodologies are usually suited to one class of application *e.g.,* diagnostic. Shells are usually limited to a single problem solving technique and they determine the styles of user interface on behalf of the expert system developer. Another very important drawback of the shells is their cost. Since the developed system needs to be distributed to many users, each copy would require a separate licence, and this would constitute a crippling amount of royalties to be paid in licensing fees.

Visual Prolog was chosen to build the current system. This was sound both financially and technically, since Visual Prolog offers very good features for developing expert systems, and no royalties are required for the distributed systems.

9.3 Design decisions

The design principle that was adopted is a top-down modular decomposition method, where each of the identified sub-processes is regarded as a separate module. This method helped during the programming of the system, since it takes less time to develop modular software, by decomposing the whole of the program to manageable smaller units. Each module can be developed, tested and corrected individually before it is linked to the main program.

The design of the structure of the present system is based on:

1. the initial model envisaged by the principal researchers of the project, included in the technical annex to the first progress report;

2. the above identified conservators' sub-processes.

The design features implemented in the final system include:

1. efficiency in terms of knowledge acquisition, editing and run cycle;
2. provision of various system consultation modes;
3. a friendly graphical user interface that incorporates several user-interfacing styles (windows, menus, icons, list boxes, radio buttons, editing fields, text editors...) to enable easy, efficient, communication with the system, and provide meaningful error and help messages that can be accessed wherever required in the system;
4. provision of an interactive multi-data visualisation mode.

9.4 System architecture

In the following sections, each of the system's main components (modules) is explained to clarify the logic behind its design and architecture decisions.

Top Level Co-ordinator (TLC)

This is the main module and is the component of the system that receives and processes the initial user requests. This is achieved by allowing the user to access any of the system's other components. It responds to the user queries from the opening screen and handles control to the relevant module to perform the required action. At the end of each requested process, control returns to the TLC. The main objective of the TLC is to facilitate the co-ordination and management of the system's various functions, by smoothly and efficiently controlling the interfacing and communications between the system modules.

File Processor Module (FP)

The FP controls all the file processing activities in the system. It achieves this by employing a number of sub-processors, each of which is explained below.

Site file management sub-processor: This sub-processor is responsible for creating new site files. This is accomplished by creating three files for every new sample (raw analytical data, graph data, and the thermodynamic model data results), assigning the sample name and the appropriate extension for each one. It checks newly created sample names and alerts for duplications within the same site folder. It is also responsible for loading existing sample data files for reprocessing, editing or visualisation purposes.

Temporary file management sub-processor: During the course of a consultation, a number of temporary files are created and deleted. This is quite an involved process that requires careful monitoring and management, and is controlled by this sub-processor.

Chemical references file management sub-processor: The chemical references are required to be processed to match the relevant references with the present sample salts and stored in a file for use by the visualisation module.

Data Entry Module

This module facilitates data acquisition. It employs highly interactive user-friendly data acquisition methods, utilising various GUI styles. These GUI styles facilitate easy data entry and are less error prone. The provision of an instant error detecting mechanism ensures a high degree of reliability in the entered data. This mechanism checks entered values against legally defined values as they are entered, and it also performs compatibility value checking by monitoring the combined allowable value for each set of data. It also advises on the course of action to be taken to rectify any error. To further reduce the possibility of error during data entry, a mechanism is adopted that bars the selection of some options if certain other options are selected. Context sensitive help is readily available when required.

Consistency Checker Module

This is a third error detection mechanism, which maintains the integrity of the entered data by checking the ion balance and triggering the relevant error messages if there is a charge imbalance between the cations and anions. It also advises on what course of action should be taken to balance ions if necessary, and transforms ionic data entered in any concentration units into molarity, and the temperature to degrees Kelvin. The module performs its tasks in conjunction with the Ion Balance Sub-Module.

Ion Balance Sub-Module: This sub-module is responsible for ensuring ionic balance before consulting the thermodynamic model, and offers the user a number of ion balancing methods.

Visualisation Module

This is the module that performs the presentation of the salts' behaviour in a graphic form. It offers an interactive multi-graphs mode (volume/temperature, volume/relative humidity, molar quantity/temperature, molar quantity/relative humidity, and stacks of up to three graphs). Data coordinates and salt identifications in these graphs can be determined using a mouse, while bibliographical references are selected automatically using an intelligent pattern matching algorithm.

10
Using ECOS

Clifford Price
Institute of Archaeology, University College London

10.1 Sampling and analysis

To use ECOS, the user requires an ionic analysis of a sample (or samples) taken from the monument or artefact under investigation.

Taking samples is easy, but taking samples that are representative and meaningful is much more difficult (*cf.* section 2.3.3).

If samples are to be taken from a monument, it may be necessary to take a great many samples in order to build up a fair and representative picture. The costs of analysis may then become unacceptable. Even worse, permission for sampling may not be forthcoming if it would be necessary to drill a large number of holes. It is often necessary to adopt a compromise that a statistician would regard as less than satisfactory.

Another problem relates to the sample itself. How should it be taken? If it is a sample of efflorescence that is scraped off the surface, it may not be representative of the salts that are present in the depth of the object/monument. To find out about the salts that are present in the interior, it may be necessary to drill out a sample. Indeed, one can take a succession of drillings from the same hole, sampling the first 5mm, for example, then from 5–10mm, then 10–15mm *etc.* In this way, one can build up a picture of the distribution of salts within the interior. Even here, however, one needs to be aware of the limitations: the distribution of salts may well vary with varying environmental conditions.

Analysis will invariably be based on an aqueous extract of the original sample: a known weight of the sample is added to a known volume of de-ionised water. After allowing time for all soluble salts to dissolve, any remaining solids are removed by filtration or by centrifuge, and the solution is used for analysis.

The appropriate proportion of sample to water will depend on the nature of the sample. If the sample consists primarily of efflorescence, less sample will be necessary than if the sample consists primarily of stone dust, for example. Advice should be sought from the laboratory undertaking the analysis. The important thing is to keep a record of the proportions used, so that total salt content may subsequently be computed where necessary. The solution should not be acidified in an attempt to dissolve sparingly soluble salts.

A number of different techniques may be used for the analysis of the aqueous extract, the most common being ion chromatography (IC), inductively-coupled plasma emission spectroscopy (ICP-ES, or simply ICP), and atomic-absorption spectroscopy (AAS). It may be necessary to dilute the solution further in order to get within the operating range of the individual technique; if this is the case, the results must be converted back to the concentration of the original solution before entering the data into this program.

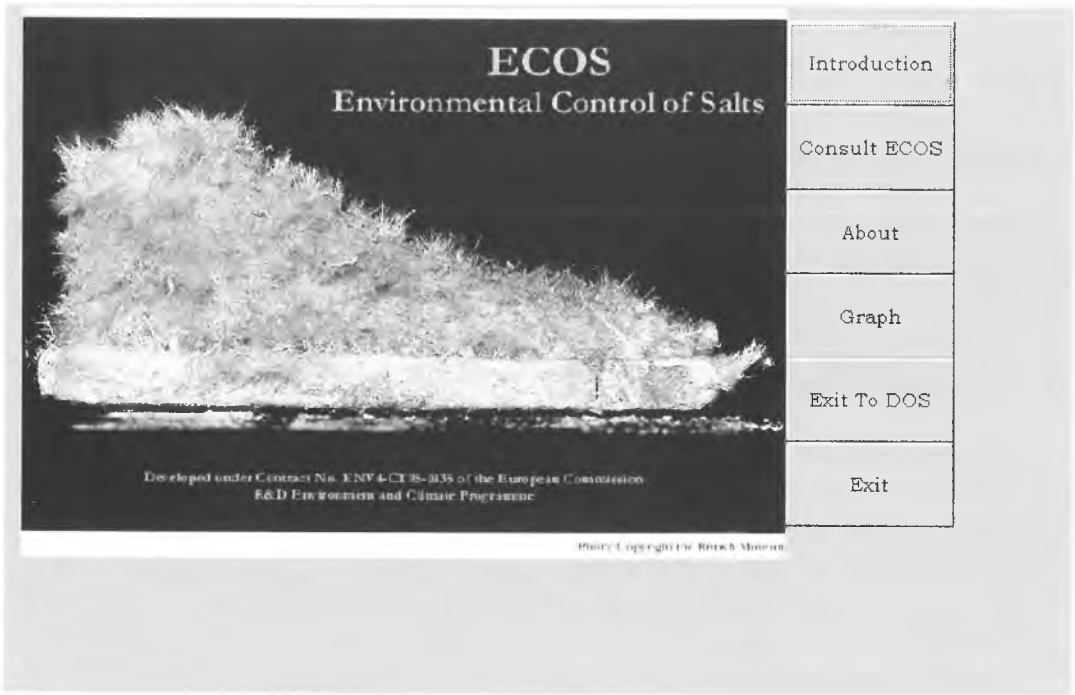

Figure 10.1: ECOS opening page.

If possible, the pH of the original solution should be measured, using a pH meter. This may assist in the subsequent interpretation of results, should there be an imbalance in the ratio of anions to cations.

ECOS is capable of handling analytical data in a number of different formats: percentage weight of sample, percentage weight of solution, g.ion/litre, molal, molar or parts per million (ppm).

10.2 Running the ECOS program

The program, which runs under Windows 32, is contained on two diskettes containing the following files:

`phas4.exe`

`ecos.hlp`

`salt.exe`

To install the application, a directory named ECOS should be created, with two sub-directories named `exe` and `sites`. The three files should be loaded into the `exe` sub-directory.

To run the program, execute the file `phas4.exe`.

10.3 Getting started with ECOS

The opening page (Fig. 10.1) gives the user three main options:

- Introduction, which provides a textual introduction to the program, with links to other help topics;

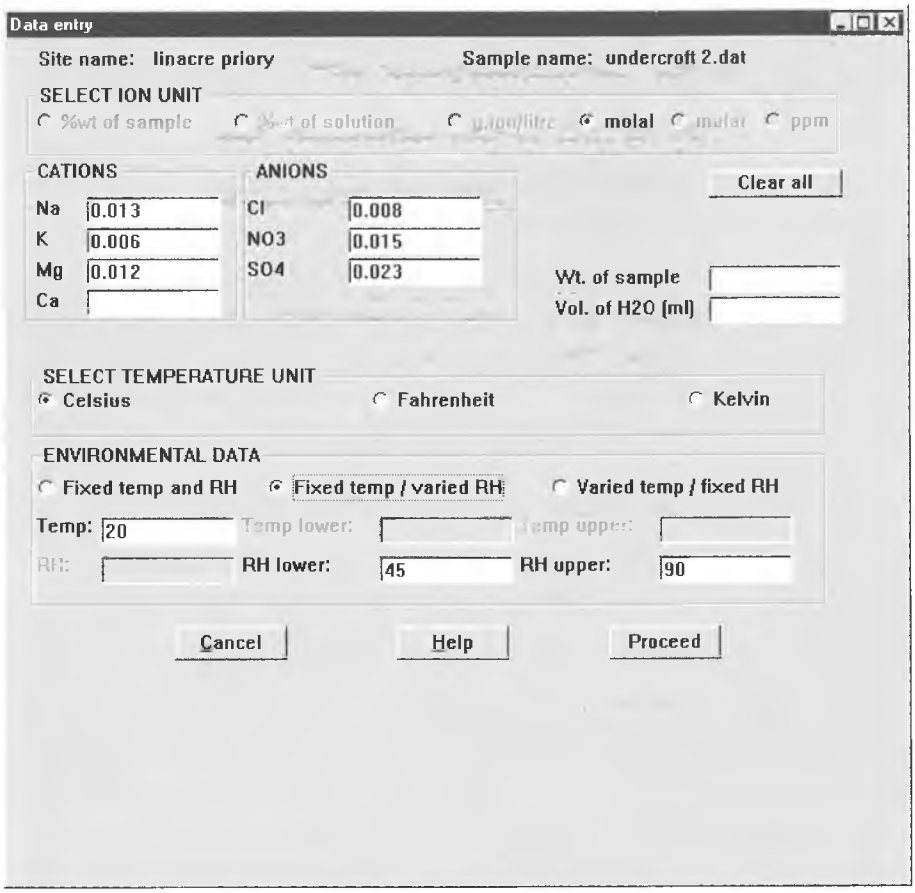

Figure 10.2: Data entry page.

- Consult ECOS, which allows for the creation of sample files or, subsequently, to view and alter existing data files; and
- Graph, which gives direct access to graphs created for existing data sets. The user is given the option of displaying up to three graphs simultaneously. This facilitates comparison of samples taken from the same site or object.

On clicking Consult ECOS, the user must create a folder for the site or object in question, open the newly created folder and then enter a sample name or number as a filename in `.dat` format. The user is then taken to the data entry page, shown in Figure 10.2.

The user first selects the units of measurement in which the analytical data are expressed, and then enters the data in the appropriate boxes.[1] Next, he/she selects the way in which the results are to be displayed:

[1] Although the system cannot handle Ca^{2+} and $SO_4{}^{2-}$ simultaneously, the analytical data received from the laboratory may show the presence of both ions, due to the sparing solubility of gypsum. The system permits the entry of both ions, but uses a value of zero for the ion of lesser concentration, and uses the difference in the two concentrations for the ion of higher concentration. Gypsum is thus effectively removed from the system.

The inability to handle Ca^{2+} and $SO_4{}^{2-}$ simultaneously is unlikely to present a problem in the majority of cases. In instances where both Ca^{2+} and $SO_4{}^{2-}$ are present, they will exist as solid gypsum under most environmental conditions below 99% RH, and will not contribute to damage by volume change.

- the state of the system at a specified temperature and relative humidity; *or*
- a graph showing the state of the system over a specified range of relative humidities and at a specified temperature; *or*
- a graph showing the state of the system over a specified range of temperatures and at a specified relative humidity.

Having entered the data, the user clicks on proceed. If the charge on the anions and cations is exactly in balance, the system displays the results in the chosen format. However, in many cases there will be an imbalance of charge, either because of inaccuracies in the analytical data or because there are some ions that have not been analysed/entered. In these cases, the system alerts the user and offers three options:

- return to the data entry page, so that the data may be corrected;
- automatic proportional scaling of the ionic concentrations, to achieve charge neutrality;
- manual tuning of selected ions, to achieve charge neutrality.

When charge neutrality has been achieved, the system displays the final results in the chosen format. In the majority of cases, one of the graphical formats will be the most useful. The graph can display either the cumulative molar concentrations of each of the minerals existing in the solid state or their cumulative volume, and the user can readily alternate between the two by clicking on the appropriate box beneath the graph. It is the volume display that will indicate the regions of temperature or relative humidity that pose the greatest/least threat to objects or sites contaminated with ions in the concentrations entered. The graphs use different colours to illustrate individual minerals, and the user can right click on each line to get further information about the mineral and about the underlying thermodynamic data, by then selecting Crystal Information or Crystal Data respectively.

10.4 Examples

Figures 10.3 and 10.4 illustrate the output of ECOS for pure sodium sulfate (*cf.* Figure 2.3). At 20°C, the system exists in the solid state below 95% RH; mirabilite ($Na_2SO_4 \cdot 10H_2O$) is stable between 95% and 76% RH. and thenardite (Na_2SO_4) below 76% RH . The 314% volume change that accompanies hydration to mirabilite is dramatically shown in Figure 10.4. (Note that ECOS does not display a vertical line at the equilibrium RH of single salts. The ERH is denoted by the right-hand end of the plotted line.)

The full power of ECOS is revealed when salt mixtures are entered. Figure 10.5 shows the graphical output for the data/options of Figure 10.2. It gives the molar quantities of those minerals that exist in equilibrium in the solid state over the specified range of relative humidities. Note that it is a cumulative plot; the quantity of each mineral is indicated by the distance of the relevant line from the line beneath. In this case, crystallisation/solution is taking place over the range 58–80%. Above 80%, all the ions are in solution; beneath 58%, the entire system is in the solid state.

Figure 10.6 shows the corresponding volume graph, in which the molar quantities of each mineral have been converted to volumes. As with Figure 10.5, the plot is

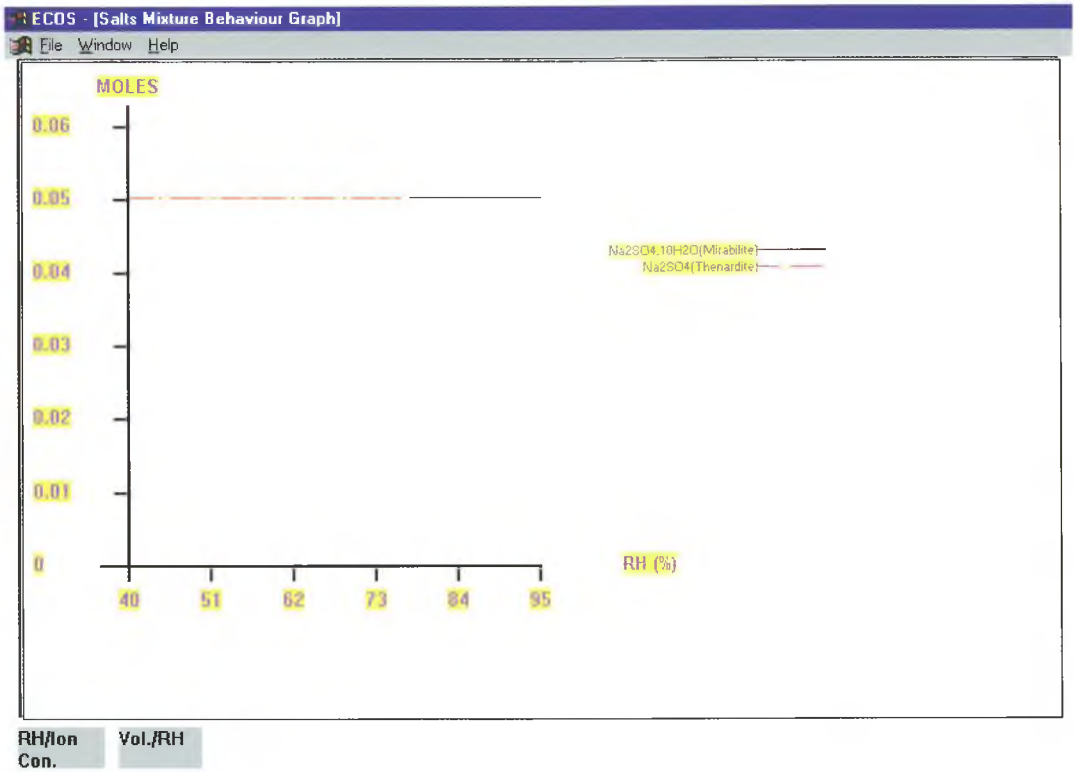

Figure 10.3: ECOS output for sodium sulfate (molar quantities).

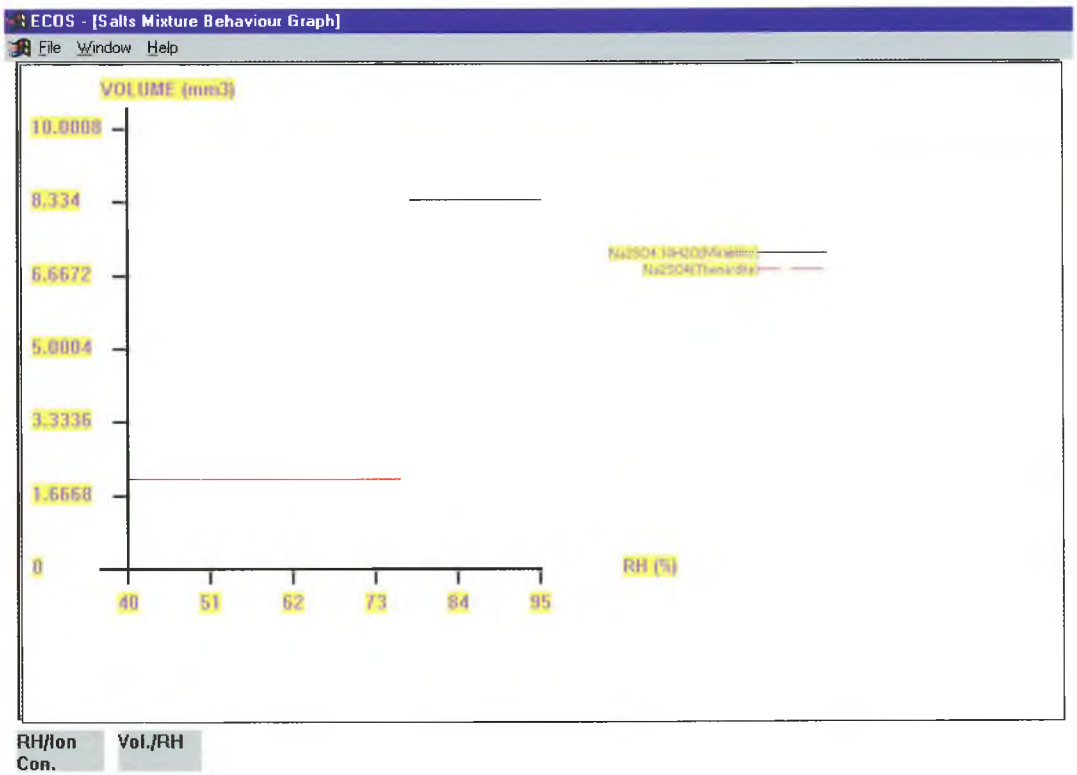

Figure 10.4: ECOS output for sodium sulfate (solid volumes).

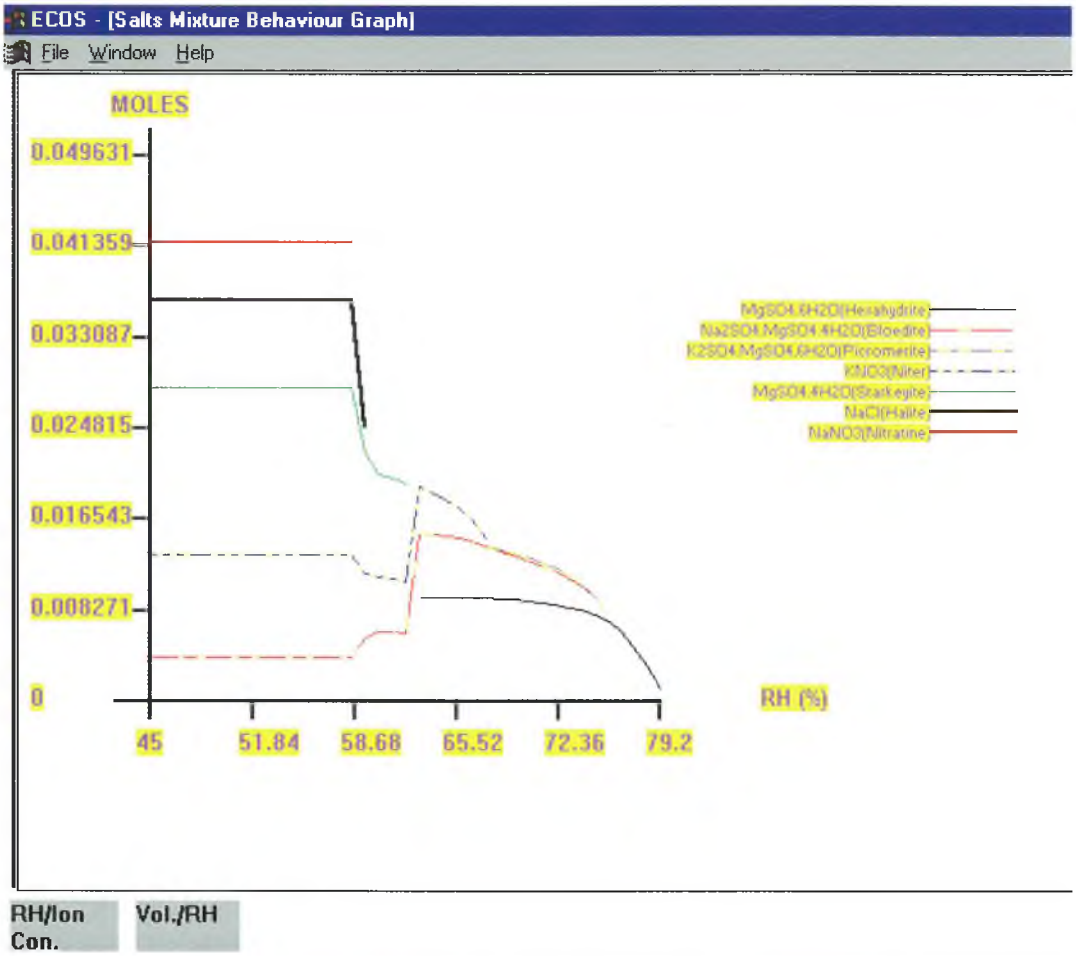

Figure 10.5: ECOS output for the data/options entered in Figure 10.2. The graph shows the cumulative quantity of salts existing in the solid state over a range of relative humidities.

cumulative; by looking at the uppermost line, the user can see the total volume of the system. There is a dip in the total volume between 58% and 63%, attributable largely to the loss of water from hydrated salts at 63%, accompanied by the crystallisation of other minerals as the RH falls towards 58%.

If the ambient RH were to be held permanently below 58%, or above 80%, then no salt damage should be encountered. No other range is entirely safe, although the range 65–70% is relatively flat. More than half the salts crystallise out in the range 70–80%, and this range is definitely to be avoided.

10.5 Advanced features of ECOS

The information in sample files can be altered at any time and the results viewed by clicking on Consult ECOS and selecting Open. It should be noted that only the final data entered are automatically saved to the file.

Figure 10.7 illustrates the facility whereby graphs may be stacked to allow comparison between samples. It is accessed from the Graph button on the opening page: select more than one graph by holding down the shift key and clicking on the graph files desired. When using this facility users should ensure that the same environmental data are entered for each of the files chosen.

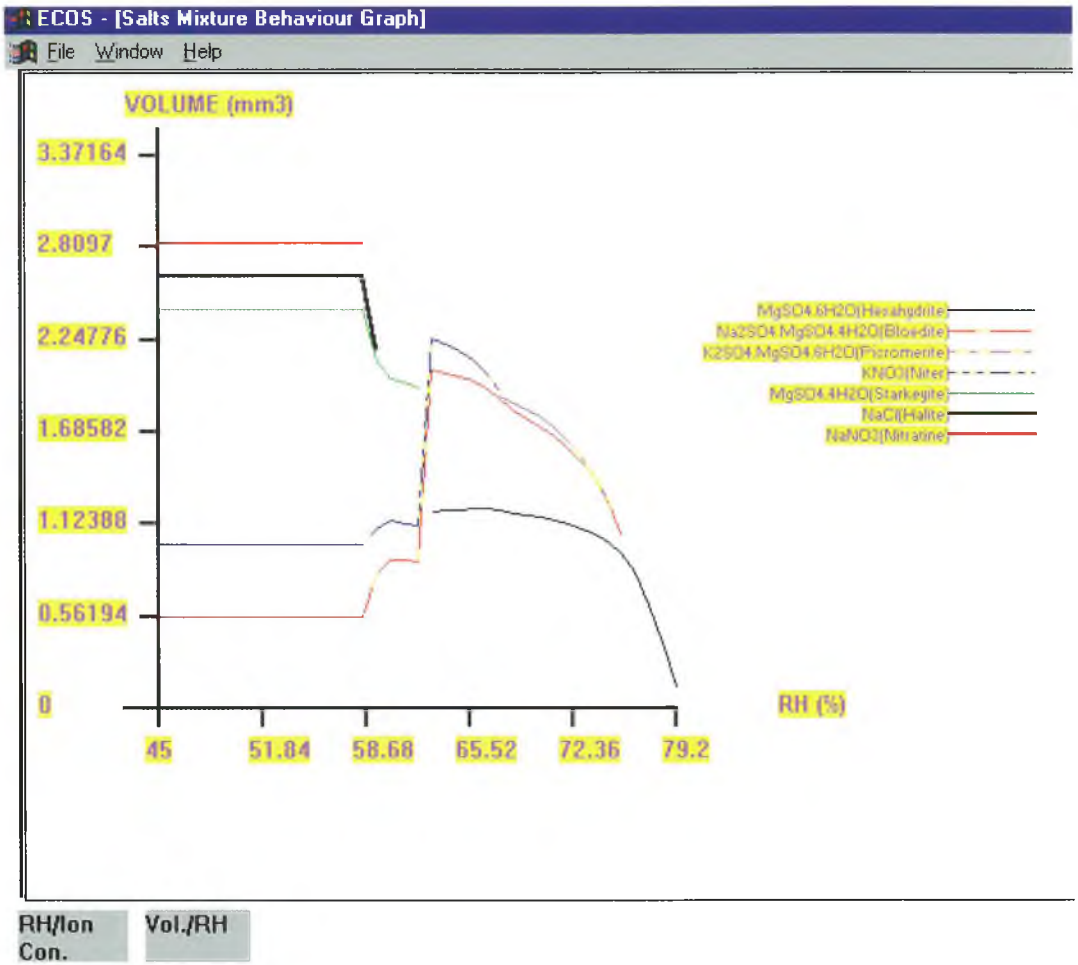

Figure 10.6: An alternative representation of the data of Figure 10.5, showing the cumulative *volume* of salts existing in the solid state under equilibrium conditions.

10.6 Evaluating ECOS

Within the three-year timescale of the contract, it was not practicable to mount full field trials of ECOS. They are now being undertaken by the project partners, and will be reported in the literature in due course. Collaboration with other researchers, conservators and conservation scientists is welcomed. Copies of the prototype version may be requested from the coordinator (`c.price@ucl.ac.uk`).

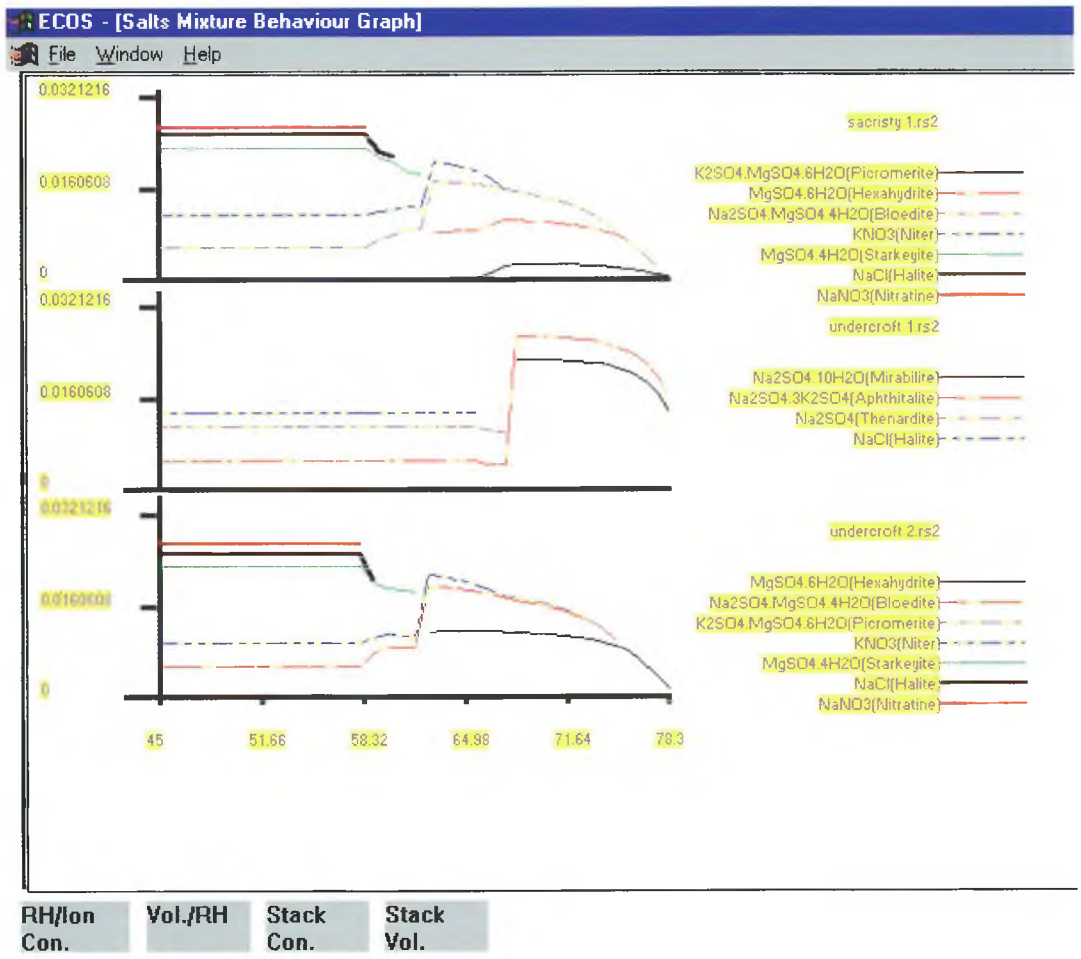

Figure 10.7: Graphs stacked to facilitate comparison.

ISBN 1-873132-52-2